

**SYNTHESIS AND CONFORMATIONAL ANALYSES OF
UNNATURAL AMINO ACIDS AND THEIR HYBRID
PEPTIDES**

By

MANISH KUMAR GUPTA

Enrolment No: **CHEM 11201704019**

National Institute of Science Education and Research (NISER)

Bhubaneswar

A thesis submitted to the

Board of Studies in Chemical Sciences

In partial fulfilment of requirements

for the Degree of

DOCTOR OF PHILOSOPHY

of

HOMI BHABHA NATIONAL INSTITUTE


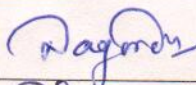
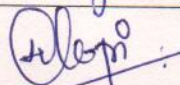
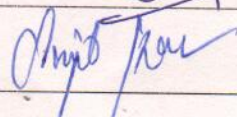
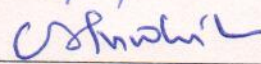
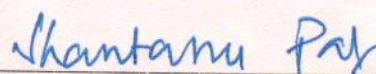


June, 2023

Homi Bhabha National Institute¹

Recommendations of the Viva Voce Committee

As members of the Viva Voce Committee, we certify that we have read the dissertation prepared by **MANISH KUMAR GUPTA** entitled: **"SYNTHESIS AND CONFORMATIONAL ANALYSES OF UNNATURAL AMINO ACIDS AND THEIR HYBRID PEPTIDES"** and recommend that it may be accepted as fulfilling the thesis requirement for the award of Degree of Doctor of Philosophy.

Chairman – Prof. A. Srinivasan		22.12.23
Guide / Convener – Dr. Nagendra K. Sharma		22/12/23
Examiner - Prof. Hosahudya N. Gopi		22/12/23
Member 1- Dr. S. Kar		22/12/23
Member 2- Dr. Chandra S. Purohit		22/12/23.
Member 3- Dr. Shantanu Pal		22.12.23

Final approval and acceptance of this thesis is contingent upon the candidate's submission of the final copies of the thesis to HBNI.

I/We hereby certify that I/we have read this thesis prepared under my/our direction and recommend that it may be accepted as fulfilling the thesis requirement.

Date: 22.12.23

Place: NISER

Bhubaneswar

Signature

Co-guide (if any)



Signature

Guide Dr. N. K. Sharma

¹ This page is to be included only for final submission after successful completion of viva voce.

STATEMENT BY AUTHOR

This dissertation has been submitted in partial fulfilment of requirements for an advanced degree at Homi Bhabha National Institute (HBNI) and is deposited in the library to be made available to borrowers under rules of the HBNI.

Brief quotations from this dissertation are allowable without special permission, provided that accurate acknowledgement of source is made. Requests for permission for extended quotation from or reproduction of this manuscript in whole or in part may be granted by the Competent Authority of HBNI when in his or her judgment the proposed use of the material is in the interests of scholarship. In all other instances, however, permission must be obtained from the author.



MANISH KUMAR GUPTA

DECLARATION

I hereby certify that the research described in the thesis has been performed by me. The work is unique and has never been submitted in full or in part for a degree or diploma at this institution or university or any other.

Manish Kumar Gupta

MANISH KUMAR GUPTA

List of Publications arising from the thesis

Publications in Refereed Journal

1. **M. K. Gupta;** N. K. Sharma.* A new amino acid, hybrid peptides and BODIPY analogs: synthesis and evaluation of 2-aminotroponyl-L-alanine (ATA) derivatives. *Org. Biomol. Chem.*, 2022, **20**, 9397-9407.
2. **M. K. Gupta;** C. K. Jena, C. Balachandra, N. K. Sharma.* Unusual Pseudopeptides: Syntheses and Structural Analyses of Ethylenedipropyl Peptides and Their Metal Complexes with Cu(II) Ion. *J. Org. Chem.* 2021, **86**, 16327-16336.
3. **M. K. Gupta;** C. K. Jena, N. K. Sharma.* Pd-Catalyzed C(sp²)-H olefination: synthesis of *N*-alkylated isoindolinone scaffolds from aryl amides of amino acid. *Org. Biomol. Chem.*, 2021, **19**, 10097-10104
4. **M. K. Gupta;** A. Panda, S. Panda, N. K. Sharma.* Synthesis and conformational analysis of isoindolinone hybrid peptide through Pd catalyzed C-H activation. *Org. Biomol. Chem.*, 2023, **21**, 5104
5. **M. K. Gupta;** A. Panda, N. K. Sharma.* Ru(II)-Catalyzed Regioselective Redox-Neutral Annulation of benzamides with diphenylacetylene at room temperature. (*Manuscript communicated*)

Conference/Symposium

1. Poster Presentation on “**Unusual Pseudopeptides: Syntheses and Structural Analyses of Ethylenedipropyl Peptides and Their Metal Complexes with Cu(II) Ion**” at NBCC Conference on 26th July 2018 in NISER Bhubaneswar, India.
2. Poster Presentation on “A new amino acid, hybrid peptides and BODIPY analogs: synthesis and evaluation of 2-aminotroponyl-L-alanine (ATA) derivatives” at IC-

CBSDD–2019 (08-10 March. 2019), Berhampur university, Odisha.

3. Oral Presentation on “**Pd-Catalyzed C(sp²)–H olefination: synthesis of N-alkylated isoindolinone scaffolds from aryl amides of amino acid esters**” at **RAIMS-2022** (18-19 November), VSSUT Burla, Sambalpur, Odisha.
4. Attended International Workshop on Organo-& Electrocatalysis for Sustainable Synthesis (**OECSS-2022**) (22-23 dec. 2022), IIT Bhubaneswar, Odisha.

ACKNOWLEDGEMENTS

I now had the chance to express my gratitude to everyone who had assisted me in reaching this point in my life. I owe God a huge debt of gratitude for blessing this life and providing me with courage.

I gratefully acknowledge the National Institute of Science Education and Research (NISER) for its thriving research environment. It is an honour for me to work in such a prestigious organisation. For the Junior/Senior Research Fellowship, I am grateful to the University Grants Commission (UGC).

I would like to express my sincere gratitude to my supervisor Dr. Nagendra Kumar Sharma for letting me to work under his supervision. I am grateful to him for his attention, assistance, support, and innumerable other things that I cannot list in this journey. He gave me what I am now because of his incredible vision, depth of understanding, and kindness. It would not have been possible without him.

I would like to thank the faculty, School of Chemical Science (SCS), my current and past research lab members Dr. Bibhuti, Dr. Smitha, Dr. Supriya, Dr. Raghunath, Sagarika, Chinmay, Subhashree, Ankita, Malobika, Subhashish. I also thank my doctoral committee Prof. A. Srinivasan, Dr. Chandrasekhar Purohit, Dr. Sanjib kar and Dr. Santanu pal.

Finally, I want to express my sincere thanks to my parents and brother for their sacrifices on my behalf, their unwavering support, and their blessings, which helped me get through numerous challenges throughout my Ph.D. and my life.

SYNOPSIS

Synthesis and conformational analyses of unnatural amino acids and their hybrid peptides

CHAPTER 1

Introduction to amino acids, peptides, and C-H activation on peptides

Amino acid and peptide derivatives are important in synthetic organic chemistry and medicinal chemistry, which attract many chemists to develop new methods for their synthesis. Amino Acids are the organic compounds that combine to form proteins; hence they are referred to as the building components of proteins. These biomolecules are involved in several biological and chemical functions in the human body and are the necessary ingredients for the growth and development of human beings. Peptides are short chains of amino acids linked by peptide bonds. A polypeptide is a longer, continuous, unbranched peptide chain. Peptides have several functions in the body. They are also the basis of various medications. Aiming to gain stronger or specific or novel biological effects and overcome the disadvantages of natural peptides, artificial hybrid peptides have been designed by combining the sequence of two or more different peptides with varied biological functions. Various hybrid peptides act as therapeutic drug. Captopril, Enalapril used for reducing blood pressure. Lisinopril increases muscle relaxing activity. Ramipril facilitates blood clotting and Fisinopril used for hypertension. Hybrid tetrapeptide folds into β -hairpin in solution state due to the presence of hydrogen bonding between them. Hybrid peptides also used as catalyst for various reactions like kinetic resolution of amino alcohols catalyst and methanolysis of oxazol-5(4H)-ones.

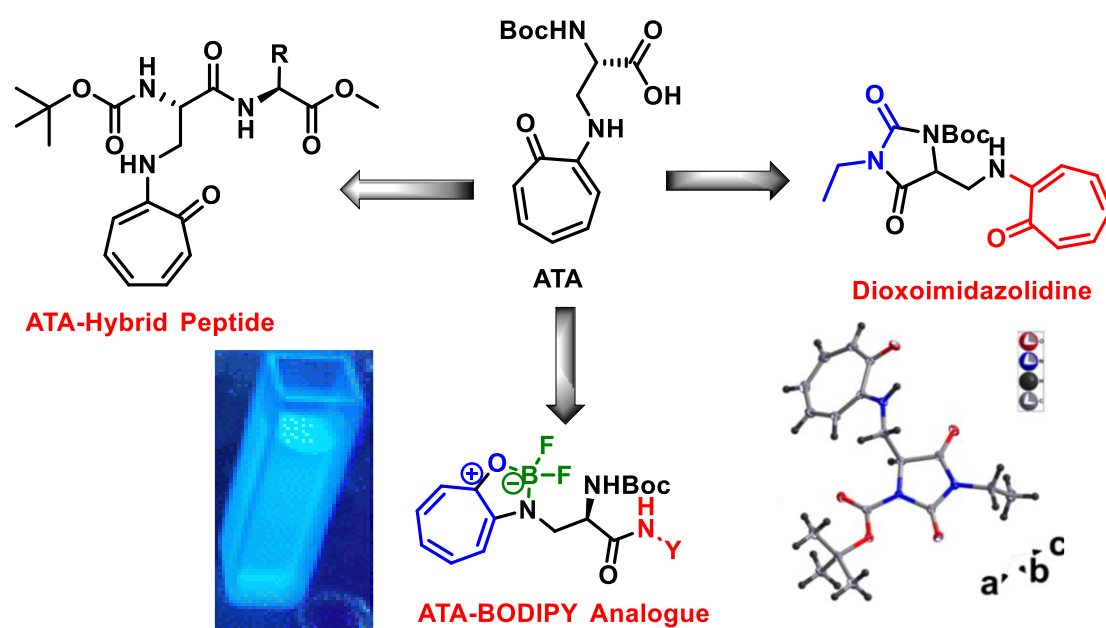
The growing importance of peptides and proteins in therapeutic and biomedical applications has provided immense motivation toward the development of new ways to construct and transform peptide molecules. As in other areas of organic synthesis, C–H functionalization (CHF) chemistry could potentially exemplify disruptive technologies for peptide engineering.

Over the past decade, the field has witnessed an exciting surge of reports of various metal-catalyzed CHF chemistry for postassembly modification of peptides and proteins. Late-stage functionalization of C–H bonds (C–H LSF) can provide a straightforward approach to the efficient synthesis of functionalized complex molecules such as peptides and, thereby, potentially useful because sought-after molecules can be made quickly for use in diverse disciplines, such as drug discovery, materials research, and molecular imaging.

CHAPTER 2

Synthesis and conformational evaluation of 2-aminotroponyl-L-alanine (ATA) derivatives

(M. K. Gupta; N. K. Sharma.* *Org. Biomol. Chem.*, 2022, **20**, 9397-9407)



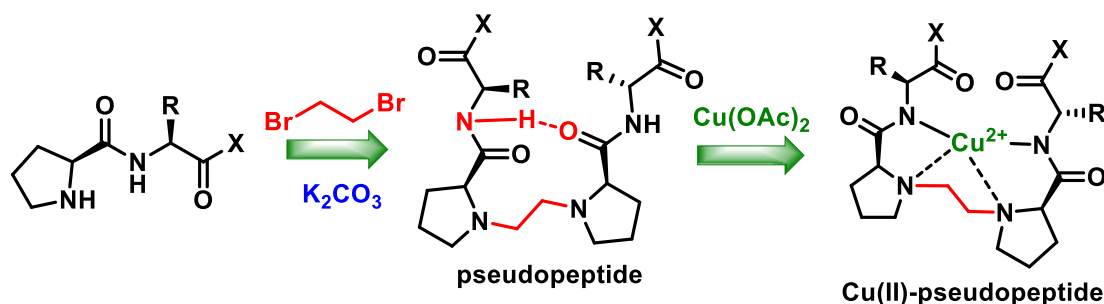
Natural aromatic α -amino acid residues play critical roles in the structural and functional organization of proteins owing to π -interactions. Their aromatic residues are derived from benzenoid scaffolds. Non-benzenoid aromatic scaffolds such as tropone and tropolone are also constituents of troponoid natural products. Tropolone has the ability to exhibit π -interactions along with additional hydrogen bonding. This chapter highlights the introduction to 2-

aminotroponyl-L-alanine and its synthetic utility towards the formation of its hybrid peptides and its fluorescent BODIPY analogue. Its unusual reactivity with the peptide coupling agent EDC forming a heterocyclic troponyl dioxoimidazolidine derivative. Conformational analyses of troponylated hybrid peptides revealed the role of the troponyl residue in the structural changes of ATA-containing peptides into β -turn/ α -helix type structures. For practical utility, their non-cytotoxicity and cell internalization into HeLa cells has been demonstrated.

CHAPTER 3

Synthesis of ethylenedipropyl pseudopeptides and their metal complexes with Cu(II) ion

(M. K. Gupta; C. K. Jena, C. Balachandra, N. K. Sharma.* *J. Org. Chem.* 2021, 86, 16327-16336)



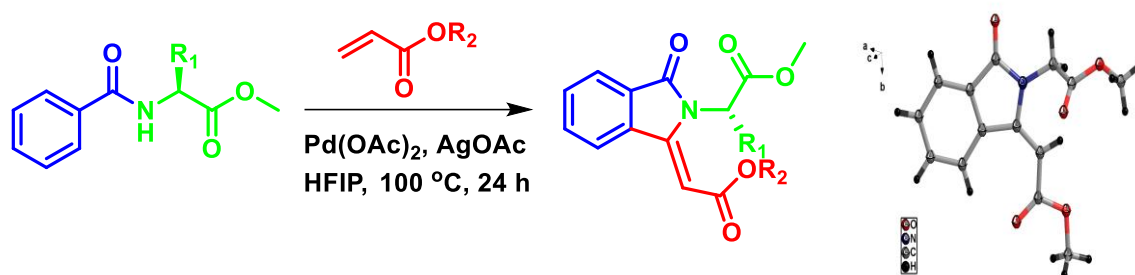
The synthetic unnatural amino acids and their peptides as peptidomimetics have shown remarkable structural and functional properties. In the repertoire of synthetic peptides, pseudopeptides have emerged as attractive small peptidomimetics that are capable of forming the characteristic secondary structures in the solid/solution phase, as in natural peptides. This report describes the synthesis and structural analyses of novel pseudopeptides as ethylenedipropyl (etpro) tetra/hexapeptides, comprising a chiral diaminedicarboxylate scaffold. Their NMR and CD spectral analyses strongly support the formation of the β -turn-type structures in organic solvents (ACN/MeOH). Further, the single-crystal X-ray studies of tetrapseudopeptide confirm the formation of a unique self-assembly structure as β -strand type in the solid state through hydrogen bonding. Importantly, their diamine moiety influences the

formation of Cu-complexes with Cu(II) ions. A tetrapseudopeptide monocarboxylate-Cu(II) complex forms the single crystal that is studied by the single-crystal X-ray diffractometer. The crystal structure of the tetrapseudopeptide-Cu(II) complex confirms the formation of the distorted square planar geometry structure, almost like the amyloid β (A β)-peptide-Cu(II) complex structural geometry. Hence, these etpro-pseudopeptides are emerging peptidomimatics that form β -turn types of structures and metal complexes mainly with Cu(II) ions. These molecules could be considered for the development of peptide-based catalysts and peptide-based therapeutic drug candidates.

CHAPTER 4a

Synthesis of isoindolinone analogues from *N*-benzoyl amino esters through Pd-catalysed C-H activation

(M. K. Gupta; C. K. Jena, N. K. Sharma.* *Org. Biomol. Chem.*, 2021, **19**, 10097-10104)



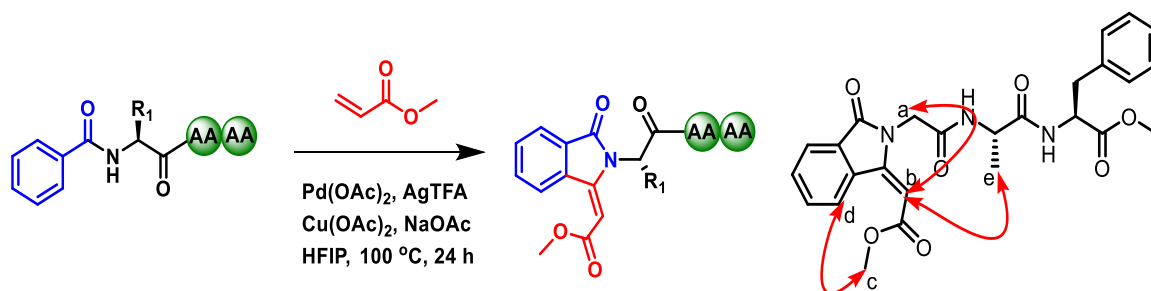
Isoindolinone is a constituent of various natural products and synthetic biologically active compounds. The classical multi-step synthetic methods used to prepare various indolinone derivatives are tedious and challenging. One-pot synthetic methods are attractive and economical. Transition-metal-catalyzed C–H activation is an emerging tool for synthesizing natural products and small organic molecules via reducing the number of synthetic steps necessary. This paper describes the synthesis of *N*-alkyl-3-methenyl chiral isoindolinone

derivatives from aryl amides of L-amino acids and non-activated alkene via Pd-catalyzed C(sp²)-H olefination. Herein, the amino acid residue acts as a directing group for olefination at the aryl ring, and then cyclization occurs at the amide NH. Hence, this methodology could be helpful to transform standard amino acids into respective chiral isoindolinone derivatives.

CHAPTER 4b

Synthesis of isoindolinone hybrid peptide from *N*-benzoyl peptide through late-stage Pd catalyzed C-H activation

(M. K. Gupta; A. Panda, S. Panda, N. K. Sharma.* *Manuscript communicated*)

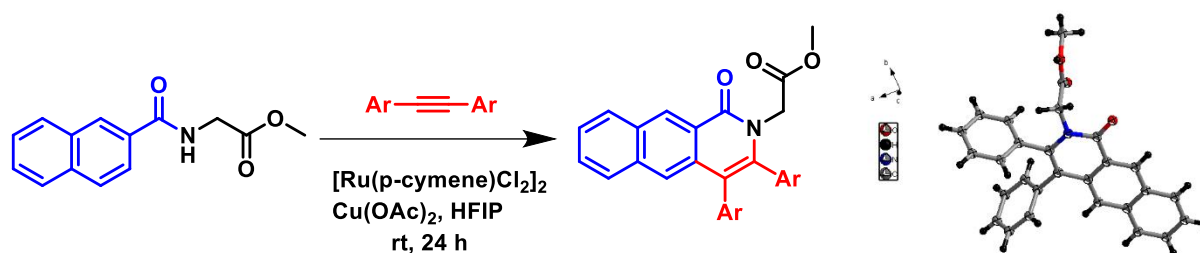


Isoindolinone is a constituent of several natural products that show wide range of bioactivities such as anticancer, antimicrobial, antiviral and anti-inflammatory properties. It would be interesting to explore the isoindolinone's carbonyl group (H-bond acceptor) in structural and conformational changes. However, synthesis of isoindolinone comprising peptides in short steps are really challenging. Herein, we have developed a synthetic methodology for introducing isoindolinone residue in peptides via Pd-catalyzed C(sp²)-H activation/olefination, and demonstrated the conformational changes owing to the isoindolinone scaffold. Hence, isoindolinonyl peptides provide an avenue for synthesis of novel foldamers and therapeutic agents.

CHAPTER 5

Ru(II)-Catalyzed regioselective redox-neutral annulation of benzamides with diphenylacetylene at room temperature

(M. K. Gupta; A. Panda, N. K. Sharma.* *Manuscript Communicated*)



One of the significant nitrogen-heterocyclic compounds with a wide range of pharmacological and physiological activities are isoquinolones (isoquinolin-1(2H)-ones), and their synthesis techniques have advanced significantly in recent years. It has been extensively studied in synthetic chemistry that annulation protocols using unsaturated hydrocarbons are essential and effective ways to synthesise cyclic molecules with high atom-utilization and step-economy. Isoquinolones are useful synthetic building blocks in addition to being intriguing and significant nitrogen-heterocyclic molecules with a variety of pharmacological and physiological functions. There are several effective methods for creating isoquinolones, and some of the earliest works have been published. This paper describes the synthesis of isoquinolones derivatives from *N*-naphthoyl amino ester/peptide and *N*-biphenayl amino ester/peptide via Ru-catalyzed C(sp²)-H annulation at room temperature. Herein, the amino acid ester/amide residue acts as a directing group for annulation at the aryl ring, and then cyclization occurs at the amide NH. Hence, this methodology could be helpful to transform

standard amino acids/peptides into respective chiral isoquinolones derivatives in room temperature.

List of Schemes

Scheme 2. 1 Synthesis of Aminotroponyl Alanine (ATA)	40
Scheme 2. 2 Synthesis of dioxoimidazolidine derivative (7)	41
Scheme 2. 3 Synthesis of ATA hybride peptides	44
Scheme 2. 4 Synthesis of ATA-BODIPY analogues	45
Scheme 3. 1 Synthesis of Ethylenyldipropyl (etpro) peptides	73
Scheme 3. 2 Synthesis of etpro-peptides-Cu(II) complexes	80
Scheme 4a. 1 Synthesis of 3-methylenyl-N-alkyl chiral isoindolin-1-one molecules	94
Scheme 4a. 2 Synthesis of Chiral isoindolinone derivative using various amino ester	97
Scheme 4a. 3 Synthesis of Chiral isoindolinone derivative using different aryl group	99
Scheme 4b. 1 Synthesis of substituted isoindolinone peptide derivative with peptide residue	120
Scheme 4b. 2 Synthesis of substituted isoindolinone peptide derivative with peptide residue	122
Scheme 4b. 3 Synthesis of substituted isoindolinone peptide derivative with 2-naphthoic acid and 4-biphenyl carboxylic acid	123
Scheme 4b. 4 Synthesis of aryl substituted isoindolinonyl peptide derivatives	124
Scheme 4b. 5 Synthesis of substituted isoindolinonyl tri-peptide	125
Scheme 5. 1 Annulation of N-naphthoyl amino ester	163
Scheme 5. 2 isoquinolone derivative using peptides and diphenyl acetylene	165
Scheme 5. 3 isoquinolone derivative using peptides and 1,3-diyne	166

List of Tables

Table 2. 1 Photophysical parameters of ATA-BODIPY analogues (in ACN)	52
Table 3. 1 Comparative HRMS analyses of Peptide ligand and their complexes	80
Table 4a. 1 Optimized reaction condition	96
Table 5. 1 Optimized reaction condition	162

List of Figures

Figure 1. 1 Carbodimides and Benzotriazoles used in (a) solution phase peptide synthesis (b) solid phase peptide synthesis	5
Figure 1. 2 General representation of solution phase peptide synthesis	6
Figure 1. 3 General representation of solid phase peptide synthesis	7
Figure 1. 4 Some of the peptide-based therapeutics	8
Figure 1. 5 Peptide based therapeutics inhibitory action against SARS-CoV-2	9
Figure 1. 6 Some of the non-ribosomal amino acids present in various natural products	12
Figure 1. 7 Bioactive natural products containing non-ribosomal amino acids	14
Figure 1. 8 (a) Tropolone (b) Hydrogen bonding in tropolone	13
Figure 1. 9 Natural products containing tropolone	14
Figure 1. 10 (a) Unnatural δ -amino acid, troponyl aminoethylglycine (b) N-troponylated peptides (c) L-aminotroponyl alanine (ATA) and its peptide	15
Figure 1. 11 Functionlization on (a) prolyl containing aminotroponone (b) sulphonation of amino tropolone	16
Figure 1. 12 Basic representation of C-H activation	17
Figure 1. 13 Modified peptides drugs by C-H functionalization	18
Figure 1. 14 C-H activation in peptides (a) Trp backbone (b) Tyr backbone (c) Phe backbone	19
Figure 1. 15 Natural products having isoindolinone unit	21
Figure 1. 16 Some natural product containing isoquinolone unit	23
Figure 1. 17 (a) 3-metoxycarbonyl isoquinolone derivative (b) 3-acyl-isoquinolone derivatives	23
Figure 2. 1 (1) previous work: (a) Achiral Troponyl amino acid derivatives (b) Hydrazino troponyl amino acid (2) This works: Chiral troponyl amino acid	38
Figure 2. 2 The plausible reaction mechanism of dioxoimidazolidine formation. (a) Reaction without HOBt; (b) Reaction with HOBt	41
Figure 2. 3 NOE's of ATA-peptide (A) di-peptide (8c), (B) tetra-peptide (8i)	45
Figure 2. 4 DMSO-d ₆ titration NMR experiments of ATA-Hybrid peptide: (A) BocNH-ATA-Val-OMe (8c), (B) Boc NH-ATA-Gly-ATA-Gly-OMe (8i), (C) BocNH-ATA-Gly-Gly-OMe (8h), (D) BocNH-Val-ATA-OMe (11b)	46

Figure 2. 5 CD spectra of (6, 8e, 8h, 8i) in acetonitrile (ACN)	47
Figure 2. 6 CD spectra of (8a-8d, 8f, 8g & 11a-11e) in acetonitrile (ACN) & in methanol (MeOH)	48
Figure 2. 7 Theoretically optimized structure of ATA-peptides 8a (A)/11a (B)/ 8i (C)	49
Figure 2. 8 (a) Sample under fluorescence light; (b) UV-Vis absorption and emission spectra of ATA-BODIPY analogs (12a/12b); (c) Computational Molecular orbital diagrams of 12a/12b	50
Figure 2. 9 (a) HOMO-LUMO of ATA-BODIPY analogs;(b) Theoratically optimized structure of 12b	51
Figure 2. 10 Confocal images of HeLa cells with 12a: (a) stained with DAPI; (b) BODIPY 12a treated cells with FITC staining (green channel); (c) merged image of DAPI and FITC staining	52
Figure 3. 1 (a) Reported model of A β -peptides-Cu(II) complex; (b) Rationally designed bioinspired ligand and metal complex from pseudopeptides	71
Figure 3. 2 2D NMR (NOE) analyses: (A) NOE interactions in hairpin peptides 4a, 4b and (B) Selective NOE assessments of peptide 4b	75
Figure 3. 3 (A) DMSO-d ₆ titration NMR profile of peptides 3a, 3b / 4a, 4b; and (B) Proposed Hydrogen bonding in etpro-peptides 3a, 3b / 4a, 4b	76
Figure 3. 4 CD spectra of control and etpro-Peptides (A) in ACN and (B) in MeOH	78
Figure 3. 5 Temperature dependent CD spectra of control and etpro-Peptides in ACN	79
Figure 3. 6 EPR spectra of etpro-peptide Cu-complex 4a-Cu (A) and 4b-Cu (B)	81
Figure 4a. 1 (a) Isoindolinone and related natural products, (b) the previously reported isoindolinone, and (c) the isoindolinone reported in this paper	93
Figure 4a. 2 (a) ORTEP diagram and (b) Unit cell of acrylatyl glycynyl Isoindolinone 6a	95
Figure 4a. 3 The proposed reaction mechanism of isoindolinone synthesis	100
Figure 4b. 1 Isoindolinone and related natural peptides	117
Figure 4b. 2 (a) The previously reported C-H hydroarylation (b) C-H functionalization and (c) This report- post synthesis of isoindolinyl peptides	119

Figure 4b. 3 The proposed mechanism for isoindolinone peptide synthesis	126
Figure 4b. 4 NOESY spectra of isoindolinone derivative 23	127
Figure 4b. 5 DMSO d6 titration NMR of isoindonyl derivatives	128
Figure 4b. 6 Conformation of isoindolinone peptides (Computationally optimized structure of isoindolinone peptides MMFF94 and GMMX)	130
Figure 4b. 7 Cell proliferation data of peptides	132
 Figure 5. 1 (a) C-H activation of ala residue via bidentate directing group (b) Backbone modification by Ru catalyst (c) Lys-based peptides are modification by Rh(III) catalyst (d) C-H activation/annulation in N-naphthoyl amino ester in rt	161
Figure 5. 2 Proposed mechanistic pathway	167

List of Abbreviations

Å	angstrom
aa	amino acid
ala	alanine
asn	asparagine
Ac	acetyl
aq.	aqueous
Bn	benzyl
Boc	<i>tert</i> -butyloxycarbonyl
BODIPY	boron-dipyrromethene
br	broad
°C	degrees Celsius
calcd.	calculated
CCDC	Cambridge Crystallographic Data Centre
CSD	Cambridge Structural Database
CD	Circular Dichroism
COSY	Correlation Spectroscopy
D	doublet
DMF	<i>N,N</i> -dimethylformamide
DCM	Dichloromethane
DMSO	dimethyl sulfoxide
DCE	dichloroethane
DIPEA	diisopropylethylamine
DIPCDI	diisopropylcarbodiimide
EDC.HCl	<i>N</i> -(3-Dimethylaminopropyl)- <i>N'</i> -ethylcarbodiimide

	hydrochloride
eq.	equivalent
ESI	Electrospray Ionization
Et	ethyl
EtOAc	Ethylacetate
FDA	Food and Drug Administration
Fmoc	Fluorenyl methoxy carbonyl
G	gram(s)
Gly	glycine
Ile	Isoleucine
HBTU	(2-(1H-benzotriazol-1-yl)-1,1,3,3-tetramethyluronium hexafluorophosphate
HATU	(1-[Bis(dimethylamino)methylene]-1H-1,2,3-triazolo[4,5-b] pyridinium 3-oxide hexafluorophosphate
HCTU	(1H-6-Chlorobenzotriazole-1-yl)-1,1,3,3-tetramethyluronium hexafluorophosphate
h	hour(s)
HRMS	High Resolution Mass Spectroscopy
HSQC	Heteronuclear Single Quantum Coherence Spectroscopy
Hz	hertz
His	histidine
IR	infrared (spectroscopy)
<i>J</i>	coupling constant
JNK	c-Jun N-terminal protein kinases
K	kelvin
λ	wavelength

L	liter
Leu	leucine
Lys	lysine
M	multiplet or milli
m/z	mass to charge ratio
μ	micro
Me	methyl
mg	milli gram
MHz	megahertz
min	minute(s)
mol	mole(s)
mL	milli litre
μ L	micro litre
μ M	micro molar
mM	milli molar
mp	melting point
NMR	Nuclear Magnetic Resonance
NMM	N-methyl morpholine
NOE	Nuclear Overhauser Effect
NOESY	Nuclear Overhauser Enhancement Spectroscopy
nm	nanometers
<i>p</i>	para
PyBOP	benzotriazol-1- yloxytripyrrolidinophosphonium hexafluorophosphate
Ph	Phenyl
pH	hydrogen ion concentration in aqueous solution

ppm	parts per million
Prop	propyl
Pro	proline
Phe	phenyalanine
q	quartet
PTSA	<i>p</i> -toluene sulfonic acid
rt	room temperature
s	singlet
t	triplet
TBTU	2-(1H-Benzotriazole-1-yl)-1,1,3,3-tetramethylaminium tetrafluoroborate
TFA	Trifluoroacetic acid
THF	Tetrahydrofuran
TFE	trifluoroethanol
TLC	thin layer chromatography
TMS	trimethylsilyl
Ts	<i>p</i> -toluenesulfonyl (tosyl)
Tyr	tyrosine
UV	ultraviolet
Val	valine
W	weak

TABLE OF CONTENTS

Chapter 1	1
1.1 Introduction to peptides	3
1.1.1 History of peptides	3
1.1.2 Amino acids and peptides	3
1.1.3 Synthesis of peptides	6
1.1.4 Peptide as therapeutic drug	8
1.1.5 Unnatural amino acids (UAAs) and its Peptides	11
1.1.6 Unnatural aromatic amino acids containing nonbenzenoid scaffold Tropolone	12
1.2 Functionalization of peptide backbone	16
1.2.1 Introduction to C-H activation on peptides	16
1.2.2 Late-stage C(sp ²)-H functionalization on peptides	20
1.2.3 Synthesis of Isoindolinone analogs via C-H activation	21
1.2.4 Synthesis of Isoquinolone via C-H activation	22
1.3 References	25
 Chapter 2	 36
2.1 Introduction	36
2.2.1 Hypothesis and objective	38
2.2 Result and discussion	38
2.2.1 Synthesis of Aminotroponyl Alanine (ATA)	38
2.2.2 Synthesis of dioxoimidazolidine derivative	39
2.2.3 Synthesis of ATA hybrid peptides	42
2.2.4 Synthesis of ATA-BODIPY analogues	44
2.2.5 Conformational analysis of ATA peptides	44
2.2.6 DMSO D6 Titration study	46
2.2.7 Circular Dichroism study	47
2.2.8 Theoretical study	49
2.2.9 Fluorescence study	50
2.2.10 HOMO & LUMO Computational study	51
2.2.11 Cell culture study	52
2.3 Conclusion	53
2.4 Experimental Section	53

2.4.1 Materials and instrumentation	53
2.4.2 General procedure for peptide coupling	54
2.4.3 Chemical shift values of NMR	54
2.5 References	63
Chapter 3	69
3.1 Introduction	69
3.1.1 Hypothesis and objective	71
3.2 Results and discussion	71
3.2.1 Synthesis of Ethylenedipropyl peptides	73
3.2.2 Conformational analyses	73
3.2.3 DMSO D6 Titration study	74
3.3.4 Circular Dichroism study	77
3.3.5 Metalation of ethylene Ethylenldipropyl peptides	78
3.3.6 EPR Study of Cu-peptides	79
3.3 Conclusions	80
3.4 Experimental Section	81
3.4.1 Material and Instrumentation	81
3.4.2 General Procedure for Peptide Coupling	81
3.4.3 General Procedure for Synthesis of dipropyl Peptides (4a, 4b)	82
3.4.4 General Procedure for Metalation of Peptides	82
3.4.5 Chemical shift values of NMR	82
3.5 References	84
Chapter 4a	90
4a.1 Introduction	90
4a.1.1 Hypothesis and objective	91
4a.2 Result and discussion	93
4a.2.1 Synthesis of Chiral isoindolinone derivatives	93
4a.2.2 Substrate scope using various amino ester	95
4a.2.3 Substrate scope using using different aryl groups	97
4a.2.4 The proposed reaction mechanism	98
4a.3 Conclusion	99

4a.4 Experimental Section	100
4a.4.1 Materials and instrumentation	100
4a.4.2 General procedure for amide synthesis	100
4a.4.3 General procedure for Pd-catalysed reactions	201
4a.4.4 Chemical shift values of NMR	101
4a.5 References	109
Chapter 4b	115
4b.1 Introduction	115
4b.1.1 Hypothesis and objective	118
4b.2 Results and Discussions	119
4b.2.1 Isoindolinone synthesis from N-Benzoyl peptide	119
4b.2.2 Substrate scope using various dipeptides	120
4b.2.3 Substrate scope using 2-naphthoic acid and 4-biphenyl carboxylic acid	122
4b.2.4 Substrate scope using various aryl groups	123
4b.2.5 Substrate scope using tripeptides	124
4b.2.6 Conformational analyses	126
4b.2.7 DMSO D6 Titration study	127
4b.2.8 Theoretical study	128
4b.2.9 Cell culture study	130
4b.3 Conclusions	131
4b.4 Experimental Details	132
4b.4.1 Material and Instrumentation	132
4b.4.2 General Procedure for benzamide derivative peptide synthesis	132
4b.4.3 General procedure for Pd-catalysed reactions	133
4b.4.4 Chemical shift values of NMR	133
4b.5 References	151
Chapter 5	158
5.1 Introduction	158
5.1.1 Hypothesis and objective	160
5.2 Result and discussion	160
5.2.1 Annulation of N-naphthoyl amino ester	162

5.2.2 Substrate scopes naphthoyl amino esters and naphthoyl aminoacid	163
5.2.3 Substrate scopes various peptides with diphenyl acetylene	164
5.2.4 The proposed reaction mechanism	165
5.3 Conclusion	166
5.4 Experimental Section	167
5.4.1 Materials and instrumentation	167
5.4.2 General procedure for amide synthesis	167
5.4.2 General procedure for Ru-catalysed reactions	168
5.4.3 Chemical shift values of NMR	168
5.5 Appendix	181
Contents	181
5.6 References	208

CHAPTER-1

Introduction

TABLE OF CONTENTS

Chapter 1	3
1.1 Introduction to peptides	3
1.1.1 History of peptides	3
1.1.2 Amino acids and peptides	3
1.1.3 Synthesis of peptides	6
1.1.4 Peptides as therapeutic drugs	8
1.1.5 Unnatural amino acids (UAAs) and Its Peptides	11
1.1.6 Unnatural aromatic amino acids containing nonbenzenoid scaffold Tropolone	12
1.2 Functionalization of peptides backbone	16
1.2.1 Introduction to C-H activation on peptides	16
1.2.2 Late-stage C(sp²)-H functionalization on peptide	20
1.2.3 Synthesis of Isoindolinone analogs via C-H activation	21
1.2.4 Synthesis of Isoquinolone via C-H activation	22
1.3 References	25

Chapter 1

1.1 Introduction to peptides

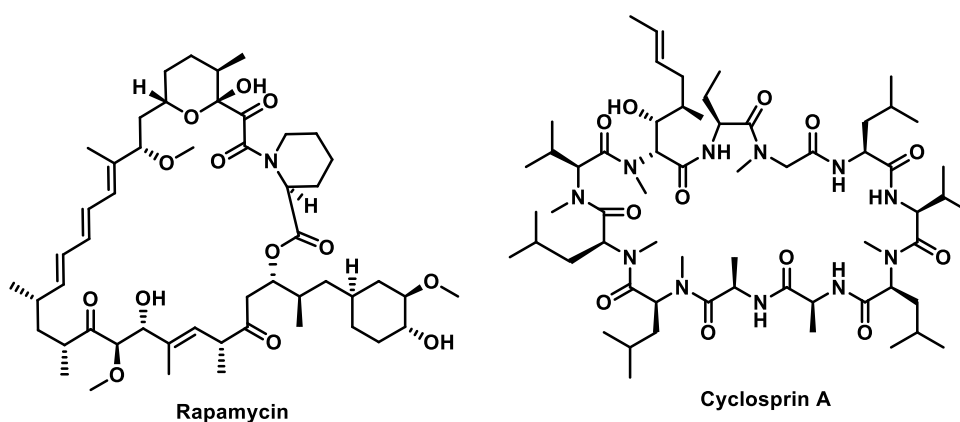
1.1.1 History of peptides

Peptides are found in living systems and indistinguishably linked to the beginning of life.¹ During every stage of chemical evolution, various types of cooperative interactions occurred between peptides and other biomolecules such as carbohydrates, nucleic acids and lipids, which served as the driving force of evolution.² Modern hypotheses on the origin of life are made easier by understanding the chemical and biological synthetic methods of peptide.³⁻⁵ Hermann Emil Fischer and Franz Hofmeister hypothesized that proteins are made up of amino acids.⁶ However the term “protein” is derived from the “proteios” (primary), i.e., representing the first position in living organisms, which is established by Jöns Jacob Berzelius in 1838.⁷⁻⁸ In the early 19th century, the first amino acid and its peptides were identified as Asparagine and related peptides, which were extracted from asparagus.⁹⁻¹¹ In 1881, Theodor Curtius produced the first *N*-protected dipeptide as Benzoylglycylglycine from a silver salt of glycine and Benzoyl chloride through the azide-coupling methods.¹² Later in 1901 Fischer and Ernest Fourneau described a more efficient synthesis of dipeptide gly-gly by hydrolysis of diketopiperazine, which regarded as the discovery of peptide chemistry.¹³ Fisher is also called as the “Father” of peptide chemistry.¹⁴

1.1.2 Amino acids and peptides

Amino acids are building block of peptides that form by their conjugation through peptide or amide bonds. These biomolecules play a critical roles in regulation of various biological processes including the gene expressions and RNA mediated protein synthesis.¹⁵ Their deficiencies suppress protein synthesis and lead to protein deficiency diseases.¹⁵ On the basis of vital requirements, there are two types of amino acids, essential and non-essential amino

acids.¹⁶ The essential amino acids are valine, isoleucine, leucine, methionine, phenylalanine, tryptophan, threonine, histidine, and lysine. Essential amino acids are consumed through diet, however non-essential amino acids are synthesized through the biosynthesis process. Although more than 300 amino acids have been identified, only 20 are involved in the synthesis of proteins known as proteogenic amino acids. A peptide typically contains two or more amino acids. A brief chain of amino acids (10–20 amino acids) is called an oligopeptide. An extended chain of amino acids is called a polypeptide (more than 20 residues). Amino acids are involved in the synthesis of tissue proteins, enzymes, physiologically active peptide glutathione and a few hormones. The well-known peptides hormones are insulin, glucagon, and growth hormone.¹⁷ Interestingly, thyroxine, nor-adrenaline, and adrenaline hormones are formed from amino acid.¹⁸ Peptide-based natural products are also found in cyclic and acyclic forms comprising D/L- α -amino acids, gem-dialkyl substituted α -amino acids, α , β -unsaturated α -amino acids (**Figure 1.1**).¹⁹ These natural products exhibit wide range of bioactivities and being used in the biomedical research and medication discovery.²⁰⁻²¹ For examples, Rapamycin, Cyclosporin, Pristinamycin, Gramicidin S have already shown promising results in therapeutic drug development. **Figure 1.1** depicts a few synthetic amino acids found in peptide natural products.



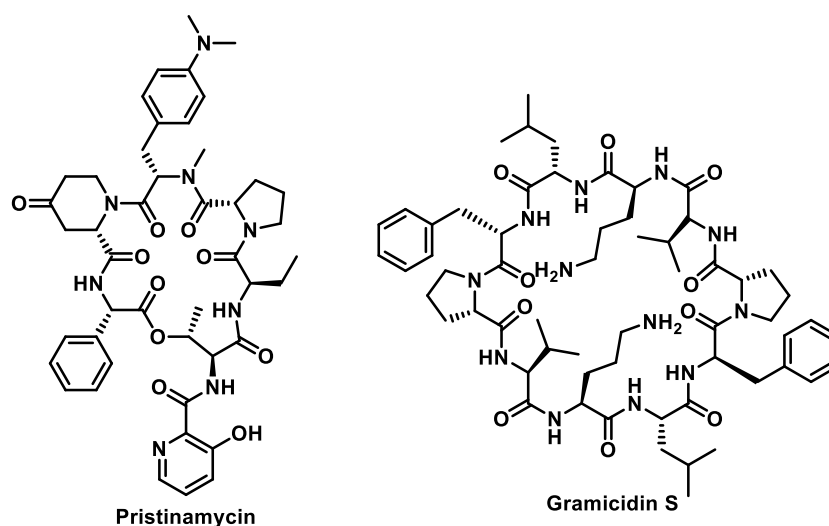


Figure 1. 1 Bioactive natural products containing non-ribosomal amino acids.

Recently, synthetic peptides have emerged as potential candidate for the development of biomaterials and therapeutic drugs owing to the characteristic structural and functional properties, which enhance interactions with specific receptors. Peptide derived drugs exhibit exceptional selectivity and minimal side effects as compared to small molecules. However, the serum stability, cell cytotoxicity and cell permeability of short peptides are still persisting as major challenges for using as therapeutic drugs. Furthermore, compared to what would be expected from the conventional mimetic approach, the number of peptides implicated in critical biological processes is steadily increasing. Peptides have evolved into exciting therapeutic agents with unlimited potential and are likely to be extensively explored. We sincerely anticipate that these straightforward biomolecules will generate wholly new insights and offer potential solutions for creating the distinctive biomedicine of the future.¹⁴

1.1.3 Synthesis of peptides

Peptide synthesis is a well-established methods from corresponding amino acids in presence of carboxylate activating agents or coupling agents.²² It involves the condensation of the carboxylate group of 1st amino acid with the amino group of 2nd amino acid. There are two typical methods for the synthesis of peptides-(i) Solution-phase synthesis and (ii) Solid-phase synthesis. In the Solution phase peptide synthesis, the amine-protected amino acid (PG-NH-aa-OH) and carboxylate-protected amino acid (NH₂-aa-OPG) are employed for the condensation reactions in presence of coupling reagents under anhydrous basic conditions that produced corresponding protected dipeptide. Its protecting group was removed sequentially and coupled with desired protected amino acid/peptides derivatives under similar coupling conditions (**Figure 1.2**). These steps are repeated to achieve the target peptides. The commonly used coupling reagents are carbodiimides (EDC.HCl, DIPCDI, PyBOP and DCC) and benzotriazole (HOBt, HOAt, and 6-Cl-HOBt) derivatives (**Figure 1.3**).

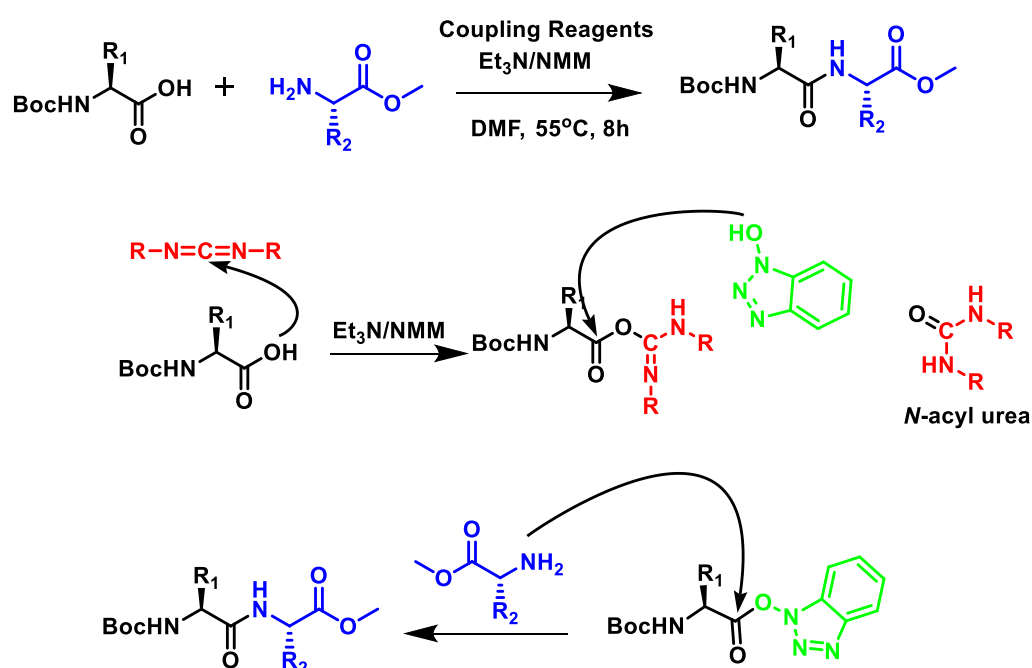


Figure 1. 2 General representation of solution phase peptide synthesis.

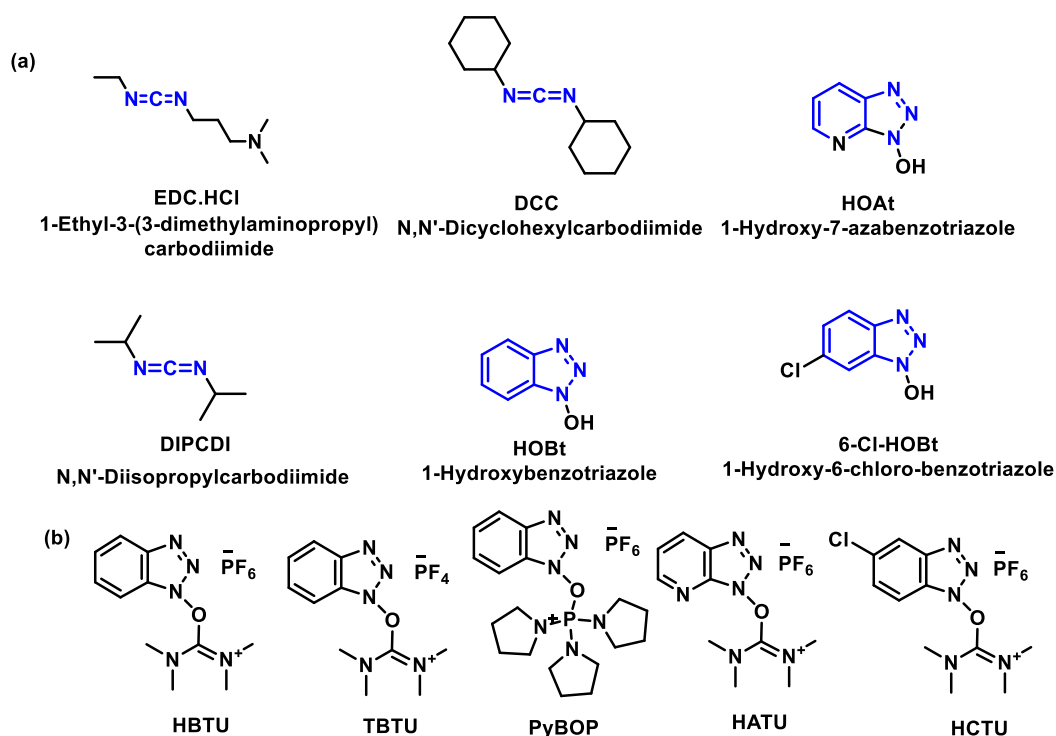


Figure 1. 3 Coupling reagents-Carbodimides and Benzotriazoles.

In solid-phase peptide synthesis, generally amino functionalized solid support resins are being used for coupling with amine-protected amino acid derivatives under similar peptide bond coupling anhydrous conditions (**Figure 1.4**). The completion of reactions is monitored by Kaiser's test (Ninhydrin test). After negative kaiser's test results, the resin is washed with anhydrous solvents to remove unreacted reagents and amino acid derivative. Then the deprotection of amino group are performed and monitored with the Kaiser's test that give positive results (Resins turn into blue colour). Then, this first amino acid linked amino functionalized resins are employed with coupling with another desired amino acids and then repeated all steps. After synthesis of target peptides, the cleavage reaction are performed with neat TFA:TIPS:H₂O that produced resin free peptides. This peptides are purified and characterized by the known analytical methods.

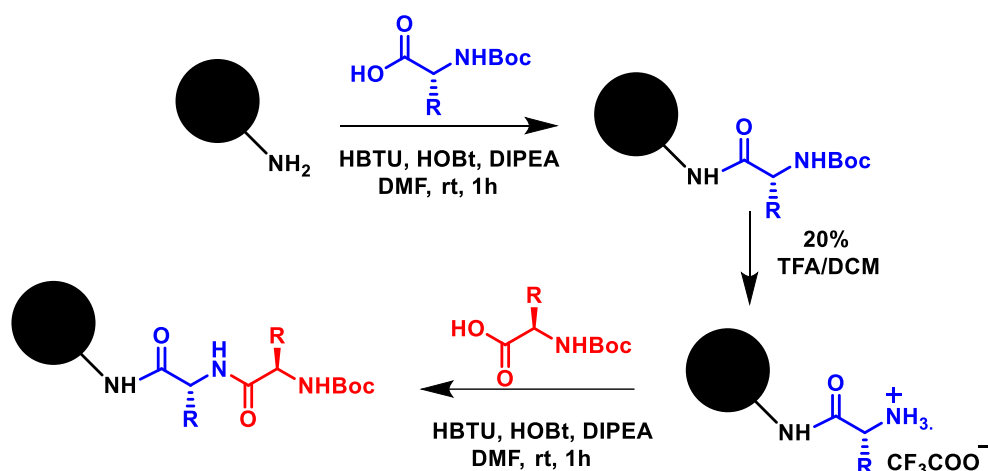


Figure 1. 4 General representation of solid phase peptide synthesis.

1.1.4 Peptides as therapeutic drugs

At the beginning of the twenty-first century, peptide drug development entered a new era. Peptide drug development has evolved, including drug discovery, drug design, synthesis, structural modification, and activity evaluation. A neurotoxic peptide called ziconotide is employed to treat extreme chronic pain.²³⁻²⁴ Some drugs currently available in the market, like Enalapril maleate and Lisinopril, are *tri*-peptides used for the treatment of hypertension and congestive heart failure. Sincalide is an *octa*-peptide used for the treatment of diagnosis of the functional state of the gallbladder and pancreas and is a stimulant of gastric secretion. Buserelin and histrelin acetates are *nona*-peptides that are gonadotropin-releasing hormone agonists. Buserelin has D-serine, whereas histrelin contains D-histidine used to treat advanced prostate cancer and central precocious puberty. Furthermore, *nona*-peptides, argipressin, lypressin, and phenylpressin are vasopressin analogues used to treat central diabetes and stomatitis. Hepatic insufficiency and wound healing are both managed with the help of the *tri*-peptide glutathione, which is made up of H-Glu, Cys, and Gly. A dipeptide of Ac-Asp-Glu-OH called spaglumag magnesium salt is used to treat allergic rhinitis and conjunctivitis. Thymopentin is a *penta*-peptide with the amino acid sequences H-Arg-Lys-Asp-Val-Tyr-OH used to treat both primary

and secondary immune systems.²⁵ Some of the presented peptide therapeutics are depicted in **Figure 1.5**.

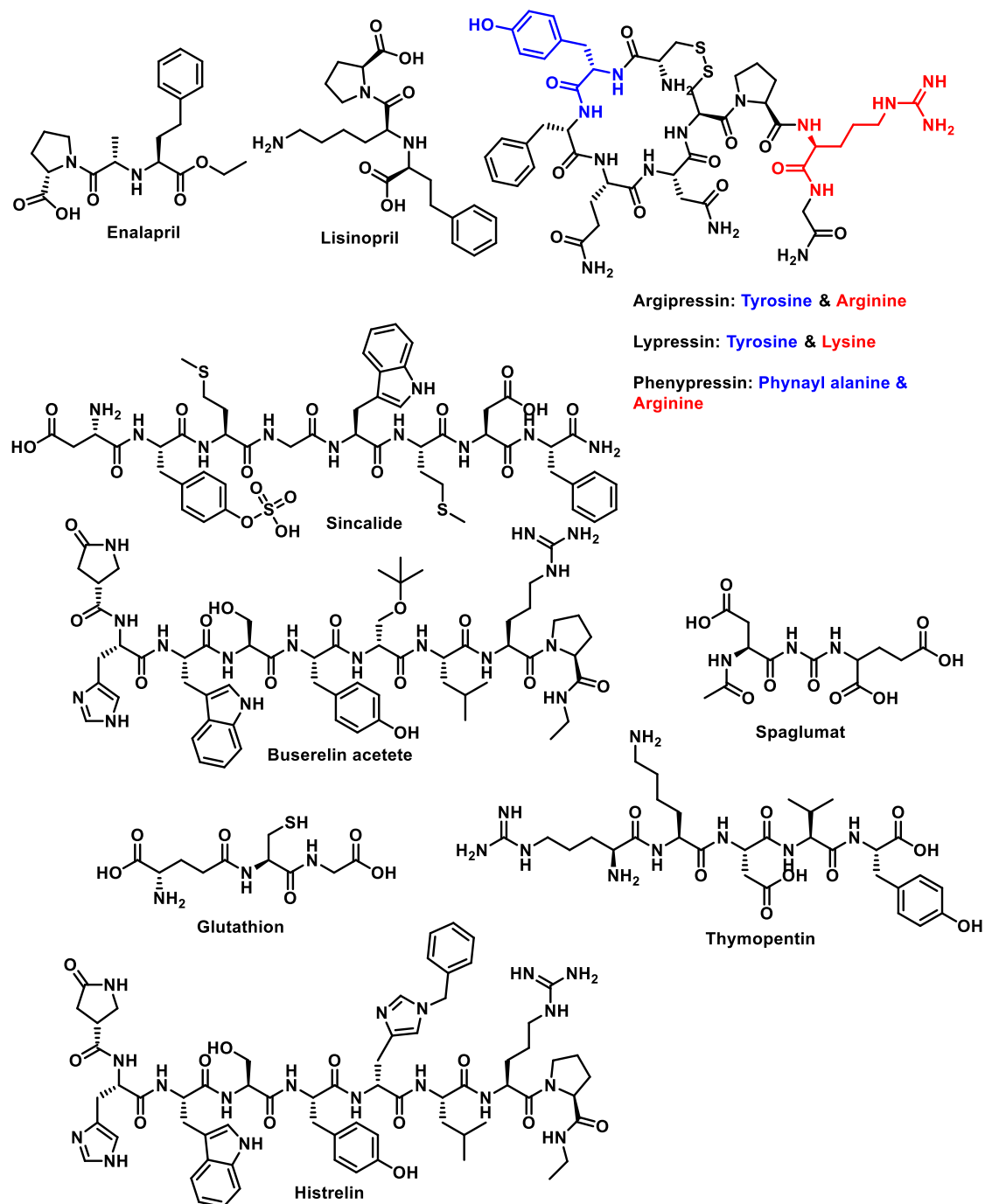


Figure 1. 5 Some of the peptide-based therapeutics.

Limitations of peptide drugs

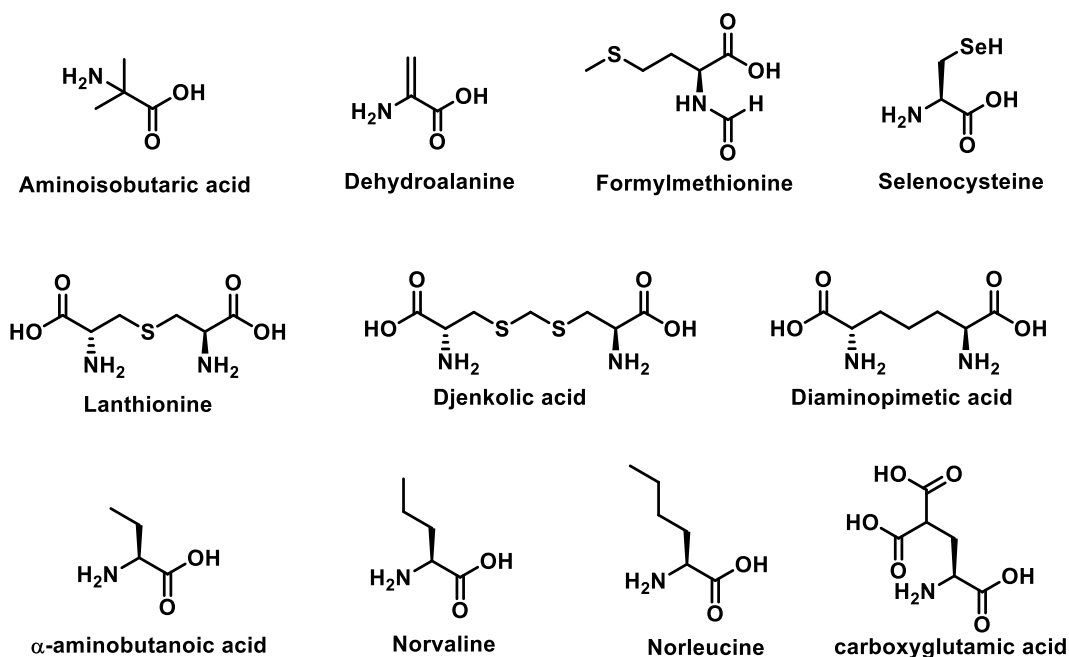
Although peptide therapeutic drugs have several benefits over small molecule therapies, they also have significant drawbacks which prevent them from being used as medicinal compounds. Numerous studies have identified that peptide has low passive membrane permeability.²⁶⁻²⁹ In addition the oral bioavailability of peptides is also hampered by a number of chemical and enzymatic barriers that occur after oral uptake. A peptide can be chemically degraded in the low pH of the stomach and enzymatically degraded by digestive enzymes.³⁰

Approaches to overcome the limitations

To overcome the limitations of peptide therapeutics, structural alterations are made to a peptide without altering the pharmacokinetic properties of the native drug.^{25,31-35} Permeability can also be raised by alterations that lock in particular conformations. For instance, α -alkylation reduces the solubility and increases permeability by rigidifying the backbone conformation.³⁶⁻³⁷ Another *N*-alkylation strategy that reduces the H-bond-donating potential and therefore increases permeability is the use of peptoid building blocks instead of peptides.³⁸ Other modification includes cyclization of the linear peptide through disulfide bonds, hydrazine bridges, and lactam formation to enhance the proteolytic stability and affinity.³⁵ Other options for modification include isosteric substitution and introducing an unnatural amino acid residues. Isosteric replacement refers to the substitution of an isosteric functional group, such as esters, thioesters, thioamides, alkenes, or fluoro-alkenes, for a specific amide functional group. Depsipeptides and thiodepsipeptides are the names of the resulting peptides when the amide link is replaced by ester and thioester, respectively. The peptides synthesized by these chemical alterations to an existing native peptide often referred to as peptidomimetics. Among all the aforementioned chemical transformations, the synthesis of unnatural amino acids as alternatives for natural amino acids attracted the scientific community in the search for new potential peptide therapeutics drugs.

1.1.5 Unnatural amino acids (UAAs) and Its Peptides

Unnatural amino acids (UAAs) are non-proteinogenic or non-canonical amino acid derivatives. UAA derivatives are synthesized by the structural modifications of native amino acids that alter their conformation and functions. In some cases, even a single incorporation of UAA into native peptides severely affects structural and functional properties.³⁹⁻⁴⁰ UAA comprising peptides increases their functional diversity in various aspects like bio-orthogonal chemistry and protein labelling, posttranslational mimetic, protein-protein interactions etc.⁴¹ In the literature, various synthetic UAAs are reported which are categorized non- α -amino acids, and side chain modified α -amino acids. Additionally, D-amino acids, C-substituted, and *N*-alkylation native amino acids are also known as UAAs (**Figure 1.6**).³⁵



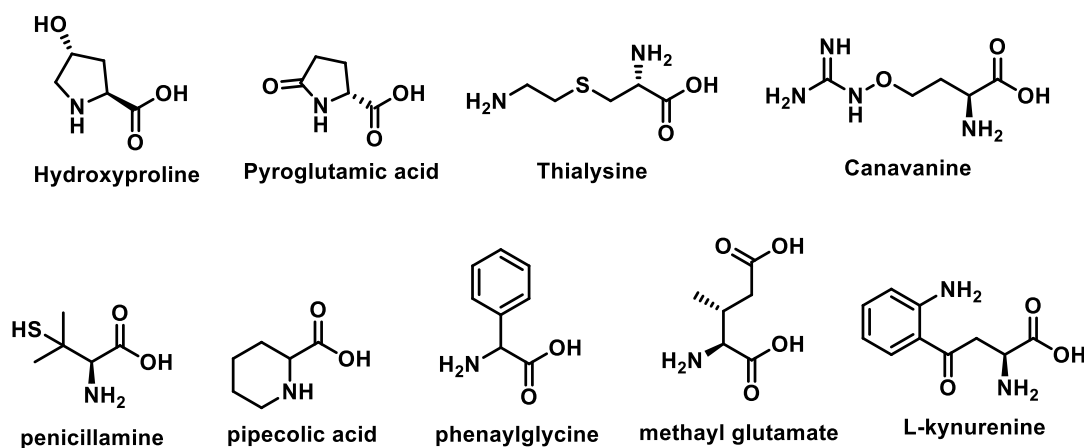


Figure 1.6 Some of the non-ribosomal amino acids present in various natural products.

Moreover, synthetic amino acids played a key role in the development of peptidomimetics and the conformational restrictions used to develop molecular scaffolds.⁴² Many of these synthetic amino acids were also used as pharmacologically effective compounds.⁴³ As a result, synthetic amino acids offer a virtually limitless variety of unique structural components for the development of novel structures and therapeutic approaches.⁴⁴

1.1.6 Unnatural aromatic amino acids containing nonbenzenoid scaffold Tropolone

Tropolone is non-benzenoid aromatic scaffolds comprising a seven-membered ring cycloheptatriene as *2-hydroxy-2,4,6-cycloheptatrien-1-one* (**Figure 1.7**).⁴⁵⁻⁴⁷ It contains conjugated carbonyl and hydroxyl functional groups at tropone aromatic ring system, which are considered as structural isomer of benzoic acid. Tropolone related derivatives are occurred in living system as troponoid natural products.⁴⁵ A few of them exhibit excellent bioactivities possessing therapeutic values such as antimicrobial and anticancer activity. Tropolone has unique photophysical properties including intramolecular charge transfer and fluorescence properties in non-polar organic solvents though its quantum yield is low.⁴⁸ Tropolone is admirable natural ligand of coordinating metals such as Be, Cu, Zn, Ni, Co, Pb, Mg, Ca, etc.

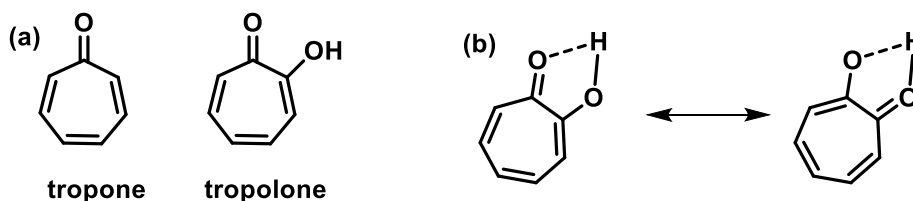
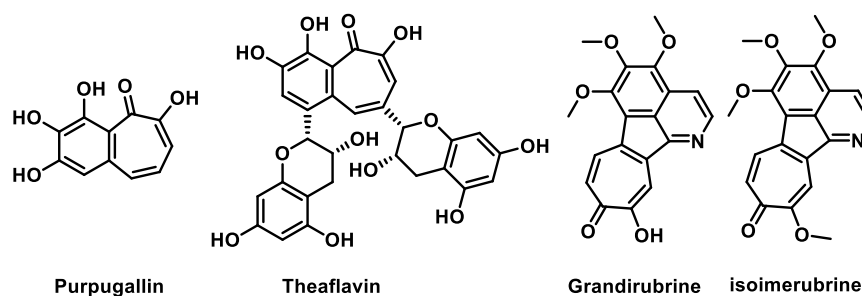


Figure 1. 7 (a) Tropolone (b) Hydrogen bonding in tropolone.

About 200 isolated and recognized natural tropolonoid molecules have been found in nature. The scientific community became attracted to tropolonoid natural products because of their interesting biological properties, including their antibacterial, antifungal, antiviral, and antitumor actions.^{46, 49-50} Tropolonoids act as selective enzyme inhibitors by chelating with metal ion co-factors (Zn, Mg, and Mn).⁴⁹ Interestingly, most of the tropolonoid natural products are the secondary metabolites of either plants or fungi, and their biosynthesis is well established.

Purpurogallin is a benzotropolone isolated from the nutgalls and oak bark used as antioxidant in nonedible oils, fuels and lubricants.⁵¹ Theaflavins were first isolated from black tea leaves, showing numerous biological activities such as antioxidant properties, anti-pathogenic, anticancer, and preventing heart diseases, hypertension, and diabetes.⁵²⁻⁵³ Grandirubrine, imerubrine, isoimerubrine, pareirubrine A and pareirubrine B are another class of tropolonoids (**Figure 1.8**).³⁹⁻⁴¹ They are generally called as tropoloisoquinolines and isolated from the Menispermaceae plants. They have also shown cytotoxic activity against selective cell-assays.



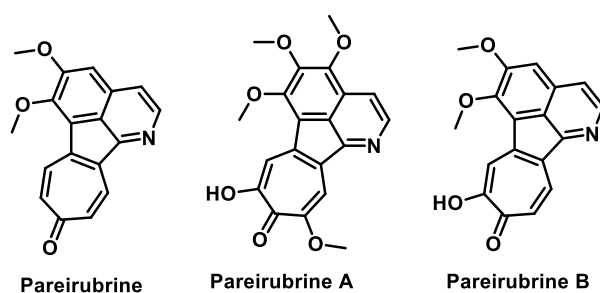


Figure 1. 8 Natural products containing tropolone.

Overall, it is important to note that most tropolonoids have a tropolone moiety, which helps to bind with the target site through noncovalent interactions to carry out specific biological functions. Sometimes, the chelation of the tropolone moiety with the appropriate enzyme metal ion co-factors results in the specific enzyme activity (inhibition or promotion) of tropolonoids. The ketone and hydroxyl functional groups of the tropolone moiety of tropolonoids, or one of them, have been extensively studied in the literature as having a vital role in the execution of specific biological activity.⁵⁴⁻⁵⁵

There is a huge demand for synthetic peptides in the development of potential peptide mimics, which may perform similarly or better than natural peptides. There has been a lot of research into aromatic amino acids and peptides bearing phenyl due to the high probability that phenyl residue will form a stable secondary structure owing to the addition of another stabilizing component in the form of π - π noncovalent interactions.³¹⁻³² A few non-benzenoid aromatic derivatives, such as tropolone, and similar compounds, are also present in nature in addition to phenyl containing benzenoid aromatic amino acids. However, the function of peptides and amino acids containing troponyl is not well understood. Additionally, tropolonyl derivatives have a carbonyl functional group, which may be important for maintaining a stable conformation in peptides.

Previously our group has designed the formation of unnatural δ -amino acid, troponyl aminoethylglycine (Tr-aeg) and its backbone derivative from tropolone and aminoethylglycine (aeg). We have also explained the troponyl motif linked covalently at aeg backbone in Tr-aeg amino acid. By using NMR techniques, we have shown the significance of the troponyl carbonyl group of Tr-aeg in hydrogen bonding with amide N-H of the peptide containing Tr-aeg residue (**Figure 1.9a**).⁵⁶ Additionally, our group has generated an array of *N*-troponylated (*di/tri*) peptides. This study illustrates how the troponyl group affects the shape and structure of *N*-troponylated short peptides using various techniques (**Figure 1.9b**).⁵⁷ Recently we have described the synthesis and structural investigations of a rationally designed chiral unnatural amino acid L-aminotroponyl alanine (ATA), which includes the tropone residue and its hybrid peptides (**Figure 1.9c**).⁵⁸ Using this unnatural amino acid, we have created a number of hybrid peptides from both the N- and C-terminal sites using various α -amino acid esters.

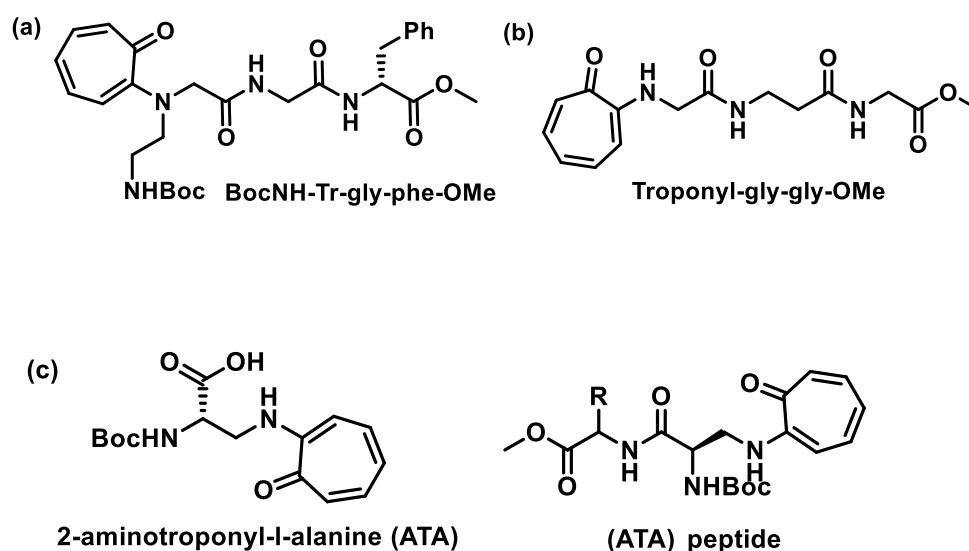


Figure 1. 9 (a) Unnatural δ -amino acid, troponyl aminoethylglycine (b) *N*-troponylated peptides (c) L-aminotroponyl alanine (ATA) and its peptide.

Animotropolone acts as a directing group for various C-H activation in the tropolone ring. The carbonyl and amino groups hold the metal catalyst and activate the C-H bond close to the carbonyl group. Using this strategy, various new psudopeptides from prolyl containing aminotroppone have been synthesized (**Figure 1.10a**).⁵⁹ Further sulphonation of amino tropolone has been synthesized by Cu-catalysed C-H activation method forming aminotroponyl sulphone (ATS). Additionally, these compounds inhibit the generation of pyocyanin, biofilm, and swarming motility, which reduce *P. aeruginosa* pathogenicity in cells. Thus potential therapeutic possibilities for the treatment of *P. aeruginosa* infections include ATS derivatives (**Figure 1.10b**).⁶⁰

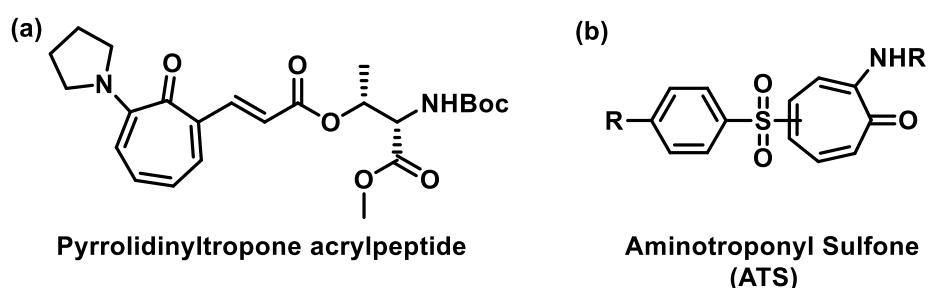


Figure 1. 10 Functionalization on (a) prolyl containing aminotroppone (b) sulphonation of amino tropolone.

1.2 Functionalization of peptides backbone

1.2.1 Introduction to C-H activation on peptides

Over the years, various C-H activation techniques have been developed, allowing a carbon-hydrogen bond change into a functional group using a metal catalyst (**Figure 1.11**).⁶¹ Usually, the metal catalyst coordinates to a directing group, forms a metal complex, and inserts into the proximal C-H bond. In contrast to traditional cross-coupling reactions, C-H activation does not require the preparation of organic halide, organic boron, or organic metal compounds, and pre-functionalization is not necessary. This makes the reaction step economical and cost-effective.

This methodology offers great features like (a) Activation of the distal Sp^2 meta or para C-H bonds and $Sp^3\beta$ or γ bonds.⁶² (b) Unique prospect for future diversification provided by remarkable compatibility with halogens and other polar functional groups.⁶³ (c) Densely functionalized molecules and natural products can be late-stage functionalized under mild reaction conditions.⁶⁴ However, there are a number of disadvantages to C-H activation method such as need to install and remove the directing group, difficult reaction conditions, residual metal impurities, and scaling-up challenges for large scale synthesis. Transient, inherent directing group or even non-directed C-H activation strategies were developed to overcome these disadvantages.⁶⁵⁻⁶⁶

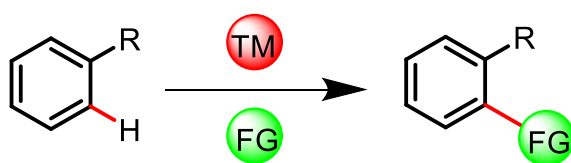


Figure 1. 11 Basic representation of C-H activation.

C-H activation of peptide offers an excellent tool for the modification of peptide-based drugs over cross-coupling of peptides which deal with several steps. Modified peptides exhibit remarkable biological function compared to natural peptides and are discovered to be more effective therapeutic agents than small molecules due to their increased target selectivity and affinity.⁶⁷⁻⁶⁸ Several peptide drugs show great biological efficacy but exhibit poor pharmacological properties and by peptide modification, the potency of such peptide can be elevated.⁶⁹⁻⁷¹ The modification of peptides takes place either through C-H functionalization of the aromatic residues or the macrocyclization of peptides.⁷²⁻⁷⁴ Wang group has synthesized Celogetin C (17-membered ring) macrocyclic peptide used for vitamin C deficiency via late-stage C-H activation in a step economical manner. Valorphin (14-membered ring) and baratin

(17-membered ring) analogues developed through late-stage C-H activation by lavilla group used to treat epilepsy and bipolar disorder (**Figure 1.12**).⁷⁵

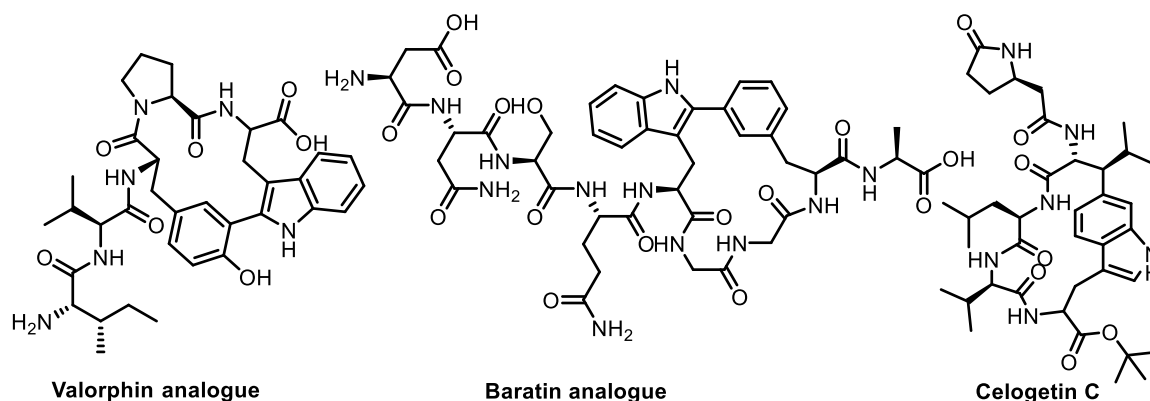


Figure 1. 12 Modified peptides drugs by C-H functionalization.

The amino acid backbone of peptide provides the regioselective modification via C-H functionalization without the assistance of any directing group. For instance, palladium (Pd) or gold (Au) catalyst shows undirected reactivity at C2 position of tryptophan (trp) in peptide. The Pd catalysis selectively activates the methyl C-H bond of alanine (Ala) in peptides and convert it to a range of functional groups using endogenous or exogenous directing groups. The iridium (Ir) catalyst allowed for the selective borylation of C-H bonds of phenylalanine (Phe) in peptides.⁷²

Pd-catalyst has proven to be the most adaptable among small molecule catalytic C-H Functionalization (CHF).⁷² Rodolfo group reported the first post-synthetic modification of peptides that is chemo selective C2 arylation of Tryptophan (Trp) in various *tri* and *tetra* peptides using Pd(OAc)₂ as a catalyst.⁷⁶ Further, J. S. Fairlamb reported the C2 arylation of Trp in peptides using aryl boronic acids, Cu(OAc)₂, and air as oxidants at 40 °C.⁷⁷ The same team altered the work and reported C2 arylation of Trp in peptides using mesityl-substituted

diaryl-iodonium reagent [MesArI]OTf and aryldiazonium salts.^{78,79} Keith James and coworkers reported Pd(II)-catalysed C2-H arylation of Trp with aryl iodides of aromatic amino acid side chains and was first method for peptide macrocyclization to be published (**Figure 1.13a**).⁸⁰

Tyrosine (Tyr) has a phenol side chain that is hydrophobic and electron-rich. Tyr side chains could occur as either phenol or phenolate due to the high acidity of OH. Tyr in proteins can undergo several posttranslational modifications owing to its nucleophilic OH group. Bedford group reported Rh(II)-catalysed C-H ortho arylation.⁸¹ Xiong group has shown Pd-catalysed C3-alkenylation of Tyr in peptides with electron-deficient terminal alkenes using an O-linked silanol as the directing group (**Figure 1.13b**).⁸² The aromatic side chain of phenylalanine is hydrophobic and electron-neutral. It frequently takes part in the binding of the hydrophobic targets. As the phenyl group is not reactive for metal complexation, C-H bond functionalization method for Phe are rare. On the other hand, by using the selectfluor reagent and photo redox catalysis, Lectka group described a radical-mediated benzylic C-H fluorination of Phe in peptides.⁸³ Yu and coworkers demonstrated the C2-H iodination, acetoxylation, and olefination of Phe ring using *N*-triflate (Tf) as a mono-dentate directing group.⁸⁴ Keith group reported an effective aryl C-H borylation of Boc-Phe-OMe using a modified Hartwig and Smith method (**Figure 1.13c**).⁸⁵

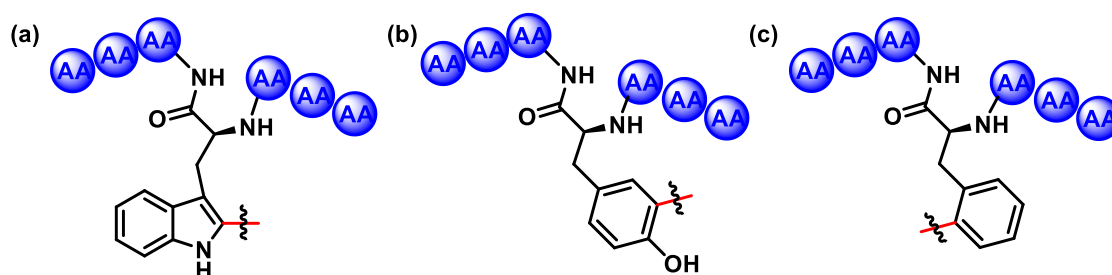


Figure 1. 13 C-H activation in peptides (a) Trp backbone (b) Tyr backbone (c) Phe backbone.

1.2.2 Late-stage C(sp²)-H functionalization on peptide

C-H activation without installation of a specific directing group producing one analogue in sufficient quantity in a complex molecule (such as a peptide) is known as late-stage functionalization (LSF). In simple words, every C-H Functionalization on a complex molecule is LSF.⁸⁶ The selective modification of proteins/peptide by late-stage biopolymer diversification is very alluring, and it offers significant potential for the direct tagging of particular structural motifs inside proteins. Developing highly chemo- and site-selective chemical transformations are required for synthetically relevant peptide modification approaches. Wang developed a peptide guided Pd(II)-catalysed C-H activation to functionalize and macrocyclize the bioactive peptidosulfonamides. The site-selective olefination of benzyisulfonamide with both activated and inactivated alkenes, as well as the cyclization of benzosulfonamide with acrylates, are excellent examples peptide guided C-H activation.⁸⁷ The same group reported late-stage peptide functionalization using Pd(II)-catalysed C(sp²)H olefination, where peptide backbone acts as the directing group. The ligation and macrocyclization of peptide aryl acetamides can be accomplished using this technique.⁸⁸ The peptide backbone facilitates Pd(II)-catalysed C(sp²)H olefination of phenylalanine residues as a highly adaptable for peptide macrocyclization. This approach works well for peptide ligation, modification, and peptide macrocycles for different sizes and sequences.⁸⁹ Ackermann group revealed the first ever metal free direct C2 arylation of synthetic indoles using diaryliodonium ions.⁹⁰ W Song and coworkers have reported site specific C(sp²)H olefination and alkynylation of phenylalanine residues in the peptides using Pd(II)-catalyst.⁹¹ Wang group have created a flexible technique for the C(sp²)H arylation by Pd(II)-catalysed modification and macrocyclization of short peptides with *N*-terminal benzamide.⁸⁸

1.2.3 Synthesis of Isoindolinone analogs via C-H activation

Isoindolinone is a chemical compound that belongs to the class of heterocyclic organic compounds. It is characterized by a bicyclic structure consisting of a six-membered benzene ring fused to a five-membered pyrrole ring. Isoindolinones have gained significant attention in the field of medicinal chemistry due to their diverse pharmacological properties and potential therapeutic applications. These compounds exhibit a wide range of biological activities, including antimicrobial, anticancer, anti-inflammatory, and antioxidant effects. The isoindolinone scaffold serves as a valuable template for the design and synthesis of novel drug candidates with improved efficacy and reduced side effects. The synthetic methods for obtaining this heterocyclic skeleton have drawn a lot of attention due to its critical function in a variety of applications. However, multistep synthesis procedures have frequently been used to generate the necessary isoindolinone derivative (Figure 1.14).⁹² Transition-metal catalysed C–C bond formation with subsequent lactamization has provided simplified access to a large variety of isoindolinone derivatives.

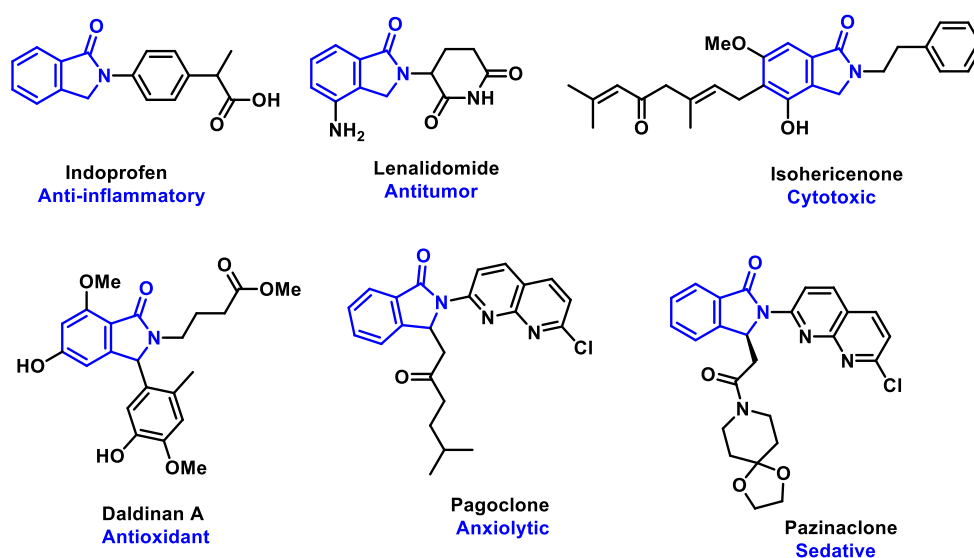


Figure 1. 14 Natural products having isoindolinone unit.

Using *N*-substituted benzamides as reactants containing either activating or directing groups is a common in most C-H functionalization strategies for isoindolinone synthesis. Li, Wrigglesworth, and Hii generated an array of isoindolinone compounds from *N*-methoxy derivatized benzamides with alkenes as reactants and Pd(II) as catalyst, using *p*-benzoquinone as oxidant and acetic acid as solvent.⁹³⁻⁹⁵ Zhu and Youn have reported the oxidative synthesis of isoindolinones using tosylated benzamides with a range of alkene reactants and either Pd(OAc)₂ and Pd(Tfa)₂ as catalysts.⁹⁶⁻⁹⁷ Dai and Yu produced 3-imino-isoindolinones from *tert*-butylisocyanides and *N*-methoxy benzamides in good yields.⁹⁸ Aldehydes have also been helpful substrates for the synthesis of isoindolinone, similar to alkenes. Zhao and Huang effectively synthesised 3-hydroxyisoindolinones from a range of aldehydes and *N*-derivatized benzamides using aqueous *tert*-butyl hydroperoxide (TBHP).⁹⁹ Li and Wang used a decarboxylation based approach for the synthesis of fused tricyclic isoindolinone derivatives and 3-hydroxy-isoindolinone that worked with a variety of substrates and could be carried out using persulfates as oxidants.¹⁰⁰⁻¹⁰¹ One of the most prominent fields of research relating to isoindolinone synthesis has been C–H functionalization reactions and these method often allow convenient routes from most commercially available compounds to isoindolinones. They are commonly prepared with super stoichiometric amounts of the oxidant or the additives. In both C–H functionalization and carbonylation based methodologies the use of temporary and sometimes permanent directing groups is a common feature.

1.2.4 Synthesis of Isoquinolone via C-H activation

The isoquinolone structure consists of a six-membered aromatic ring (benzene ring) fused to a six membered nitrogen containing ring. The nitrogen atom in the quinolone ring is in the ortho position to the fused benzene ring. These are among the most prominent structural motifs present in a variety of naturally occurring alkaloids, pharmaceuticals, and biologically active compounds.¹⁰²⁻¹⁰³ Dorianine, *N*-methylcoryaldine, and its 3,4-dihydro analogue,

hydroxyhydrastinine, are some of them (**Figure 1.15**).¹⁰⁴ Isoquinolones exhibit various biological activities and are of interest in medicinal chemistry. They serve as important building blocks in the synthesis of many pharmaceuticals, including drugs with antiviral, antibacterial, antifungal, and anticancer properties.¹⁰⁵⁻¹⁰⁶ The derivatives of 1(2H)-isoquinolones have been discovered to be antagonists of the receptors 5-HT₃, 5-HT₂, glycoprotein IIb, and tachykinin receptors.¹⁰⁴

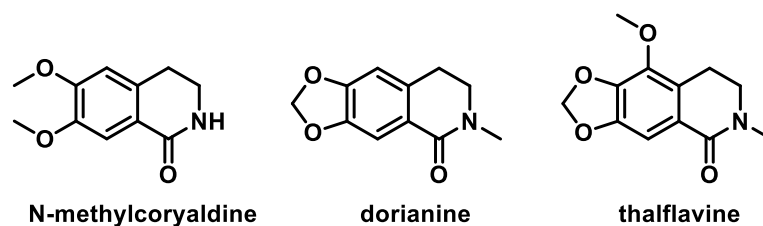


Figure 1. 15 Some natural product containing isoquinolone unit.

A powerful JNK inhibitor 3-metoxycarbonyl isoquinolone has been found to drastically reduce heart hypertrophy in rats (**Fig 1.16**).¹⁰² Further efforts were made to increase the 3-metoxycarbonyl isoquinolone's JNK inhibitory action and it was found that the JNK inhibitory action of 3-acyl-isoquinolone derivatives was more powerful than that of 3-metoxycarbonyl isoquinolone.¹⁰²

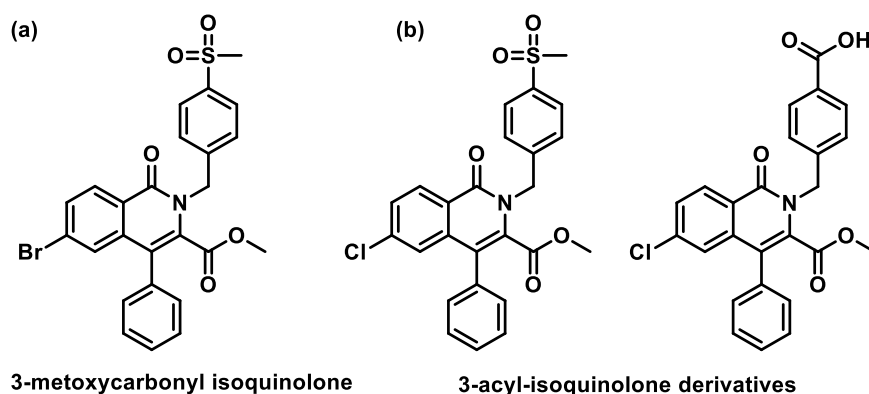


Figure 1. 16 (a) 3-metoxycarbonyl isoquinolone derivative (b) 3-acyl-isoquinolone derivatives.

There is a constant demand in synthetic chemistry and drug discovery for the development of useful and effective synthetic pathways to manufacture isoquinolones and their equivalents quickly. Conventional processes for making isoindolinone derivatives rely on organometallic compounds and metal-complex catalyst reactions.¹⁰⁴ Thus, methods for the synthesis of isoquinolone derivatives without the use of organometallic reagents were introduced. These methods are also useful and economical. For instance, the Gabriel-Coleman synthesis of isoquinolones, which entails expanding the phthalimide ring with a strong base like alkoxide.¹⁰⁷

The group of reactions that include the formation of a C-C bond are comparable to the traditional techniques for the synthesis of isoquinoline derivatives, i.e., Bischler–Napieralski and Pictet–Spengler reactions. The reaction includes condensing agent Ti_2O_3 /4-dimethylaminopyridine (DMAP) in methylene chloride followed by hydrolysis to form 1(2H)-isoquinolones derivative.¹⁰⁸⁻¹⁰⁹ Using the Simig approach lithiation of Phenethylamine the required synthesis of isoquinolone has been developed.¹¹⁰ The isoquinolone derivative can be generated by the intramolecular cyclization of o-ethynylbenzamide $\text{PdCl}_2 \cdot 2\text{CH}_3\text{CN}$ is used as a catalyst. Also, a method based on an intramolecular Heck reaction proved very helpful for this approach.¹⁰⁴

Through the decades, rapidly evolving procedures for the inter-/intramolecular annulation of unsaturated hydrocarbons with nitrogen-containing reaction partners have led to the formation of isoquinolone. The cyclocondensation of *N*-alkoxybenzamides with internal alkynes was initially investigated by Guimond and coworkers. They synthesized N-H isoquinolones by activating C-H/N-O bonds using Rh(II)-catalyst in methanol.¹¹¹ Additionally, for the construction of isoquinolone ring, functionalized arenes have been utilized as coupling partners in [4+2] annulations with alkynes. Using Rh(II)-catalyst, the annulation with *N*-iminopyridinium ylides has been performed, forming the desired product.¹¹² At room temperature, Co(II)-catalysed [4+2] annulation of *N*-chloro benzamides with alkynes in TFE

occurs with the selective breaking of C-H/N-Cl bonds in the presence of KOAc.¹¹³ A recent extension of the work has performed by Pawar and coworkers using Ru(II)-catalyst with 1,3-diyne in *N*-chlorobenzamide at room temperature to produce an isoquinolone derivative.¹¹⁴ Dandela group has reported the regioselective synthesis of isoquinolone derivatives by double annulation of *N*-methoxy benzamide with alkynes and alkenes using Ru(II) catalyst.¹¹⁵ Eycken group reported Ru-catalysed annulation of *N*-benzoyl-amino ester derivatives with diphenyl acetylene using microwave radiation.¹¹⁶ Further they have extended their work chemo selective diversification on peptide backbone on *N*-benzoyl-peptide and Lys based peptide with diphenyl acetylene followed by using Ru(II) and Rh(II)-catalyst.¹¹⁷⁻¹¹⁸ Liu and his coworkers developed isoquinolone derivative by annulating 2 phenyloxoline with iodonium ylide in the presence of Rh(II)-catalyst.¹¹⁹

1.3 References

1. Bojarska, J.; Kaczmarek, K.; Zabrocki, J.; Wolf, W., Amino Acids: Molecules of life. *Int. J. Nutr. Sci* **2019**, 4, 1035-1037.
2. Frenkel-Pinter, M.; Samanta, M.; Ashkenasy, G.; Leman, L. J., Prebiotic peptides: Molecular hubs in the origin of life. *Chemical reviews* **2020**, 120 (11), 4707-4765.
3. Muchowska, K. B.; Moran, J., Peptide synthesis at the origin of life. *Science* **2020**, 370 (6518), 767-768.
4. Schiller, M. R., The minimotif synthesis hypothesis for the origin of life. *J Transl Sci* **2016**, 2 (5), 289-296.
5. Greenwald, J.; Kwiatkowski, W.; Riek, R., Peptide Amyloids in the Origin of Life. *J Mol Biol* **2018**, 430 (20), 3735-3750.
6. Fruton, J. S., Contrasts in scientific style. Emil Fischer and Franz Hofmeister: their research groups and their theory of protein structure. *Proc Am Philos Soc* **1985**, 129 (4), 313-70.
7. Mulder, G., Sur la composition de quelques substances animales. *Bulletin des sciences physiques et naturelles en Neerlande* **1838**, 104 (1838), 9.
8. Hartley, H., Origin of the word 'protein'. *Nature* **1951**, 168 (4267), 244.

9. Vauquelin, L.-N.; Robiquet, P. J., The discovery of a new plant principle in *Asparagus sativus*. *Ann Chim* **1806**, 57 (88-93), 14.
10. Anfinsen, C. B., The formation and stabilization of protein structure. *Biochemical Journal* **1972**, 128 (4), 737.
11. Vickery, H. B.; Schmidt, C. L., The History of the Discovery of the Amino Acids. *Chemical reviews* **1931**, 9 (2), 169-318.
12. Sachdeva, S., Peptides as 'drugs': the journey so far. *International journal of peptide research and therapeutics* **2017**, 23 (1), 49-60.
13. Chandrudu, S.; Simerska, P.; Toth, I., Chemical methods for peptide and protein production. *Molecules* **2013**, 18 (4), 4373-4388.
14. Grant, G. A., *Synthetic peptides: a user's guide*. Oxford University Press on Demand: 2002.
15. Kimball, S. R.; Jefferson, L. S., New functions for amino acids: effects on gene transcription and translation. *The American journal of clinical nutrition* **2006**, 83 (2), 500S-507S.
16. Hellwinkel, D., *Systematic Nomenclature of Organic Chemistry*. Springer: 2001.
17. Bonora, E.; Orioli, S.; Coscelli, C.; Buzzelli, G.; Gentilini, P.; Butturini, U., Possible roles of insulin, glucagon, growth hormone and free fatty acids in the pathogenesis of insulin resistance of subjects with chronic liver diseases. *Acta diabetologia latina* **1984**, 21, 241-250.
18. Akram, M.; Asif, H.; Uzair, M.; Akhtar, N.; Madni, A.; Shah, S. A.; Hasan, Z. U.; Ullah, A., Amino acids: A review article. *Journal of Medicinal Plants Research* **2011**, 5 (17), 3997-4000.
19. Walsh, C. T.; O'Brien, R. V.; Khosla, C., Nonproteinogenic amino acid building blocks for nonribosomal peptide and hybrid polyketide scaffolds. *Angewandte Chemie International Edition* **2013**, 52 (28), 7098-7124.
20. Albericio, F.; Kruger, H. G., Therapeutic peptides. *Future medicinal chemistry* **2012**, 4 (12), 1527-1531.
21. Nixon, A. E., *Therapeutic peptides*. Springer: 2014.
22. Lubell, W. D., Peptide chemistry. 2012; Vol. 14, pp 4297-4302.
23. Bourinet, E.; Zamponi, G. W., Block of voltage-gated calcium channels by peptide toxins. *Neuropharmacology* **2017**, 127, 109-115.
24. Deer, T. R.; Pope, J. E.; Hanes, M. C.; McDowell, G. C., Intrathecal therapy for chronic pain: a review of morphine and ziconotide as firstline options. *Pain Medicine* **2019**, 20 (4), 784-798.

25. Vlieghe, P.; Lisowski, V., J. Martinez i M. Khrestchatisky. *Drug Discovery Today* **2010**, *15*, 40-56.
26. Fouche, M.; Schäfer, M.; Berghausen, J.; Desrayaud, S.; Blatter, M.; Piéchon, P.; Dix, I.; Martin Garcia, A.; Roth, H. J., Design and development of a cyclic decapeptide scaffold with suitable properties for bioavailability and oral exposure. *ChemMedChem* **2016**, *11* (10), 1048-1059.
27. Hill, T. A.; Lohman, R.-J.; Hoang, H. N.; Nielsen, D. S.; Scully, C. C.; Kok, W. M.; Liu, L.; Lucke, A. J.; Stoermer, M. J.; Schroeder, C. I., Cyclic penta- and hexaleucine peptides without N-methylation are orally absorbed. *ACS medicinal chemistry letters* **2014**, *5* (10), 1148-1151.
28. White, T. R.; Renzelman, C. M.; Rand, A. C.; Rezai, T.; McEwen, C. M.; Gelev, V. M.; Turner, R. A.; Linington, R. G.; Leung, S. S.; Kalgutkar, A. S., On-resin N-methylation of cyclic peptides for discovery of orally bioavailable scaffolds. *Nature chemical biology* **2011**, *7* (11), 810-817.
29. Rezai, T.; Yu, B.; Millhauser, G. L.; Jacobson, M. P.; Lokey, R. S., Testing the conformational hypothesis of passive membrane permeability using synthetic cyclic peptide diastereomers. *Journal of the American Chemical Society* **2006**, *128* (8), 2510-2511.
30. Yin, N.; Brimble, M. A.; Harris, P. W.; Wen, J., Enhancing the oral bioavailability of peptide drugs by using chemical modification and other approaches. *Med. Chem* **2014**, *4* (12), 763-769.
31. Seebach, D.; Gardiner, J., β -Peptidic peptidomimetics. *Accounts of chemical research* **2008**, *41* (10), 1366-1375.
32. Horne, W. S.; Gellman, S. H., Foldamers with heterogeneous backbones. *Accounts of chemical research* **2008**, *41* (10), 1399-1408.
33. Lubell, W. D., *Peptidomimetics I*. Springer: 2017; Vol. 48.
34. Pelay-Gimeno, M.; Glas, A.; Koch, O.; Grossmann, T. N., Structure-based design of inhibitors of protein-protein interactions: mimicking peptide binding epitopes. *Angewandte Chemie International Edition* **2015**, *54* (31), 8896-8927.
35. Avan, I.; Hall, C. D.; Katritzky, A. R., Peptidomimetics via modifications of amino acids and peptide bonds. *Chemical Society Reviews* **2014**, *43* (10), 3575-3594.
36. Kessler, H., Peptoids a new approach to the development of pharmaceuticals. *Angewandte Chemie International Edition in English* **1993**, *32* (4), 543-544.
37. Witek, J.; Wang, S.; Schroeder, B.; Lingwood, R.; Dounas, A.; Roth, H.-J. r.; Fouché, M.; Blatter, M.; Lemke, O.; Keller, B., Rationalization of the membrane permeability differences in a series of analogue cyclic decapeptides. *Journal of chemical information and modeling* **2018**, *59* (1), 294-308.

38. Wu, H.; Mousseau, G.; Mediouni, S.; Valente, S. T.; Kodadek, T., Cell-Permeable Peptides Containing Cycloalanine Residues. *Angewandte Chemie* **2016**, *128* (41), 12827-12832.
39. Budisa, N.; Völler, J.; Koksche, B.; Acevedo-Rocha, C.; Kubyskhin, V.; Agostini, F., Xenobiology meets enzymology: exploring the potential of unnatural building blocks in biocatalysis. *Angew. Chem. Int. Ed* **2017**, *56*, 9680-9703.
40. Narancic, T.; Almahboub, S. A.; O'Connor, K. E., Unnatural amino acids: production and biotechnological potential. *World Journal of Microbiology and Biotechnology* **2019**, *35*, 1-11.
41. Davis, L.; Chin, J. W., Designer proteins: applications of genetic code expansion in cell biology. *Nature reviews Molecular cell biology* **2012**, *13* (3), 168-182.
42. Venkatraman, J.; Shankaramma, S. C.; Balaram, P., Design of folded peptides. *Chemical reviews* **2001**, *101* (10), 3131-3152.
43. Saladino, R.; Botta, G.; Crucianelli, M., Advances in the synthesis of bioactive unnatural amino acids and peptides. *Mini reviews in medicinal chemistry* **2012**, *12* (4), 277-300.
44. Pless, S. A.; Ahern, C. A., Unnatural amino acids as probes of ligand-receptor interactions and their conformational consequences. *Annual review of pharmacology and toxicology* **2013**, *53*, 211-229.
45. Pauson, P. L., Tropones and tropolones. *Chemical Reviews* **1955**, *55* (1), 9-136.
46. Liu, N.; Song, W.; Schienebeck, C. M.; Zhang, M.; Tang, W., Synthesis of naturally occurring tropones and tropolones. *Tetrahedron* **2014**, *70* (49), 9281.
47. Nozoe, T., Substitution products of tropolone and allied compounds. *Nature* **1951**, *167*, 1055-1057.
48. Takagi, K.; Saiki, K.; Mori, K.; Yuki, Y.; Suzuki, M., Synthesis of tropolone-containing conjugated polymers and their optical properties. *Polymer journal* **2007**, *39* (8), 813-821.
49. Bentley, R., A fresh look at natural tropolonoids. *Natural product reports* **2008**, *25* (1), 118-138.
50. Zhao, J., Plant troponoids: chemistry, biological activity, and biosynthesis. *Current medicinal chemistry* **2007**, *14* (24), 2597-2621.
51. Prasad, K.; Kapoor, R.; Lee, P., Purpurogallin, a scavenger of polymorphonuclear leukocyte-derived oxyradicals. *Molecular and cellular biochemistry* **1994**, *139*, 27-32.
52. Mukamal, K. J.; Maclure, M.; Muller, J. E.; Sherwood, J. B.; Mittleman, M. A., Tea consumption and mortality after acute myocardial infarction. *Circulation* **2002**, *105* (21), 2476-2481.

53. MacKenzie, T.; Comi, R.; Sluss, P.; Keisari, R.; Manwar, S.; Kim, J.; Larson, R.; Baron, J. A., Metabolic and hormonal effects of caffeine: randomized, double-blind, placebo-controlled crossover trial. *Metabolism* **2007**, *56* (12), 1694-1698.
54. Harmon, K. M.; Davis, S., Carbonium Ion Salts. VI. Tropenium Hydrogen Dihalides and an Improved Route to Tropenium Chloride. *Journal of the American Chemical Society* **1962**, *84* (22), 4359-4360.
55. Barton, D.; Magnus, P.; Smith, G.; Zurr, D., Oxidation of ketone acetals by hydride transfer. *Journal of the Chemical Society D: Chemical Communications* **1971**, (15), 861-863.
56. Balachandra, C.; Sharma, N. K., Synthesis and conformational analysis of new troponyl aromatic amino acid. *Tetrahedron* **2014**, *70* (41), 7464-7469.
57. Palai, B. B.; Sharma, N. K., N-Arylated peptide: troponyl residue influences the structure and conformation of N-troponylated-(di/tri)-peptides. *CrystEngComm* **2021**, *23* (1), 131-139.
58. Gupta, M. K.; Sharma, N. K., A new amino acid, hybrid peptides and BODIPY analogs: synthesis and evaluation of 2-aminotroponyl-L-alanine (ATA) derivatives. *Organic & Biomolecular Chemistry* **2022**, *20* (47), 9397-9407.
59. Jena, C. K.; Sharma, N. K., Novel cinnamic acid analogues: synthesis of aminotroponyl acrylates by Pd (ii)-catalysed C (sp²)-H olefination. *Chemical Communications* **2022**, *58* (58), 8077-8080.
60. Meher, S.; Kumari, S.; Dixit, M.; Sharma, N. K., Cu-Catalyzed Synthesis of Alkylaminotroponyl Sulfones as Pseudomonas Aeruginosa Quorum Sensing Inhibitors Targeting lasI/R QS Circuitry. *Chemistry—An Asian Journal* **2022**, *17* (23), e202200866.
61. Chen, X.; Engle, K. M.; Wang, D. H.; Yu, J. Q., Palladium (II)-catalyzed C–H activation/C–C cross-coupling reactions: versatility and practicality. *Angewandte Chemie International Edition* **2009**, *48* (28), 5094-5115.
62. Ghosh, M.; De Sarkar, S., meta- and para-Selective C–H Functionalization using Transient Mediators and Noncovalent Templates. *Asian Journal of Organic Chemistry* **2018**, *7* (7), 1236-1255.
63. Yang, J., Transition metal catalyzed meta-C–H functionalization of aromatic compounds. *Organic & Biomolecular Chemistry* **2015**, *13* (7), 1930-1941.
64. Franzoni, I.; Mazet, C., Recent trends in Pd-catalyzed remote functionalization of carbonyl compounds. *Organic & biomolecular chemistry* **2014**, *12* (2), 233-241.
65. Higham, J. I.; Bull, J. A., Transient imine directing groups for the C–H functionalisation of aldehydes, ketones and amines: an update 2018–2020. *Organic & Biomolecular Chemistry* **2020**, *18* (37), 7291-7315.
66. Rani, G.; Luxami, V.; Paul, K., Traceless directing groups: a novel strategy in regiodivergent C–H functionalization. *Chemical Communications* **2020**, *56* (83), 12479-12521.

67. Li, W.; Separovic, F.; O'Brien-Simpson, N. M.; Wade, J. D., Chemically modified and conjugated antimicrobial peptides against superbugs. *Chemical Society Reviews* **2021**, *50* (8), 4932-4973.
68. Lee, A., Harris JL Khanna KK Hong J.-H. *Int. J. Mol. Sci* **2019**, *20*, 2383.
69. Bird, G. H.; Madani, N.; Perry, A. F.; Princiotto, A. M.; Supko, J. G.; He, X.; Gavathiotis, E.; Sodroski, J. G.; Walensky, L. D., Hydrocarbon double-stapling remedies the proteolytic instability of a lengthy peptide therapeutic. *Proceedings of the National Academy of Sciences* **2010**, *107* (32), 14093-14098.
70. Driggers, E. M.; Hale, S. P.; Lee, J.; Terrett, N. K., The exploration of macrocycles for drug discovery—an underexploited structural class. *Nature Reviews Drug Discovery* **2008**, *7* (7), 608-624.
71. Szewczuk, Z.; Gibbs, B. F.; Yue, S. Y.; Purisima, E. O.; Konishi, Y., Conformationally restricted thrombin inhibitors resistant to proteolytic digestion. *Biochemistry* **1992**, *31* (38), 9132-9140.
72. Tong, H.-R.; Li, B.; Li, G.; He, G.; Chen, G., Postassembly modifications of peptides via metal-catalyzed C–H functionalization. *CCS Chemistry* **2021**, *3* (3), 1797-1820.
73. Lu, X.; He, S.-J.; Cheng, W.-M.; Shi, J., Transition-metal-catalyzed CH functionalization for late-stage modification of peptides and proteins. *Chinese Chemical Letters* **2018**, *29* (7), 1001-1008.
74. Sengupta, S.; Mehta, G., Late stage modification of peptides via CH activation reactions. *Tetrahedron Letters* **2017**, *58* (14), 1357-1372.
75. Tang, J.; He, Y.; Chen, H.; Sheng, W.; Wang, H., Synthesis of bioactive and stabilized cyclic peptides by macrocyclization using C (sp³)–H activation. *Chemical Science* **2017**, *8* (6), 4565-4570.
76. Ruiz-Rodríguez, J.; Albericio, F.; Lavilla, R., Postsynthetic modification of peptides: chemoselective C-arylation of tryptophan residues. *Chemistry—A European Journal* **2010**, *16* (4), 1124-1127.
77. Williams, T. J.; Reay, A. J.; Whitwood, A. C.; Fairlamb, I. J., A mild and selective Pd-mediated methodology for the synthesis of highly fluorescent 2-arylated tryptophans and tryptophan-containing peptides: a catalytic role for Pd 0 nanoparticles? *Chemical Communications* **2014**, *50* (23), 3052-3054.
78. Reay, A. J.; Williams, T. J.; Fairlamb, I. J., Unified mild reaction conditions for C2-selective Pd-catalysed tryptophan arylation, including tryptophan-containing peptides. *Organic & biomolecular chemistry* **2015**, *13* (30), 8298-8309.
79. Reay, A. J.; Hammarback, L. A.; Bray, J. T.; Sheridan, T.; Turnbull, D.; Whitwood, A. C.; Fairlamb, I. J., Mild and regioselective Pd (OAc)₂-catalyzed C–H arylation of tryptophans by [ArN₂] X, promoted by tosic acid. *ACS catalysis* **2017**, *7* (8), 5174-5179.

80. Dong, H.; Limberakis, C.; Liras, S.; Price, D.; James, K., Peptidic macrocyclization via palladium-catalyzed chemoselective indole C-2 arylation. *Chemical Communications* **2012**, 48 (95), 11644-11646.
81. Bedford, R. B.; Haddow, M. F.; Webster, R. L.; Mitchell, C. J., The catalytic ortho-arylation of tyrosine. *Organic & Biomolecular Chemistry* **2009**, 7 (15), 3119-3127.
82. Hu, Q.-L.; Hou, K.-Q.; Li, J.; Ge, Y.; Song, Z.-D.; Chan, A. S.; Xiong, X.-F., Silanol: a bifunctional group for peptide synthesis and late-stage functionalization. *Chemical Science* **2020**, 11 (23), 6070-6074.
83. Bume, D. D.; Pitts, C. R.; Jokhai, R. T.; Lectka, T., Direct, visible light-sensitized benzylic CH fluorination of peptides using dibenzosuberone: selectivity for phenylalanine-like residues. *Tetrahedron* **2016**, 72 (40), 6031-6036.
84. Li, J. J.; Mei, T. S.; Yu, J. Q., Synthesis of Indolines and Tetrahydroisoquinolines from Arylethylamines by PdII-Catalyzed C-H Activation Reactions. *Angewandte Chemie* **2008**, 120 (34), 6552-6555.
85. Meyer, F.-M.; Liras, S.; Guzman-Perez, A.; Perreault, C.; Bian, J.; James, K., Functionalization of Aromatic Amino Acids via Direct C–H Activation: Generation of Versatile Building Blocks for Accessing Novel Peptide Space. *Organic Letters* **2010**, 12 (17), 3870-3873.
86. Guillemard, L.; Kaplaneris, N.; Ackermann, L.; Johansson, M. J., Late-stage C–H functionalization offers new opportunities in drug discovery. *Nature Reviews Chemistry* **2021**, 5 (8), 522-545.
87. Tang, J.; Chen, H.; He, Y.; Sheng, W.; Bai, Q.; Wang, H., Peptide-guided functionalization and macrocyclization of bioactive peptidosulfonamides by Pd(II)-catalyzed late-stage C–H activation. *Nature Communications* **2018**, 9 (1), 3383.
88. Tan, J.; Wu, J.; Liu, S.; Yao, H.; Wang, H., Macrocyclization of peptidoarylacetamides with self-assembly properties through late-stage palladium-catalyzed C (sp²)-H olefination. *Science Advances* **2019**, 5 (3), eaaw0323.
89. Bai, Z.; Cai, C.; Yu, Z.; Wang, H., Backbone-Enabled Directional Peptide Macrocyclization through Late-Stage Palladium-Catalyzed δ -C (sp²)-H Olefination. *Angewandte Chemie* **2018**, 130 (42), 14108-14112.
90. Zhu, Y.; Bauer, M.; Ploog, J.; Ackermann, L., Late-Stage Diversification of Peptides by Metal-Free C-H Arylation. *Chemistry—A European Journal* **2014**, 20 (41), 13099-13102.
91. Zheng, Y.; Song, W., Pd-Catalyzed Site-Selective C (sp²)-H Olefination and Alkynylation of Phenylalanine Residues in Peptides. *Organic letters* **2019**, 21 (9), 3257-3260.
92. Savela, R.; Méndez-Gálvez, C., Isoindolinone Synthesis via One-Pot Type Transition Metal Catalyzed C-C Bond Forming Reactions. *Chemistry (Weinheim an der Bergstrasse, Germany)* **2021**, 27 (17), 5344-5378.

93. Li, D.-D.; Yuan, T.-T.; Wang, G.-W., Synthesis of isoindolinones via palladium-catalyzed C–H activation of N-methoxybenzamides. *Chemical Communications* **2011**, 47 (48), 12789-12791.
94. Wigglesworth, J. W.; Cox, B.; Lloyd-Jones, G. C.; Booker-Milburn, K. I., New heteroannulation reactions of N-alkoxybenzamides by Pd (II) catalyzed C–H activation. *Organic letters* **2011**, 13 (19), 5326-5329.
95. Xia, C.; White, A. J.; Hii, K. K. M., Synthesis of isoindolinones by Pd-catalyzed coupling between N-methoxybenzamide and styrene derivatives. *The Journal of Organic Chemistry* **2016**, 81 (17), 7931-7938.
96. Zhu, C.; Falck, J., N-acylsulfonamide assisted tandem C–H olefination/annulation: synthesis of isoindolinones. *Organic letters* **2011**, 13 (5), 1214-1217.
97. Youn, S. W.; Ko, T. Y.; Kim, Y. H.; Kim, Y. A., Pd (II)/Cu (II)-Catalyzed regio-and stereoselective synthesis of (E)-3-arylmethyleneisoindolin-1-ones using air as the terminal oxidant. *Organic letters* **2018**, 20 (24), 7869-7874.
98. Liu, Y.-J.; Xu, H.; Kong, W.-J.; Shang, M.; Dai, H.-X.; Yu, J.-Q., Overcoming the limitations of directed C–H functionalizations of heterocycles. *Nature* **2014**, 515 (7527), 389-393.
99. Yu, Q.; Zhang, N.; Huang, J.; Lu, S.; Zhu, Y.; Yu, X.; Zhao, K., Efficient Synthesis of Hydroxyl Isoindolones by a Pd-Mediated C-H Activation/Annulation Reaction. *Chemistry–A European Journal* **2013**, 19 (34), 11184-11188.
100. Menglei, Y.; Yu, S.; Hui, Y., Room-temperature one-pot palladium-catalyzed synthesis of 3-hydroxyisoindolin-1-ones from phenylglyoxylic acids. *Heterocycles: an international journal for reviews and communications in heterocyclic chemistry* **2016**, 92 (3), 560-572.
101. Jing, K.; Wang, X.-N.; Wang, G.-W., Diastereoselective Synthesis of Oxazoloisoindolinones via Cascade Pd-Catalyzed ortho-Acylation of N-Benzoyl α -Amino Acid Derivatives and Subsequent Double Intramolecular Cyclizations. *The Journal of Organic Chemistry* **2018**, 84 (1), 161-172.
102. Asano, Y.; Kitamura, S.; Ohra, T.; Itoh, F.; Kajino, M.; Tamura, T.; Kaneko, M.; Ikeda, S.; Igata, H.; Kawamoto, T., Discovery, synthesis and biological evaluation of isoquinolones as novel and highly selective JNK inhibitors (2). *Bioorganic & medicinal chemistry* **2008**, 16 (8), 4699-4714.
103. Cushman, M., Design and synthesis of indenoisoquinolines targeting topoisomerase I and other biological macromolecules for cancer chemotherapy. *Journal of Medicinal Chemistry* **2021**, 64 (24), 17572-17600.
104. Glushkov, V.; Shklyayev, Y. V., Synthesis of 1 (2H)-Isoquinolones. *Chemistry of Heterocyclic Compounds* **2001**, 37, 663-687.

105. Sheng, C.; Miao, Z.; Zhang, W., New strategies in the discovery of novel non-camptothecin topoisomerase I inhibitors. *Current medicinal chemistry* **2011**, *18* (28), 4389-4409.
106. Wang, K.-B.; Elsayed, M. S.; Wu, G.; Deng, N.; Cushman, M.; Yang, D., Indenoisoquinoline topoisomerase inhibitors strongly bind and stabilize the MYC promoter G-quadruplex and downregulate MYC. *Journal of the American Chemical Society* **2019**, *141* (28), 11059-11070.
107. Gabriel, S.; Colman, J., Ueber 4-Oxyisocarbostyryl. *Berichte der deutschen chemischen Gesellschaft* **1900**, *33* (1), 996-1000.
108. Gonzalez, D.; Martinot, T.; Hudlicky, T., A short chemoenzymatic synthesis of (+)-narciclasine. *Tetrahedron letters* **1999**, *40* (16), 3077-3080.
109. Akgün, H.; Hudlicky, T., Total syntheses of ert-conduramine A and ent-7-deoxypancratistatin. *Tetrahedron letters* **1999**, *40* (16), 3081-3084.
110. Simig, G., A new route to isoindole intermediates. *Synlett* **1990**, *1990* (07), 425-426.
111. Guimond, N.; Gouliaras, C.; Fagnou, K., Rhodium (III)-catalyzed isoquinolone synthesis: the N–O bond as a handle for C–N bond formation and catalyst turnover. *Journal of the American Chemical Society* **2010**, *132* (20), 6908-6909.
112. Zhu, H.; Zhuang, R.; Zheng, W.; Fu, L.; Zhao, Y.; Tu, L.; Chai, Y.; Zeng, L.; Zhang, C.; Zhang, J., Synthesis of isoquinolone via rhodium (III)-catalyzed CH activation with 1, 4, 2-dioxazol-5-ones as oxidizing directing group. *Tetrahedron* **2019**, *75* (23), 3108-3112.
113. Yu, X.; Chen, K.; Guo, S.; Shi, P.; Song, C.; Zhu, J., Direct access to cobaltacycles via C–H activation: N-Chloroamide-enabled room-temperature synthesis of heterocycles. *Organic letters* **2017**, *19* (19), 5348-5351.
114. Ghosh, A.; Sapkal, G. T.; Pawar, A. B., Ru(II)-Catalyzed Regioselective Redox-Neutral [4 + 2] Annulation of N-Chlorobenzamides with 1,3-Diynes at Room Temperature for the Synthesis of Isoquinolones. *The Journal of Organic Chemistry* **2023**, *88* (7), 4704-4719.
115. Naikawadi, P. K.; Mucherla, L.; Dandela, R.; Sambari, M.; Kumar, K. S., One-Pot Two-Step Double Annulation of N-Methoxybenzamides with Alkynes and Alkenes: Regioselective Construction of Isoindolo [2, 1-b] isoquinolin-5 (7H)-ones. *Advanced Synthesis & Catalysis* **2021**, *363* (15), 3796-3802.
116. Sharma, N.; Bahadur, V.; Sharma, U. K.; Saha, D.; Li, Z.; Kumar, Y.; Colaers, J.; Singh, B. K.; Van der Eycken, E. V., Microwave-Assisted Ruthenium-Catalysed ortho-C–H Functionalization of N-Benzoyl α -Amino Ester Derivatives. *Advanced Synthesis & Catalysis* **2018**, *360* (16), 3083-3089.
117. Song, L.; Ojeda-Carralero, G. M.; Parmar, D.; González-Martínez, D. A.; Van Meervelt, L.; Van der Eycken, J.; Goeman, J.; Rivera, D. G.; Van der Eycken, E. V., Chemoselective Peptide Backbone Diversification and Bioorthogonal Ligation by Ruthenium-Catalyzed C–H Activation/Annulation. *Advanced Synthesis & Catalysis* **2021**, *363* (13), 3297-3304.

118. Song, L.; Lv, Z.; Li, Y.; Zhang, K.; Van der Eycken, E. V.; Cai, L., Construction of Peptide–Isoquinolone Conjugates via Rh (III)-Catalyzed C–H Activation/Annulation. *Organic Letters* **2023**.
119. Yang, Z.; Liu, J.; Li, Y.; Ding, J.; Zheng, L.; Liu, Z.-Q., Three-Component Synthesis of Isoquinolone Derivatives via Rh (III)-Catalyzed C–H Activation and Tandem Annulation. *The Journal of Organic Chemistry* **2022**, 87 (21), 14809-14818.

CHAPTER-2

2-Aminotroponyl-L-alanine (ATA) derivatives are synthesised and evaluated as a novel amino acid, hybrid peptides, and BODIPY analogues

TABLE OF CONTENTS

Chapter 2	37
2.1 Introduction.....	37
2.2.1 Hypothesis and objective	39
2.2 Result and discussion	39
2.2.1 Synthesis of Aminotroponyl Alanine (ATA).....	39
2.2.2 Synthesis of dioxoimidazolidine derivative.....	40
2.2.3 Synthesis of ATA hybrid peptides	43
2.2.4 Synthesis of ATA-BODIPY analogues	45
2.2.5 Conformational analysis of ATA peptides	45
2.2.6 DMSO D ₆ Titration study.....	47
2.2.7 Circular Dichroism study	48
2.2.8 Theoretical study	50
2.2.9 Fluorescence study	51
2.2.10 HOMO & LUMO Computational study.....	52
2.2.11 Cell culture study	53
2.3 Conclusion	54
2.4 Experimental Section.....	54
2.4.1 Materials and instrumentation	54
2.4.2 General procedure for peptide coupling	55
2.4.3 Chemical shift values of NMR	55
2.5 References.....	64

Chapter 2

2.1 Introduction

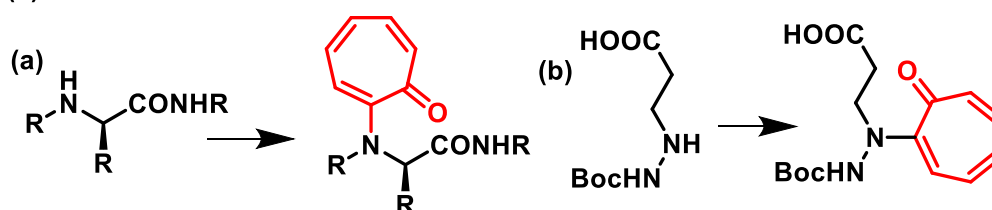
Native aromatic amino acids like phenylalanine (Phe), tyrosine (Tyr), tryptophan (Trp), and histidine (His) serve crucial roles in the structural and functional organisation of peptides and proteins. These amino acids are produced from benzenoid scaffolds.¹ Different enzymes have the functional group-containing aromatic amino acids Tyr, His, and Trp in their active sites, and these amino acids are essential to the catalytic activity of those enzymes.² Additionally, Trp is a fluorescent amino acid. Typically, native amino acids undergo extensive structural alterations that drastically change both their structure and activities. As noted in the literature, structurally altered aromatic amino acid analogues have shown promise as constituents of a variety of peptidomimetics and foldamers.³⁻⁵ Svendsen, for instance, has shown how bulky bovine lactoferricin peptides with aromatic amino acids increase antibacterial action.⁶ Huc has rationally created aromatic oligoamides from synthetic aromatic amino acids, and because of the face-to-face π - π interactions between the aromatic residues, they fold into β -sheet type foldamers.⁷ Due to π - π interactions, aromatic amino acids are also implicated in the development of amyloid self assembling structures.⁸ Sanjayan has studied a peptide oligomer that is coupled with anthranilic acid and creates distinct (1-2) type helical turns.⁹ Unnatural aromatic acids synthesised from benzotriazoles that display charge transfer-based luminous compounds with large Stokes shifts have been described by Sutherland.¹⁰ Utilizing an artificial starter tRNA, Cate has demonstrated the beginning of protein synthesis with synthetic aromatic amino acids produced from phenylalanine.¹¹ Recently, it was discovered that a phenylalanine analogue can create a hydrogel even when combined with single amino acid derivatives that have strong antibacterial properties.¹² Parang has created a number of cyclic peptides with the diphenylalanine residue and assessed the effectiveness of their transportation.¹³ Raman spectroscopy investigation by Tannenbaum assessed aromatic amino acids as potential

indicators in breast cancer.¹⁴ The benzenoid aromatic ring is the source of the majority of synthetic aromatic amino acids. Tropolone, a non-benzenoid aromatic scaffold, is a part of troponoid natural products.¹⁵⁻¹⁶ It has capabilities for metal complexing and intramolecular proton transfer with coordinating metal ions. Due to charge transfer, $\pi-\pi^*$, $n-\pi^*$ interactions, it also displays distinctive photophysical features. Tropolone-related substances have a wide range of biological actions, including antiviral, antifungal, antiviral, antibiotic, antimitotic, and anticancer properties.¹⁷⁻¹⁸ Recently, we created hybrid peptides of achiral troponyl amino acids with a tropone carbonyl group that generate a unique folding due to their aminoethyl backbone and achiral troponyl amino acid structure (**Figure 2.1 1a**).¹⁹ However, in mildly acidic environments, their amide bonds can be hydrolyzed.²⁰⁻²¹ The troponyl-containing hydrazine amino acid also demonstrates foldamer characteristics with exceptional amide bond reactivity in mild acidic conditions (**Figure 2.1 1b**).²² In the past, we have also shown that the native *di-/tri*-peptide's folding behaviour is considerably changed when the troponyl scaffold is added to the N-terminus.²³ The creation of a stable compound with BF_2 by 2-aminotropoimine derivatives has been documented in the literature.²⁴ On the other hand, the synthesis of many fluorescent BODIPY molecules has utilised dipyrromethene, a versatile N,N-ligand of boron.²⁵⁻²⁷ Additionally, N,N-/N,O-chelation has been employed to create fluorescent compounds of the BODIPY type and BODIPY analogues using the non-dipyrromethene scaffold.²⁸⁻³⁰ In the past, it has been investigated how to create novel fluorescent compounds called BODIPY analogues from aminotropone derivatives by complexing with BF_2 by N,N-/N,O chelation.³¹⁻³³

2.2.1 Hypothesis and objective

Inspired from results we have created chiral amino acids with the troponyl ring that may be inserted between peptides to change the structure of peptides. Here, we report the synthesis and structural investigations of a chiral, unnatural, aromatic amino acid (UAA) that was rationally designed and contains the tropone residue and its peptides (**Figure 2.1**). The synthesis and photophysical characteristics of its BODIPY analogue are also reported.

(1) Previous works



(2) This work

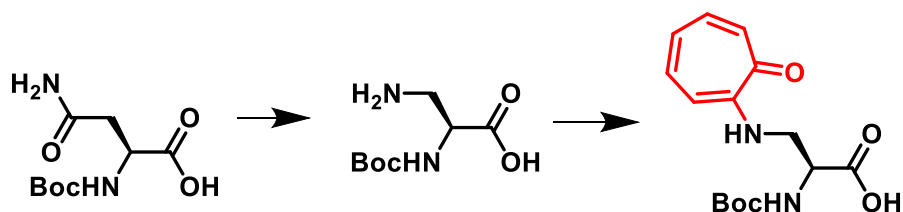


Figure 2.1 (1) previous work: (a) Achiral Troponyl amino acid derivatives (b) Hydrazino troponyl amino acid (2) This work: chiral troponyl amino acid.

2.2 Result and discussion

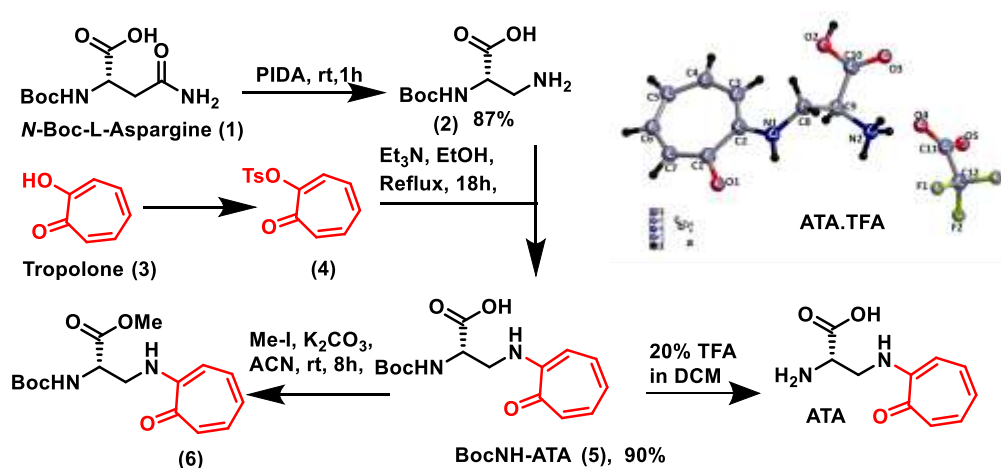
2.2.1 Synthesis of Aminotroponyl Alanine (ATA)

We started the synthesis of the unnatural, non-benzenoid, aromatic amino acid aminotroponyl alanine (ATA) using the tropolone scaffold and the amino acid asparagine (Asn) (**Scheme 2.1**). Using PIDA as oxidising agent in accordance with a known approach, N-Boc-L-asparagine (**1**) was transformed into a chiral diamine, namely 2-amino-L-alanine derivative (**2**).³⁴ The required BocNH-L-aminotroponyl alanine derivative was then generated by N-troponylation of diamine

carboxylate after tropolone (**3**) had been transformed into O-tosyltropolone (**4**) under refluxing conditions which produced the desired BocNH-L-aminotroponyl alanine derivative (**5**). NMR and ESI-HRMS were used to describe the product after it was separated by silica column purification (2 % MeOH/DCM). We attempted to crystallise the unprotected unnatural aromatic acid ATA after removing the Boc group with 20% TFA/DCM.

Along with TFA salt, we also got a single crystal of ATA. its ORTEP diagram is presented (**Scheme 2.1**). The Cambridge Crystallographic Data Centre (CCDC) has received its crystal data under reference number 2174977.

Scheme 2.1 Synthesis of Aminotroponyl Alanine (ATA)

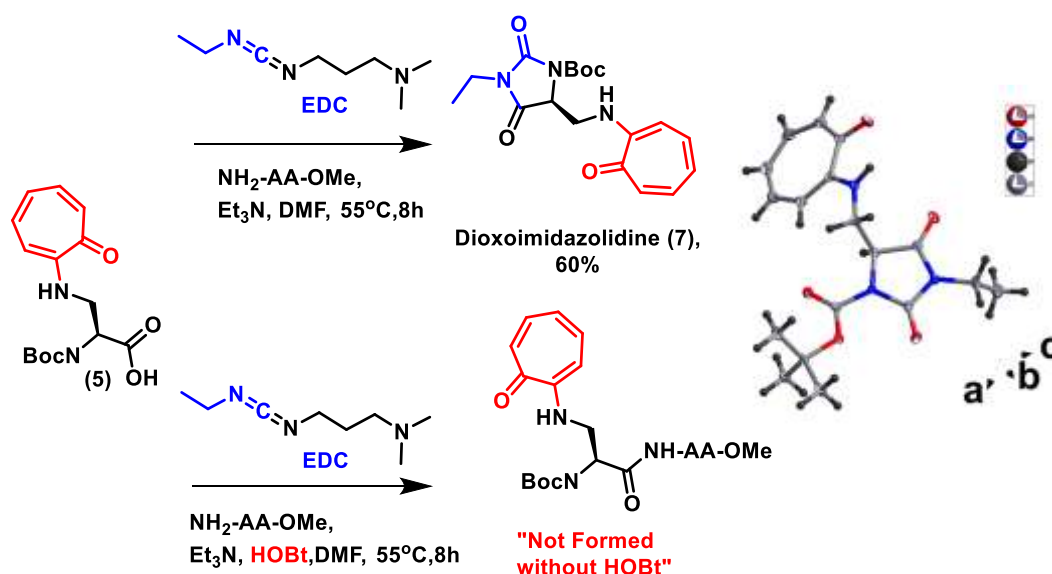


2.2.2 Synthesis of dioximidazolidine derivative

We tried to make hybrid peptides from native amino acids of the ATA. Under basic conditions, the ATA derivative (**5**) was exposed to peptide coupling with amino acid ester in the presence of versatile coupling agents, ethyl carbodiimide (EDC) (**Scheme 2.2**). Sadly, we were unable to obtain the desired hybrid dipeptide. But we discovered a novel heterocyclic dioximidazolidine derivative (**7**) with an amino troponyl residue after rigorous analysis. In a DCM:MeOH solvent solution, we produced a single crystal of compound (**7**). We investigated the crystal using an X-ray diffractometer which revealed the structure of compound **7** to be a

dioxoimidazolidine derivative. The solved X-ray data have been submitted to the CCDC with reference number 2212187. With other amino acid ester, we carried out the same reaction and separated the same compound. However, the reaction was carried out with the addition of hydroxyl benzotriazole (HOBt), which resulted in the production of the required *di*-peptide. For comparative investigations, the same reaction was carried out using dioxoimidazolidine derivative rather than amino acid ester and BocNH-amino acid derivatives, which produced *di*-peptides with efficiency. Thus, troponyl residue rather than *di*-peptides play a crucial role in the synthesis of dioxoimidazolidine derivative by unique C-N bond cleavage in EDC (coupling reagent). Including protease inhibitors³⁵⁻³⁶ the troponyl bearing dioxoimidazolidine molecule (7) can be considered as a therapeutic drug candidate.

Scheme 2.2 Synthesis of dioxoimidazolidine derivative (7)



We provide a likely mechanism for how the novel dioxoimidazolidine heterocyclic compound is created (**Figure 2.2**). In the absence of HOBt, the carboxylate of BocATA (5) combines with the coupling agent EDC to generate an adduct (**Int-1**) that transforms into the seven-membered reactive lactone (**Int-2**) with the creation of an asymmetric urea derivative. This urea side product combines with the lactone intermediate (**Int-2**) to produce another intermediate, (**Int-**

3), which unexpectedly breaks the C-N bond of the urea derivative to produce (**Int-4**). Then, (**Int-4**) provides the derivative of dioxoimidazolidine (**7**) containing the aminotroponyl residue. (**Int-1**) produces a reactive acyclic ester and urea derivative when HOBt is present. Then, peptides are produced when the amine group of the amino acid ester derivative combines with the benzotriazolyl acyclic ester (**Figure 2.2**).

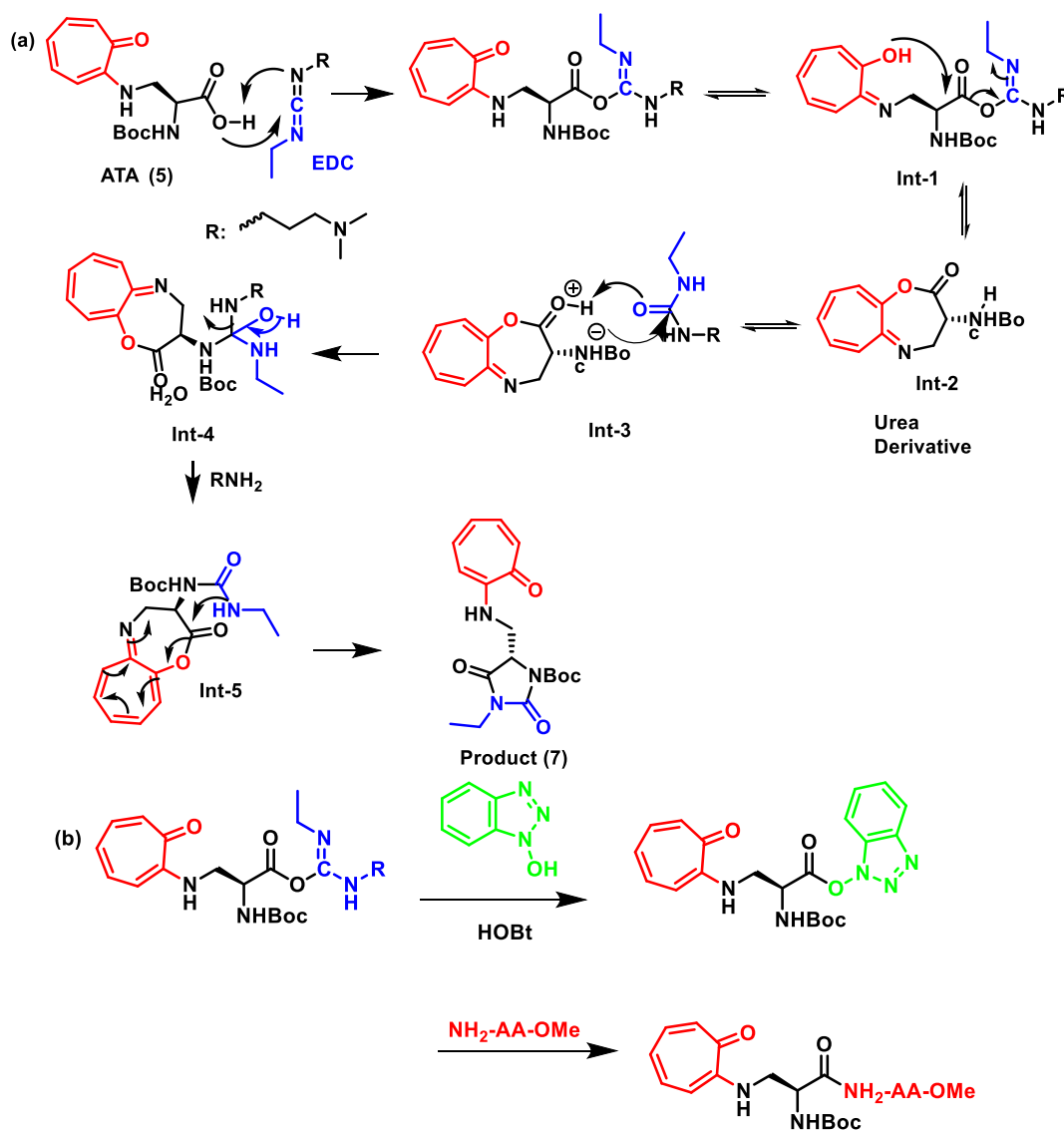
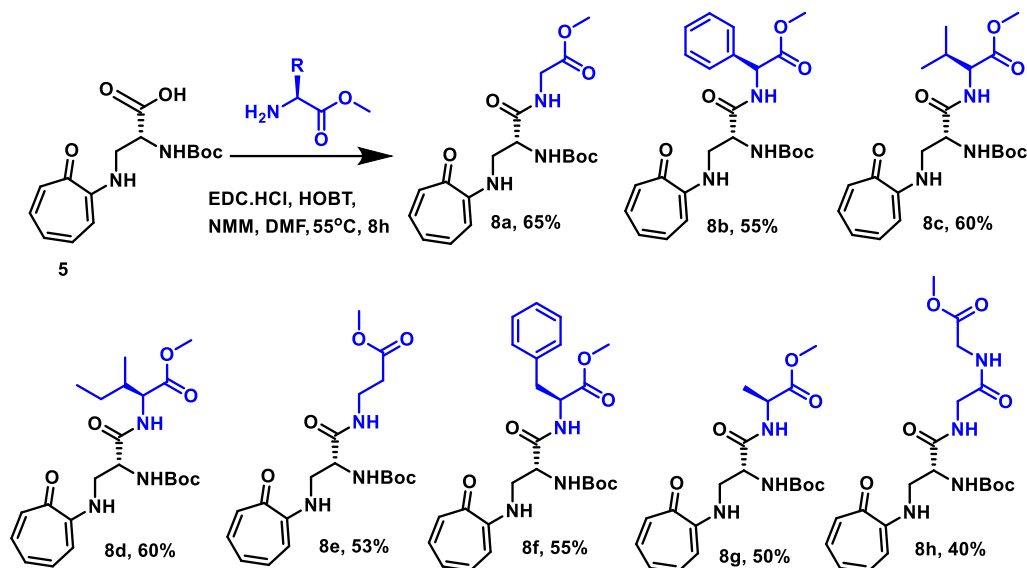
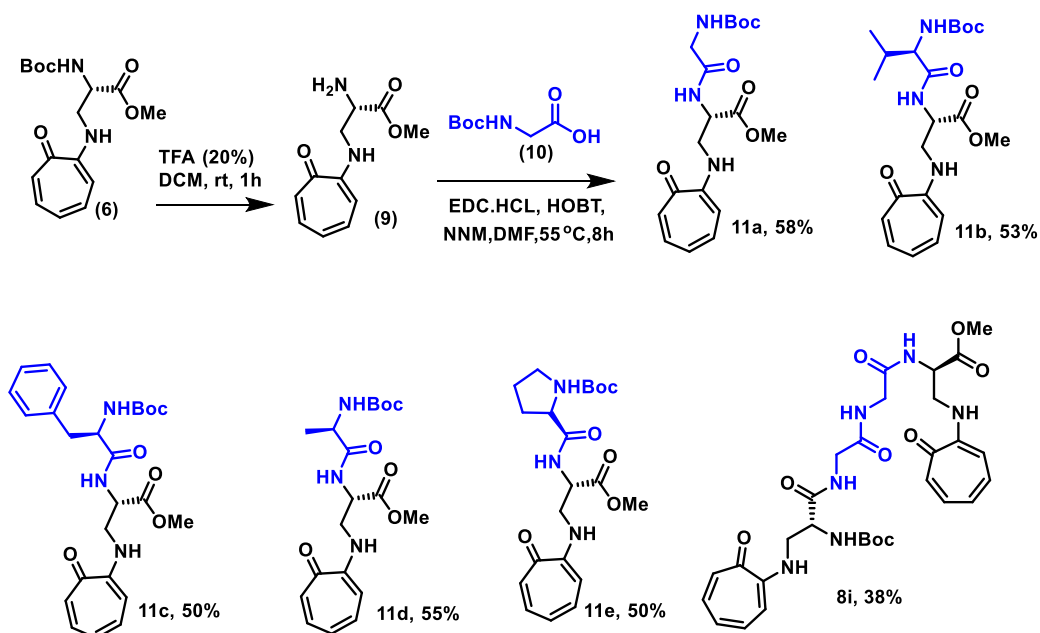


Figure 2.2 The plausible reaction mechanism of dioxoimidazolidine formation (a) Reaction without HOBt (b) Reaction with HOBt.

2.2.3 Synthesis of ATA hybrid peptides

Additionally, we created hybrid *di*-peptides utilising the peptide coupling processes with EDC and HOBt to investigate the function of the troponyl residue in the conformational alterations of hybrid peptides. (**Scheme 2.3**) Using the coupling reagent the free carboxylate group of BocNH-ATA (**5**) was linked with the free amine group of the amino acid ester NH₂-AA-OMe (**10a**), resulting in a hybrid dipeptide with the troponyl residue at the N-terminal end. Here, we applied Gly, Phe, Val, Ile, Pheg, and Ala neutral amino acid ester derivatives (NH₂-AA-OMe) to create the corresponding hybrid ATA di-peptides (**8a-8g**). Using the same peptide coupling conditions, we also synthesized the native *di*-peptide (NH₂-Gly-Gly-OMe) and the hybrid *tri*-peptide (**8h**) from BocNH-ATA. We coupled the carboxylate group of the Boc protected native amino acid derivative BocNH-AA-OH (**10b**) with the Boc group of the ATA ester (**6**) under peptide coupling conditions after removing the Boc group of the ATA ester (**6**) with (20% TFA/DCM). In this work, we provide hybrid peptides **11a-11e** that contain a troponyl residue at the C-terminus. By using NMR and HRMS, all hybrid peptides (**8/11**) were identified. Under identical peptide coupling conditions, we were able to successfully create the heterodimer with glycine serving as the pacer from the hybrid ATA dipeptide (BocNH-ATA-Gly-OMe, **8a**). *Di*-peptide **8a** was converted into building blocks (NH₂-ATA-Gly-Ome/BocNH-ATA-Gly-OH) by removing the Boc group and ester hydrolysis. Under identical conditions, these building blocks were joined by an amide bond using EDC/HOBt, resulting in the ATA-heterodimer (**8i**). Therefore, ATA serves as a non-benzenoid artificial aromatic amino acid building block to produce hybrid ATA-peptides.

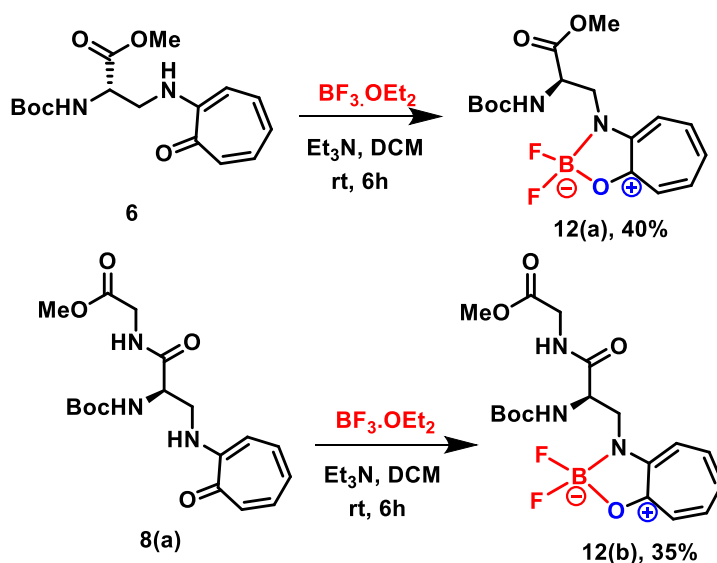
Scheme 2.3 Synthesis of ATA hybriide peptides

(a) ATA hybriide peptides from *N*-terminal(b) ATA hybriide peptides from *C*-terminal

2.2.4 Synthesis of ATA-BODIPY analogues

We have also investigated alkyl aminotroponyl scaffolds for producing fluorescent BODIPY analogues with quantum yields of 10-15%.³¹⁻³² We tried to make a different BODIPY analogue, the boron difluoro-ATA complex, an unnatural aromatic amino acid. (**Scheme 2.4**) Under mildly basic conditions, the boronating agent BF_3OEt_2 was used to boronate the ATA derivative (**6**), resulting in the formation of the borondifluoro-ATA complex (**12a**). The ATA-containing hybrid dipeptide (**8a**) was similarly treated with the boronating agent BF_3OEt_2 , resulting in the formation of the borondifluoro-ATA peptide complex (**12b**). Both BODIPY analogs (**12a/12b**) were characterized by respective NMR ($^1\text{H}/^{13}\text{C}/^{11}\text{B}/^{19}\text{F}$). The late-stage production of the peptide BODIPY analogue is highly supported by our findings.

Scheme 2.4 Synthesis of ATA-BODIPY analogs



2.2.5 Conformational analysis of ATA peptides

By placing a troponyl scaffold at the N-terminal of peptides, we have investigated the role of the troponyl residue in the structural and conformational alterations of peptides.²³ Here, we used NMR (1D/2D) and circular dichroism (CD) methods to investigate the structural changes

of ATA hybrid peptides (**8/11**) in organic solvents. We first determined the chemical shift of the ATA-peptide's protons from their corresponding ^1H - ^1H -COSY (2D-NMR) spectra, and then we determined their NOE connectivity from corresponding ^1H - ^1H -NOESY NMR spectra. **Figure 2.3** provides the extended NOESY spectra of the representative *di*-peptides (**8c**) and (**11b**). The troponyl ring protons (C3-H/C4-H) of the C-terminal ATA-peptide (**8c**) displayed potent NOEs with the alanyl CH_2 of the ATA residue. And the aminotroponone's N-H is attached to the $\alpha\text{C-H}$ of the alanyl residue (**Figure 2.3A**). Additional NOE peaks, troponyl ring protons (C3-H/C4-H) with CH_2 of alanyl residue in the ATA unit, were also seen in the instance of the *N*-terminal ATA-peptide (**11b**). Similar NOEs were observed with other *di*-peptides and *tri*-peptides. The troponyl ring protons (C3-H/C4-H) in heterodimer ATA-tetrapeptides (**8i**) displayed significant NOEs with both the alanyl CH_2 of ATA and the $-\text{CH}_2$ of the peptide. These NMR data demonstrated the troponyl carbonyl's near proximity to the *N*-terminal sides of the respective hybrid peptides in chloroform, which may have been caused by an intramolecular hydrogen bond between the troponyl carbonyl and backbone amine N-H.

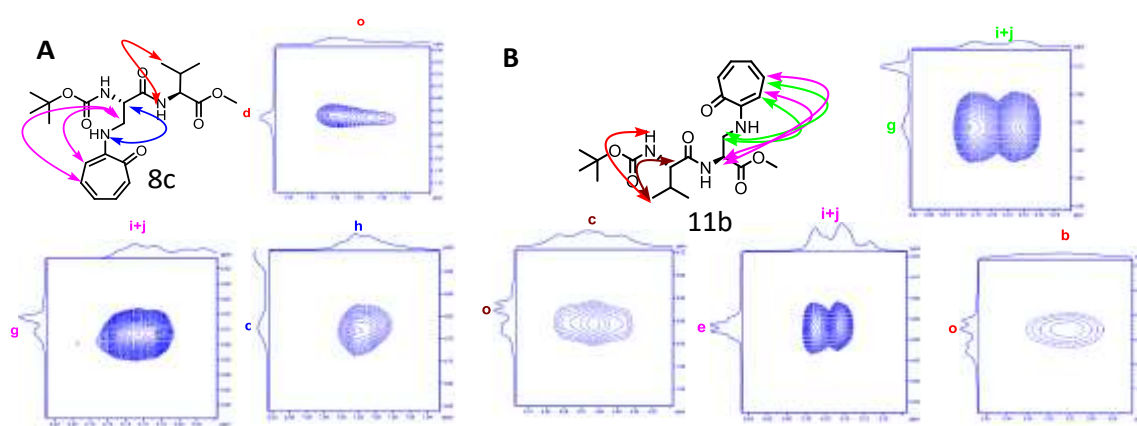


Figure 2.3 NOE's of ATA-peptide (A) *di*-peptide (**8c**) & (B) *di*-peptide (**11b**).

2.2.6 DMSO D₆ Titration study

Additionally, using the DMSO-d₆ titration ¹H-NMR method, we looked at the intra/inter molecular hydrogen bonding in ATA-peptide derivatives. The DMSO-d₆ titration-¹H-NMR experiments revealed the type of hydrogen bonding.²³ **Figure 2.4** shows the titration curves of the hybrid peptides (**8c/8i/8h/11b**), DMSO-d₆ vs. chemical shift. The chemical shifts of BocN–H, amide-N–H, and troponyl-N–H were almost the same with the increase the concentration of DMSO-d₆. However, with increasing DMSO-d₆, we observed a downfield shift in amide-N-H and BocN-H and a slight upfield shift of aminotroponyl-N-H. Thus, the hybrid peptide's amino troponyl N-Hs are implicated in intramolecular hydrogen bonding in their respective peptides.

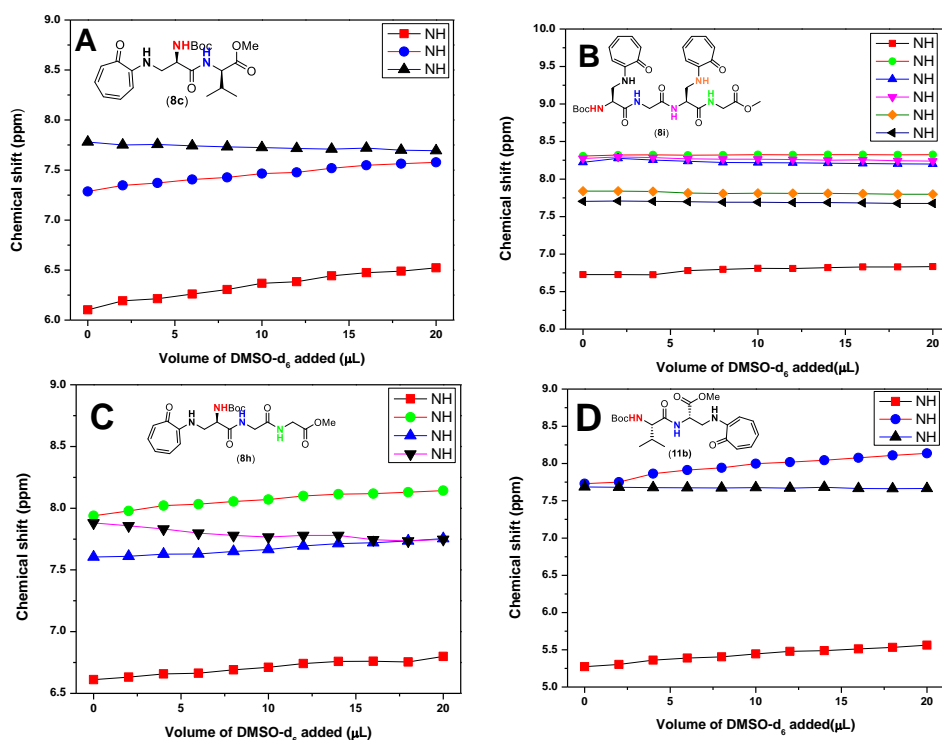


Figure 2.4 DMSO-d₆ titration NMR experiments of ATA-Hybrid peptide: (A) BocNH-ATA-Val-OMe (**8c**), (B) Boc NH-ATA-Gly-ATA-Gly-OMe (**8i**), (C) BocNH-ATA-Gly-Gly-OMe (**8h**), (D) BocNH-Val-ATA-OMe (**11b**).

2.2.7 Circular Dichroism study

Additionally, using CD experiments, we investigated the foldameric characteristics of hybrid peptides (**8/11**) in polar protic and polar aprotic solvents. We recorded the circular dichroism (CD) spectra of hybrid ATA-peptides (**8/11**) in acetonitrile (ACN) and methanol (MeOH). The aromatic ATA residue generates positive and negative signals above $\lambda_{220\text{ nm}}$ in the CD spectra of hybrid peptides (**8/11**) in ACN. The electronic transition of the troponyl ring may be the cause of the two peaks in the CD spectra of the monomer (**6**) at the wavelengths (λ) 240 nm/265 nm ($\lambda_{240\text{ nm}}/\lambda_{260\text{ nm}}$) (**Figure 2.5**). Additionally, their comparative CD studies to those of native *di*-peptides are explained. The CD spectra of ATA-peptide (**8c**) show a maximum at $\lambda_{210\text{ nm}}$ and minimum at $\lambda_{265\text{ nm}}$, which strongly encourage the formation of a structure of the turn type while the peptide (**11b**), has one maximum and two minima $\lambda_{234\text{ nm}}$ and $\lambda_{265\text{ nm}}$, respectively, which support helix type structures (**Figure 2.6**). The CD spectra of the ATA *tri*-peptide (**8h**) displays two minima ($\lambda_{260\text{ nm}}$ and $\lambda_{218\text{ nm}}$), along with a little blue shift that may be caused by the presence of an additional non-ATA amide bond.) (**Figure 2.5**). The CD spectra of the ATA *tetra*-peptide (**8i**) show a noticeable minimum ($\lambda_{265\text{ nm}}$), which may be a random coil or other non-characteristic structure (**Figure 2.5**). In methanol, Only the ATA *di*-peptide (**11b**) displays an almost turn-like maximum ($\lambda_{265\text{ nm}}$)/minimum ($\lambda_{215\text{ nm}}$) structure, the other ATA-peptides display random coils, probably as a result of the absence of intramolecular hydrogen bonding (**Figure 2.6**).

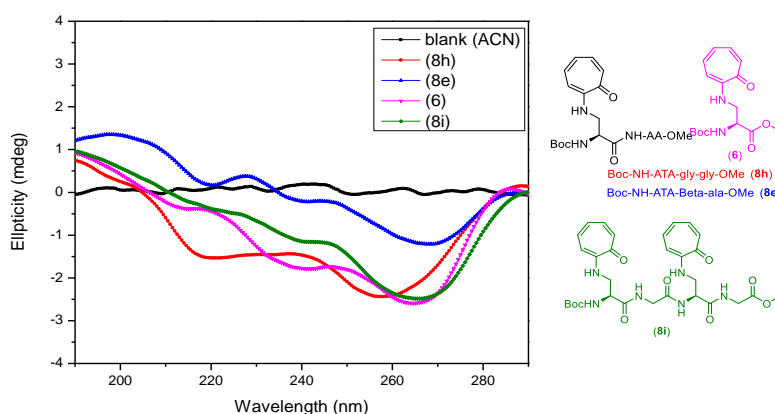


Figure 2.5 CD spectra of (**6**, **8e**, **8h**, **8i**) in acetonitrile (ACN).

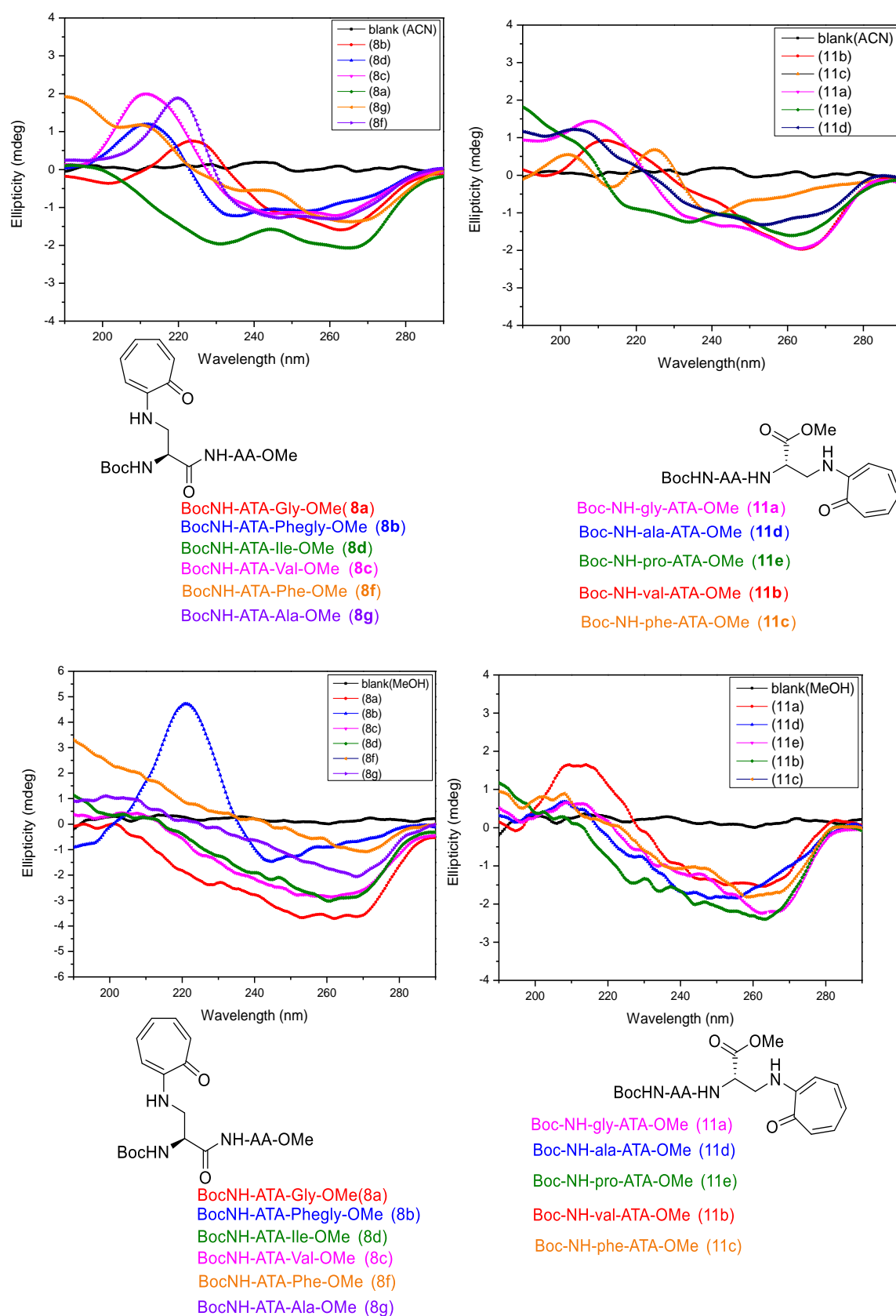


Figure 2.6 CD spectra of (8a-8d, 8f, 8g & 11a-11e) in acetonitrile (ACN) & in methanol (MeOH).

2.2.8 Theoretical study

The most stable conformation of peptides and associated derivatives has been identified in the literature using energy minimization (GMMX) and DFT calculations³⁷. We carried theoretical investigations to verify the structural changes of ATA-peptides. Here we have tried to optimized the conformations of the ATA-monomer (**6**), ATA *di*-peptides (**8a/8c/11a**), ATA-*tri*-peptide (**8h**), and ATA *tetra*-peptide (**8i**) using GMMX and DFT calculations. The hybrid peptides (**8a/11a**) exhibit stable conformers as a result of intramolecular hydrogen bonding. We also extracted the hydrogen bonding from the stable conformer of ATA *tetra*-peptide (**8i**) (**Figure 2.7**). We noticed that in ATA-peptides, the distance between troponyl Carbonyl C=O and the amide N-H is less than 2.0 within a suitable hydrogen bonding bond angle. Theoretical investigations thus confirm the role of the troponyl carbonyl C=O of ATA-peptides by hydrogen bonding with amide N-H.

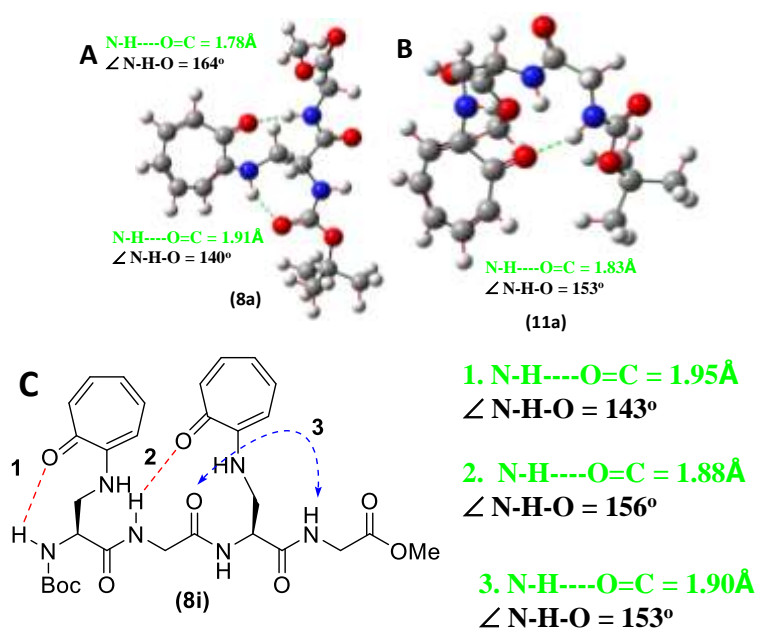


Figure 2.7 Theoretically optimized structure of ATA-peptides **8a** (A)/**11a** (B)/ **8i** (C).

2.2.9 Fluorescence study

Tropolone is a naturally occurring chromophore and fluorophore, although its quantum yield in an aprotic organic solvent is exceedingly low less than 1%. Previously we have explored novel BODIPY analogs from tropolone, which exhibit reasonably high quantum yields (10–15%).³¹⁻³² The photophysical characteristics of the ATA derivative (**6**) and its BODIPY analogues (**12a/12b**) have also been examined in this article. In MeOH and ACN, we recorded their emission and absorption spectra. The absorption and emission spectra of the BODIPY analogues (**12a/12b**) in ACN reveal that they are fluorescent molecules. with λ_{em} , 450 nm with Stokes shifts of 65 nm (**12a**) and 71 nm (**12b**) (**Figure 2.8 and Table 2.1**). These spectra also show that fluorescence intensity of (**12b**) is greater than (**12a**). Then, with reference to quinine sulphate, we determined their photophysical characteristics and relative quantum yields (QY) (**Table 2.1**). The molar absorptivity (ϵ , $M^{-1} cm^{-1}$, $\lambda_{382} nm$) and quantum yield of the BODIPY analog **12a** (9.1%) are higher than those of **12b** (5.5%). Additionally, we found that in the protic solvent MeOH, their photophysical characteristics are nearly identical.

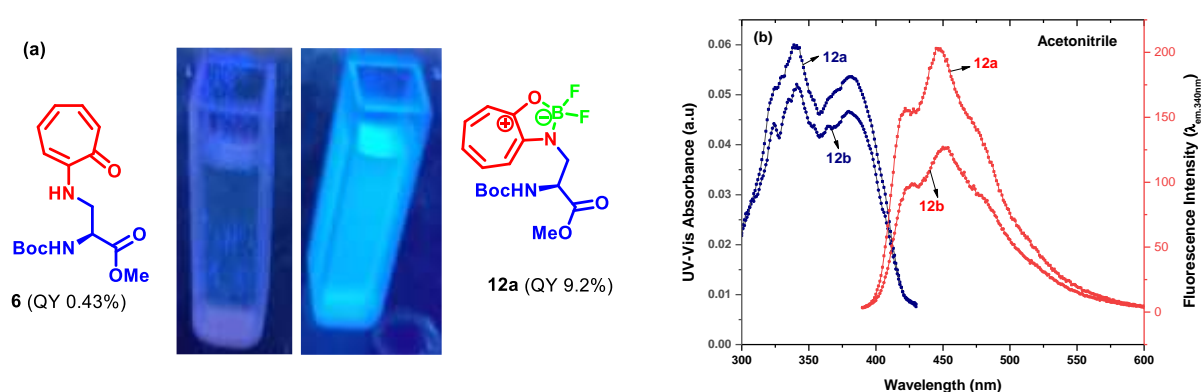


Figure 2.8 (a) Sample under fluorescence light; (b) UV-Vis absorption and emission spectra of ATA-BODIPY analogs (**12a/12b**)

Table 2.1 Photophysical parameters of ATA-BODIPY analogues

Entry		λ_{abs}	$\epsilon(\lambda_{382\text{nm}})$ ($\text{M}^{-1}\text{cm}^{-1}$)	λ_{em} ($\lambda_{\text{ex},340\text{nm}}$)	Stokes Shift (nm)	QY (%)
1	12a	248, 341, 382	5363	448	65	9.1
2	12b	246, 342, 382	4640	453	71	5.5

Solvent ACN.

2.2.10 HOMO & LUMO Computational study

Here, we found that the amino acid ester BODIPY analogue (**12a**) showed significantly more fluorescence quenching than the hybrid peptide BODIPY analogue (**12b**). To learn more about the actual causes we produced the HOMO-LUMO of BODIPY analogues (**12a/12b**) Using computational DFT (B3LYP) techniques. Their HOMO-LUMO diagrams shows in **Figure 2.9**. Troponyl and the backbone of the amino acid contribute to the HOMOs of both analogues (**12a** and **12b**), whereas the troponyl residue contributes to the LUMOs. In both analogues, the energy difference between the HOMO-LUMO is nearly identical. However, the quantum yield BODIPY analogue (**12b**) is considerably lower than that of analogue (**12a**). With a distance of 1.8Å, the theoretically optimized structure of analogue (**12b**) displays intramolecular hydrogen bonding as N-H.....F-B which possibly partially quenches the fluorescence owing to the perturbation of electron delocalization in the troponyl *di*-fluoroboron complex residue.

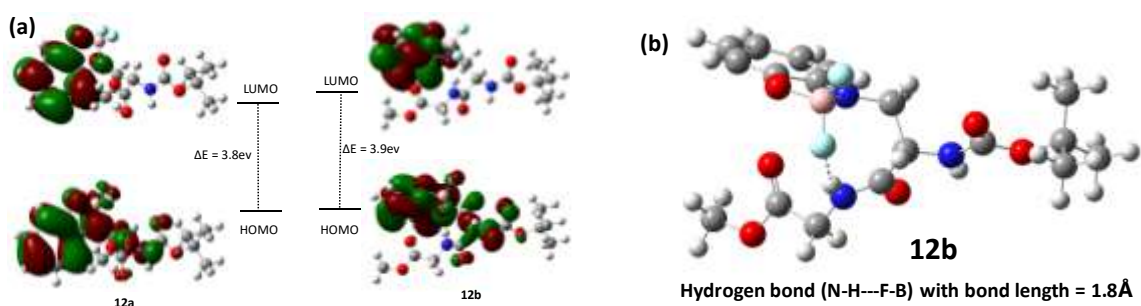


Figure 2.9 (a) HOMO-LUMO of ATA-BODIPY analogs;(b) Theoratically optimized structure of **12b**.

2.2.11 Cell culture study

In order to be useful, we examined the cytotoxicity of the BODIPY amino acid derivative (**ATA/12a**) by MTT assay and cell-internalization in HeLa cells by confocal studies. According to the MTT assay results, (**ATA/12a**) is nontoxic at a concentration of 50 μ M for both normal (HEK293T) and cancerous (HeLa) cells. However, at high concentrations, cell growth was impeded. The HeLa cells were then incubated to the ATA-BODIPY analogue for 18 hours and observed under a confocal microscope using various channels such as DAPI (blue channel), FITC (green channel, $\sim\lambda_{ex.500}$ nm), and TRITC (red channel, $\sim\lambda_{ex.550}$ nm) (**Figure 2.10**). Localization in the cellular nucleus is seen in the DAPI-stained image (**2.10a**). The picture demonstrates that ATA-BODIPY (**12a**) molecules have entered the cells in the FITC channel. The merged images indicate the cytoplasmic localization of ATA-BODIPY (**12a**). Similar results were obtained in Under TRITC, (red channel). As a result, the ATA-BODIPY analogue may be utilised as a fluorescent probe of target specific peptides.

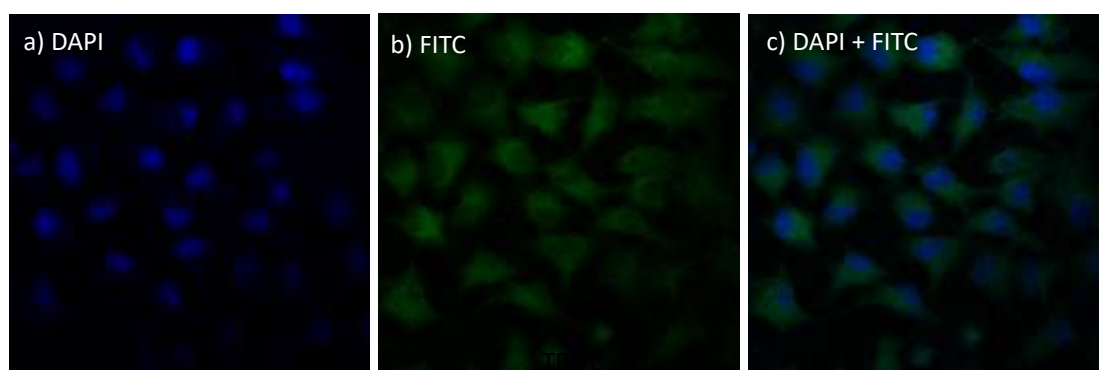


Figure 2.10 Confocal images of HeLa cells with (**12a**): (a) stained with DAPI; (b) BODIPY (**12a**) treated cells with FITC staining (green channel); (c) merged image of DAPI and FITC staining.

2.3 Conclusion

The hybrid *di*-, *tri*-, and *tetra*-peptides of the chiral L-aminotroponyl amino acid (ATA) have been successfully synthesised. It is significant that we have discovered novel heterocycle compounds, during the creation of hybrid peptides, dioxoimidazolidine derivatives. We also created the fluorescent BODIPY analogue derived from the ATA/ATA-peptide with a quantum yield of between 6% and 9%. According to our conformational investigations, troponyl residues play a crucial role in the structural transformation of ATA-containing peptides into β -turn/ α -helix type structures. We have shown that they are not cytotoxic and that they internalize into HeLa cells, where they are found in the cytoplasm, for use in real-world applications. As a result, ATA, ATA-peptides, and ATA BODIPY analogues are brand-new non-benzenoid artificial aromatic amino acid derivatives that may be used to create new peptidomimetics.

2.4 Experimental Section

2.4.1 Materials and instrumentation

The materials were purchased from commercial suppliers and used without purification. Anhydrous DMF was freshly prepared by distilling over calcium hydride. Reactions were monitored by thin-layer chromatography, visualized with UV irradiation and ninhydrin. Column chromatography was performed using 100–200 mesh silica. Mass spectra were obtained using a Bruker MicroTOF-Q II spectrometer. NMR spectra were recorded on a Bruker AV-700 MHz and a Bruker AV-400 MHz ^1H (400 MHz), ^{13}C (100.6 MHz). ^1H and ^{13}C NMR chemical shifts were recorded in ppm downfield from tetramethylsilane, and the splitting patterns are abbreviated as s, singlet; d, doublet; dd, doublet of doublet; t, triplet q, quartet; dq,

doublet of the quartet; m, multiplet. CD experiments were performed on a JASCO-J 1500. All CD experiments were performed at 25°C, and the two recorded scans were averaged and from 290 to 190 nm wavelengths.

2.4.2 General procedure for peptide coupling

N-Boc protected amino acid (**ATA 5**) was dissolved in DMF before triethylamine (TEA, 3.0 eq.), EDC.HCl (1.3 eq.) and HOBt (1.3 eq.) were added, resulting in the amino acid methyl ester (1.2 eq.). Further, this mixture was heated to 60°C for 8–12 h. The reaction was monitored by TLC. The crude reaction mixture was concentrated under reduced pressure before water was added. The aqueous layer was extracted with EtOAc. The organic layer was combined, dried over anhydrous Na₂SO₄, and concentrated under reduced pressure. The residue was purified with column chromatography using an EtOAc/hexane solvent system to yield the corresponding substrates.

2.4.3 Chemical shift values of NMR

(S)-2-((*tert*-Butoxycarbonyl)amino)-3-((7-oxocyclohepta-1,3,5-trien-1-yl)amino)propanoic acid (**5**). Compound **5** was purified by column chromatography with the solvent system methanol: dichloromethane (2:98) and obtained as a yellow solid (2.0 g, 81% yield) *R*_f = 0.23 (3% MeOH/DCM). ¹H NMR (400 MHz, CDCl₃) δ 8.11 (s, 1H), 7.73 (s, 1H), 7.31–7.09 (m, 3H), 6.83 (d, *J* = 8 Hz, 1H), 6.71 (d, *J* = 8 Hz, 1H), 5.86 (s, 1H), 4.53 (s, 1H), 3.78 (s, 2H), 1.34 (s, 9H). ¹³C NMR (101 MHz, CDCl₃) δ 175.57 (s), 172.44 (s), 156.48 (s), 155.67 (s), 138.28 (s), 137.59 (s), 128.42 (s), 124.26 (s), 111.65 (s), 80.30 (s), 52.88 (s), 44.35 (s), 28.31 (s). HRMS (ESI) *m/z*: [M + Na]⁺ calcd for C₁₅H₂₀N₂O₅ 331.1270; found 331.1273

(*S*)-2-Amino-3-((7-oxocyclohepta-1,3,5-trien-1-yl)amino)propanoic acid (**ATA**). **ATA** was purified by column chromatography with the solvent system MeOH:DCM (15:85) and obtained as a brown solid (0.5 g, 71% yield) $R_f = 0.83$ (30% MeOH/DCM). ^1H NMR (700 MHz, DMSO) δ 7.79 (d, $J = 4$ Hz, 1H), 7.30 (m, 1H), 6.98 (d, $J = 12$ Hz, 1H), 6.87–6.58 (m, 1H), 4.06 (t, 1H), 3.87–3.67 (m, 1H). ^{13}C NMR (101 MHz, DMSO) δ 176.67 (s), 169.78 (s), 155.44 (s), 137.63 (s), 136.73 (s), 129.30 (s), 123.10 (s), 109.15 (s), 51.31 (s), 42.55 (s). HRMS (ESI) m/z : $[\text{M} + \text{H}]^+$ calcd for $\text{C}_{10}\text{H}_{12}\text{N}_2\text{O}_5$ 209.0926; found 209.0909.

Methyl(*S*)-2-((*tert*-butoxycarbonyl)amino)-3-((7-oxocyclohepta-1,3,5-trien-1-yl)amino)propanoate (**6**). Compound **6** was purified by column chromatography with the solvent system ethylacetate:hexane (20:80) and obtained as a yellow solid (0.5 g, 71% yield) $R_f = 0.83$ (50% EtOAc/hexane). ^1H NMR (400 MHz, CDCl_3) δ 7.8–7.4 (m, 1H), 7.4–7.1 (m, $J = 23.7, 10.7$ Hz, 3H), 6.8–6.5 (m, $J = 16.5, 7.2$ Hz, 2H), 5.7 (d, $J = 6.1$ Hz, 1H), 4.6 (d, $J = 5.3$ Hz, 1H), 3.8–3.8 (m, 1H), 3.8 (s, 1H), 1.4 (s, 9H). ^{13}C NMR (101 MHz, CDCl_3) δ 176.8 (s), 170.8 (s), 155.5 (s), 155.3 (s), 137.4 (s), 136.2 (s), 129.4 (s), 123.2 (s), 109.1 (s), 80.4 (s), 53.0 (s), 52.9 (s), 44.3 (s), 28.3 (s). HRMS (ESI) m/z : $[\text{M} + \text{Na}]^+$ calcd for $\text{C}_{16}\text{H}_{22}\text{N}_2\text{O}_5$ 345.1421; found 345.1417.

tert-Butyl(*S*)-3-ethyl-2,4-dioxo-5-(((7-oxocyclohepta-1,3,5-trien-1-yl)amino)methyl)imidazolidine-1-carboxylate (**7**). Compound **7** was prepared by heating **5** with EDC.HCl and Et_3N in DMF at 60 °C for 8 h and purified by column chromatography with the solvent system ethylacetate:hexane (35:65) and obtained as a brown solid (60% yield). $R_f = 0.50$ (40% EtOAc/hexane). ^1H NMR (400 MHz, CDCl_3) δ 7.29–7.00 (m, 1H), 6.72–6.56 (m, 1H), 4.51 (dd, $J = 17.5, 14.2$ Hz, 1H), 4.17–3.91 (m, 1H), 3.46 (dt, $J = 13.5, 6.6$ Hz, 1H), 1.52 (s, 3H), 1.04 (t, $J = 7.1$ Hz, 1H). ^{13}C NMR (101 MHz, CDCl_3) δ 176.81 (s), 169.31 (s), 155.32 (s), 151.60 (s), 149.11 (s), 137.49 (s), 135.88 (s), 129.95 (s), 123.81 (s), 108.92 (s), 85.18 (s), 59.28

(s), 41.75 (s), 34.40 (s), 28.02 (s), 12.89 (s). HRMS (ESI) m/z : $[M + Na]^+$ calcd for $C_{18}H_{23}N_3O_5$ 384.1524; found 384.1535

Methyl(S)-2-((tert-butoxycarbonyl)amino)-3-((7-oxocyclohepta-1,3,5-triyl)amino)

propanoyl) glycinate (8a). Peptide **8a** was synthesized using a general procedure for peptide coupling (the above-mentioned procedure) and purified by column chromatography with the solvent system ethylacetate:hexane (40:60) and obtained as a yellow gummy solid (65% yield). $R_f = 0.33$ (50% EtOAc/hexane). 1H NMR (400 MHz, $CDCl_3$) δ 7.9–7.8 (m, 2H), 7.2 (t, $J = 8$ Hz, 2H), 7.1 (d, $J = 8$ Hz, 1H), 6.7 (d, $J = 12$ Hz, 1H), 6.7–6.6 (m, 2H), 4.8–4.6 (m, 1H), 4.0 (d, $J = 3.6$ Hz, 2H), 3.8–3.7 (m, 2H), 3.7 (s, 3H), 1.4 (s, 10H). ^{13}C NMR (101 MHz, $CDCl_3$) δ 176.5, 170.8, 170.0, 155.9, 155.8, 137.4, 136.6, 128.8, 123.1, 109.8, 80.2, 53.3, 52.3, 44.7, 41.3, 28.2. HRMS (ESI) m/z : $[M + Na]^+$ calcd for $C_{18}H_{25}N_3O_6$ 402.1636; found 402.1616.

Methyl2-((S)-2-((tert-butoxycarbonyl)amino)-3-((7-oxocyclohepta-1,3,5-trien-1-yl)amino)

propanamido)-2-phenylacetate (8b). Peptide **8b** was synthesized using a general procedure for peptide coupling (the above-mentioned procedure) and purified by column chromatography with the solvent system ethylacetate:hexane (40:60) and obtained as a yellow gummy solid (55% yield). $R_f = 0.83$ (50% EtOAc/hexane). 1H NMR (400 MHz, $CDCl_3$) δ 7.9–7.7 (m, 2H), 7.3–7.2 (m, 5H), 7.2–7.0 (m, 3H), 6.8–6.6 (m, 2H), 6.3 (d, $J = 8$ Hz, 1H), 5.5 (d, $J = 8$ Hz, 1H), 4.6–4.5 (m, 1H), 3.8–3.7 (m, 2H), 3.7 (s, 3H), 1.4 (s, 9H). ^{13}C NMR (101 MHz, $CDCl_3$) δ 176.7 (s), 170.7 (s), 169.8 (s), 155.8 (s), 155.6 (s), 137.4 (s), 136.5 (s), 135.9 (s), 129.2 (s), 128.9 (s), 128.5 (s), 127.3 (s), 123.2 (s), 109.7 (s), 80.5 (s), 56.9 (s), 52.9 (s), 52.8 (s), 44.5 (s), 28.3 (s). HRMS (ESI) m/z : $[M + Na]^+$ calcd for $C_{24}H_{29}N_3O_6$ 478.1949; found 478.1978.

Methyl((S)-2-((tert-butoxycarbonyl)amino)-3-((7-oxocyclohepta-1,3,5-trien-1-yl)amino)

propanoyl)-D-valinate (8c). Peptide **8c** was synthesized using a general procedure for peptide coupling (the above-mentioned procedure) and purified by column chromatography with the

solvent system ethylacetate:hexane (40:60) and obtained as a yellow gummy solid (60% yield). $R_f = 0.50$ (50% EtOAc/hexane). ^1H NMR (400 MHz, CDCl_3) δ 7.9 (d, $J = 4$ Hz, 1H), 7.5 (s, 1H), 7.3–7.1 (m, 3H), 6.8–6.6 (m, 2H), 6.4 (d, $J = 8$ Hz, 1H), 4.7–4.6 (m, 1H), 4.5 (dd, $J = 4$, 4 Hz, 1H), 3.7 (d, $J = 8$ Hz, 2H), 3.7 (s, 3H), 2.2–2.1 (m, 1H), 1.4 (s, 9H), 0.9 (d, 6H). ^{13}C NMR (101 MHz, CDCl_3) δ 176.6 (s), 171.9 (s), 170.4 (s), 156.0 (s), 155.7 (s), 137.4 (s), 136.5 (s), 128.9 (s), 123.0–120.4 (m), 109.7 (s), 80.3 (s), 57.5 (s), 53.3 (s), 52.2 (s), 44.7 (s), 31.1 (s), 28.3 (s), 18.7 (s), 17.8 (s). HRMS (ESI) m/z : $[\text{M} + \text{Na}]^+$ calcd for $\text{C}_{21}\text{H}_{31}\text{N}_3\text{O}_6$ 444.2105; found 444.2107.

Methyl(2R)-2-((S)-2-((tert-butoxycarbonyl)amino)-3-((7-oxocyclohepta-1,3,5-trien-1-yl)amino) propanamido)-3-methylpentanoate (8d). Peptide **8d** was synthesized using a general procedure for peptide coupling (the above-mentioned procedure) and purified by column chromatography with the solvent system ethylacetate:hexane (40:60) and obtained as a yellow gummy solid (58% yield). $R_f = 0.54$ (50% EtOAc/hexane). ^1H NMR (400 MHz, CDCl_3) δ 8.0 (t, $J = 5.4$ Hz, 1H), 7.6–7.5 (m, 1H), 7.3–7.1 (m, 1H), 6.8–6.6 (m, 1H), 6.5 (d, $J = 6.3$ Hz, 1H), 4.7–4.6 (m, $J = 11.4$ Hz, 1H), 4.5 (dd, $J = 7.9$, 5.3 Hz, 1H), 3.8–3.7 (m, $J = 21.2$, 5.0 Hz, 1H), 3.7 (s, 1H), 1.9–1.7 (m, 1H), 1.4 (s, 9H), 0.9–0.9 (m, 2H), 0.9–0.8 (m, 6H). ^{13}C NMR (101 MHz, CDCl_3) δ 176.6 (s), 171.8 (s), 170.2 (s), 156.0 (s), 155.7 (s), 137.4 (s), 136.5 (s), 128.9 (s), 123.1 (s), 109.8 (s), 80.3 (s), 56.8 (s), 53.4 (s), 52.1 (s), 44.6 (s), 37.8 (s), 28.3 (s), 25.1 (s), 15.3 (s), 11.5 (s). HRMS (ESI) m/z : $[\text{M} + \text{Na}]^+$ calcd for $\text{C}_{22}\text{H}_{33}\text{N}_3\text{O}_6$ 458.2262; found 458.2259.

Methyl(S)-3-(2-((tert-butoxycarbonyl)amino)-3-((7-oxocyclohepta-1,3,5-trien-1-yl)amino) propanamido) propanoate (8e). Peptide **8e** was synthesized using a general procedure for peptide coupling (the above-mentioned procedure) and purified by column chromatography

with the solvent system ethylacetate:hexane (40:60) and obtained as a yellow gummy solid (53% yield). $R_f = 0.25$ (50% EtOAc/hexane). ^1H NMR (400 MHz, CDCl_3) δ 7.8 (t, 1H), 7.4 (s, 1H), 7.3–7.2 (m, 2H), 7.2 (d, $J = 12$ Hz, 1H), 6.8–6.7 (m, 2H), 6.4 (d, 1H), 4.6–4.4 (m, 1H), 3.8–3.7 (m, 2H), 3.6 (s, 3H), 3.6–3.4 (m, 2H), 2.7–2.4 (m, 2H), 1.4 (s, 9H). ^{13}C NMR (101 MHz, CDCl_3) δ 176.6 (s), 172.6 (s), 170.3 (s), 161.5 (s), 155.8 (s), 137.6 (s), 136.7 (s), 128.9 (s), 123.3 (s), 109.9 (s), 80.3 (s), 53.5 (s), 51.8 (s), 44.7 (s), 35.1 (s), 33.6 (s), 28.2 (s). HRMS (ESI) m/z : $[\text{M} + \text{Na}]^+$ calcd for $\text{C}_{19}\text{H}_{27}\text{N}_3\text{O}_6$ 416.1792; found 416.1792.

Methyl((S)-2-((tert-butoxycarbonyl)amino)-3-((7-oxocyclohepta-1,3,5-trien-1-yl)amino)propanoyl)phenylalaninate (8f). Peptide **8f** was synthesized using a general procedure for peptide coupling (the above-mentioned procedure) and purified by column chromatography with the solvent system ethylacetate:hexane (40:60) and obtained as a yellow gummy solid (55% yield). $R_f = 0.66$ (50% EtOAc/hexane). ^1H NMR (400 MHz, CDCl_3) δ 7.9 (t, $J = 8$ Hz, 1H), 7.3–7.1 (m, 6H), 7.1–7.0 (m, 3H), 6.8–6.6 (m, 2H), 6.3 (d, $J = 8$ Hz, 1H), 4.9–4.8 (m, 1H), 4.6–4.5 (m, 1H), 3.8–3.7 (m, 2H), 3.6 (s, 3H), 3.0 (m, 2H), 1.4 (s, 9H). ^{13}C NMR (101 MHz, CDCl_3) δ 176.7 (s), 171.5 (s), 170.0 (s), 155.8 (s), 155.6 (s), 137.4 (s), 136.5 (s), 135.8 (s), 129.2 (s), 128.5 (s), 127.0 (s), 123.2 (s), 109.8 (s), 80.3 (s), 65.0 (s), 53.5 (s), 52.4 (s), 44.4 (s), 37.9 (s), 28.3 (s). HRMS (ESI) m/z : $[\text{M} + \text{Na}]^+$ calcd for $\text{C}_{25}\text{H}_{31}\text{N}_3\text{O}_6$ 492.2105; found 492.2114.

Methyl((S)-2-((tert-butoxycarbonyl)amino)-3-((7-oxocyclohepta-1,3,5-trien-1-yl)amino)propanoyl)alaninate (8g). Peptide **8g** was synthesized using a general procedure for peptide coupling (the above-mentioned procedure) and purified by column chromatography with the solvent system ethylacetate:hexane (40:60) and obtained as a yellow gummy solid (50% yield).

R_f = 0.40 (50% EtOAc/hexane). ¹H NMR (400 MHz, CDCl₃) δ 7.8 (t, J = 8 Hz, 1H), 7.5 (s, 1H), 7.3–7.1 (m, 3H), 6.8 (d, J = 8 Hz, 1H), 6.7 (t, J = 8 Hz, 1H), 6.2 (d, J = 4 Hz, 1H), 4.6 (dt, 2H), 3.8–3.7 (m, 2H), 3.7 (s, 3H), 1.4 (s, 9H), 1.3 (d, J = 8 Hz, 3H). ¹³C NMR (101 MHz, CDCl₃) δ 176.5 (s), 172.9 (s), 169.9 (s), 155.8 (s), 150.3 (s), 137.7 (s), 136.8 (s), 129.0 (s), 123.5 (s), 110.1 (s), 80.5 (s), 53.3 (s), 52.5 (s), 48.3 (s), 44.7 (s), 28.3 (s), 17.9 (s). HRMS (ESI) m/z: [M + Na]⁺ calcd for C₁₉H₂₇N₃O₆ 416.1792; found 416.1796.

Methyl(S)-2-(2-((tert-butoxycarbonyl)amino)acetamido)-3-((7-oxocyclohepta-1,3,5-trien-1-yl)amino) propanoate (11a). Peptide **11a** was synthesized using a general procedure for peptide coupling (the above-mentioned procedure) and purified by column chromatography with the solvent system ethylacetate:hexane (40:60) and obtained as a yellow gummy solid (58% yield). R_f = 0.16 (50% EtOAc/hexane). ¹H NMR (400 MHz, CDCl₃) δ 7.9 (t, 1H), 7.7 (d, 1H), 7.3–7.2 (m, J = 8.1 Hz, 1H), 7.2–7.1 (m, J = 11.1 Hz, 1H), 6.8–6.7 (m, J = 8.1 Hz, 1H), 5.6–5.5 (m, 1H), 5.0–4.8 (m, 1H), 3.9–3.8 (m, 4H), 3.7 (s, 3H), 1.4 (s, 9H). ¹³C NMR (101 MHz, CDCl₃) δ 176.7 (s), 170.6 (s), 170.2 (s), 156.0 (s), 155.5 (s), 137.7 (s), 136.5 (s), 129.2 (s), 123.5 (s), 109.5 (s), 80.0 (s), 53.0 (s), 51.6 (s), 44.0 (s), 43.7 (s), 28.3 (s). HRMS (ESI) m/z: [M + Na]⁺ calcd for C₁₈H₂₅N₃O₆ 402.1636; found 402.1637

Methyl(S)-2-((S)-2-((tert-butoxycarbonyl)amino)-3-methylbutanamido)-3-((7-oxocyclohepta-1,3,5-trien-1-yl) amino)propanoate (11b). Peptide **11b** was synthesized using a general procedure for peptide coupling (the above-mentioned procedure) and purified by column chromatography with the solvent system ethylacetate:hexane (40:60) and obtained as a yellow gummy solid (53% yield). R_f = 0.53 (50% EtOAc/hexane). ¹H NMR (400 MHz, CDCl₃) δ 7.7 (t, 1H), 7.3–7.1 (m, 3H), 6.8–6.7 (m, 2H), 5.3 (s, 1H), 4.9–4.8 (m, 1H), 4.1–4.0 (m, 1H), 3.9–3.8 (m, 2H), 3.7 (s, 3H), 2.2–2.0 (m, 1H), 1.4 (s, 9H), 0.9 (dd, J = 8 Hz, 6H). ¹³C NMR (101 MHz, CDCl₃) δ 176.7 (s), 172.3 (s), 170.6 (s), 155.8 (s), 155.5 (s), 137.6 (s), 136.5 (s), 129.3

(s), 123.5 (s), 109.6 (s), 79.7 (s), 59.6 (s), 52.9 (s), 51.6 (s), 43.6 (s), 31.2 (s), 28.3 (s), 19.2 (s), 16.6 (s). HRMS (ESI) m/z : $[M + Na]^+$ calcd for $C_{21}H_{31}N_3O_6$ 444.2124; found 444.2105.

Methyl(S)-2-((S)-2-((tert-butoxycarbonyl)amino)-3-phenylpropanamido)-3-((7-oxocyclohepta-1,3,5-trien-1-yl) amino)propanoate (11c). Peptide **11c** was synthesized using a general procedure for peptide coupling (the above-mentioned procedure) and purified by column chromatography with the solvent system ethylacetate:hexane (40:60) and obtained as a yellow gummy solid (50% yield). R_f = 0.50 (50% EtOAc/hexane). 1H NMR (400 MHz, $CDCl_3$) δ 7.6 (m, 2H), 7.3–7.1 (m, 8H), 6.8–6.7 (m, 2H), 4.9–4.8 (m, 1H), 4.5–4.4 (m, 1H), 3.8 (t, J = 4 Hz, 2H), 3.7 (s, 1H), 3.2–2.9 (m, 2H), 1.3 (s, 9H). ^{13}C NMR (101 MHz, $CDCl_3$) δ 176.7 (s), 172.0 (s), 170.3 (s), 155.5 (s), 155.4 (s), 137.7 (s), 136.5 (s), 129.3 (s), 129.3 (s), 128.5 (s), 126.9 (s), 123.5 (s), 109.6 (s), 80.1 (s), 52.9 (s), 51.6 (s), 43.8 (s), 38.4 (s), 28.2 (s). HRMS (ESI) m/z : $[M + Na]^+$ calcd for $C_{25}H_{31}N_3O_6$ 492.2105; found 492.2125.

Methyl2-(2-((tert-butoxycarbonyl)amino)propanamido)-3-((7-oxocyclohepta-1,3,5-trien-1-yl)amino) propanoate (11d). Peptide **11d** was synthesized using a general procedure for peptide coupling (the above-mentioned procedure) and purified by column chromatography with the solvent system ethylacetate:hexane (40:60) and obtained as a yellow gummy solid (55% yield). R_f = 0.33 (50% EtOAc/hexane). 1H NMR (400 MHz, $CDCl_3$) δ 7.8 (s, 1H), 7.6 (s, 1H), 7.3–7.1 (m, J = 16.3, 8.9 Hz, 1H), 7.1–7.0 (m, J = 11.6 Hz, 1H), 6.7–6.5 (m, J = 10.5 Hz, 1H), 5.4 (s, 1H), 4.8–4.7 (m, J = 11.7, 5.6 Hz, 1H), 4.2–4.1 (m, J = 6.1 Hz, 1H), 3.8–3.7 (m, J = 11.1, 5.5 Hz, 1H), 3.7 (s, 1H), 1.3 (s, 3H), 1.3 (d, J = 7.0 Hz, 1H). ^{13}C NMR (101 MHz, $CDCl_3$) δ 176.7 (s), 173.5 (s), 170.6 (s), 155.5 (s), 155.4 (s), 137.6 (s), 136.5 (s), 129.2 (s), 123.4 (s), 109.6 (s), 79.8 (s), 52.9 (s), 51.6 (s), 50.1 (s), 43.5 (s), 28.2 (s), 18.6 (s). HRMS (ESI) m/z : $[M + Na]^+$ calcd for $C_{19}H_{27}N_3O_6$ 416.1792; found 416.1801.

tert-Butyl-(2*S*)-2-((1-methoxy-1-oxo-3-((7-oxocyclohepta-1,3,5-trien-1-yl)amino)propan-2-yl)carbamoyl) pyrrolidine-1-carboxylate (**11e**). Peptide **11e** was synthesized using a general procedure for peptide coupling (the above-mentioned procedure) and purified by column chromatography with the solvent system ethylacetate:hexane (40:60) and obtained as a yellow gummy solid (50% yield). $R_f = 0.40$ (50% EtOAc/hexane). ^1H NMR (400 MHz, CDCl_3) δ 7.7–7.3 (m, 1H), 7.3–7.0 (m, 1H), 6.7–6.6 (m, $J = 9.5$ Hz, 1H), 4.9–4.7 (m, 1H), 4.3–4.1 (m, 1H), 3.8–3.7 (m, 2H), 3.7 (s, 3H), 3.4–3.2 (m, 2H), 2.3–1.7 (m, 4H), 1.3 (s, 9H). ^{13}C NMR (101 MHz, CDCl_3) δ 176.7 (s), 173.5 (s), 172.8 (s), 170.4 (s), 155.4 (s), 137.5 (s), 136.3 (s), 129.2 (s), 123.2 (s), 109.2 (s), 80.4 (s), 60.9 (s), 60.0 (s), 52.9 (s), 47.1 (s), 43.6 (s), 28.2 (s), 24.4 (s), 23.6 (s). HRMS (ESI) m/z : $[\text{M} + \text{Na}]^+$ calcd for $\text{C}_{21}\text{H}_{29}\text{N}_3\text{O}_6$ 442.1949; found 442.1966.

Methyl(*R*)-(*R*)-(2-((*tert*-butoxycarbonyl)amino)-3-((7-oxocyclohepta-1,3,5-trien-1-yl)amino)propanoyl)glycylglycinate (**8h**). Peptide **8h** was synthesized using a general procedure for peptide coupling (the above-mentioned procedure) and purified by column chromatography with the solvent system ethylacetate:hexane (40:60) and obtained as a yellow solid (40% yield). $R_f = 0.40$ (100% EtOAc/hexane). ^1H NMR (400 MHz, CDCl_3) δ 8.0 (s, 1H), 7.9 (s, 1H), 7.6 (s, 1H), 7.3–7.1 (m, $J = 39.2, 22.4, 81$ Hz), 6.7–6.6 (m, 2H), 4.7–4.6 (m, 1H), 4.2–3.9 (m, 4H), 3.8–3.7 (m, 2H), 3.7 (s, 3H), 1.4 (s, 9H). ^{13}C NMR (101 MHz, CDCl_3) δ 176.5 (s), 170.9 (s), 170.3 (s), 169.5 (s), 156.3 (s), 155.9 (s), 137.7 (s), 136.3–136.2 (m), 128.9 (s), 123.4 (s), 110.2 (s), 80.6 (s), 53.9 (s), 52.3 (s), 44.7 (s), 43.0 (s), 41.1 (s), 28.3 (s). HRMS (ESI) m/z : $[\text{M} + \text{H}]^+$ calcd for $\text{C}_{20}\text{H}_{28}\text{N}_4\text{O}_7$ 437.2036; found 437.2017.

Methyl((*S*)-2-(2-((*S*)-2-((*tert*-butoxycarbonyl)amino)-3-((7-oxocyclohepta-1,3,5-trien-1-yl)amino)propanamido)acetamido)-3-((7-oxocyclohepta-1,3,5-trien-1-yl)amino)propanoyl)glycinate (**8i**). Peptide **8i** was synthesized using a general procedure for peptide coupling (the above-mentioned procedure) and purified by column chromatography with the solvent system MeOH:DCM (03:97) and obtained as a yellow gummy solid (38% yield). $R_f =$

0.43 (100% EtOAc/hexane). ^1H NMR (400 MHz, CDCl_3) δ 8.4–8.2 (m, 3H), 7.9–7.8 (t, 1H), 7.7 (t, 1H), 7.2–7.1 (m, 4H), 7.1–6.9 (m, 2H), 6.9–6.7 (m, 2H), 6.7–6.5 (m, 3H), 5.2–4.9 (m, 1H), 4.8–4.6 (m, 1H), 4.0 (t, J = 8 Hz, 4H), 3.9–3.7 (m, 4H), 3.6 (s, 3H), 1.3 (s, 9H). ^{13}C NMR (101 MHz, CDCl_3) δ 176.4 (s), 171.6 (s), 170.4 (s), 170.3 (s), 170.2 (s), 156.1 (s), 155.7 (s), 137.6 (s), 137.5 (s), 136.7 (s), 128.8 (s), 128.7 (s), 123.2 (s), 123.1 (s), 110.0 (s), 80.2 (s), 52.3 (s), 52.3 (s), 52.1 (s), 52.0 (s), 44.6 (s), 43.3 (s), 41.3 (s), 28.3 (s). HRMS (ESI) m/z : $[\text{M} + \text{Na}]^+$ calcd for $\text{C}_{30}\text{H}_{38}\text{N}_6\text{O}_9$ 649.2592; found 649.2620.

Methyl (S)-2-((tert-butoxycarbonyl)amino)-3-(2,2-difluoro113,214-cyclohepta[d][1,3,2]oxazaborol-3(2H)-yl)propanoate (12a). Bodipy **12a** was synthesized using the above-mentioned procedure and purified by column chromatography with the solvent system ethylacetate:hexane (40:60) and obtained as a yellow gummy solid (40% yield). R_f = 0.40 (50% EtOAc/hexane). ^1H NMR (400 MHz, CDCl_3) δ 7.69–7.61 (m, 1H), 7.56 (t, J = 10.2 Hz, 1H), 7.44–7.32 (m, 1H), 7.16 (t, J = 9.6 Hz, 1H), 5.54 (d, J = 4 Hz, 1H), 4.58 (m, 1H), 4.34–3.97 (m, 2H), 3.79 (s, 3H), 1.42 (s, 9H). ^{13}C NMR (101 MHz, CDCl_3) δ 170.25 (s), 167.76 (s), 155.52 (s), 141.70 (s), 140.04 (s), 128.57 (s), 128.48 (s), 120.18 (s), 118.49 (s), 80.42 (s), 52.95 (s), 44.12 (s), 29.70 (s), 28.27 (s). ^{11}B NMR (128 MHz, CDCl_3) δ 5.77 (t, J = 18.0 Hz). ^{19}F NMR (377 MHz, CDCl_3) δ –134.80––139.97 (m). HRMS (ESI) m/z : $[\text{M} + \text{Na}]^+$ calcd for $\text{C}_{16}\text{H}_{21}\text{BF}_2\text{N}_2\text{O}_5$ 393.1556; found 393.1446.

Methyl (S)-2-((tert-butoxycarbonyl)amino)-3-(2,2-difluoro113,214-cyclohepta[d][1,3,2]oxazaborol-3(2H)-yl)propanoyl)glycinate (12b). Bodipy **12b** was synthesized by stirring 6 with $\text{BF}_3 \cdot \text{OEt}_2$ with Et_3N in DCM for 1 h–2 h at rt. The reaction mixture was monitored by TLC and purified by column chromatography with the solvent system ethylacetate:hexane (40:60) and **12b** was obtained as a yellow gummy solid (35% yield). R_f = 0.40 (50%

EtOAc/hexane). ^1H NMR (400 MHz, CDCl_3) δ 7.77–7.68 (m, 1H), 7.59 (t, J = 10.2 Hz, 1H), 7.50 (d, J = 10.4 Hz, 1H), 7.39 (d, J = 10.0 Hz, 1H), 7.21 (t, J = 9.7 Hz, 1H), 6.96 (s, 1H), 5.84 (s, 1H), 4.62 (dd, J = 13.0, 6.7 Hz, 1H), 4.14–3.96 (m, 4H), 3.67 (s, 3H), 1.43 (s, 9H). ^{13}C NMR (101 MHz, CDCl_3) δ 170.42 (s), 169.51 (s), 167.71 (s), 160.83 (s), 155.58 (s), 142.01 (s), 140.01 (s), 128.82 (s), 120.31 (s), 119.11 (s), 52.30 (s), 41.30 (s), 41.25 (s), 29.68 (s), 28.17 (s). ^{11}B NMR (128 MHz, CDCl_3) δ 5.87 (t, J = 16.9 Hz). ^{19}F NMR (377 MHz, CDCl_3) δ –136.05 (dd, J = 233.4, 88.6 Hz). HRMS (ESI) m/z : $[\text{M} + \text{Na}]^+$ calcd for $\text{C}_{18}\text{H}_{24}\text{BF}_2\text{N}_2\text{O}_5$ 450.1671; found 450.1660.

2.5 References

1. Parthasarathy, A.; Cross, P. J.; Dobson, R. C.; Adams, L. E.; Savka, M. A.; Hudson, A. O., A three-ring circus: metabolism of the three proteogenic aromatic amino acids and their role in the health of plants and animals. *Frontiers in molecular biosciences* **2018**, *5*, 29.
2. Hufton, S. E.; Jennings, I.; Cotton, R., Structure and function of the aromatic amino acid hydroxylases. *Biochemical Journal* **1995**, *311* (Pt 2), 353.
3. Horne, W. S.; Gellman, S. H., Foldamers with heterogeneous backbones. *Accounts of chemical research* **2008**, *41* (10), 1399-1408.
4. John, E. A.; Massena, C. J.; Berryman, O. B., Helical anion foldamers in solution. *Chemical reviews* **2020**, *120* (5), 2759-2782.
5. Yoo, S. H.; Lee, H.-S., Foldectures: 3D molecular architectures from self-assembly of peptide foldamers. *Accounts of Chemical Research* **2017**, *50* (4), 832-841.
6. Haug, B. E.; Skar, M. L.; Svendsen, J. S., Bulky aromatic amino acids increase the antibacterial activity of 15-residue bovine lactoferricin derivatives. *Journal of peptide science: an official publication of the European Peptide Society* **2001**, *7* (8), 425-432.
7. Sebaoun, L.; Maurizot, V.; Granier, T.; Kauffmann, B.; Huc, I., Aromatic oligoamide β -sheet foldamers. *Journal of the American Chemical Society* **2014**, *136* (5), 2168-2174.
8. Stanković, I. M.; Niu, S.; Hall, M. B.; Zarić, S. D., Role of aromatic amino acids in amyloid self-assembly. *International journal of biological macromolecules* **2020**, *156*, 949-959.

9. Prabhakaran, P.; Kale, S. S.; Puranik, V. G.; Rajamohanam, P.; Chetina, O.; Howard, J. A.; Hofmann, H.-J. r.; Sanjayan, G. J., Sequence-specific unusual (1→2)-type helical turns in α/β -hybrid peptides. *Journal of the American Chemical Society* **2008**, *130* (52), 17743-17754.
10. Bell, J. D.; Morgan, T. E.; Buijs, N.; Harkiss, A. H.; Wellaway, C. R.; Sutherland, A., Synthesis and photophysical properties of benzotriazole-derived unnatural α -amino acids. *The Journal of Organic Chemistry* **2019**, *84* (16), 10436-10448.
11. Tharp, J. M.; Ad, O.; Amikura, K.; Ward, F. R.; Garcia, E. M.; Cate, J. H.; Schepartz, A.; Söll, D., Initiation of Protein Synthesis with Non-Canonical Amino Acids In Vivo. *Angewandte Chemie International Edition* **2020**, *59* (8), 3122-3126.
12. Misra, S.; Mukherjee, S.; Ghosh, A.; Singh, P.; Mondal, S.; Ray, D.; Bhattacharya, G.; Ganguly, D.; Ghosh, A.; Aswal, V., Single Amino-Acid Based Self-Assembled Biomaterials with Potent Antimicrobial Activity. *Chemistry–A European Journal* **2021**, *27* (67), 16744-16753.
13. Salehi, D.; Mozaffari, S.; Zoghebi, K.; Lohan, S.; Mandal, D.; Tiwari, R. K.; Parang, K., Amphiphilic cell-penetrating peptides containing natural and unnatural amino acids as drug delivery agents. *Cells* **2022**, *11* (7), 1156.
14. Contorno, S.; Darienzo, R. E.; Tannenbaum, R., Evaluation of aromatic amino acids as potential biomarkers in breast cancer by Raman spectroscopy analysis. *Scientific Reports* **2021**, *11* (1), 1-9.
15. Bentley, R., A fresh look at natural tropolonoids. *Natural product reports* **2008**, *25* (1), 118-138.
16. Guo, H.; Roman, D.; Beemelmans, C., Tropolone natural products. *Natural product reports* **2019**, *36* (8), 1137-1155.
17. Sekine, S.; Shimodaira, C.; Uesawa, Y.; Kagaya, H.; Kanda, Y.; Ishihara, M.; Amano, O.; Sakagami, H.; Wakabayashi, H., Quantitative structure–activity relationship analysis of cytotoxicity and anti-uv activity of 2-aminotropones. *Anticancer Research* **2014**, *34* (4), 1743-1750.
18. Narita, T.; Suga, A.; Kobayashi, M.; Hashimoto, K.; Sakagami, H.; Motohashi, N.; Kurihara, T.; Wakabayashi, H., Tumor-specific Cytotoxicity and Type of Cell Death Induced by Benzo [b] cyclohept [e][1, 4] oxazine and 2-Aminotropone Derivatives. *Anticancer Research* **2009**, *29* (4), 1123-1130.
19. Balachandra, C.; Sharma, N. K., Synthesis and conformational analysis of new troponyl aromatic amino acid. *Tetrahedron* **2014**, *70* (41), 7464-7469.
20. Balachandra, C.; Sharma, N. K., Direct/reversible amidation of troponyl alkylglycinates via cationic troponyl lactones and mechanistic insights. *ACS omega* **2018**, *3* (1), 997-1013.
21. Balachandra, C.; Sharma, N. K., Instability of amide bond comprising the 2-aminotropone moiety: cleavable under mild acidic conditions. *Organic letters* **2015**, *17* (16), 3948-3951.

22. Dalabehera, N. R.; Meher, S.; Bhusana Palai, B.; Sharma, N. K., Instability of amide bond with trifluoroacetic acid (20%): synthesis, conformational analysis, and mechanistic insights into cleavable amide bond comprising β -troponylhydrazino acid. *ACS omega* **2020**, 5 (40), 26141-26152.
23. Palai, B. B.; Sharma, N. K., N-Arylated peptide: troponyl residue influences the structure and conformation of N-troponylated-(di/tri)-peptides. *CrystEngComm* **2021**, 23 (1), 131-139.
24. Holmquist, H.; Benson, R., 2-Bora-and 2-Thia-1, 3-diazaazulenes. *Journal of the American Chemical Society* **1962**, 84 (24), 4720-4722.
25. Loudet, A.; Burgess, K., BODIPY dyes and their derivatives: syntheses and spectroscopic properties. *Chemical reviews* **2007**, 107 (11), 4891-4932.
26. Patalag, L. J.; Ahadi, S.; Lashchuk, O.; Jones, P. G.; Ebbinghaus, S.; Werz, D. B., GlycoBODIPYs: Sugars Serving as a Natural Stock for Water-soluble Fluorescent Probes of Complex Chiral Morphology. *Angewandte Chemie* **2021**, 133 (16), 8848-8853.
27. Sibold, J.; Kettelhoit, K.; Vuong, L.; Liu, F.; Werz, D. B.; Steinem, C., Synthesis of Gb3 Glycosphingolipids with Labeled Head Groups: Distribution in Phase-Separated Giant Unilamellar Vesicles. *Angewandte Chemie* **2019**, 131 (49), 17969-17977.
28. Alsimaree, A. A.; Alatawi, O. M.; Waddell, P. G.; Day, D. P.; Alsenani, N. I.; Knight, J. G., Pyrrolylquinoline-BF₂ and BPh₂ BODIPY-Type Analogues: Synthesis, Structural Analysis and Photophysical Properties. *Crystals* **2021**, 11 (9), 1103.
29. Schrage, B. R.; Nemykin, V. N.; Ziegler, C. J., BOSHYPY fluorophores: BODIPY analogues with single atom controlled aggregation. *Organic Letters* **2021**, 23 (13), 5246-5250.
30. Liu, B.; Li, J.; Yang, W.; Yan, H.; Gao, X.; Zhang, Q., Naphthalene imide derived BODIPY analogues as n-channel semiconductors. *Dyes and Pigments* **2022**, 199, 110053.
31. Palai, B. B.; Soren, R.; Sharma, N. K., BODIPY analogues: synthesis and photophysical studies of difluoro boron complexes from 2-aminotropone scaffolds through N, O-chelation. *Organic & Biomolecular Chemistry* **2019**, 17 (26), 6497-6505.
32. Bhusana Palai, B.; Kumari, S.; Dixit, M.; Sharma, N. K., Nonbenzenoid BODIPY Analogues: Synthesis, Structural Organization, Photophysical Studies, and Cell Internalization of Biocompatible N-Alkyl-Aminotroponyl Difluoroboron (Alkyl-ATB) Complexes. *ACS omega* **2022**, 7 (31), 27347-27358.
33. Balachandra, C.; Sharma, N. K., Novel fluorophores: Syntheses and photophysical studies of boron-aminotroponimines. *Dyes and Pigments* **2017**, 137, 532-538.
34. Zhang, L.-h.; Kauffman, G. S.; Pesti, J. A.; Yin, J., Rearrangement of N α -protected L-asparagines with iodosobenzene diacetate. A practical route to β -amino-L-alanine derivatives. *The Journal of Organic Chemistry* **1997**, 62 (20), 6918-6920.

35. Konnert, L.; Lamaty, F.; Martinez, J.; Colacino, E., Recent advances in the synthesis of hydantoins: the state of the art of a valuable scaffold. *Chemical Reviews* **2017**, *117* (23), 13757-13809.
36. Park, J.-H.; Lee, G.-E.; Lee, S.-D.; Hien, T. T.; Kim, S.; Yang, J. W.; Cho, J.-H.; Ko, H.; Lim, S.-C.; Kim, Y.-G., Discovery of novel 2, 5-dioxoimidazolidine-based P2X7 receptor antagonists as constrained analogues of KN62. *Journal of medicinal chemistry* **2015**, *58* (5), 2114-2134.
37. Biswas, S.; Abo-Dya, N. E.; Oliferenko, A.; Khiabani, A.; Steel, P. J.; Alamry, K. A.; Katritzky, A. R., Oxyzaopeptides: Synthesis, Structure Determination, and Conformational Analysis. *The Journal of Organic Chemistry* **2013**, *78* (17), 8502-8509.

CHAPTER-3

Unusual Pseudopeptides: Syntheses and Structural Analyses of Ethylenediproyl Peptides and Their Metal Complexes with Cu(II) Ion

TABLE OF CONTENTS

Chapter 3	70
3.1 Introduction.....	70
3.1.1 Hypothesis and objective	72
3.2 Results and discussion	72
3.2.1 Synthesis of Ethylenedipropyl peptides	73
3.2.2 Conformational analyses	74
3.2.3 DMSO D6 Titration study	75
3.3.4 Circular Dichroism study	78
3.3.5 Metalation of ethylene Ethylenedipropyl peptides.....	79
3.3.6 EPR Study of Cu-peptides.....	80
3.3 Conclusions.....	81
3.4 Experimental Section.....	82
3.4.1 Material and Instrumentation	82
3.4.2 General Procedure for Peptide Coupling	82
3.4.3 General Procedure for Synthesis of dipropyl Peptides (4a, 4b)	83
3.4.4 General Procedure for Metalation of Peptides.....	83
3.4.5 Chemical shift values of NMR	83
3.5 References.....	85

Chapter 3

3.1 Introduction

Many biological processes involve protein-protein interactions (PPIs) and protein-nucleic acid interactions (PNIs).¹⁻² The potential for therapeutic benefit from the development of medicines that target these interactions is substantial. Yet, due to the wide and shallow binding surface, tiny molecules hardly ever target these interactions. Structured peptides are thought to be prospective therapeutic medication options due to their positive results in binding to protein and nucleic acids in the repertoire of macromolecular ligands.³⁻⁴ To control numerous biochemical processes, proteins and peptides create distinctive secondary structures, such as α -helix, β -sheet, and β -turn.⁵⁻⁷ Peptides are susceptible to proteolysis and are likely to lose their secondary structure in solutions, which reduces their target selectivity. Further limitations of peptides include low selectivity and poor cell permeability.⁸ By limiting conformational flexibility to increase metabolic stability and target specificity, various structurally modified artificial amino acids and associated peptides are created as peptidomimetics to address these issues.⁹⁻¹⁰ The different peptidomimetics of the α -helix, β -sheet, and β -turn are created and investigated for a variety of applications, such as medicinal behaviors and catalytic capabilities in chemical synthesis.¹¹⁻¹⁷ The β -hairpin, which is created by joining two β -strands through a loop in an antiparallel manner, is another significant peptidomimetics.¹⁸⁻²² The development of novel peptide-based nanomaterials and selective antibody binding are both greatly facilitated by the antiparallel-hairpin peptides.²³ D-pro/L-Pro and D-pro/L-Gly turns are incorporated into peptides to create stable β -hairpins. Yet, in nature, β -hairpins with parallel strands are uncommon. Using a dimethyl diamine linker, Gellman and colleagues created novel parallel β -hairpin peptides and thoroughly investigated their structural analyses utilising NMR and X-ray analyses.²⁴ In addition, the amide bonds and functional side chains of peptides act as naturally

occurring coordinating metal ligands. For instance, Fe/Cu/Zn ions-peptide complexes have important roles in controlling fundamental biological processes.²⁵ In the emerging field of biochemical research for developing therapeutic drugs and diagnostic probes, reactive oxygen species (ROS) generation regulation in living systems, metallopeptides play a major role.²⁶⁻²⁷ The most prevalent Copper-peptide, GHK-Cu(II), for instance, is thought of as a natural antioxidant and collagen-stimulating agent and may be found in human plasma and saliva.²⁸ Additional copper peptides (Cu(II)-Amyloid β -peptides) are related to ROS regulation in Alzheimer's disease.²⁹ Cu(II) ion coordinates with two histidine residues and the terminal Asp1-Ala2 dipeptide, according to the structural analysis of the Cu(II)-A peptide(**Figure 3.1a**).³⁰⁻³¹

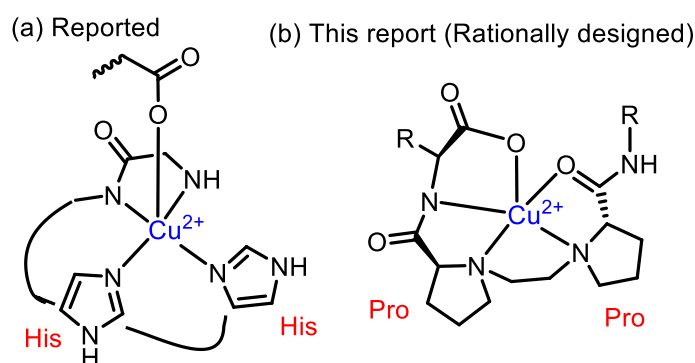


Figure 3.1 (a) Reported model of A β -peptides-Cu(II) complex; (b) Rationally designed bioinspired ligand and metal complex from pseudopeptides.

Cu-Peptidomimetics may therefore be used in the creation of new medicinal medicines. In addition to forming stable β -turn/sheet/hairpin structures, unnatural amino acids are being investigated as peptide ligands for metal complexation. Pseudopeptides, the bioinspired peptide ligands, have recently been created from achiral diamine and derivatives of amino acids such amino amides and bioamine acids (amino amides).³²⁻³³ The Cu(II) ions can also form complexes with these pseudopeptides. A different analogue, ethylenedipropyl acid, is said to create an EDTA-meditated Cu(II)-complex in aqueous solution. Because of their cyclic structures and flexibility, Pro and Gly residues are favoured in the literature for the

development of β -turn type structures.³⁴ Here, we present the rational design of novel pseudopeptides that bind two short peptides together via an ethylenedipropyl (etpro) scaffold. These pseudopeptides are likely to produce novel Cu(II)-peptidomimetics and secondary structures of the β -turn type in the presence of Cu(II)-ions. The creation of ethylenedipropyl (etpro) peptides, conformational analysis of those peptides, and Cu(II)-complexation using NMR, CD, Mass, EPR, and single crystal X-ray techniques are all included in this article.

3.1.1 Hypothesis and objective

In this article, the structural studies and synthesis of new pseudopeptides called ethylenedipropyl (etpro) tetra/hexapeptides, which contain a chiral diamine dicarboxylate scaffold, are discussed. It is highly supported by their NMR and CD spectrum investigations that the β -turn-type structures occur in organic solvents (ACN/MeOH). Also, the tetra pseudopeptide single-crystal X-ray experiments demonstrate that hydrogen bonding causes a distinctive self-assembly structure of the β -strand type to develop in the solid state. Significantly, its diamine moiety affects how Cu-complexes with Cu(II) ions form. These compounds might be taken into account for the development of peptide-based catalysts and medicinal medication candidates.

3.2 Results and discussion

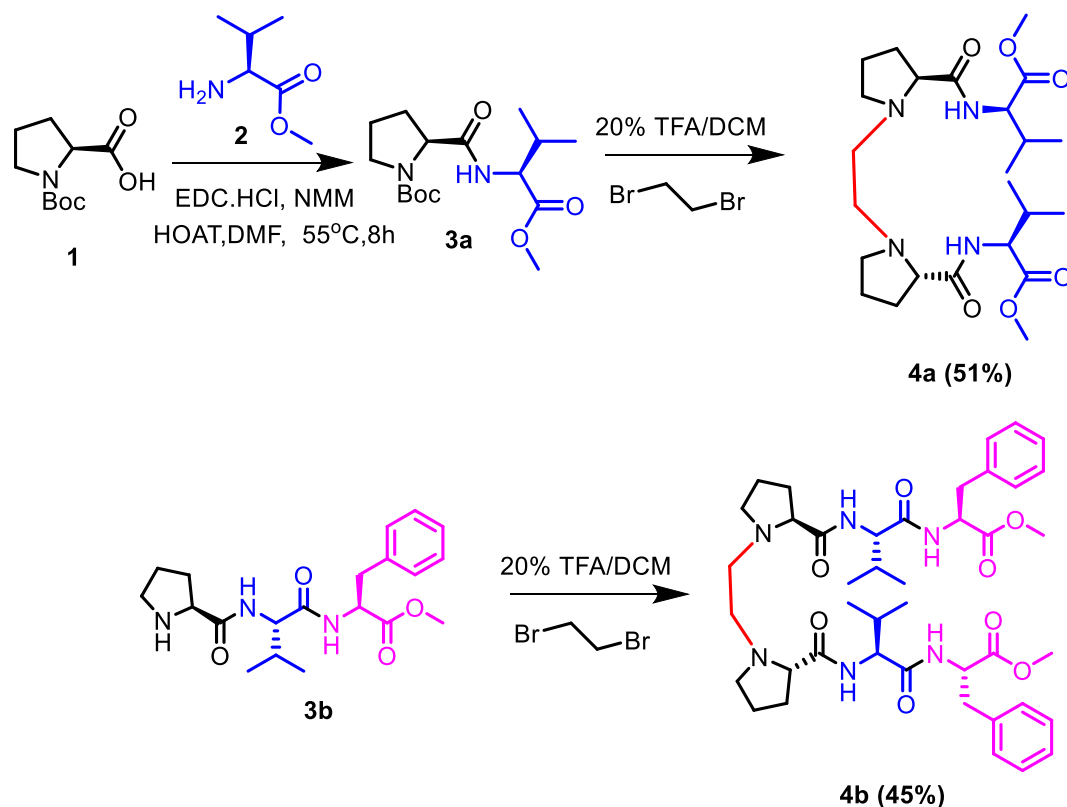
Here, we present a facile and elegant technique for joining two peptides at their *N*-termini through an ethylene bridge. In order to improve the intramolecular hydrogen bonding in the peptide backbone, which often affects the formation of β -turn forms of secondary structure, we planned to manufacture organic solvent-soluble peptides, mostly using aprotic solvents. Since Val and Phe are among the hydrophobic residues in non-polar amino acids and are therefore simple to dissolve in organic solvents, we solely used these residues. Crucially, the steric

effects of these thick side chain residues may allow for good selectivity over the structural alterations of their peptides in solution. Using commercially available native L-amino acids.

3.2.1 Synthesis of Ethylenediprollyl peptides

we started the synthesis of *etpro*-peptide ligands with L-Proline residue at the *N*-terminus (**Scheme 3.1**). The usual synthetic method of an amide bond was used. First the NBoc-Proline (**1**), which was coupled with valine methyl ester (**2**) by amide bond, producing *N*-prolyl terminated *di*-peptide (**3a**). For the formation of tripeptide (**3b**), boc deprotection of *di*-peptide (val-phe) was done and then coupled with boc proline. In order to create free amine at the *N*-terminus of prolyl peptides, their NBoc groups of proline residue were then removed under acidic conditions (20% TFA). This allowed for the *N*-alkylation with 1,2-dibromo ethane to occur under basic conditions. As a result, the intended *etpro*-tetra-peptides (**4a**) was extracted from the corresponding *di*-peptides (**3a**) whereas the desired *etpro*-hexapeptides (**4b**) were obtained in good yield from the *tri*-peptides (**3b**).

Scheme 3.1 Synthesis of Ethylenyldiprollyl (*etpro*) peptides



Our analysis of their 1D/2D-NMR and HRMS spectra revealed the structure of the corresponding peptides (**4a**, **4b**). In the literature, the synthesis of metalated peptides using achiral diamines as peptide-based ligands is described.³² The freshly formed pseudopeptides (**4a**, **4b**) contain chiral diamine residues, which may offer a special opportunity to control the secondary structure in small peptides and novel chiral peptide ligand for the synthesis of metallopeptides with coordinating metals.

3.2.2 Conformational analyses

Also, using 2D-NMR techniques, we looked at the potential structure of those pseudopeptides (**4a**, **4b**) in the solution phase. As a result, we captured the 2D NMR (COSY/NOESY) spectra of peptides in solvent CDCl₃. We also looked in to the 2D NMR spectra of control peptides (**3a**, **3b**) for comparison. We attributed the chemical shift of protons in pseudopeptides (**4a**, **4b**). In 2D-NOESY NMR spectra, the control di-peptide (**3a**) only displays two NOE cross-peaks, such as Val-CH₃ with BocCH₃ and Val-CH with BocCH₃, but no NOE with amide NH. Amide NH(e) displays NOE cross-peaks with Val-CH₃ in its tetra-peptide (**4a**), as well as other NOE interactions with Val-CH(d) with Val-CH₃(b), Val-CH(d) with OCH₃, and Val-CH₃ with OCH₃. Tetra-peptide (**4a**) had more divergent NOE interactions than the control *di*-peptide (**3a**), which may be related to the formation of the hairpin configuration (**Figure 3.2A**). Both amide NH do not display NOE interactions in the control *tri*-peptide **3c**. They do, however exhibit NOE cross-peaks like BocCH₃ with side chain Val (β -CH₃/ α -CH). In its hairpin *hexa*-peptide (**4b**), amide NH's have NOE cross-peaks such as NH(K) with Pro-CH/Val- α -CH/Val- β -CH₃ and NH(g) with Val-CH/Val-CH₃/Phe- α -CH/Phe- β -CH₂. In contrast to the corresponding control di-/tri-peptides, the amide NH of the *tetra*-/*hexa*-peptides (**4a**, **4b**) has NOE cross-peaks with other CH peaks (**3a**, **3b**). These findings clearly suggest that a β -turn kind of structure, most likely a β -turn type of structure, formed (**Figure 3.2A**).

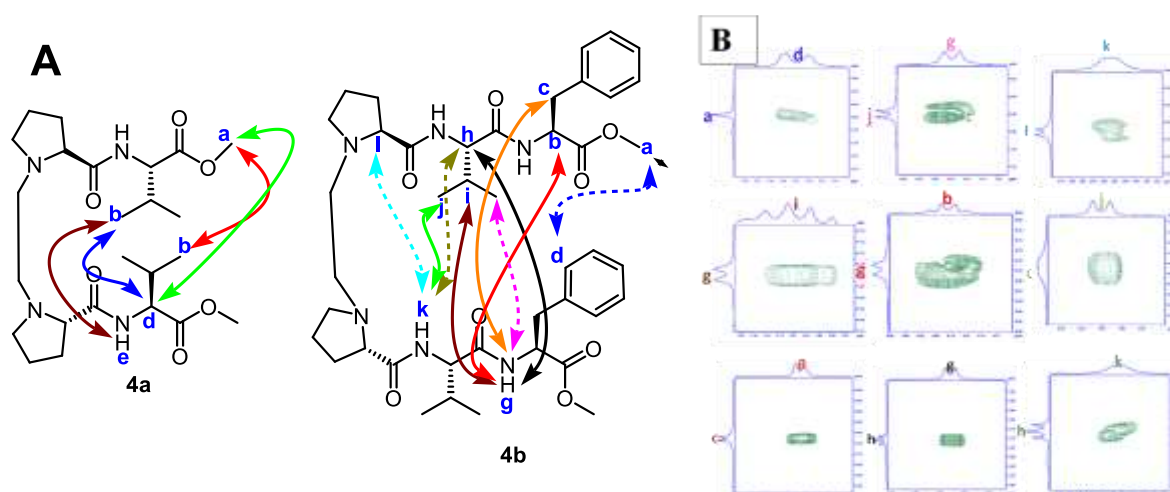


Figure 3.2 2D NMR (NOE) analyses: (A) NOE interactions in hairpin peptides **4a**, **4b** and (B) Selective NOE assessments of peptide **4b**.

3.2.3 DMSO D6 Titration study

By using ^1H -NMR techniques, we also investigated the hydrogen bonding between amide N-H and C=O of peptides. One of the well-known method to identify the intramolecular/intermolecular hydrogen-bonded amide N-H is DMSO- d_6 titration ^1H -NMR experiment in solution phase.³⁵ In order to compare tetra pseudopeptides to the control peptides **3a**, **3b** we did the DMSO- d_6 titration ^1H NMR experiment with peptides **4a**, **4b** in CDCl_3 . We plotted the NMR titration profiles (Chemical shift of amide NH vs. concentration of DMSO- d_6) and extracted the chemical shift values of their amide NHs in varied concentrations of DMSO- d_6 . Prolyl acetamide N-H of Pro-Val in peptides **3a**, **3b/4a**, **4b** exhibit nearly identical chemical shifts when DMSO- d_6 concentration increases.

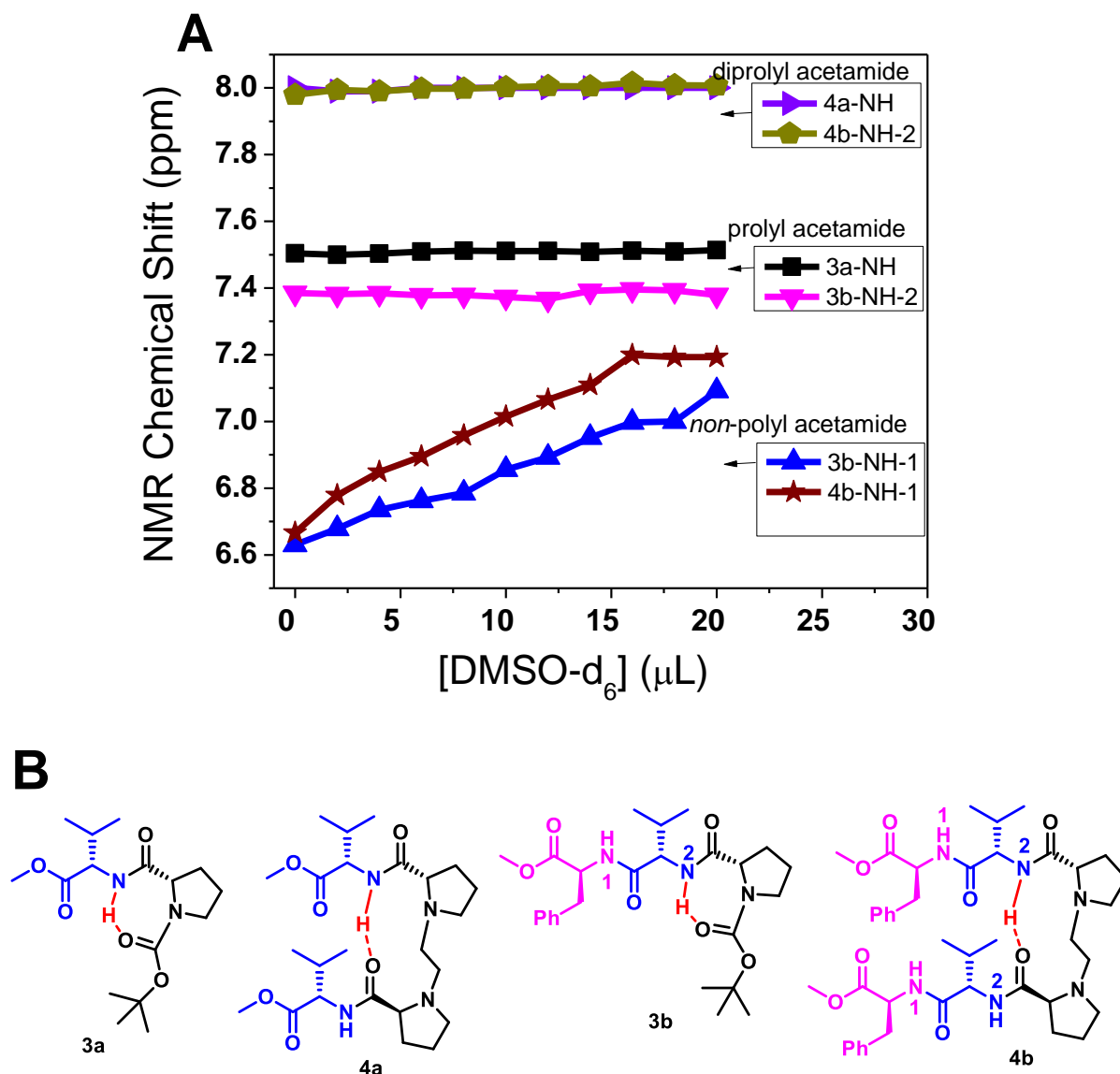


Figure 3.3 (A) DMSO- d_6 titration NMR profile of peptides **3a**, **3b/4a**, **4b**; and (B) Proposed Hydrogen bonding in *etpro*-peptides **3a**, **3b/4a**, **4b**.

However, non-prolyl amide N-H's (Val-Phe) of **3b/4b** are significantly downfield shifted with the increasing concentration of DMSO- d_6 . Thus, only prolyl acetamide N-H's of **3a**, **3b/4a**, **4b** are involved in the intramolecular hydrogen bonding in solution

(CDCl₃), with the NBoc carbonyl group. In literature, the prolyl *di*-peptides (X_{aa}-Pro/Pro-X_{aa}) reportedly form the β -/ γ -turn and open type conformation in solid states.^{25, 36-37} Hence we proposed the possible intramolecular hydrogen bonding (N-H---O=C) in control peptides (**3a**, **3b**) form γ -turn (**Figure 3.3A**), while *etpro*-peptides (**4a**, **4b**) form β -turn types structure in chloroform (CDCl₃) solution (**Figure 3.3B**).

Further, we recorded circular dichroism (CD) spectra of *etpro*-peptides (**4a**, **4b**) in acetonitrile (ACN)/methanol (MeOH) and compare with control peptides (**3a**, **3b**). In literature, β -/ γ -turn/ β -sheet also exhibit characteristic signal as maxima $\lambda_{200\text{nm}}$ and minima $\lambda_{220\text{nm}}$.³⁸⁻³⁹ The control dipeptide **3a** exhibit γ -turn type weak CD signal (max/min) only in ACN, while control tripeptides **3b** possibly exhibit β -/ γ -turn type signal in both solvents ACN/MeOH (**Figure 3.4**). The CD spectra of *etpro*-peptide **4a** exhibit characteristics β -turn/ β -strand type of CD signal such as maxima at wavelength 210nm ($\lambda_{210\text{nm}}$) and minima at 230nm ($\lambda_{230\text{nm}}$) in both solvents ACN/MeOH. However, the CD spectra of **4b** exhibit two maxima at wavelength ~200nm/220nm and one minima at wavelength ~230nm in both solvents ACN/MeOH. The typical CD signal of peptides appears mainly due to electronic transitions of amide bonds as n- π^* at wavelength ~222nm and π - π^* (parallel and perpendicular) at ~199nm and ~208nm.⁴⁰ The bathochromic and hypsochromic shifts are also observed in CD spectra of peptides in the different dielectric constant solvent environments. However, there is no linear correlation between CD signal and the dielectric constant of the solvents. Hence, CD spectra of *etpro*-pseudopeptides (**4a**, **4b**) exhibit a marginal bathochromic shift of β -turn type structure in organic solvents. However, the CD signals of *etpro*-peptide (**4a**) are more prominent than *etpro*-peptides (**4b**). Since peptide **4b** have additional phe residue which probably enhance the hydrophobic interactions with Val side chains and perturb the hydrogen bonding (N-H---O=C). As resultant regular β -turn structures are affected.

The DMSO NMR titration studies also suggest that phenyl-NH's are not involved in intramolecular hydrogen bonding.

3.3.4 Circular Dichroism study

We have also recorded the temperature-dependent CD spectra of annealed *etpro*-peptides (**4a**, **4b**) and control peptides (**3a**, **3b**) in ACN as solvent. The characteristic CD signal of control peptides (**3a**, **3b**) significantly decreases with temperature compared to the *etpro*-peptides **4a**, **4b**. These results strongly support the formation of thermally stable β -turn type of structure with *etpro*-peptides, prominently in **4a**, in organic solvent ACN. The β -turn is a structural motif common to many proteins and cyclic peptides, which are considered as potential mimicry of drug like small molecules such as ligand of GPCR (G-protein coupled receptor).⁴¹ Recently, Miller and co-workers have explored β -turn peptide motif in development of peptide based catalyst.³⁶ Hence these pseudopeptides (**4a**, **4b**) could be a new analogues of native β -turn motifs.

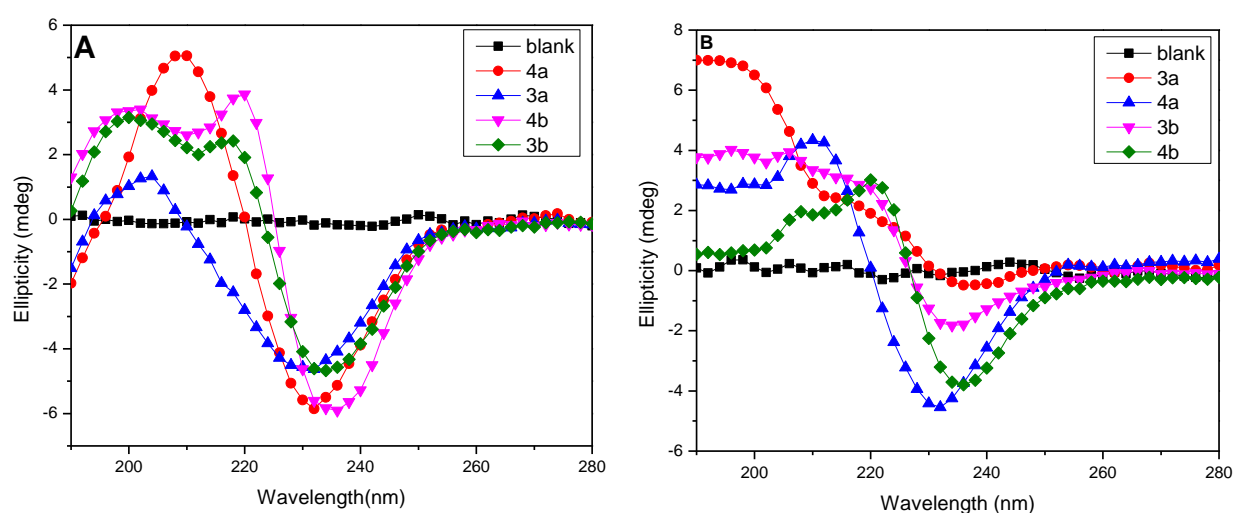


Figure 3.4 CD spectra of control and *etpro*-Peptides (**A**) in ACN and (**B**) in MeOH.

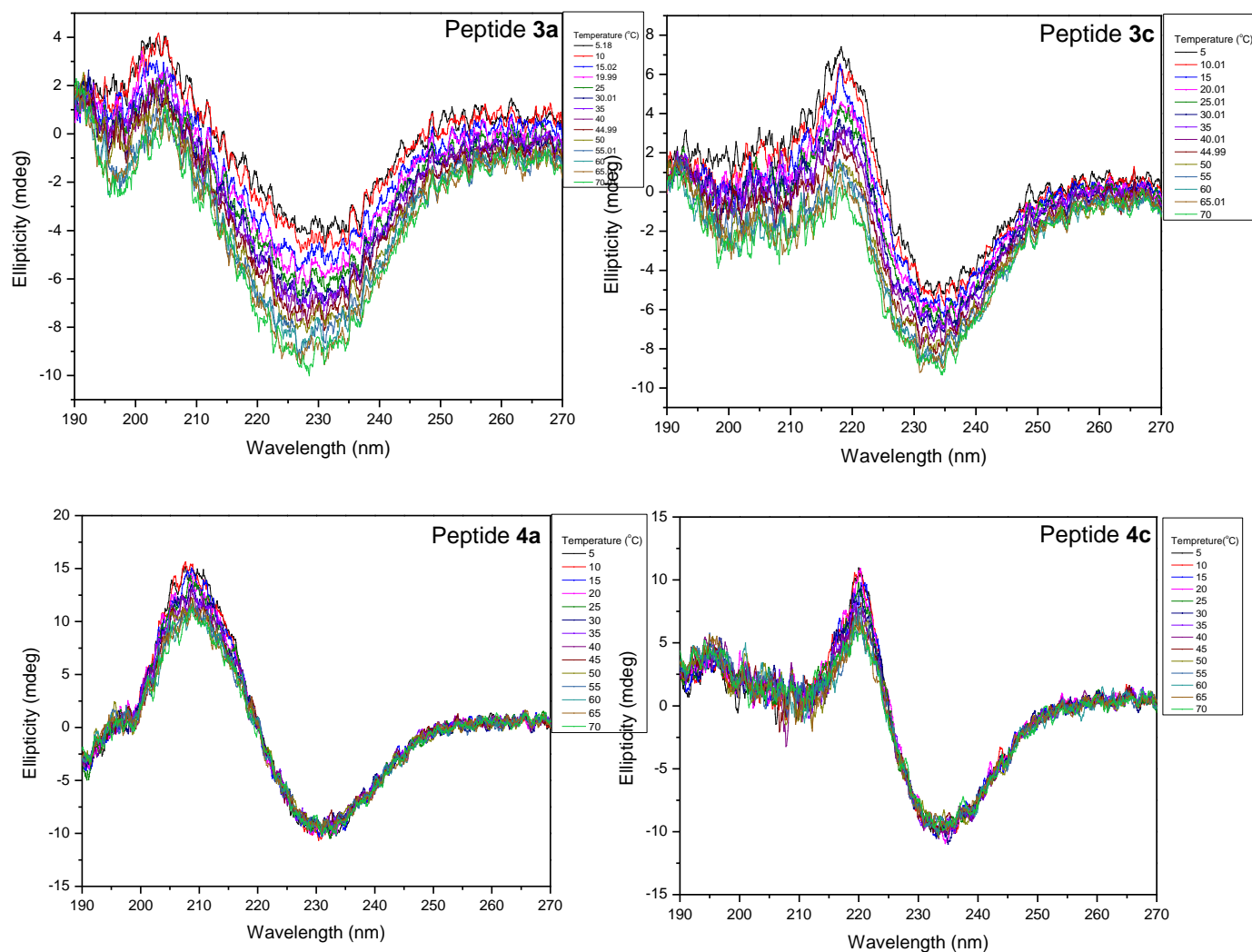


Figure 3.5 Temperature dependent CD spectra of control and *etpro*-Peptides in ACN.

3.3.5 Metalation of ethylene Ethylenediproyl peptides

To explore metal coordinating properties of *etpro*-Peptides, we treated pseudopeptides **4a**, **4b** with $\text{Cu}(\text{OAc})_2$ under basic reflux conditions in ethanol and then characterized by ESI-HRMS (**Scheme 3.2**). We compared the observed HRMS values of peptide ligands (**4a**, **4b**) and their complexes (**Table 3.1**). In the case of peptide **4a**, the observed HRMS values of *etpro*-peptide is increased by $m/z \sim 61.0$ that matches with m/z of $[\text{Cu}^{2+}]$, which strongly supported the formation of Cu(II) complex by deprotonation of two amide N-H's of peptide **4a** as the proposed structure **4a-Cu**. We also obtained the similar mass results with other peptides **4b**.

Thus our HRMS analyses strongly supports the formation of *etpro*-peptide-Cu(II) complex stoichiometrically with 1:1 ratio of peptides (**4a**, **4b**) and Cu ions.

Scheme 3.2 Synthesis of *etpro*-peptides-Cu(II) complexes

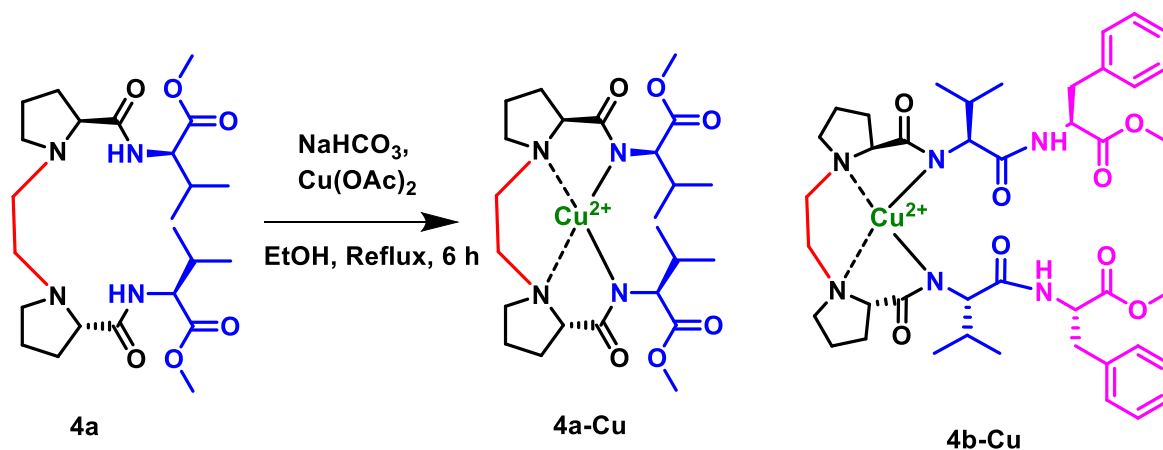


Table 3.1 Comparative HRMS analyses of Peptide ligand and their complexes

Entry	<i>Etpro</i> -Peptides	HRMS-Ligand	HRMS-Complex	Δ_{HRMS}^*
1	4a	483.3174 (Obs.) 483.3177 (Calcd.)	544.2313 (Obs) 544.2317 (Calcd.)	60.9139 (Obs)
2	4b	777.4552 (Obs.) 777.4545 (Calcd.)	838.3751 (Obs) 838.3685 (Calcd)	60.9199 (Obs)

3.3.6 EPR Study of Cu-peptides

The Cu(II)-complex with pseudopeptides ligands are well studied by EPR.⁴² We also recorded EPR spectra of *etpro*-peptides **4a-4b** Cu(II) in solvent MeOH at freezing temperature 100K. The EPR spectra of **4a-Cu(II)** and **4b-Cu(II)** complex is depicted in (Figure 3.6). The EPR spectra of peptide (**4a**)-Cu(II) complex indicate the g_{\parallel} values (2.4-2.1) are higher than g_{\perp} (2.03) and g_e as agreement $g_{\parallel} > g_{\perp} > g_e$. The EPR spectra of

Cu(II)-peptide distorted square planar/pyramidal are reported and exhibit nearly the same.⁴³⁻⁴⁴ The results are consistent with other pseudopeptides **4b** under similar freezing conditions. Hence *etpro*-peptides **4a-4d** form a stable distorted square planar complex with Cu(II) stoichiometric ratio (1:1). The metal complex of pseudopeptides comprising non-chiral diamine has shown remarkable self-assembly structural and functional properties.⁴⁵ Hence the Cu(II) complexes of pseudopeptides (**4a**, **4b**) containing chiral ligands could exhibit the similar structures and functions.

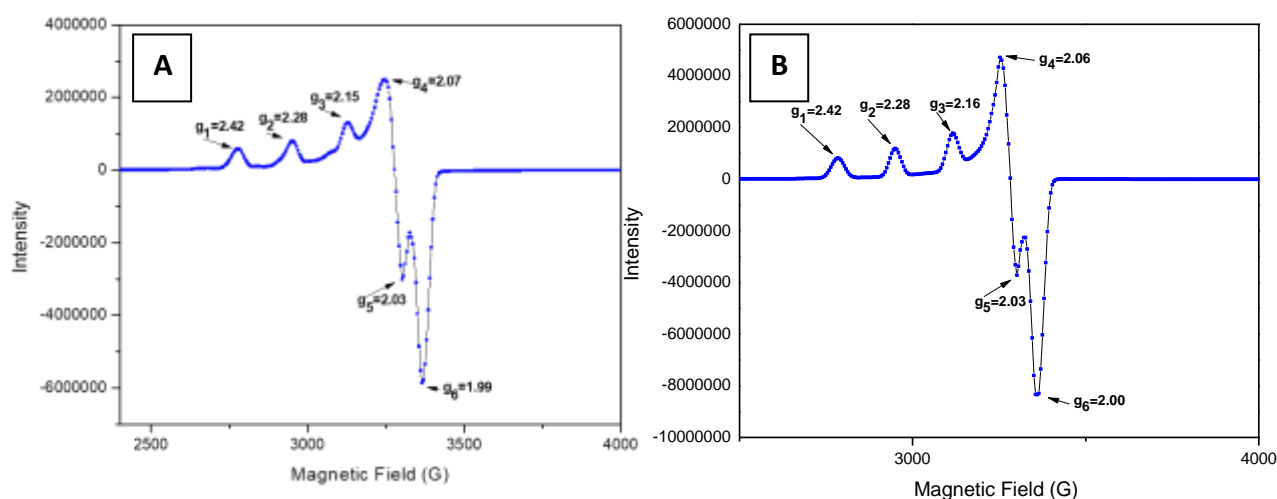


Figure 3.6 EPR spectra of *etpro*-peptide Cu-complex **4a-Cu** (A) and **4b-Cu** (B).

3.3 Conclusions

The syntheses of ethylenediproyl (*etpro*) pseudopeptides, comprising achiral diamine linker, are accomplished from native *di/tri*-peptides using amino acids like pro, val, and phe. The DMSO d_6 titration NMR suggests the possible intramolecular hydrogen bonding (N-H---O=C) in control peptides (**3a**, **3b**) form γ -turn while *etpro*-peptides (**4a**, **4b**) form β -turn types structure in chloroform in $CDCl_3$. Their NMR and CD analytical results reveals the formation of a unique β -turn type of conformational structure in organic solvents (ACN/MeOH) in solution phase. The formation of Cu(II) complex with *etpro*-pseudopeptides are demonstrated successfully by HRMS and EPR techniques.

Hence ethylenedipropyl pseudopeptides are new peptidomimics to form β -turn type of secondary structure in solution state and Cu(II)-complex. These peptide could be considered as an potential pseudopeptides ligand for various applications including inhibitor of A β -peptides and synthesis of metallopeptide based catalyst which are emerging area of research.

3.4 Experimental Section

3.4.1 Material and Instrumentation

The materials were purchased from commercial suppliers and used without purification. Anhydrous DMF was freshly prepared by distilling over calcium hydride. Reactions were monitored by thin-layer chromatography, visualized by UV and ninhydrin. Column chromatography was performed in 230–400 and 100–200 mesh silica. Mass spectra were obtained from a Bruker MicroTOF-Q II spectrometer. NMR spectra were recorded on Bruker AV-700 MHz and Bruker AV-400 ^1H (400 MHz), ^{13}C (100.6 MHz). ^1H and ^{13}C NMR chemical shifts were recorded in ppm downfield from tetramethylsilane, and splitting patterns are abbreviated as s, singlet; d, doublet; dd, doublet of doublet; t, triplet; q, quartet; dq, doublet of the quartet; m, multiplet. CD experiments were performed on JASCO-J 1500. All CD experiments were performed at 20°C, and the recorded two scans were averaged and from 310 to 190 nm wavelengths.

3.4.2 General Procedure for Peptide Coupling

NBoc protected amino acid (1.0 eq.) and amino acid ester (1.2 eq.), HOAt (1.3 eq.), were dissolved in dry DMF solvent. This reaction mixture was stirred for 10 min, then N-methyl morpholine (3.0 eq.) was added dropwise and cooled to 0°C followed by addition of EDC.HCl (1.3 eq.). Further, this mixture was heated to 55°C for 8–12h. The reaction was monitored by TLC. After completion of reaction, the crude reaction mixture was concentrated under reduced

pressure. This crude mixture was purified by column chromatography with organic solvent system, EtOAc, and hexane. The purified peptide was characterized by $^1\text{H}/^{13}\text{C}$ NMR and ESI-HRMS (ESI-ToF) techniques.

3.4.3 General Procedure for Synthesis of diprolyl Peptides (4a, 4b)

The *di/tripeptides* (2.0 eq.) were added to ACN along with base K_2CO_3 and allowed to stir at room temperature (rt) for 30 min. Dibromoethane (1 eq.) was added to the mixture at rt followed by heating at 65°C . The completion of reaction was monitored by TLC. The crude reaction mixture was concentrated under reduced pressure. The concentrated crude mixture was purified by column chromatography with organic solvent system MeOH and DCM. The obtained product was characterized by $^1\text{H}/^{13}\text{C}$ NMR and ESI-HRMS techniques.

3.4.4 General Procedure for Metalation of Peptides

Corresponding peptides (1 eq.) were dissolved in EtOH. To this solution, NaHCO_3 was added, and pH 9 was maintained. Then the solution was allowed to stir for 15 min at rt. Two eq. of $\text{Cu}(\text{OAc})_2$ was added to this reaction mixture followed by refluxing for 6 h. The completion of reaction was monitored by TLC. The crude reaction mixture was filtered through Celite, and the filtrate was evaporated under reduced pressure.

3.4.5 Chemical shift values of NMR

Dimethyl-2,2'-(((2S,2'S)-1,1'-(ethane-1,2-diyl)bis(pyrrolidine-1,2-diyl-carbonyl))bis(azanediyl)) (2S,2'S) bis(3-methylbutanoate) (4a). Peptide **4a** was synthesized by the general procedure for synthesis of hairpin peptide (the above-mentioned procedure) and purified by column chromatography with solvent system methanol:dichloromethane (2:98) as a pale yellow semiliquid (0.5 g, 51% yield). ^1H NMR (400 MHz, CDCl_3) δ (ppm) 8.01 (d, $J = 8.0$ Hz, 2H), 4.52 (dd, $J = 4.0, 8.0$ Hz, 2H), 3.74 (s, 6H), 3.27 (m, 2H), 3.12 (dd, $J = 4.0, 4.0$ Hz,

2H), 2.82–2.77 (m, 2H), 2.77–2.68 (m, 2H), 2.41–2.36 (m, 2H), 2.23–2.18 (m, 4H), 1.91–1.76 (m, 6H), 0.93 (dd, $J = 4.0, 8.0$ Hz, 12H). ^{13}C NMR (101 MHz, CDCl_3) δ (ppm) 174.8, 172.1, 67.7, 56.2, 55.1, 54.4, 51.8, 31.2, 30.8, 24.2, 18.9, 17.6. HRMS (ESI) m/z : $[\text{M} + \text{H}]^+$ calcd for $\text{C}_{24}\text{H}_{43}\text{N}_4\text{O}_6$ 483.3177; found 483.3174.

Dimethyl-2,2'-(((2S,2'S)-2,2'-(((2S,2'S)-1,1'-(ethane-1,2-diyl)bis-(pyrrolidine-1,2-diyl-2-carbonyl))bis(azanediyl))bis(3-methylbutanoyl))bis(azanediyl))(2S,2'S)bis(3-phenylpropanoate) (**4b**). Peptide **4b** was synthesized by the general procedure and purified by column chromatography with solvent system methanol:dichloromethane (3:97) as a pale yellow semiliquid (1.0 g, 45% yield). ^1H NMR (400 MHz, CDCl_3) δ (ppm) 7.97 (d, $J = 4.0$ Hz, 2 H), 7.30–7.28 (m, 4 H), 7.24–7.22 (m, 2 H), 7.14 (d, $J = 8.0$ Hz, 4 H), 6.68 (d, $J = 8.0$ Hz, 2 H), 4.79 (d, $J = 4.0$ Hz, 2 H), 4.17–4.13 (m, 2 H), 3.68(s, 6H), 3.09–3.07 (m, 8 H), 2.66–2.64 (m, 2 H), 2.50–2.48 (m, 2 H), 2.25–2.19 (m, 2 H), 2.13–2.08 (m, 4 H), 1.88–1.85 (m, 2 H), 1.74–1.73 (m, 4 H), 0.90 (d, $J = 8.0$ Hz, 12 H). $^{13}\text{C}\{^1\text{H}\}$ NMR (101 MHz, CDCl_3) δ (ppm) 175.2, 171.8, 170.8, 135.9, 129.2, 128.6, 127.1, 67.9, 58.3, 54.9, 54.1, 53.3, 52.2, 37.8, 30.8, 30.6, 24.2, 19.2, 18.2. HRMS (ESI) m/z : $[\text{M} + \text{H}]^+$ calcd for $\text{C}_{42}\text{H}_{61}\text{N}_6\text{O}_8$ 777.4545; found 777.4552.

Tetrapeptide-Cu(II) Complex (4a-Cu). **4a-Cu** was synthesized by the general procedure as a dark blue semiliquid. HRMS (ESI) m/z : $[\text{M} + \text{H}]^+$ calcd for $\text{C}_{24}\text{H}_{41}\text{N}_4\text{O}_6\text{Cu}$ 544.2317; found 544.2313.

Hexapeptide-Cu(II) Complex (4b-Cu). **4b-Cu** was synthesized by the general procedure as a blue semiliquid. HRMS (ESI) m/z : $[\text{M} + \text{H}]^+$ calcd for $\text{C}_{42}\text{H}_{59}\text{N}_6\text{O}_8\text{Cu}$ 838.3685; found 838.3751.

3.5 References

1. Ngounou Wetie, A. G.; Sokolowska, I.; Woods, A. G.; Roy, U.; Loo, J. A.; Darie, C. C., Investigation of stable and transient protein–protein interactions: past, present, and future. *Proteomics* **2013**, *13* (3-4), 538-557.
2. Yoo, J.; Winogradoff, D.; Aksimentiev, A., Molecular dynamics simulations of DNA–DNA and DNA–protein interactions. *Current Opinion in Structural Biology* **2020**, *64*, 88-96.
3. Fosgerau, K.; Hoffmann, T., Peptide therapeutics: current status and future directions. *Drug discovery today* **2015**, *20* (1), 122-128.
4. Lenci, E.; Trabocchi, A., Peptidomimetic toolbox for drug discovery. *Chemical Society Reviews* **2020**, *49* (11), 3262-3277.
5. Eisenberg, D., The discovery of the α -helix and β -sheet, the principal structural features of proteins. *Proceedings of the National Academy of Sciences* **2003**, *100* (20), 11207-11210.
6. Cheng, R. P.; Gellman, S. H.; DeGrado, W. F., β -Peptides: from structure to function. *Chemical reviews* **2001**, *101* (10), 3219-3232.
7. Girvin, Z. C.; Andrews, M. K.; Liu, X.; Gellman, S. H., Foldamer-templated catalysis of macrocycle formation. *Science* **2019**, *366* (6472), 1528-1531.
8. Van Regenmortel, M., Antigenicity and immunogenicity of synthetic peptides. *Biologicals* **2001**, *29* (3-4), 209-213.
9. Guarna, A.; Trabocchi, A., *Peptidomimetics in organic and medicinal chemistry: the art of transforming peptides in drugs*. John Wiley & Sons: 2014.
10. Kreutzer, A. G.; Nowick, J. S., Elucidating the structures of amyloid oligomers with macrocyclic β -hairpin peptides: insights into Alzheimer's disease and other amyloid diseases. *Accounts of chemical research* **2018**, *51* (3), 706-718.
11. Girvin, Z. C.; Gellman, S. H., Foldamer catalysis. *Journal of the American Chemical Society* **2020**, *142* (41), 17211-17223.
12. Fremaux, J.; Mauran, L.; Pulka-Ziach, K.; Kauffmann, B.; Odaert, B.; Guichard, G., α -Peptide–Oligourea Chimeras: Stabilization of Short α -Helices by Non-Peptide Helical Foldamers. *Angewandte Chemie* **2015**, *127* (34), 9954-9958.
13. Hanessian, S.; Luo, X.; Schaum, R.; Michnick, S., Design of Secondary Structures in Unnatural Peptides: Stable Helical gamma-Tetra-Hexa-, and Octapeptides and Consequences of -Substitution. *JOURNAL-AMERICAN CHEMICAL SOCIETY* **1998**, *120*, 8569-8570.

14. Simonovsky, E.; Miller, Y., Controlling the properties and self-assembly of helical nanofibrils by engineering zinc-binding β -hairpin peptides. *Journal of Materials Chemistry B* **2020**, 8 (33), 7352-7355.
15. Tang, Q.; Zhong, Y.; Miller, D. P.; Liu, R.; Zurek, E.; Lu, Z.-L.; Gong, B., Reverse turn foldamers: an expanded β -turn motif reinforced by double hydrogen bonds. *Organic letters* **2020**, 22 (3), 1003-1007.
16. Bomar, M. G.; Song, B.; Kibler, P.; Kodukula, K.; Galande, A. K., An enhanced β turn in water. *Organic Letters* **2011**, 13 (21), 5878-5881.
17. Zhai, L.; Otani, Y.; Hori, Y.; Tomita, T.; Ohwada, T., Peptide-based short single β -strand mimics without hydrogen bonding or aggregation. *Chemical Communications* **2020**, 56 (10), 1573-1576.
18. de Alba, E.; Jiménez, M. A.; Rico, M., Turn residue sequence determines β -hairpin conformation in designed peptides. *Journal of the American Chemical Society* **1997**, 119 (1), 175-183.
19. Robinson, J. A., β -Hairpin peptidomimetics: design, structures and biological activities. *Accounts of chemical research* **2008**, 41 (10), 1278-1288.
20. Blandl, T.; Cochran, A. G.; Skelton, N. J., Turn stability in β -hairpin peptides: Investigation of peptides containing 3: 5 type I G1 bulge turns. *Protein Science* **2003**, 12 (2), 237-247.
21. Liu, Y.; Xia, X.; Xu, L.; Wang, Y., Design of hybrid β -hairpin peptides with enhanced cell specificity and potent anti-inflammatory activity. *Biomaterials* **2013**, 34 (1), 237-250.
22. Tatko, C. D.; Waters, M. L., Selective aromatic interactions in β -hairpin peptides. *Journal of the American Chemical Society* **2002**, 124 (32), 9372-9373.
23. Hong, M.; Lyu, W.; Wang, Y.; Zou, J.; Chen, Z.-G., Establishing the golden range of Seebeck coefficient for maximizing thermoelectric performance. *Journal of the American Chemical Society* **2020**, 142 (5), 2672-2681.
24. Freire, F.; Almeida, A. M.; Fisk, J. D.; Steinkruger, J. D.; Gellman, S. H., Impact of Strand Length on the Stability of Parallel- β -Sheet Secondary Structure. *Angewandte Chemie International Edition* **2011**, 50 (37), 8735-8738.
25. Mir, F. M.; Crisma, M.; Toniolo, C.; Lubell, W. D., Isolated α -turn and incipient γ -helix. *Chemical Science* **2019**, 10 (28), 6908-6914.
26. Chassaing, S.; Collin, F.; Dorlet, P.; Gout, J.; Hureau, C.; Faller, P., Copper and heme-mediated Abeta toxicity: redox chemistry, Abeta oxidations and anti-ROS compounds. *Current topics in medicinal chemistry* **2012**, 12 (22), 2573-2595.
27. Tupe, S.; Deshpande, M., Current status and new directions in antifungal drug development. 2013; pp 241-252.

28. Espino, J.; Pariente, J. A.; Rodríguez, A. B., Oxidative Stress and Immunosenescence: Therapeutic Effects of Melatonin. *Oxidative Medicine and Cellular Longevity* **2012**, 2012, 670294.
29. Arrigoni, F.; Prosdocimi, T.; Mollica, L.; De Gioia, L.; Zampella, G.; Bertini, L., Copper reduction and dioxygen activation in Cu–amyloid beta peptide complexes: insight from molecular modelling. *Metallomics* **2018**, 10 (11), 1618-1630.
30. Cheignon, C.; Jones, M.; Atrián-Blasco, E.; Kieffer, I.; Faller, P.; Collin, F.; Hureau, C., Identification of key structural features of the elusive Cu-A β complex that generates ROS in Alzheimer's disease. *Chemical science* **2017**, 8 (7), 5107-5118.
31. Hureau, C., Coordination of redox active metal ions to the amyloid precursor protein and to amyloid- β peptides involved in Alzheimer disease. Part 1: An overview. *Coordination Chemistry Reviews* **2012**, 256, 2164-2174.
32. Luis, S. V.; Alfonso, I., Bioinspired chemistry based on minimalistic pseudopeptides. *Accounts of chemical research* **2014**, 47 (1), 112-24.
33. Faggi, E.; Gavara, R.; Bolte, M.; Fajari, L.; Juliá, L.; Rodríguez, L.; Alfonso, I., Copper(ii) complexes of macrocyclic and open-chain pseudopeptidic ligands: synthesis, characterization and interaction with dicarboxylates. *Dalton Transactions* **2015**, 44 (28), 12700-12710.
34. Metrano, A. J.; Abascal, N. C.; Mercado, B. Q.; Paulson, E. K.; Hurtley, A. E.; Miller, S. J., Diversity of Secondary Structure in Catalytic Peptides with β -Turn-Biased Sequences. *Journal of the American Chemical Society* **2017**, 139 (1), 492-516.
35. Dalabehera, N. R.; Meher, S.; Bhusana Palai, B.; Sharma, N. K., Instability of Amide Bond with Trifluoroacetic Acid (20%): Synthesis, Conformational Analysis, and Mechanistic Insights into Cleavable Amide Bond Comprising β -Troponylhydrazino Acid. *ACS omega* **2020**, 5 (40), 26141-26152.
36. Metrano, A. J.; Abascal, N. C.; Mercado, B. Q.; Paulson, E. K.; Hurtley, A. E.; Miller, S. J., Diversity of secondary structure in catalytic peptides with β -turn-biased sequences. *J. Am. Chem. Soc.* **2017**, 139 (1), 492-516.
37. Organic & biomolecular chemistry Sengupta, A.; Aravinda, S.; Shamala, N.; Raja, K. M. P.; Balaram, P., Structural studies of model peptides containing β -, γ -and δ -amino acids. *Org. Biomol. Chem.* **2006**, 4 (22), 4214-4222.
38. Migliore, M.; Bonvicini, A.; Tognetti, V.; Guilhaudis, L.; Baaden, M.; Oulyadi, H.; Joubert, L.; Ségalas-Milazzo, I., Characterization of β -turns by electronic circular dichroism spectroscopy: a coupled molecular dynamics and time-dependent density functional theory computational study. *Phys. Chem. Chem. Phys.* **2020**, 22 (3), 1611-1623.
39. De La Paz, M. L.; Goldie, K.; Zurdo, J.; Lacroix, E.; Dobson, C. M.; Hoenger, A.; Serrano, L., De novo designed peptide-based amyloid fibrils. *Proc Natl Acad Sci U S A* **2002**, 99 (25), 16052-16057.

40. Miles, A. J.; Wallace, B. A., Circular dichroism spectroscopy of membrane proteins. *Chem. Soc. Rev.* **2016**, *45* (18), 4859-4872.
41. Craik, D. J.; Fairlie, D. P.; Liras, S.; Price, D., The future of peptide-based drugs. *Chem. Biol. Drug. Des.* **2013**, *81* (1), 136-147.
42. Faggi, E.; Gavara, R.; Bolte, M.; Fajari, L.; Juliá, L.; Rodriguez, L.; Alfonso, I., Copper (ii) complexes of macrocyclic and open-chain pseudopeptidic ligands: synthesis, characterization and interaction with dicarboxylates. *Dalton Transactions* **2015**, *44* (28), 12700-12710.
43. Cheignon, C.; Jones, M.; Atrián-Blasco, E.; Kieffer, I.; Faller, P.; Collin, F.; Hureau, C., Identification of key structural features of the elusive Cu–A β complex that generates ROS in Alzheimer's disease. *Chemical science* **2017**, *8* (7), 5107-5118.
44. Yako, N.; Young, T. R.; Cottam Jones, J. M.; Hutton, C. A.; Wedd, A. G.; Xiao, Z., Copper binding and redox chemistry of the A β 16 peptide and its variants: insights into determinants of copper-dependent reactivity. *Metallomics* **2017**, *9* (3), 278-291.
45. Luis, S. V.; Alfonso, I., Bioinspired chemistry based on minimalistic pseudopeptides. *Acc. Chem. Res.* **2014**, *47* (1), 112-124.

CHAPTER-4a

**Pd(II)-Catalysed C(sp²)-H olefination: synthesis of *N*-alkylated isoindolinone scaffolds
from aryl amides of amino acid esters**

TABLE OF CONTENTS

Chapter 4a	91
4a.1 Introduction.....	91
4a.1.1 Hypothesis and objective	92
4a.2 Result and discussion.....	93
4a.2.1 Synthesis of <i>Chiral</i> isoindolinone derivatives	94
4a.2.2 Substrate scope using various amino ester	96
4a.2.3 Substrate scope using using different aryl groups	98
4a.2.4 The proposed reaction mechanism	99
4a.3 Conclusion	100
4a.4 Experimental Section.....	101
4a.4.1 Materials and instrumentation	101
4a.4.2 General procedure for amide synthesis.....	101
4a.4.3 General procedure for Pd-catalysed reactions	102
4a.4.4 Chemical shift values of NMR	102
4a.5 References	110

Chapter 4a

4a.1 Introduction

A broad variety of naturally occurring, synthetic, biologically and pharmaceutically active compounds contain the structural motif of the isoindolinone scaffold. Pagoclone, indoprofen, erinacerins, lennoxamine, lenalidomide, isohericenone, pazinaclone are some of the examples (**Figure 4a.1a**).¹⁻³ These molecule show, antioxidant, antifungal, anti-parkinsons, anti-inflammatory, antipsychotic, antihypertensive, anesthetic, vasodilatory, anxiolytic, antiviral, anti-cancer activities. The classical synthesis of isoindolinone derivatives involves challenging multi-step synthetic strategies.⁴⁻⁶ Recent years have seen the emergence of C-H olefination and C-H activation as synthetic techniques for the synthesis of different natural products and their precursors.⁷⁻⁹ With Pd-catalyst, Maiti and colleagues have created a number of impressive C(sp²)-H olefination methods.¹⁰⁻¹⁸ He has also explored substrate-specific C(sp²)-H olefination with Co-/Rh catalysts.¹⁹⁻²¹ In the presence of transition metal catalysts, (Au, Co, Cu, In, Ir, Ni, Pd, Rh, Ru, Sc, Yb, and Zn) the synthesis of isoindolinone derivatives has also been achieved using activated arylamides and non-reactive olefins (**Figure 4a.1b**).²² The arylamide-containing tolyl sulfonate (Ts), methyl sulfonate (Ms), and alkoxides are capable of complexing metals in the presence of external ligands.

Additionally, the directing group with acrylamides has been utilised in the synthesis of isoindolinone derivatives from non-activated olefins through C-(sp²)-H olefination.²³ For example in the presence of a Pd(II)-catalyst, the quinoline directing group with arylamides produces *N*-quinolinyl substituted isoindolinones from acrylate. *N*-tosylated benzamide, however, requires the ligand to produce isoindolinone derivatives from olefins using Pd-catalyzed olefination.²⁴⁻²⁵ Peptides and amino acids have been used as directing groups and ligands in a variety of transition metal-catalysed C-H olefination and activation reactions

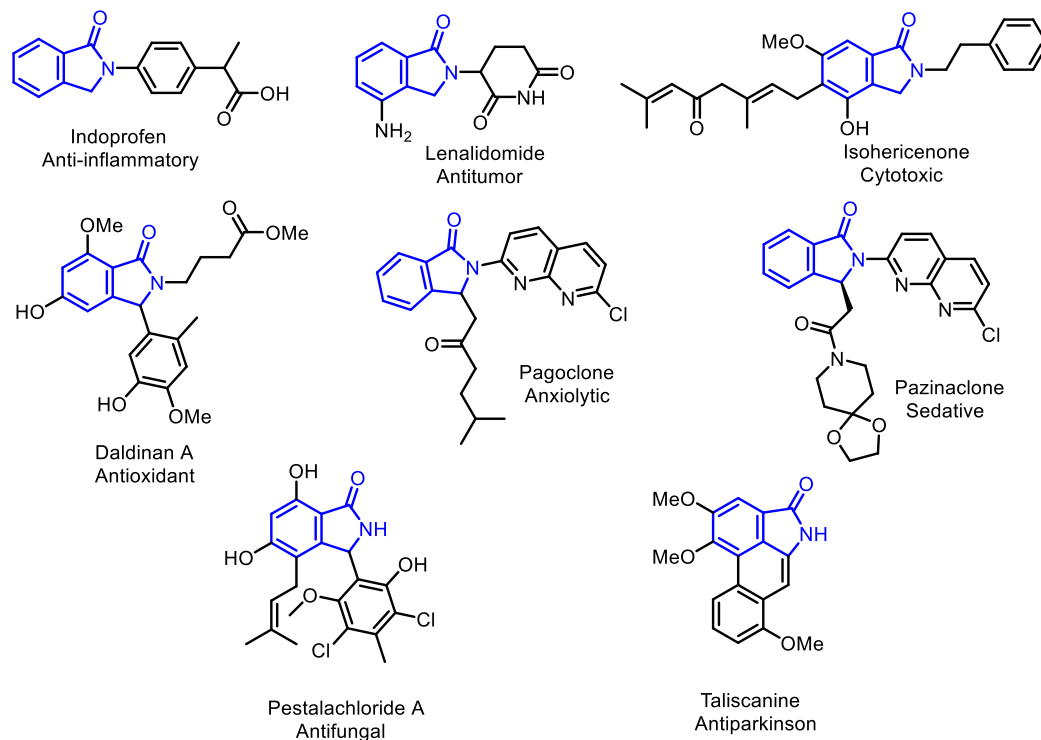
because they are natural ligands of many transition metals.²⁶ Yu and coworkers have investigated employing amino acids/peptides as the ligand or directing group in the metal-catalysed C(sp³)-H functionalization of *di-/tri/tetra*-peptides at the *N*-terminus/site-specific C-H alkynylation/ β -C-H arylation.²⁷⁻²⁹ Albericio has demonstrated the synthesis of stapled-peptides by the late-stage C(sp³)-H activation.³⁰⁻³¹ 2-Thiomethylaniline used as a directing group for C(sp³)-H functionalization of *N*-protected amino acids at the β -position with different aryl halides shown by Tran and Daugulis.³² The metal-catalysed C-H olefination amino acids and peptides has opened up possibilities for the synthesis of numerous synthetic and natural peptide analogues.³³⁻³⁴ A new approach for synthesising substituted aryl amide derivatives, metal catalysed olefination of ligand-enabled aryl amide with olefins is an emerging synthetic methodology.^{16, 35-41} Recently, Maiti and co-workers have investigated template-based regioselective C-H olefinations with inactive aliphatic olefins using Pd(II)-catalysed 8-AQ as a directing group.³⁷⁻⁴³ Wang and colleagues showed how to produce benzosultam peptidomimetics at benzyisulfonamide by the ortho-olefination reaction and cyclization reaction by Pd(II)-catalysed reactions.⁴⁴ These findings motivated the investigation of the synthesis of isoindolinone derivatives from arylamides of naturally occurring amino acids and olefins. This study describes the synthesis of N/C3-substituted isoindolinone molecules using a Pd(II)-catalyst from benzamides of natural amino acid derivatives.

4a.1.1 Hypothesis and objective

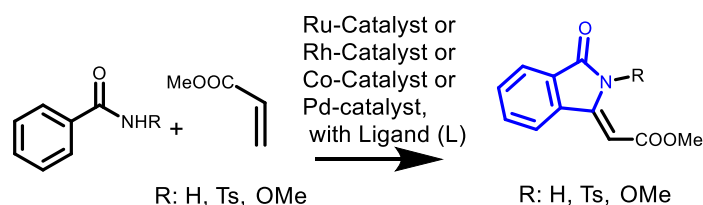
This study discusses the Pd-catalysed C(sp²)-H olefination process used to produce N-alkyl-3-methenyl chiral isoindolinone derivatives from aryl amides of L-amino acids and non-activated alkene. Here, the olefination of aryl ring is directed by the amino acid residue, and the amide NH then undergoes cyclization. Therefore, this approach may be useful to convert

common amino acids into their corresponding chiral isoindolinone derivatives (**Figure 4a.1c**).

(a) Natural Products



(b) Previous work



(c) This work

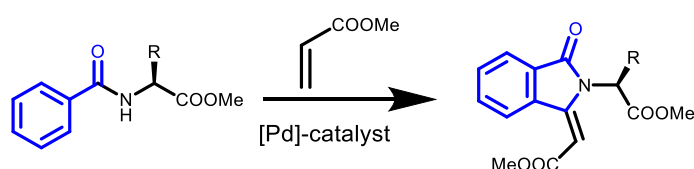


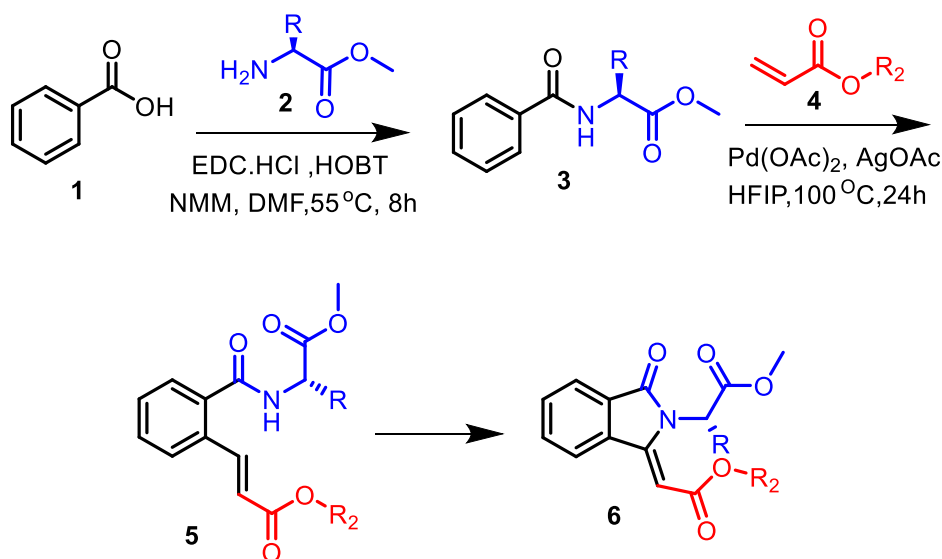
Figure 4a.1 (a) Isoindolinone and related natural products, (b) the previously reported isoindolinone, and (c) the isoindolinone reported in this paper.

4a.2 Result and discussion

4a.2.1 Synthesis of *Chiral* isoindolinone derivatives

This research began by synthesizing isoindolinone derivatives from the natural amino acid glycine (**Scheme 4a.1**). Using amide coupling conditions, the benzoic acid (**2**) was transformed into benzamide glycinate (**3**) and then olefination took place in sp^2 C–H bond of benzamide (**3**) with nonreactive acrylate (**4**) in the presence of the catalyst $Pd(OAc)_2$ (10 mol%) and the additive $AgOAc$ (oxidant) under the heating conditions ($100^\circ C$). There was only one product isolated with silica gel column and it was characterized by NMR, and ESI-HRMS. The analytical findings provided solid support for the development of 3-acrylatyl-*N*-glycinyloxy isoindolinone derivatives (**6**) rather than an olefin compound **5**.

Scheme 4a.1 Synthesis of 3-methylenyl-*N*-alkyl chiral isoindolin-1-one molecules



The same results were carried out using other acrylates such as ethyl acrylate (**4b**) and n-butyl acrylate (**4c**) which also produced isoindolinone derivatives (**6b-6c**) respectively. Compound **6a** was isolated into a single crystal, which was then examined using X-ray diffraction. The CCDC received the solved X-ray data under reference number 2098113. Along with the unit cell packing diagrams, the ORTEP diagram is also shown (**Figure 4a.2**). Compound **6a**'s trans-(E)-acrylatyl glyciny isoindolinone molecule was identified by its crystal structure. Its packing diagram shows how a supramolecular structure of the β -sheet type self-assembles. By carrying out identical reactions repeatedly with various substrate benzamide/acrylate, catalyst Pd(OAc)₂, oxidant (AgOAc), solvent, reaction time and temperature concentrations, the reaction conditions were also optimized for the highest yield (**Table 4a.1**). With 10% mole Pd(OAc)₂ and 3.0 eq. of AgOAc the optimal conditions resulted in a maximum yield of 80% in HFIP after 24 hours at 100 °C.

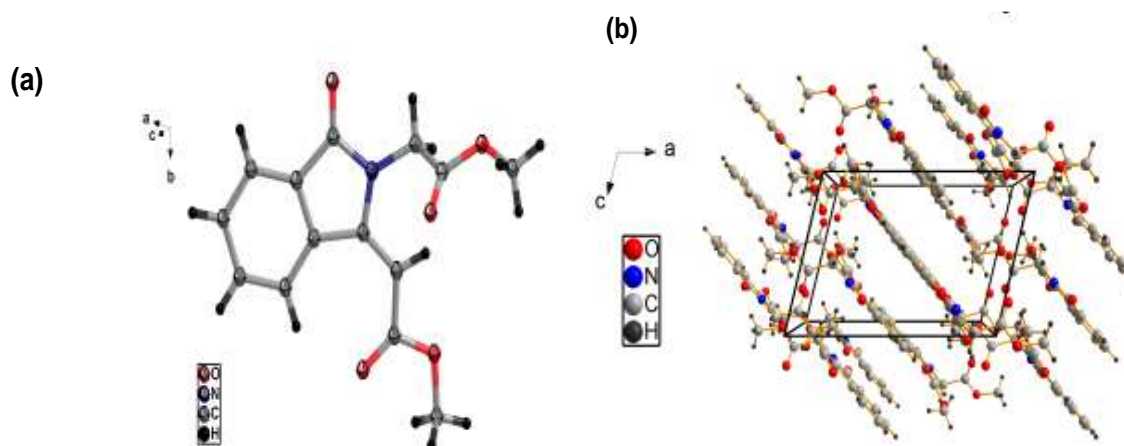
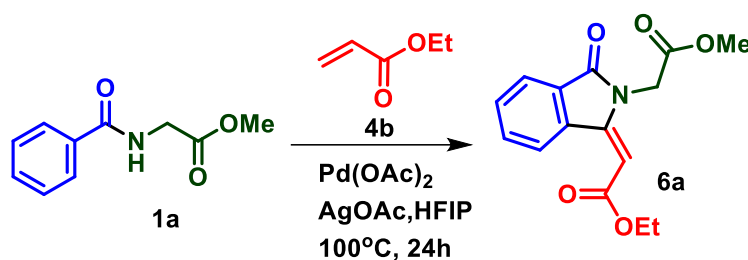


Figure 4a.2 (a) ORTEP diagram and (b) Unit cell of acrylatyl glyciny Isoindolinone **6a**.

Table 4a.1 Optimized reaction condition



Entry	Solvent	Ethylacrylate (eq)	AgOAc (eq)	$\text{Pd}(\text{OAc})_2$ (mol %)	Time (h)	Temperature ($^\circ\text{C}$)	Yield (%)
1	DCE	2	3	10	24	100	47
2	Dry DMF	2	3	10	24	100	24
3	Dry ACN	2	3	10	24	100	Trace
4	HFIP	2	3	10	24	100	81
5	t BuOH	2	3	10	24	100	77
6	HFIP	2	3	10	24	100	39
			(AgCO_3)				
7	HFIP	2	2	10	24	100	54
			(AgCO_3)				
8	HFIP	2	3	10	24	100	52
9	HFIP	2	3	0.5	24	100	62
10	HFIP	3	3	10	24	100	69
11	HFIP	4	3	10	24	100	80
12	HFIP	2	3	10	24	70	56
13	HFIP	2	3	10	24	130	68
14	HFIP	2	3	10	24	150	65
15	HFIP	2	3	10	6	150	Nd
16	HFIP	2	3	10	18	150	65
17	HFIP	2	3	10	30	150	68

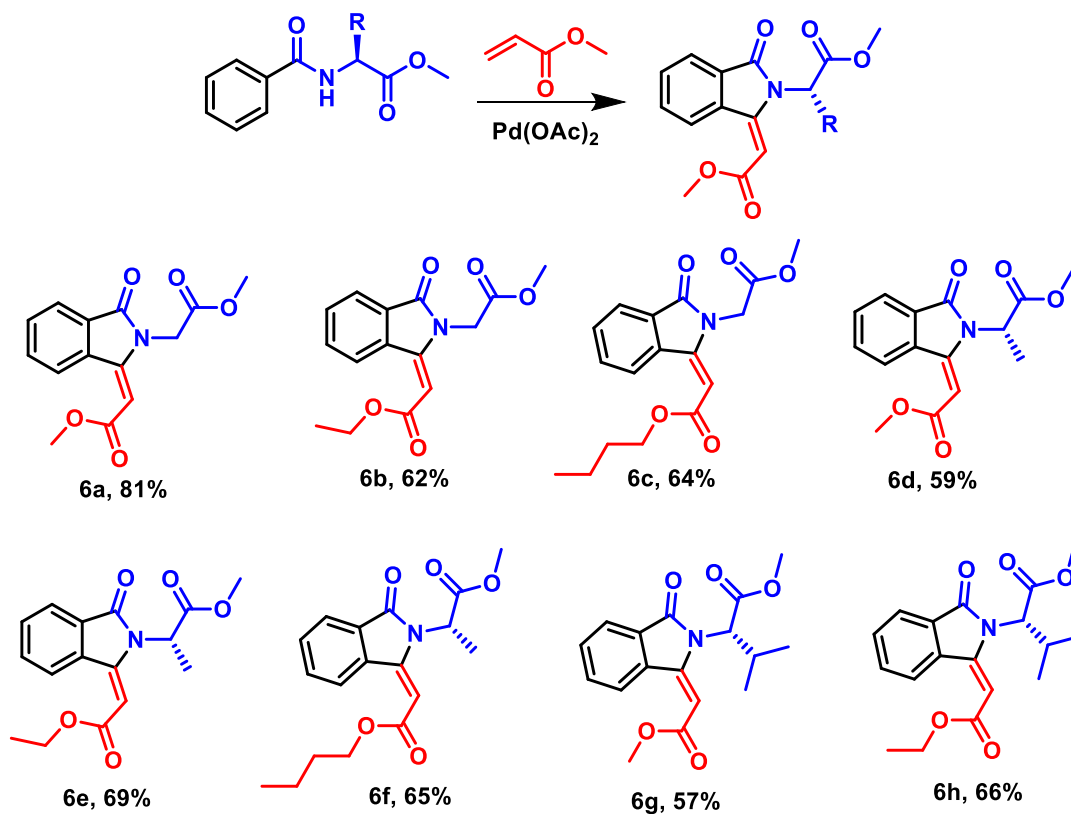
4a.2.2 Substrate scope using various amino ester

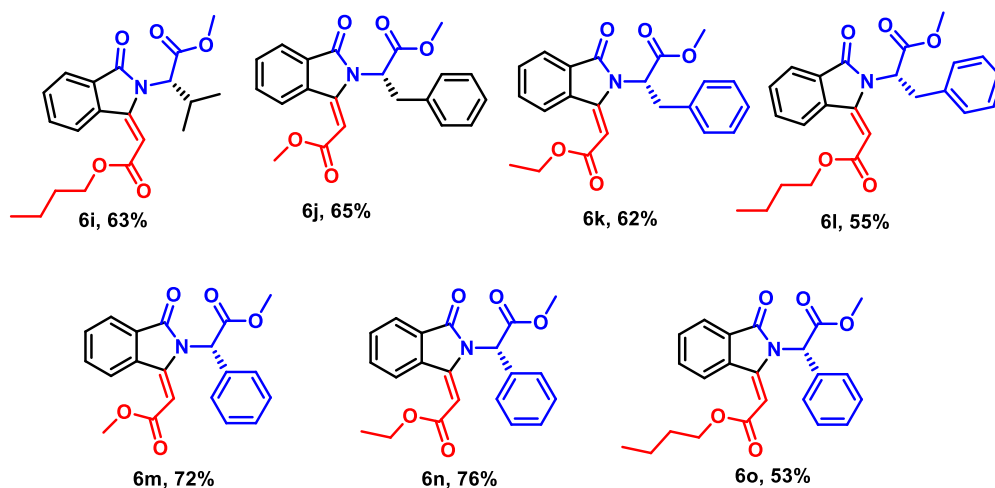
For the synthesis of chiral isoindolinone derivatives, chiral benzamide was synthesized from naturally occurring chiral L-amino acid esters (Ala-OMe/Val-OMe/Phe-OMe/phenylglycine-OMe) (**Scheme 4a.2**). Different acrylates (**4**) were treated with these chiral benzamides under the previously optimized conditions for Pd(II)-catalysed olefination and cyclization reactions. As a result, 3-acrylatyl-N-alanyl isoindolinone derivatives (**6d– 6f**) were prepared from an

alanine ester benzamide (**3b**), and the respective methyl acrylate (**4a**), ethyl acrylate (**4b**) and butyl acrylate (**4c**). Similarly, 3-acrylatyl-*N*-valinyl isoindolinone derivatives (**6g–6i**) were prepared from a valine ester benzamide (**3b**) and the respective methyl/ethyl/butyl acrylates (**4a–4c**).

3-acrylatyl-*N*-phenylalanyl isoindolinone derivatives (**6j–6l**) from benzamide of phenylalanine ester (**3c**) and respective methyl/ethyl/butyl acrylates (**4a–4c**), the 3-acrylatyl *N*-phenylglycinyl isoindolinone derivatives (**6m–6o**) from a phenylglycine ester benzamide (**3d**) and respective methyl/ethyl/butyl acrylates (**4a–4c**) with moderate to good yield. Therefore, using alternative chiral amino acid esters as a starting point, this synthetic approach might be used to create substituted chiral isoindolinone derivatives.

Scheme 4a.2 Synthesis of Chiral isoindolinone derivative using various amino ester



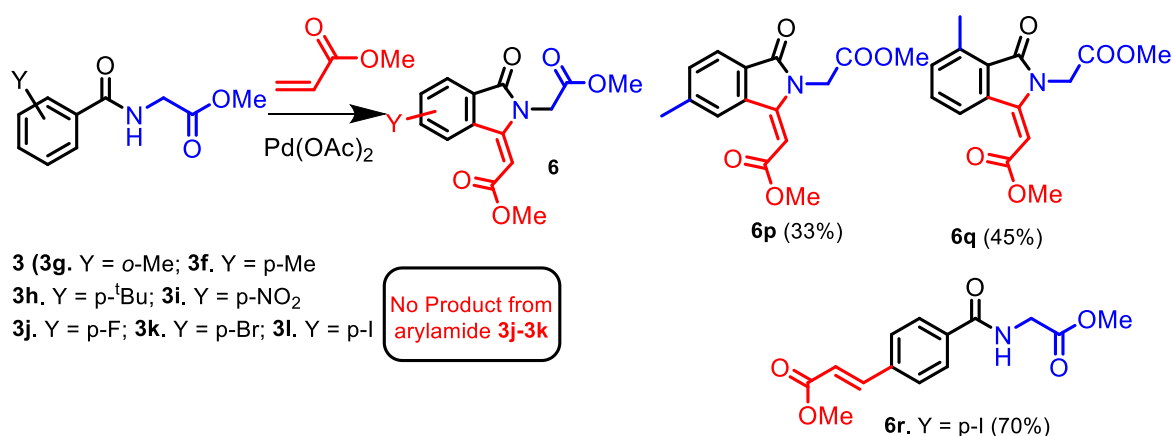


4a.2.3 Substrate scope using using different aryl groups

Additionally, under Pd-catalysed optimised reaction conditions, the synthesis of aryl-substituted isoindolinones from various arylamides of glycines and methyl acrylate was investigated (**Scheme 4a.2**). The isoindolinone derivatives (**6p/6q**), generated by the ortho/para-methyl substituted benzamides (**3g/3f**), respectively. However, isoindolino derivatives were not formed by p-tert-butyl benzamide (**3h**), p-nitro benzamide (**3i**), p-fluoro benzamide (**3j**), p-bromo benzamide (**3k**), and p-iodo benzamide (**3l**). It's interesting to note that p-iodo benzamide produced Heck arylated olefin product as p-acrylatyl benzamide (**6r**) instead of isoindolinone derivatives. The p-tert-butyl substituted benzamide could become vinyl substituted benzamide and prevent the Pd(II)-complex formation and the inhibit ortho-C–H activation (**Scheme 4a.3**). The electron density at the aryl ring of benzamide may have dropped due to the electron-withdrawing groups that destabilized the Pd(II)–aryl complexation before the C–H activation. Therefore, a benzamide containing an electron-donating group produced substituted isoindolinone derivatives with the Pd(II)-catalyst. The viability of employing acrylic acid and acrylonitrile in the previously optimised conditions to synthesise isoindolinones from benzamide of amino acid esters (Gly/Ala/Val) was then

evaluated. There was no evidence of the required isoindolinone production. For the Pd-catalysed C-H activation and production of cyclic isoindolinone compounds, benzamide is therefore essential.

Scheme 4a.3 Synthesis of *Chiral* isoindolinone derivative using different aryl groups



4a.2.4 The proposed reaction mechanism

The reaction mechanism for the Pd(II)-catalysed synthesis of isoindolinone is proposed here. The amino acid residue of *N*-benzoyl of amino acid (**3**) to serve as a directing group and form a Pd(II)-complex with Pd(OAc)₂ as a bicyclic palladacycle intermediate (**I-1**) by the C(sp²)-H activation of the ortho-aryl C-H bond. In step 2, the development of another intermediate (**I-2**) by insertion of an acrylate olefin at Pd-complex (**I-1**) by replacing the acetate ligand. In step 3 Another reactive bicyclic palladacycle intermediate is influenced by the migration of the olefin to the aryl group (ortho-position) (**I-3**), which facilitates the β-hydride elimination and forms unstable orthoolefinated aryl amide (**5**) in situ. In step 4, Compound **5** again generates bicyclic palladacycle intermediate **I-4** from intramolecular olefin C(sp²)-H activation. In step 5 The stable cyclic molecule isoindolinone (**6**) is formed when the intermediate (**I-4**) is reductively eliminated by the formation of a C-N bond. In the last step, by oxidising Pd(0) to Pd(II) using the oxidant AgOAc, the Pd(II)-catalyst is regenerated. The

double C(sp²)-H activations therefore involved the production of isoindolinones from *N*-benzoyl amino acid and acrylate olefin in the presence of the Pd(II)-catalyst (**Figure 4a.3**).

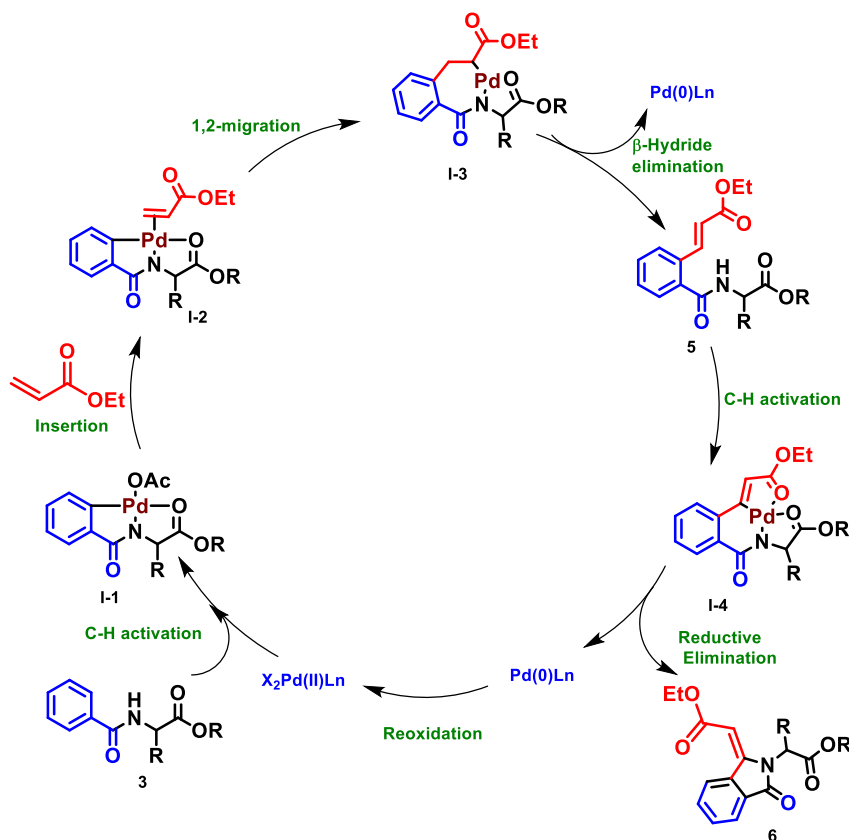


Figure 4a.3 The proposed reaction mechanism of isoindolinone synthesis.

4a.3 Conclusion

In the presence of a Pd(II)-catalyst, *N*-substituted trans-isoindolinones have been effectively synthesised from *N*-benzamide/arylamide of L-amino acid derivatives and inactivated olefins. The amino acid residue in this case served as a guiding group for mono ortho-olefination at the aryl (phenyl) ring by in situ C(sp²)-H activation, which was followed by a cyclization reaction with a second C-H activation at the intermediate aryl-olefin. Therefore, using naturally occurring L-amino acid residues as starting points and analogues of erinacerin

natural products as starting points, this approach might be employed to manufacture different *N*-substituted isoindolinone derivatives.

4a.4 Experimental Section

4a.4.1 Materials and instrumentation

All the required materials were obtained from commercial suppliers and used without purification. The dry DMF and ACN were freshly prepared by distilling them over calcium hydride. The reactions were monitored using thin-layer chromatography, and visualized using UV light and ninhydrin. Column chromatography was performed through 100–200 mesh silica. Mass spectra were obtained using a Bruker micrO TOF-Q II spectrometer. The ^{13}C - and ^1H -NMR spectra were recorded on a Bruker AV-400 NMR spectrometer ^1H (400 MHz), ^{13}C (100.6 MHz). ^1H and ^{13}C -NMR chemical shifts were recorded in ppm downfield from the tetramethyl silane, and the splitting patterns are abbreviated as s, singlet; d, doublet; dd, doublet of doublets; t, triplet; q, quartet; dq, doublet of a quartet; m, multiplet.

4a.4.2 General procedure for amide synthesis

Benzoic acid was dissolved in DMF and then the triethylamine (TEA, 3.0 eq.), EDC.HCl (1.3 eq.) and HOAt (1.3 eq.) were added, followed by the resulting amino acid methyl ester (1.2 eq.). Next, this mixture was heated to 60 °C for 8–12 h, and the reaction was monitored by TLC. The crude reaction mixture was concentrated under reduced pressure before water was added. The aqueous layer was extracted with EtOAc. The organic layer was combined, dried over anhydrous Na_2SO_4 , and concentrated under reduced pressure. The residue was purified by column chromatography with an EtOAc/hexane solvent system to yield the corresponding substrates.

4a.4.3 General procedure for Pd-catalysed reactions

Typically, the amide substrates were placed in a 15 ml sealed reaction tube under the indicated reaction conditions. The mixture was stirred at 100 °C for 12–24 h, cooled to room temperature, and then diluted with EtOAc. The resulting solution was filtered through a celite pad, concentrated under reduced pressure and the product was further purified by column chromatography with an EtOAc/hexane solvent system and was typically obtained as a white solid.

4a.4.4 Chemical shift values of NMR

Methyl 2-benzamidoacetate (3a). ¹H-NMR (400 MHz, CDCl₃) δ 7.82 (d, J = 7.5 Hz, 2H), 7.48–7.38 (m, 1H), 7.38–7.26 (m, 2H), 4.12 (d, J = 5.5 Hz, 2H), 3.65 (s, 3H). ¹³C-NMR (101 MHz, CDCl₃) δ 170.55, 168.11, 133.48, 131.67, 128.40, 127.22, 52.13, 41.62. Pale yellow solid (77% yield). ESI-HRMS m/z [M + Na]⁺ calcd for C₁₀H₁₁NO₃ 216.0621, found 216.0631.

Methyl (E)-2-(2-(2-methoxy-2-oxoethyl)-3-oxoisindolin-1-ylidene) acetate (6a). ¹H-NMR (400 MHz, CDCl₃) δ 9.02 (d, J = 7.9 Hz, 1H), 7.82 (d, J = 7.4 Hz, 1H), 7.63 (t, J = 7.7 Hz, 1H), 7.54 (t, J = 7.4 Hz, 1H), 5.46 (s, 1H), 4.51 (s, 2H), 3.74 (s, 3H), 3.70 (s, 3H). ¹³C-NMR (101 MHz, CDCl₃) δ 165.67, 164.80, 163.92, 145.95, 131.70, 131.52, 129.39, 127.42, 126.16, 121.42, 96.17, 50.67, 49.65, 38.87. White solid (81% yield). ESI-HRMS m/z [M + H]⁺ calcd for C₁₄H₁₃NO₅ 276.0866, found 276.0839.

Ethyl (E)-2-(2-(2-methoxy-2-oxoethyl)-3-oxoisindolin-1-ylidene) acetate (6b). ¹H-NMR (400 MHz, CDCl₃) δ 9.10 (d, J = 7.9 Hz, 1H), 7.89 (d, J = 7.4 Hz, 1H), 7.69 (t, 1H), 7.60 (t, J = 7.3 Hz, 1H), 5.53 (s, 1H), 4.58 (s, 2H), 4.27 (q, J = 7.1 Hz, 2H), 3.78 (s, 3H), 1.35 (t, J = 7.1 Hz, 3H). ¹³C-NMR (101 MHz, CDCl₃) δ 167.84, 166.96, 165.64, 147.84, 133.88, 133.59,

131.43, 129.55, 128.32, 123.51, 98.86, 60.68, 52.79, 40.99, 14.31. Yellow solid (62% yield). ESI-HRMS m/z $[M + H]^+$ calcd for $C_{15}H_{15}NO_5$ 290.1023, found 290.0990.

Butyl (E)-2-(2-(2-methoxy-2-oxoethyl)-3-oxoisindolin-1-ylidene acetate (6c). 1H -NMR (400 MHz, $CDCl_3$) δ 9.10 (d, $J = 7.9$ Hz, 1H), 7.89 (d, $J = 7.3$ Hz, 1H), 7.69 (t, $J = 7.7$ Hz, 1H), 7.61 (t, $J = 7.4$ Hz, 1H), 5.50 (s, 1H), 4.59 (s, 2H), 4.21 (t, $J = 6.7$ Hz, 2H), 3.78 (s, 3H), 1.75–1.62 (m, 2H), 1.51–1.38 (m, 2H), 0.97 (t, $J = 7.2$ Hz, 3H). ^{13}C -NMR (101 MHz, $CDCl_3$) δ 167.83, 166.94, 165.74, 147.81, 133.91, 133.57, 131.40, 129.55, 128.32, 123.49, 98.83, 64.62, 52.76, 41.00, 30.74, 19.20, 13.74. Yellow solid (64% yield). ESI-HRMS m/z $[M + H]^+$ calcd for $C_{17}H_{19}NO_5$ 318.1336, found 318.1311.

Methyl 2-benzamidopropanoate (3b). 1H -NMR (400 MHz, $CDCl_3$) δ 7.81 (d, $J = 7.8$ Hz, 1H), 7.46 (t, $J = 7.2$ Hz, 1H), 7.37 (t, $J = 7.4$ Hz, 1H), 7.21 (s, 1H), 4.76 (q, $J = 7.2$ Hz, 1H), 3.73 (s, 2H), 1.49 (d, $J = 7.2$ Hz, 2H). ^{13}C -NMR (101 MHz, $CDCl_3$) δ 173.66, 166.65, 133.67, 131.62, 128.30, 126.93, 52.18, 48.13, 18.15. Light yellow jelly (72% yield). ESI-HRMS m/z $[M + H]^+$ calcd for $C_{11}H_{13}NO_3$ 208.0968, found 208.0979.

Methyl (E)-2-(1-(2-methoxy-2-oxoethylidene)-3-oxoisindolin-2-yl) propanoate (6d). 1H -NMR (700 MHz, $CDCl_3$) δ 9.00 (d, $J = 7.9$ Hz, 1H), 7.79 (d, $J = 7.4$ Hz, 1H), 7.61 (t, $J = 7.7$ Hz, 1H), 7.52 (t, $J = 7.3$ Hz, 1H), 5.52 (s, 1H), 5.15 (q, $J = 14.3, 7.1$ Hz, 1H), 3.73 (s, 3H), 3.67 (s, 3H), 1.57 (d, $J = 7.3$ Hz, 3H). ^{13}C -NMR (101 MHz, $CDCl_3$) δ 170.62, 166.70, 166.11, 146.80, 133.87, 133.52, 131.39, 129.33, 128.14, 123.42, 98.80, 52.86, 51.75, 48.38, 14.72. Light yellow solid (59% yield). ESI-HRMS m/z $[M + H]^+$ calcd for $C_{15}H_{15}NO_5$ 290.1023, found 290.1015.

Methyl (E)-2-(1-(2-ethoxy-2-oxoethylidene)-3-oxoisindolin-2-yl) propanoate (6e). 1H -NMR (700 MHz, $CDCl_3$) δ 8.99 (d, $J = 8.0$ Hz, 1H), 7.79 (d, $J = 7.5$ Hz, 1H), 7.60 (t, $J = 7.7$ Hz, 1H), 7.51 (t, $J = 7.4$ Hz, 1H), 5.52 (s, 1H), 5.12 (q, $J = 7.1$ Hz, 1H), 4.19 (m, 2H), 3.66 (s,

3H), 1.57 (d, $J = 7.3$ Hz, 3H), 1.27 (t, $J = 7.2$ Hz, 3H). ^{13}C -NMR (101 MHz, CDCl_3) δ 170.63, 166.69, 165.71, 146.57, 133.93, 133.45, 131.31, 129.35, 128.15, 123.35, 99.31, 60.66, 52.83, 48.43, 14.75, 14.29. Light yellow solid (69% yield). ESI-HRMS m/z $[\text{M} + \text{H}]^+$ calcd for $\text{C}_{16}\text{H}_{17}\text{NO}_5$ 326.0999, found 326.0991.

Methyl (E)-2-(1-(2-butoxy-2-oxoethylidene)-3-oxoisindolin-2-yl) propanoate (6f). ^1H -NMR (400 MHz, CDCl_3) δ 9.08 (d, $J = 7.9$ Hz, 1H), 7.87 (d, $J = 7.4$ Hz, 1H), 7.68 (t, $J = 7.7$ Hz, 1H), 7.60 (t, $J = 7.4$ Hz, 1H), 5.60 (s, 1H), 5.19 (q, $J = 7.1$ Hz, 1H), 4.21 (t, $J = 5.8$ Hz, 2H), 3.75 (s, 3H), 1.76–1.69 (m, 2H), 1.66 (d, $J = 7.2$ Hz, 3H), 1.46–1.41 (m, 2H), 0.97 (t, $J = 7.4$ Hz, 3H). ^{13}C -NMR (101 MHz, CDCl_3) δ 170.66, 166.72, 165.84, 146.59, 133.95, 133.46, 131.31, 129.36, 128.18, 123.37, 99.27, 64.65, 52.84, 48.47, 30.71, 19.20, 14.78, 13.76, –0.00. Light yellow solid (65% yield). ESI-HRMS m/z $[\text{M} + \text{H}]^+$ calcd for $\text{C}_{18}\text{H}_{21}\text{NO}_5$ 332.1492, found 332.1487.

Methyl 2-benzamido-3-methylbutanoate (3c). ^1H -NMR (700 MHz, CDCl_3) δ 7.81 (d, $J = 7.1$ Hz, 2H), 7.53–7.47 (m, 1H), 7.46–7.40 (m, 2H), 6.84 (s, 1H), 4.81–4.76 (m, 1H), 3.75 (s, 3H), 2.31–2.24 (m, 1H), 1.03–0.97 (m, 6H). ^{13}C -NMR (176 MHz, CDCl_3) δ 172.69 (s), 167.38 (s), 134.09 (s), 131.69 (s), 128.54 (s), 127.09 (s), 57.51 (s), 52.20 (d, $J = 2.2$ Hz), 31.51 (s), 19.00 (s), 18.02 (s). White solid (78% yield). ESI-HRMS m/z $[\text{M} + \text{H}]^+$ calcd for $\text{C}_{13}\text{H}_{17}\text{NO}_3$ 258.1101, found 258.1103.

Methyl (E)-2-(1-(2-methoxy-2-oxoethylidene)-3-oxoisindolin-2-yl)-3-methylbutanoate (6g).

^1H -NMR (700 MHz, CDCl_3) δ 9.08 (d, $J = 7.9$ Hz, 1H), 7.91 (d, $J = 7.4$ Hz, 1H), 7.70 (t, $J = 8.2$ Hz, 1H), 7.62 (t, $J = 7.4$ Hz, 1H), 5.88 (s, 1H), 4.89 (d, $J = 8$ Hz, 1H), 3.82 (s, 3H), 3.72 (s, 3H), 2.80–2.71 (m, $J = 13.1, 6.5$ Hz, 1H), 1.22 (d, $J = 6.4$ Hz, 3H), 0.80 (d, $J = 6.8$ Hz, 3H). ^{13}C -NMR (176 MHz, CDCl_3) δ 169.99, 167.24, 166.26, 147.24, 133.56, 133.53, 131.38,

129.08, 128.08, 123.61, 99.31, 58.66, 52.58, 51.73, 29.69, 27.38, 21.29, 18.54. Light yellow solid (57% yield). ESI-HRMS m/z $[M + H]^+$ calcd for $C_{16}H_{17}NO_5$ 318.1336, found 318.1333.

Methyl (E)-2-(1-(2-ethoxy-2-oxoethylidene)-3-oxoisindolin-2-yl)-3-methylbutanoate (6h).

1H -NMR (700 MHz, $CDCl_3$) δ 9.06 (d, $J = 7.9$ Hz, 1H), 7.89 (d, $J = 7.4$ Hz, 1H), 7.68 (t, $J = 7.7$ Hz, 1H), 7.60 (t, $J = 7.4$ Hz, 1H), 5.85 (s, 1H), 4.88 (d, $J = 8$ Hz, 1H), 4.31–4.22 (m, 2H), 3.73 (s, 3H), 2.80–2.71 (m, 1H), 1.35 (t, 3H), 1.22 (d, $J = 6.4$ Hz, 3H), 0.80 (d, $J = 6.8$ Hz, 3H). ^{13}C -NMR (176 MHz, $CDCl_3$) δ 170.03, 167.26, 165.91, 147.01, 133.61, 133.51, 131.30, 129.10, 128.09, 123.58, 99.87, 60.71, 58.67, 52.58, 27.40, 21.33, 18.59, 14.31. Light yellow solid (66% yield). ESI-HRMS m/z $[M + H]^+$ calcd for $C_{18}H_{21}NO_5$ 354.1312, found 354.1305.

Methyl (E)-2-(1-(2-butoxy-2-oxoethylidene)-3-oxoisindolin-2-yl)-3-methylbutanoate (6i).

1H -NMR (400 MHz, $CDCl_3$) δ 9.06 (d, $J = 7.9$ Hz, 1H), 7.89 (d, $J = 7.4$ Hz, 1H), 7.69 (t, $J = 7.7$ Hz, 1H), 7.61 (t, $J = 7.4$ Hz, 1H), 5.84 (s, 1H), 4.87 (d, $J = 10.0$ Hz, 1H), 4.21 (t, $J = 6.7$ Hz, 2H), 3.70 (s, 3H), 2.83–2.68 (m, 1H), 1.76–1.65 (m, 2H), 1.49–1.38 (m, 2H), 1.22 (d, $J = 6.2$ Hz, 3H), 0.97 (t, $J = 7.3$ Hz, 3H), 0.80 (d, $J = 6.7$ Hz, 3H). ^{13}C -NMR (101 MHz, $CDCl_3$) δ 170.03, 167.26, 166.02, 147.01, 133.61, 133.51, 131.30, 129.10, 128.11, 123.58, 99.82, 64.69, 58.65, 52.58, 30.70, 27.42, 21.35, 19.22, 18.59, 13.78. Yellow solid (63% yield). ESI-HRMS m/z $[M + H]^+$ calcd for $C_{20}H_{25}NO_5$ 382.1625, found 382.1606.

Methyl 2-benzamido-3-phenylpropanoate (3d). 1H -NMR (700 MHz, $CDCl_3$) δ 7.71 (d, $J = 7.3$ Hz, 2H), 7.47–7.42 (m, 1H), 7.35 (d, $J = 13.2, 6.0$ Hz, 2H), 7.29–7.24 (m, 2H), 7.24–7.20 (m, 1H), 7.16–7.13 (m, 2H), 6.89 (d, $J = 6.8$ Hz, 1H), 5.08–5.05 (m, 1H), 3.70 (s, 3H), 3.30–3.24 (m, 1H), 3.22–3.17 (m, 1H). ^{13}C -NMR (176 MHz, $CDCl_3$) δ 172.19, 167.07, 136.06, 133.85, 131.78, 129.34, 128.63, 128.59, 127.17, 127.12, 53.70, 52.42, 37.82. Yellow solid (65% yield). ESI-HRMS m/z $[M + H]^+$ calcd for $C_{17}H_{17}NO_3$ 306.1101, found 306.1101.

Methyl (E)-2-(1-(2-methoxy-2-oxoethylidene)-3-oxoisindolin-2-yl)-3-phenylpropanoate (6j).

¹H-NMR (400 MHz, CDCl₃) δ 9.03 (d, J = 7.9 Hz, 1H), 7.78 (d, J = 7.4 Hz, 1H), 7.65 (t, J = 7.7 Hz, 1H), 7.55 (t, J = 7.4 Hz, 1H), 7.21–7.09 (m, 5H), 5.57 (s, 1H), 5.34–5.26 (m, 1H), 3.79 (s, 3H), 3.75 (s, 3H), 3.61 (dd, J = 14.2, 5.2 Hz, 1H), 3.37 (dd, J = 13.9, 10.6 Hz, 1H). ¹³C-NMR (101 MHz, CDCl₃) δ 169.83, 166.88, 166.08, 147.27, 136.53, 133.68, 133.49, 131.35, 129.00, 128.96, 128.58, 128.06, 126.97, 123.43, 98.88, 54.69, 52.95, 51.76, 34.81. Light yellow solid (65% yield). ESI-HRMS m/z [M + H]⁺ calcd for C₂₁H₁₉NO₅ 366.1369, found 366.1336.

Methyl (E)-2-(1-(2-ethoxy-2-oxoethylidene)-3-oxoisindolin-2-yl)-3-phenylpropanoate (6k).

¹H-NMR (400 MHz, CDCl₃) δ 9.03 (d, J = 7.9 Hz, 1H), 7.78 (d, J = 7.4 Hz, 1H), 7.64 (t, J = 7.7 Hz, 1H), 7.55 (t, J = 7.4 Hz, 1H), 7.22–7.03 (m, 5H), 5.55 (s, 1H), 5.35–5.26 (m, 1H), 4.25 (q, J = 6.9 Hz, 2H), 3.76 (s, 3H), 3.62 (dd, J = 14.2, 5.1 Hz, 1H), 3.38 (dd, J = 13.9, 10.6 Hz, 1H), 1.35 (t, J = 7.1 Hz, 3H). ¹³C-NMR (101 MHz, CDCl₃) δ 169.88, 166.90, 165.69, 147.01, 136.59, 133.74, 133.44, 131.26, 129.02, 128.99, 128.58, 128.09, 126.96, 123.40, 99.46, 60.67, 54.74, 52.95, 34.84, 14.33. Light yellow solid (62% yield). ESI-HRMS m/z [M + H]⁺ calcd for C₂₂H₂₁NO₅ 380.1521, found 380.1492.

Methyl (E)-2-(1-(2-butoxy-2-oxoethylidene)-3-oxoisindolin-2-yl)-3-phenylpropanoate (6l).

¹H-NMR (400 MHz, CDCl₃) δ 9.02 (d, J = 7.9 Hz, 1H), 7.78 (d, J = 7.4 Hz, 1H), 7.64 (t, J = 7.6 Hz, 1H), 7.55 (t, J = 7.2 Hz, 1H), 7.16 (m, 5H), 5.52 (s, 1H), 5.33–5.20 (m, 1H), 4.19 (t, J = 6.6 Hz, 2H), 3.76 (s, 3H), 3.62 (dd, J = 8.0 Hz, 1H), 3.37 (dd, J = 8.0 Hz, 1H), 1.74–1.63 (m, 2H), 1.49–1.38 (m, 2H), 0.98 (t, J = 7.3 Hz, 3H). ¹³C-NMR (101 MHz, CDCl₃) δ 169.87, 166.91, 165.78, 147.01, 136.61, 133.75, 133.44, 131.25, 129.03, 128.99, 128.58, 128.09, 126.96, 123.39, 99.40, 64.60, 54.82, 52.94, 34.89, 30.71, 19.22, 13.79. Yellow solid (55% yield). ESI-HRMS m/z [M + H]⁺ calcd for C₂₄H₂₅NO₅ 408.1837, found 408.1805.

Methyl 2-benzamido-2-phenylacetate (3e). $^1\text{H-NMR}$ (700 MHz, CDCl_3) δ 7.81 (d, J = 8.2 Hz, 2H), 7.48 (m, 1H), 7.43 (d, J = 7.7 Hz, 2H), 7.40 (m, 2H), 7.35 (m, 2H), 7.31 (m, 1H), 5.77 (d, J = 4.0 Hz, 1H), 3.73 (s, 3H). $^{13}\text{C-NMR}$ (176 MHz, CDCl_3) δ 171.55, 166.65, 136.55, 133.59, 131.89, 129.04, 128.63, 128.60, 127.40, 127.22, 56.86, 52.91. White solid (65% yield). ESI-HRMS m/z $[\text{M} + \text{H}]^+$ calcd for $\text{C}_{16}\text{H}_{15}\text{NO}_3$ 270.1160, found 270.1145.

Methyl (E)-2-(1-(2-methoxy-2-oxoethylidene)-3-oxoisindolin-2-yl)-2-phenylacetate (6m).

$^1\text{H-NMR}$ (700 MHz, CDCl_3) δ 9.07 (d, J = 7.9 Hz, 1H), 7.93 (d, J = 7.5 Hz, 1H), 7.72–7.68 (m, 1H), 7.62 (m, 1H), 7.39–7.31 (m, 5H), 6.33 (s, 1H), 5.67 (s, 1H), 3.82 (s, 3H), 3.73 (s, 3H). $^{13}\text{C-NMR}$ (101 MHz, CDCl_3) δ 168.70, 167.18, 166.04, 146.66, 134.00, 133.74, 133.27, 131.42, 129.09, 128.73, 128.42, 128.19, 128.02, 123.66, 100.86, 56.57, 53.05, 51.70. Light yellow solid (72% yield). ESI-HRMS m/z $[\text{M} + \text{Na}]^+$ calcd for $\text{C}_{20}\text{H}_{17}\text{NO}_5$ 374.1002, found 374.0999.

Methyl (E)-2-(1-(2-ethoxy-2-oxoethylidene)-3-oxoisindolin-2-yl)-2-phenylacetate (6n).

$^1\text{H-NMR}$ (700 MHz, CDCl_3) δ 9.06 (d, J = 7.9 Hz, 1H), 7.92 (d, J = 7.5 Hz, 1H), 7.69 (t, J = 7.7 Hz, 1H), 7.61 (t, J = 7.4 Hz, 1H), 7.40–7.30 (m, 5H), 6.28 (s, 1H), 5.66 (s, 1H), 4.19 (q, J = 7.1 Hz, 2H), 3.82 (s, 3H), 1.28 (t, J = 7.1 Hz, 3H). $^{13}\text{C-NMR}$ (101 MHz, CDCl_3) δ 168.74, 167.18, 165.67, 146.50, 134.06, 133.69, 133.33, 131.35, 129.11, 128.71, 128.41, 128.21, 128.08, 123.62, 101.22, 60.66, 56.68, 53.06, 14.26. Yellow solid (76% yield). ESI-HRMS m/z $[\text{M} + \text{Na}]^+$ calcd for $\text{C}_{21}\text{H}_{19}\text{NO}_5$ 388.1159, found 388.1155.

Methyl (E)-2-(1-(2-butoxy-2-oxoethylidene)-3-oxoisindolin-2-yl)-2-phenylacetate (6o).

$^1\text{H-NMR}$ (400 MHz, CDCl_3) δ 9.06 (d, J = 7.9 Hz, 1H), 7.93 (d, J = 7.4 Hz, 1H), 7.69 (t, J = 7.7 Hz, 1H), 7.62 (t, J = 7.4 Hz, 1H), 7.41–7.29 (m, 5H), 6.27 (s, 1H), 5.66 (s, 1H), 4.14 (t, J = 6.2 Hz, 2H), 3.82 (s, 3H), 1.68–1.59 (m, 2H), 1.42–1.31 (m, 3H), 0.93 (t, J = 7.4 Hz, 3H). $^{13}\text{C-NMR}$ (101 MHz, CDCl_3) δ 168.75, 167.19, 165.76, 146.48, 134.06, 133.68, 133.34,

131.34, 129.10, 128.69, 128.40, 128.22, 128.10, 123.62, 101.23, 64.61, 56.69, 53.05, 30.62, 19.16, 13.75. Yellow solid (53% yield). ESI-HRMS m/z $[M + Na]^+$ calcd for $C_{23}H_{23}NO_5$ 416.1480, found 416.1468.

Methyl 2-(4-methylbenzamido) acetate (3f). 1H -NMR (400 MHz, $CDCl_3$) δ 7.72 (d, $J = 7.8$ Hz, 1H), 7.40 (s, 1H), 7.16 (d, $J = 7.7$ Hz, 1H), 4.15 (d, $J = 5.2$ Hz, 1H), 3.71 (s, 2H), 2.35 (s, 2H). ^{13}C -NMR (101 MHz, $CDCl_3$) δ 170.68, 167.80, 142.13, 130.72, 129.12, 127.19, 52.25, 41.62, 21.40. White solid (40% yield). ESI-HRMS m/z $[M + Na]^+$ calcd for $C_{11}H_{13}NO_5$ 230.0793, found 230.0788.

Methyl (E)-2-(2-(2-methoxy-2-oxoethyl)-6-methyl-3-oxoisindolin-1-ylidene) acetate (6p).

1H -NMR (400 MHz, $CDCl_3$) δ 8.85 (s, 1H), 7.70 (d, $J = 7.8$ Hz, 1H), 7.34 (d, $J = 7.9$ Hz, 1H), 5.43 (s, 1H), 4.48 (s, 2H), 3.74 (s, 3H), 3.69 (s, 4H), 2.45 (s, 3H). ^{13}C -NMR (101 MHz, $CDCl_3$) δ 167.87, 166.95, 166.14, 148.36, 144.65, 134.14, 132.30, 128.74, 127.03, 123.37, 97.90, 52.74, 51.72, 40.96, 22.37. White solid (26% yield). ESI-HRMS m/z $[M + H]^+$ calcd for $C_{15}H_{15}NO_5$ 290.1017, found 290.1023.

Methyl 2-(2-methylbenzamido) acetate (3g). 1H -NMR (400 MHz, $CDCl_3$) δ 7.38 (d, $J = 7.4$ Hz, 1H), 7.30 (d, $J = 7.6$ Hz, 1H), 7.22–7.15 (m, 2H), 6.57 (s, 1H), 4.15 (d, $J = 2.0$ Hz, 2H), 3.75 (s, 3H), 2.43 (s, 3H). ^{13}C -NMR (101 MHz, $CDCl_3$) δ 170.41, 170.26, 136.32, 135.49, 131.03, 130.16, 126.93, 125.71, 52.39, 41.42, 19.75. Light yellow solid (45% yield). ESI-HRMS m/z $[M + Na]^+$ calcd for $C^{11}H^{13}NO^3$ 230.0784, found 230.0788.

Methyl (E)-2-(2-(2-methoxy-2-oxoethyl)-4-methyl-3-oxoisindolin-1-ylidene) acetate (6q).

1H -NMR (400 MHz, $CDCl_3$) δ 8.96 (d, $J = 7.9$ Hz, 1H), 7.55 (t, $J = 8.0$ Hz, 1H), 7.36 (d, $J = 7.7$ Hz, 1H), 5.48 (s, 1H), 4.55 (s, 2H), 3.80 (s, 3H), 3.77 (s, 3H), 2.72 (s, 3H). ^{13}C -NMR (101 MHz, $CDCl_3$) δ 167.97, 167.51, 166.16, 147.99, 137.83, 134.28, 133.86, 133.09,

126.41, 125.83, 97.31, 52.75, 51.67, 40.77, 17.63. White solid (33% yield). ESI-HRMS m/z $[M + Na]^+$ calcd for $C_{15}H_{15}NO_5$ 312.0845, found 312.0842.

Methyl 2-(4-(tert-butyl) benzamido) acetate (3h). 1H -NMR (400 MHz, $CDCl_3$) δ 7.78 (d, J = 7.8 Hz, 2H), 7.44 (s, 1H), 7.39 (d, J = 7.6 Hz, 2H), 4.18 (d, J = 5.3 Hz, 2H), 3.72 (s, 3H), 1.30 (s, 9H). ^{13}C -NMR (101 MHz, $CDCl_3$) δ 170.73, 167.78, 155.15, 130.67, 127.08, 125.41, 52.27, 41.64, 34.87, 31.11. White solid (65% yield). ESI-HRMS m/z $[M + Na]^+$ calcd for $C_{14}H_{19}NO_3$ 272.1282, found 272.1257.

Methyl 2-(4-nitrobenzamido) acetate (3i). 1H -NMR (400 MHz, $CDCl_3$) δ 8.30 (d, J = 8.5 Hz, 1H), 7.99 (d, J = 8.5 Hz, 1H), 6.95 (s, 1H), 4.27 (d, J = 5.0 Hz, 1H), 3.83 (s, 1H). ^{13}C -NMR (101 MHz, $CDCl_3$) δ 170.23, 165.50, 149.79, 139.13, 128.36, 123.89, 52.74, 41.86. Yellow solid (52% yield). ESI-HRMS m/z $[M + Na]^+$ calcd for $C_{10}H_{10}N_2O_5$ 261.0495, found 261.0482.

Methyl 2-(4-fluorobenzamido) acetate (3j). 1H -NMR (400 MHz, $CDCl_3$) δ 7.83 (dd, J = 7.6, 5.5 Hz, 2H), 7.09 (t, J = 8.3 Hz, 2H), 6.96 (s, 1H), 4.21 (d, J = 5.1 Hz, 2H), 3.79 (s, 3H). ^{13}C -NMR (101 MHz, $CDCl_3$) δ 170.61, 166.54, 166.15, 163.65, 129.55, 129.46, 115.74, 115.52, 52.50, 41.72. White solid (66% yield). ESI-HRMS m/z $[M + Na]^+$ calcd for $C_{10}H_{10}FNO_3$ 234.0545, found 234.0537.

Methyl 2-(4-bromobenzamido) acetate (3k). 1H -NMR (400 MHz, $CDCl_3$) δ 7.67 (d, J = 8.2 Hz, 2H), 7.54 (d, J = 8.2 Hz, 2H), 7.06 (s, 1H), 4.20 (d, J = 5.2 Hz, 2H), 3.78 (s, 3H). ^{13}C -NMR (101 MHz, $CDCl_3$) δ 170.56, 166.69, 132.36, 131.80, 128.74, 126.58, 52.55, 41.71. White solid (63% yield). ESI-HRMS m/z $[M + Na]^+$ calcd for $C_{10}H_{10}BrNO_3$ 293.9746, found 293.9736.

Methyl 2-(4-iodobenzamido) acetate (3l). $^1\text{H-NMR}$ (400 MHz, CDCl_3) δ 7.77 (d, $J = 7.8$ Hz, 2H), 7.52 (d, $J = 7.8$ Hz, 2H), 6.90 (s, 1H), 4.22 (d, $J = 5.0$ Hz, 2H), 3.80 (s, 3H). $^{13}\text{C-NMR}$ (101 MHz, CDCl_3) δ 170.54, 166.81, 137.83, 132.96, 128.69, 98.99, 52.59, 41.73. White solid (63% yield). ESI-HRMS m/z $[\text{M} + \text{Na}]^+$ calcd for $\text{C}_{10}\text{H}_{10}\text{INO}_3$ 341.9616, found 341.9616.

Methyl (E)-3-(4-((2-methoxy-2-oxoethyl) carbamoyl) phenyl) acrylate (3n). $^1\text{H-NMR}$ (400 MHz, CDCl_3) δ 7.83 (d, $J = 8.0$ Hz, 1H), 7.70 (d, $J = 16.0$ Hz, 1H), 7.58 (d, $J = 8.0$ Hz, 1H), 6.83 (s, 1H), 6.50 (d, $J = 16.0$ Hz, 1H), 4.26 (d, $J = 5.0$ Hz, 1H), 3.82 (s, $J = 5.7$ Hz, 1H), 3.81 (s, 2H). $^{13}\text{C-NMR}$ (101 MHz, CDCl_3) δ 170.49, 167.05, 166.67, 143.41, 137.62, 134.86, 128.19, 127.71, 119.85, 52.58, 51.91, 41.76. White solid (70% yield). ESI-HRMS m/z $[\text{M} + \text{Na}]^+$ calcd for $\text{C}_{14}\text{H}_{15}\text{NO}_5$ 300.0836, found 300.0842.

4a.5 References

1. Şener, B.; Gözler, B.; Minard, R. D.; Shamma, M., Alkaloids of *Fumaria vaillantii*. *Phytochemistry* **1983**, 22 (9), 2073-2075.
2. Blaskó, G.; Gula, D. J.; Shamma, M., The phthalideisoquinoline alkaloids. *Journal of Natural Products* **1982**, 45 (2), 105-122.
3. Upadhyay, S. P.; Thapa, P.; Sharma, R.; Sharma, M., 1-Isoindolinone scaffold-based natural products with a promising diverse bioactivity. *Fitoterapia* **2020**, 146, 104722.
4. Thapa, P.; Corral, E.; Sardar, S.; Pierce, B. S.; Foss Jr, F. W., Isoindolinone synthesis: selective dioxane-mediated aerobic oxidation of isoindolines. *The Journal of Organic Chemistry* **2018**, 84 (2), 1025-1034.
5. Anamimoghadam, O.; Mumtaz, S.; Nietsch, A.; Saya, G.; Motti, C. A.; Wang, J.; Junk, P. C.; Qureshi, A. M.; Oelgemöller, M., The photodecarboxylative addition of carboxylates to phthalimides as a key-step in the synthesis of biologically active 3-arylmethylene-2, 3-dihydro-1H-isoindolin-1-ones. *Beilstein Journal of Organic Chemistry* **2017**, 13 (1), 2833-2841.

6. Abell, A.; Oldham, M.; Taylor, J., Synthesis of Cyclic Acylated Enamino Esters from Enol Lactones, 4-Keto amides, and 5-Hydroxy Lactams. *The Journal of Organic Chemistry* **1995**, *60* (5), 1214-1220.
7. Chalker, J. M.; Bernardes, G. J.; Davis, B. G., A “tag-and-modify” approach to site-selective protein modification. *Accounts of chemical research* **2011**, *44* (9), 730-741.
8. Ali, W.; Prakash, G.; Maiti, D., Recent development in transition metal-catalysed C–H olefination. *Chemical Science* **2021**, *12* (8), 2735-2759.
9. Reddy, M. C.; Jeganmohan, M., Total synthesis of aristolactam alkaloids via synergistic C–H bond activation and dehydro-Diels–Alder reactions. *Chemical Science* **2017**, *8* (5), 4130-4135.
10. Deb, A.; Hazra, A.; Peng, Q.; Paton, R. S.; Maiti, D., Detailed mechanistic studies on palladium-catalyzed selective C–H olefination with aliphatic alkenes: a significant influence of proton shuttling. *Journal of the American Chemical Society* **2017**, *139* (2), 763-775.
11. Bag, S.; Patra, T.; Modak, A.; Deb, A.; Maity, S.; Dutta, U.; Dey, A.; Kancharla, R.; Maji, A.; Hazra, A., Remote para-C–H functionalization of arenes by a D-shaped biphenyl template-based assembly. *Journal of the American Chemical Society* **2015**, *137* (37), 11888-11891.
12. Deb, A.; Bag, S.; Kancharla, R.; Maiti, D., Palladium-catalyzed aryl C–H olefination with unactivated, aliphatic alkenes. *Journal of the American Chemical Society* **2014**, *136* (39), 13602-13605.
13. Seth, K.; Bera, M.; Brochetta, M.; Agasti, S.; Das, A.; Gandini, A.; Porta, A.; Zanoni, G.; Maiti, D., Incorporating unbiased, unactivated aliphatic alkenes in Pd (II)-catalyzed olefination of benzyl phosphonamide. *ACS Catalysis* **2017**, *7* (11), 7732-7736.
14. Thrimurtulu, N.; Dey, A.; Singh, A.; Pal, K.; Maiti, D.; Volla, C. M., Palladium Catalyzed Regioselective C4-Arylation and Olefination of Indoles and Azaindoles. *Advanced Synthesis & Catalysis* **2019**, *361* (6), 1441-1446.
15. Maity, S.; Hoque, E.; Dhawa, U.; Maiti, D., Palladium catalyzed selective distal C–H olefination of biaryl systems. *Chemical Communications* **2016**, *52* (97), 14003-14006.
16. Manoharan, R.; Sivakumar, G.; Jeganmohan, M., Cobalt-catalyzed C–H olefination of aromatics with unactivated alkenes. *Chemical Communications* **2016**, *52* (69), 10533-10536.
17. Patra, T.; Watile, R.; Agasti, S.; Naveen, T.; Maiti, D., Sequential meta-C–H olefination of synthetically versatile benzyl silanes: effective synthesis of meta-olefinated toluene, benzaldehyde and benzyl alcohols. *Chemical Communications* **2016**, *52* (10), 2027-2030.
18. Achar, T. K.; Ramakrishna, K.; Pal, T.; Porey, S.; Dolui, P.; Biswas, J. P.; Maiti, D., Regiocontrolled remote C–H olefination of small heterocycles. *Chemistry–A European Journal* **2018**, *24* (68), 17906-17910.

19. Dutta, U.; Maiti, S.; Pimparkar, S.; Maiti, S.; Gahan, L.; Krenke, E.; Lupton, D.; Maiti, D., Rhodium catalyzed template-assisted distal para-CH olefination, *Chem. Sci.* 2019.
20. Maity, S.; Kancharla, R.; Dhawa, U.; Hoque, E.; Pimparkar, S.; Maiti, D., *ACS Catal.*, 2016, 6, 5493–5499 CrossRef CAS;(b) S. Maity, P. Dolui, R. Kancharla and D. Maiti, *Chem. Sci* **2017**, 8, 5181-5185.
21. Baccalini, A.; Vergura, S.; Dolui, P.; Maiti, S.; Dutta, S.; Maity, S.; Khan, F. F.; Lahiri, G. K.; Zannoni, G.; Maiti, D., Cobalt-catalyzed C (sp²)-H allylation of biphenyl amines with unbiased terminal olefins. *Organic letters* **2019**, 21 (21), 8842-8846.
22. Savelle, R.; Méndez-Gálvez, C., Isoindolinone Synthesis via One-Pot Type Transition Metal Catalyzed C–C Bond Forming Reactions. *Chemistry–A European Journal* **2021**, 27 (17), 5344-5378.
23. Xia, C.; White, A. J.; Hii, K. K. M., Synthesis of isoindolinones by Pd-catalyzed coupling between N-methoxybenzamide and styrene derivatives. *The Journal of Organic Chemistry* **2016**, 81 (17), 7931-7938.
24. Zhu, C.; Falck, J., N-acylsulfonamide assisted tandem C–H olefination/annulation: synthesis of isoindolinones. *Organic letters* **2011**, 13 (5), 1214-1217.
25. Youn, S. W.; Ko, T. Y.; Kim, Y. H.; Kim, Y. A., Pd (II)/Cu (II)-Catalyzed regio- and stereoselective synthesis of (E)-3-aryl-methyleneisoindolin-1-ones using air as the terminal oxidant. *Organic letters* **2018**, 20 (24), 7869-7874.
26. Noisier, A. F.; Brimble, M. A., C–H functionalization in the synthesis of amino acids and peptides. *Chemical Reviews* **2014**, 114 (18), 8775-8806.
27. Gong, W.; Zhang, G.; Liu, T.; Giri, R.; Yu, J.-Q., Site-selective C (sp³)-H functionalization of di-, tri-, and tetrapeptides at the N-terminus. *Journal of the American Chemical Society* **2014**, 136 (48), 16940-16946.
28. Chen, G.; Zhuang, Z.; Li, G. C.; Saint-Denis, T. G.; Hsiao, Y.; Joe, C. L.; Yu, J. Q., Ligand-Enabled β -C–H Arylation of α -Amino Acids Without Installing Exogenous Directing Groups. *Angewandte Chemie* **2017**, 129 (6), 1528-1531.
29. Liu, T.; Qiao, J. X.; Poss, M. A.; Yu, J. Q., Palladium (II)-Catalyzed Site-Selective C (sp³)-H Alkynylation of Oligopeptides: A Linchpin Approach for Oligopeptide–Drug Conjugation. *Angewandte Chemie International Edition* **2017**, 56 (36), 10924-10927.
30. Mendive-Tapia, L.; Preciado, S.; García, J., Ramón; R.; Kielland, N.; Albericio, F.; Lavilla, R. New peptide architectures through C–H activation stapling between tryptophan–phenylalanine/tyrosine residues. *Nat. Commun* **2015**, 6, 1-9.
31. Noisier, A. F.; García, J.; Ionuț, I. A.; Albericio, F., Stapled Peptides by Late-Stage C (sp³)-H Activation. *Angewandte Chemie* **2017**, 129 (1), 320-324.
32. Tran, L. D.; Daugulis, O., Nonnatural amino acid synthesis by using carbon–hydrogen bond functionalization methodology. *Angewandte Chemie* **2012**, 124 (21), 5278-5281.

33. Lu, Y.; Wang, D.-H.; Engle, K. M.; Yu, J.-Q., Pd (II)-catalyzed hydroxyl-directed C–H olefination enabled by monoprotected amino acid ligands. *Journal of the American Chemical Society* **2010**, *132* (16), 5916-5921.
34. He, J.; Li, S.; Deng, Y.; Fu, H.; Laforteza, B. N.; Spangler, J. E.; Homs, A.; Yu, J.-Q., Ligand-controlled C (sp³)–H arylation and olefination in synthesis of unnatural chiral α -amino acids. *Science* **2014**, *343* (6176), 1216-1220.
35. Sevov, C. S.; Hartwig, J. F., Iridium-catalyzed oxidative olefination of furans with unactivated alkenes. *Journal of the American Chemical Society* **2014**, *136* (30), 10625-10631.
36. Lu, M.-Z.; Chen, X.-R.; Xu, H.; Dai, H.-X.; Yu, J.-Q., Ligand-enabled ortho-C–H olefination of phenylacetic amides with unactivated alkenes. *Chemical Science* **2018**, *9* (5), 1311-1316.
37. Bera, M.; Modak, A.; Patra, T.; Maji, A.; Maiti, D., Meta-selective arene C–H bond olefination of arylacetic acid using a nitrile-based directing group. *Organic letters* **2014**, *16* (21), 5760-5763.
38. Agasti, S.; Mondal, B.; Achar, T. K.; Sinha, S. K.; Sarala Suseelan, A.; Szabo, K. J.; Schoenebeck, F.; Maiti, D., Orthogonal selectivity in C–H olefination: synthesis of branched vinylarene with unactivated aliphatic substitution. *ACS Catalysis* **2019**, *9* (10), 9606-9613.
39. Bera, M.; Sahoo, S.; Maiti, D., *ACS Catal.* **2016**, *6*, 3575– 3579.(d) Maji, A.
40. Achar, T. K.; Zhang, X.; Mondal, R.; Shanavas, M.; Maiti, S.; Maity, S.; Pal, N.; Paton, R. S.; Maiti, D., Palladium-catalyzed directed meta-selective C–H allylation of arenes: Unactivated internal olefins as allyl surrogates. *Angewandte Chemie* **2019**, *131* (30), 10461-10468.
41. Achar, T. K.; Biswas, J. P.; Porey, S.; Pal, T.; Ramakrishna, K.; Maiti, S.; Maiti, D., Palladium-catalyzed template directed C-5 selective olefination of thiazoles. *The Journal of Organic Chemistry* **2019**, *84* (12), 8315-8321.
42. Bag, S.; Jana, S.; Pradhan, S.; Bhowmick, S.; Goswami, N.; Sinha, S. K.; Maiti, D., Imine as a linchpin approach for meta-C–H functionalization. *Nature Communications* **2021**, *12* (1), 1393.
43. Bag, S.; Maiti, D., Palladium-catalyzed olefination of aryl C–H bonds by using directing scaffolds. *Synthesis* **2016**, *48* (06), 804-815.
44. Tang, J.; Chen, H.; He, Y.; Sheng, W.; Bai, Q.; Wang, H., Peptide-guided functionalization and macrocyclization of bioactive peptidosulfonamides by Pd (II)-catalyzed late-stage C–H activation. *Nature Communications* **2018**, *9* (1), 3383.

CHAPTER-4b

Synthesis of Biocompatible *N*-Isoindolinonyl Peptides via Pd(II)-Catalysed C(sp²)-H Olefination/activation and Their Conformational Evaluation

TABLE OF CONTENTS

Chapter 4b	116
4b.1 Introduction.....	116
4b.1.1 Hypothesis and objective.....	119
4b.2 Results and Discussions	120
4b.2.1 Isoindolinone synthesis from <i>N</i>-Benzoyl peptide	120
4b.2.2 Substrate scope using various dipeptides	121
4b.2.3 Substrate scope using 2-napthoic acid and 4-biphenayl carboxylic acid	123
4b.2.4 Substrate scope using various aryl groups	124
4b.2.5 Substrate scope using tripeptides	125
4b.2.6 Conformational analyses	127
4b.2.7 DMSO D6 Titration study	128
4b.2.8 Theoretical study	129
4b.2.9 Cell culture study	131
4b.3 Conclusions.....	132
4b.4 Experimental Details	133
4b.4.1 Material and Instrumentation	133
4b.4.2 General Procedure for benzamide derivative peptide synthesis.....	133
4b.4.3 General procedure for Pd-catalysed reactions	134
4b.4.4 Chemical shift values of NMR	134
4b.5 References.....	152

Chapter 4b

4b.1 Introduction

Isoindolinone is heterocyclic compound with benzo fused γ -lactam scaffold that is constituent of various natural products and synthetic bioactive molecules such as Pagoclone, Indoprofen, Erinacerins, lennoxamine, lenalidomide, Isohercenone, and pazinacolone (**Figure 4b.1a**).¹⁻³ These molecules show antimicrobial, antioxidant, antifungal, antiviral, anxiolytic, anti-parkinsons, anti-inflammatory, antihypertension, and anticancer activities.⁴ In repertoire of isoindoline scaffold into peptides, the incorporation of isoindolinone moiety into naturally occurring bioactive cyclic peptides enhance their bioactivity. Fenestin A and Zygosporamide are marine-derived natural cyclic peptides possessing wide range of bioactivities including anticancer. Jin has synthesized Fenestin analogues containing isoindolinone derivatives that improved their apoptosis of tumor cells and lead to cycle arrest in the G2/M phase.⁵ Zygosporamide cyclic depsipetides isolated from marine derived fungus and its analogues are also synthesized by incorporating isoindolinone moiety that significantly improve their bioactivities (**Figure 4b.1b**).⁶ Nevertheless, Chen has synthesized various stappled peptides by incorporating isoindolinone derivatives (**Figure 4b.1c**).⁷ Thus, demand of isoindolinone containing peptides has suddenly increased and become lucrative research area for both chemists and biologists. In the literature, various heterocyclic scaffold has been used for the structural and conformational changes of native peptides.⁸⁻¹⁰ Isoindolinone moiety of Isoindolinonyl peptides could also participate in an intramolecular hydrogen bonding with other amide N-H of peptides and play significant roles in conformational changes of peptides.

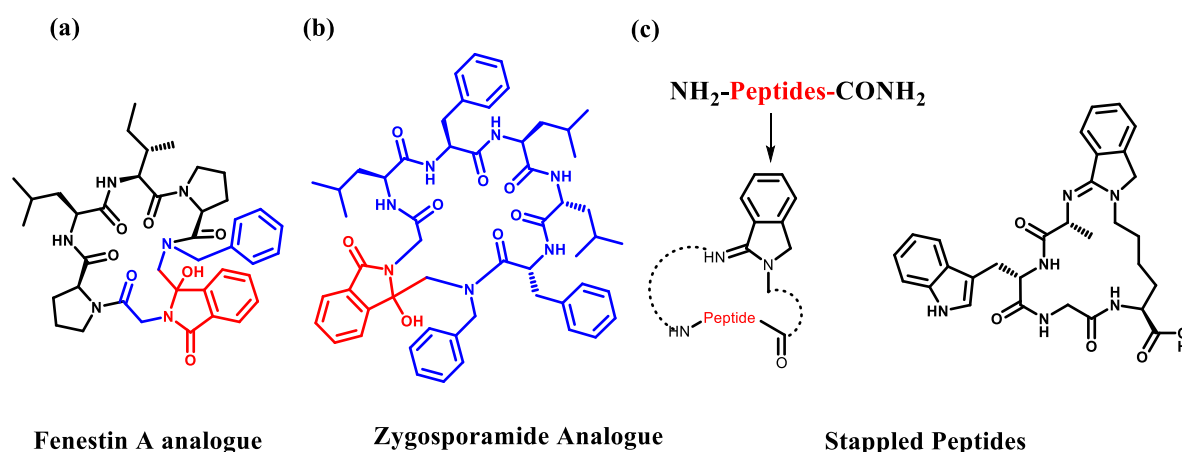


Figure 4b.1 Isoindolinone and related natural peptides.

The classical synthesis of Isoindolinone compounds is achieved through multiple challenging steps.¹¹⁻¹³ In recent times, various heterocycle compounds are synthesized in one step from economical reactant precursor through the metal catalyzed C-H activation which is modern synthetic methodology. However, the incorporation of isoindolinone residue in the native peptides are challenging through chemical synthesis. Recently, we have reported the synthesis of isoindolinone containing amino acid ester derivatives through Pd(II)-catalyzed C-H activation/olefination from *N*-benzoyl amino acid esters and olefins without using auxiliary directing group, modern synthetic methodology by C-H activations.¹⁴ Transition metal-catalyzed C-H activation and C-H olefination are emerging synthetic methodologies for synthesis of various natural products and their precursors, including isoindolinone derivatives.¹⁵⁻¹⁸ The Pd(II) catalysed C(sp²)-H olefination methodologies have reached a new milestone owing to its easy handling and cost effective.¹⁸⁻²⁹ The Co-/Rh-catalysed substrate-specific C(sp²)-H olefination are also known.³⁰⁻³² The regioselective metal catalysed C-H activation also require directing group and ligand for metal complexation before inert C-H activation and functionalization. The directing groups could be auxiliary, transient, or intrinsic. The directing group containing arylamides has also been

used for synthesizing isoindolinone derivatives from non-activated olefins through C-(sp²)-H olefination.³³ For example, the quinoline directing group containing arylamides gives *N*-quinolinyl substituted isoindolinones from acrylate in presence of Pd(II)-catalyst. However, *N*-tosylated benzamide requires a ligand to prepare isoindolinone derivatives from olefin through Pd(II)-catalysed olefination.³⁴⁻³⁵ Amino acids and peptides are natural ligands of various transition metals and are being used as directing group/ligand in the different transition metal-catalysed C–H activation/C–Olefination.³⁶ Yu has explored amino acids/peptides as the ligand or directing group in the metal-catalysed C(sp³)-H functionalization of *di-/tri/tetra*-peptides at the *N*-terminus/site-specific C–H alkynylation/ β -C–H arylation.³⁷⁻³⁹ Albericio has shown the synthesis of stapled-peptides by the late-stage C(sp³)-H activation of peptides.⁴⁰⁻⁴¹ Daugulis has used 2-thiomethylaniline as directing group for C(sp³)-H functionalization of *N*-protected amino acids at β -position with the different aryl halide.⁴² The metal-catalysed C–H olefinations of amino acid/peptide related compounds have generated opportunities to prepare various synthetic and natural peptide analogues.⁴³⁻⁴⁴ Metal catalysed olefination of ligand enabled aryl amide with olefin are emerging synthetic methodologies attracting towards the synthesis of substituted aryl amide derivatives.^{24, 45-51} Recently, Maiti has explored Pd(II)-catalysed 8-AQ directed and template based regioselective C–H olefinations with non-active aliphatic olefins.⁴⁷⁻⁵³ Wang has demonstrated the Pd(II)-catalysed ortho-olefination reaction and the cyclization reaction at benzyisulfonamide to yield benzosultam peptidomimetics.⁵⁴ The synthesis of Isoindolinone derivatives without comprising amino acid are accomplished from activated arylamides and non-reactive olefins through transition metal catalyzed C–H activation using metal ions-Sc, Yb, Au, Rh, Ir, Ru, Co, Cu, Ni, Zn, In, and Pd (**Figure. 4b.2a-b**).⁵⁵ Herein, we have rationally designed peptides containing isoindolinone olefin ester at *N*-

terminal to explore the role of isoindolinone's lactam carbonyl in the folding of peptide structure through non-covalent interactions (**Figure 4b.2c**). This report describes the post synthesis isoindolinonyl peptides from *N*-arylamide peptides and olefins through Pd(II)-catalysed C(sp²)-H olefination. Their conformational analysis is also studied by NMR and computational technique. To examine the biocompatibility and therapeutic values, their cell cytotoxicity studies are also performed before exploring their therapeutic values.

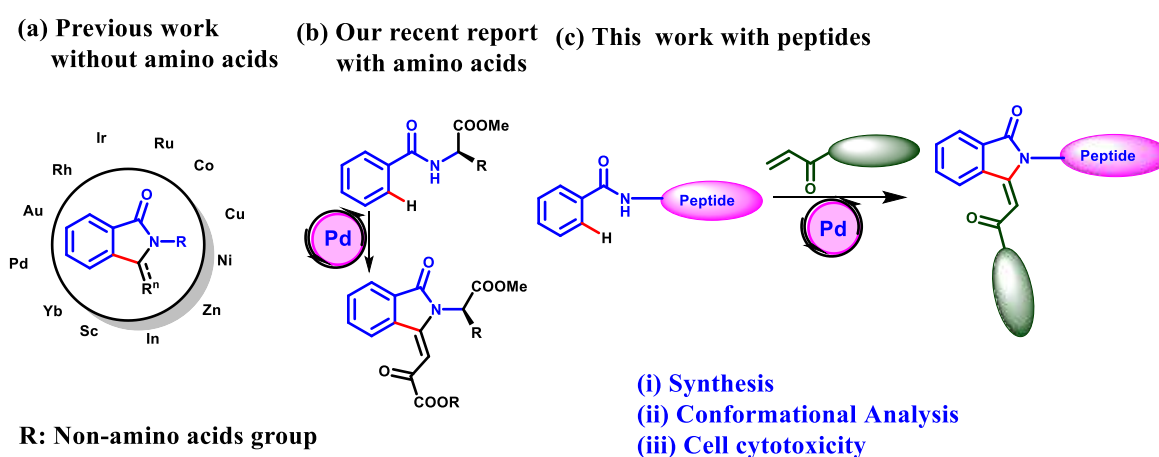


Figure 4b.2 (a) The previously reported C-H hydroarylation (b) C-H functionalization and (c) This report- post synthesis of isoindolinyl peptides.

4b.1.1 Hypothesis and objective

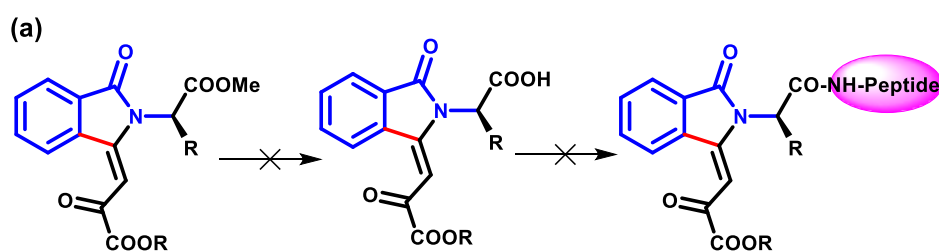
Here, we describe a method for chemo-selectively altering peptides by C-H activation/olefination catalysed by palladium with cost-effective production of functionalized isoindolinone scaffolds with strong regioselectivity. This approach offers a chemical method for the creation of novel peptide-isoindolinone conjugates and is characterised by racemization-free conditions, the generation of peptide conjugates to pharmaceuticals, natural products, and other peptide fragments. This study offers a novel illustration of peptide backbone diversity.

4b.2 Results and Discussions

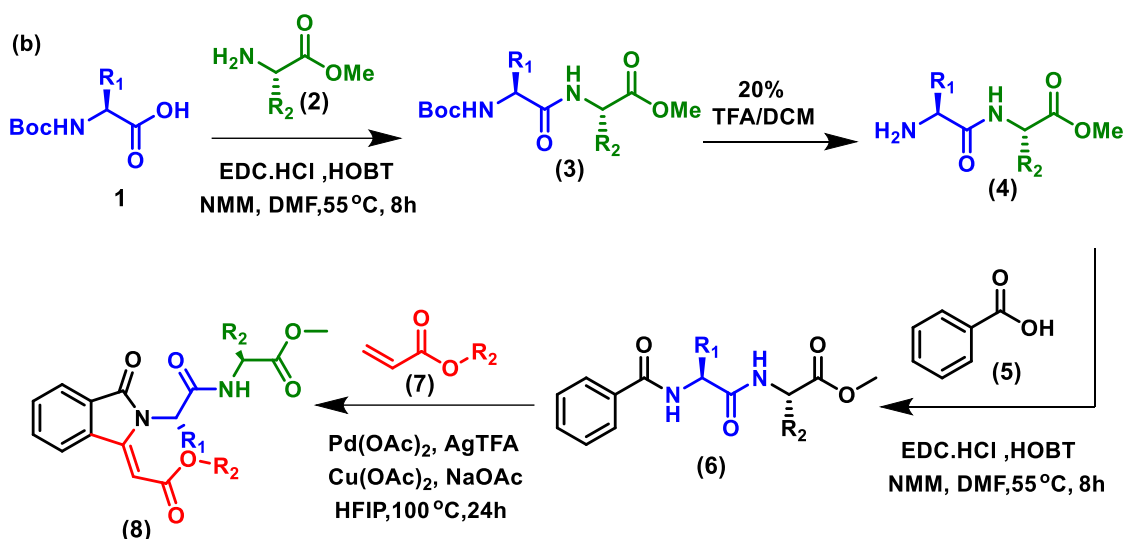
4b.2.1 Isoindolinone synthesis from *N*-Benzoyl peptide

The conjugation of isoindolinone scaffold at peptides could be achieved by two ways: (a) Coupling of previously synthesized isoindolinonyl amino acid carboxylates at free NH group of designed peptides; (b) C(sp²)-H olefination/activation reaction at *N*-benzamide of target peptides. However, we were unable to achieve its mono carboxylate derivative of isoindolinonyl amino acid ester through the base catalysed hydrolysis under mild condition (**Scheme 4b.1a**). Thus, we attempted for C(sp²)-H olefination/activation at *N*-benzamide of peptides. We synthesized dipeptides (**1-4**), containing glycine, valine, phenyl alanine and phenyl glycine ester, and their *N*-benzamide peptides (**6a-6d**) with benzoic acid under peptide coupling conditions. These peptides were subjected for Pd(II)-catalysed C-H activation/olefination reactions with different olefins by using our previously reported method.⁵⁶ Unfortunately, we could not get any olefinated/activated product. We noticed the formation of isoindolinonyl peptides (**8a**) from peptide **6a** and olefin methyl acrylate (**7a**) under Cu(OAc)₂/NaOAc at 100°C in the presence of Pd(II)-catalyst.⁵⁴ Importantly, additive Cu(OAc)₂/NaOAc was found essential for *mono* C-H olefination/activation reaction in *N*-benzamide peptides (**Scheme 4b.2a**).

Scheme 4b.1 Synthesis of substituted isoindolinone peptide derivative with peptide residue



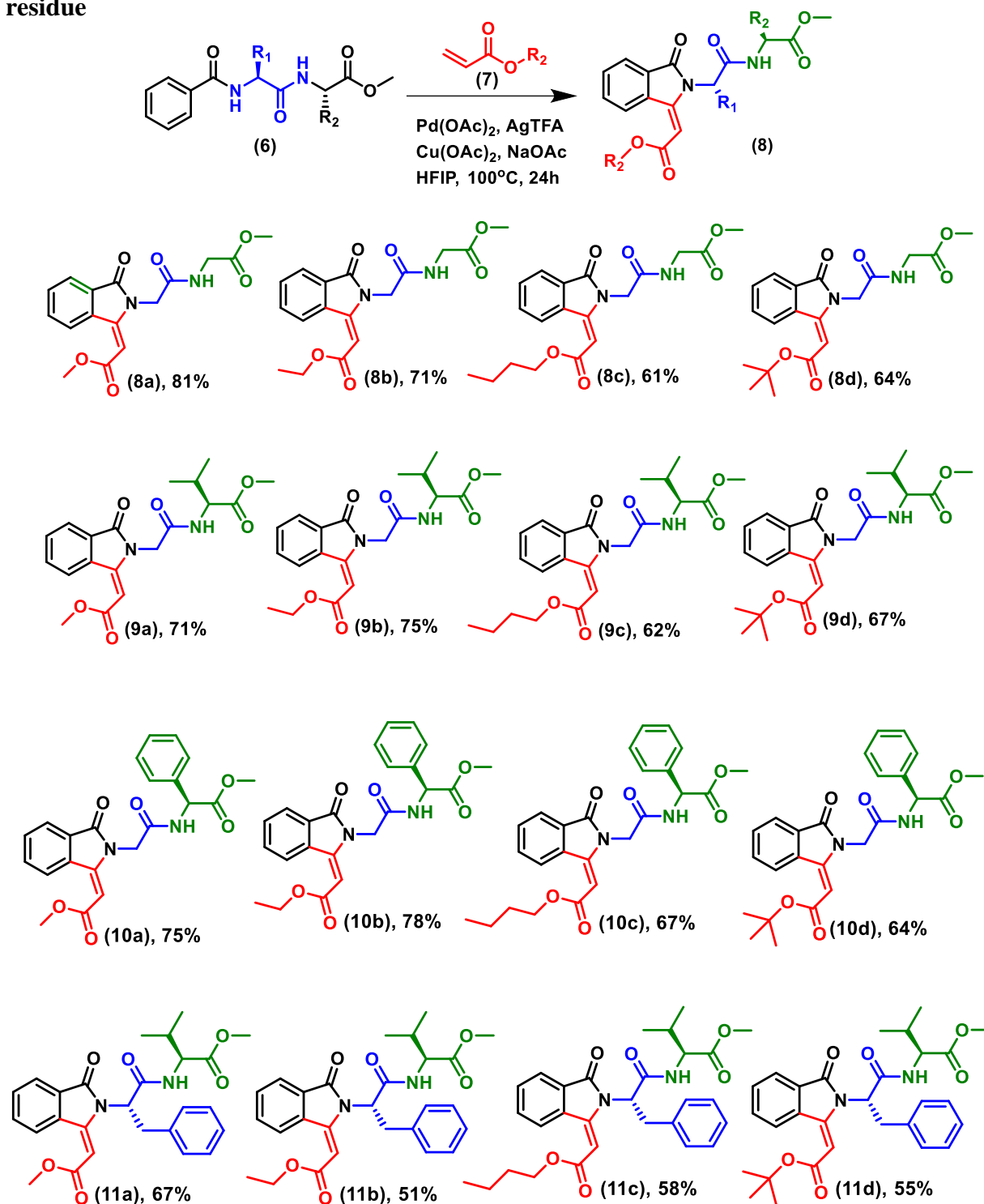
Challenges for mono ester hydrolysis



4b.2.2 Substrate scope using various dipeptides

Similarly, we synthesized other isoindolinonyl peptides **8b-8d** from peptide **6a** and different olefins- ethyl acrylate (**7b**), n-butyl acrylate (**7c**), and t-butyl acrylate (**7d**). Next, peptide **6b** were treated with various olefins (**7a-7d**) under similar optimized reaction conditions of *mono* C(sp²)-H olefination/activations that produced isoindolinonyl peptides **9a-9d** (Scheme 4b.2). We performed similar reaction with *N*-benzamide of additional *phenyl ring* containing dipeptides (**6c-6d**) and different olefins (**7a-7d**). Pleasantly, we isolated isoindolinonyl peptides **10a-10d/11a-11d** from the respective peptides and olefins through chemoselective/regioselective C-H olefination/activation at only benzamide ring. Herein, we could not get C(sp²)-H olefination reaction at phenyl glycine residue of peptide **6c** and phenyl alanine residue of peptide **6d** though there is presence of probable intrinsic amide directing group. Thus, only benzamide ring is susceptible for C-H olefination which lead to the formation of isoindolinonyl peptides.

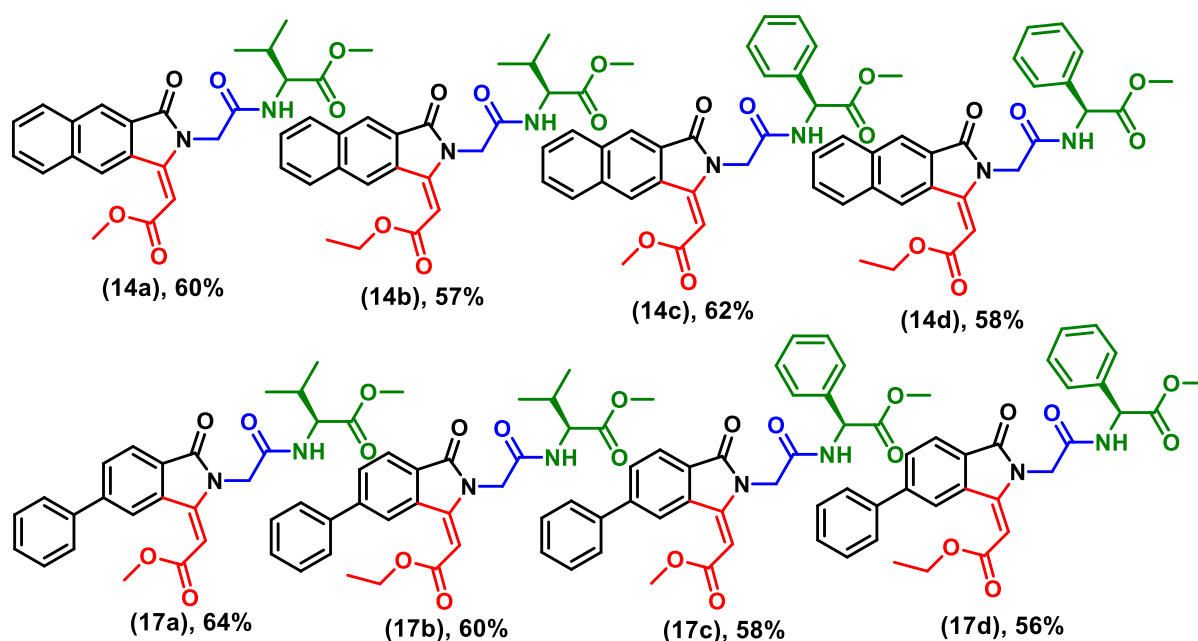
Scheme 4b.2 Synthesis of substituted isoindolinone peptide derivative with peptide residue



4b.2.3 Substrate scope using 2-napthoic acid and 4-biphenayl carboxylic acid

To explore the diversity of arylamide substrates for Pd(II)-catalysed isoindolinonyl peptide synthesis, we synthesized arylamide dipeptides **13a/13b** from 2-napthoic acid and dipeptides **4b/4c** (Scheme 4b.3). Similarly, we synthesized arylamide peptide substrates **16a/16b** from 4-biphenyl carboxylic acid and peptides **4b/4c**. These peptides were subjected for Pd catalysed olefination reaction under optimized conditions. Importantly, these peptides also produced chemo selective naphthyl isoindolinonyl peptides **14a-14d** from respective 2-napthoyl peptides **13a/13b** and acrylate **7a/7b**, while biphenyl isoindolinonyl peptides **17a-17d** from respective 4-biphenyl containing peptides **16a/16b** and acrylate **7a/7b**. Here too, we could not get C(sp²)-H olefination reaction at phenyl glycine residue of peptide **13b/16b** though there is presence of probable intrinsic amide directing group.

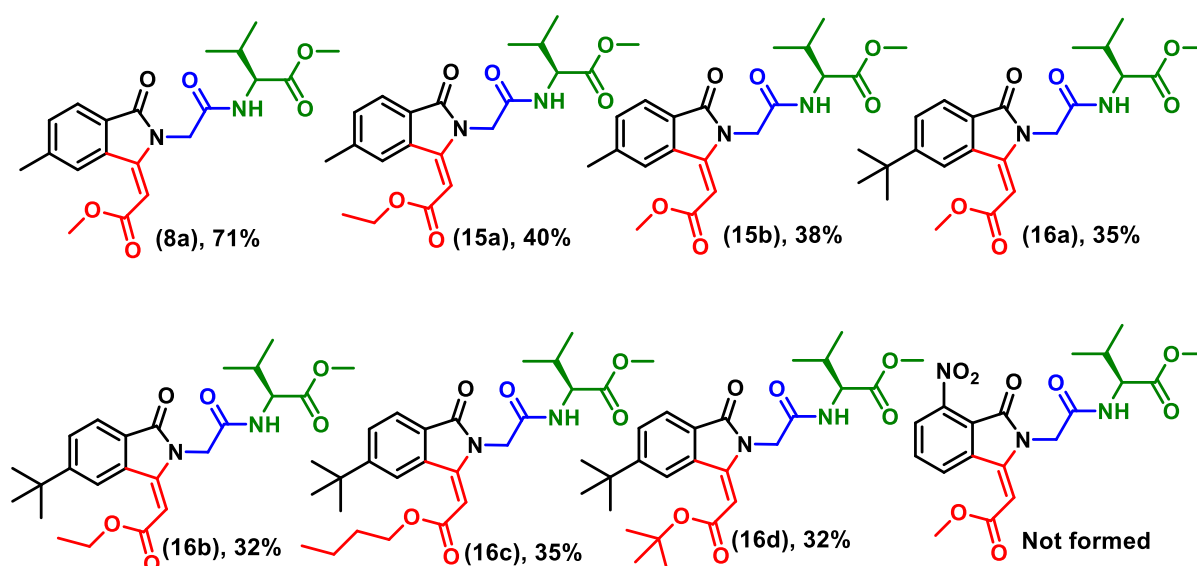
Scheme 4b.3 Synthesis of substituted isoindolinone peptide derivative with 2-napthoic acid and 4-biphenayl carboxylic acid



4b.2.4 Substrate scope using various aryl groups

Further, we examined C-H olefination/isoindolinonylation reaction with different *N*-benzamide dipetides and olefines under Pd-catalysed optimized reaction conditions. We synthesized arylamide peptides **19a-19c** containing different types of benzoyl residue such as *p*-methyl benzoyl in **19a**, *p*-*tert*-butylbenzoyl in peptide **19b**, and *m*-nitrobenzoyl in peptide **19c** (Scheme 4b.4). These peptides were subjected to olefination with different acrylates (**7**) under Pd-catalyzed olefination reaction condition. We isolated isoindolinone derivatives **20a-20b** from *p*-methylbenzoyl peptide and **21a-21d** from *p*-*tert*-butyl benzoyl peptides though their yields are low. However, nitrobenzoyl peptide (**19c**) could not give any C-H olefinated/activated product. It seems electron withdrawing group possibly perturb the metal Pd(II) complexation of phenyl ring of nitrobenzoyl peptide. Thus, unsubstituted aryl amides are more suitable substrates for Pd catalysed C(sp²)-H olefination/activation reactions under optimized condition.

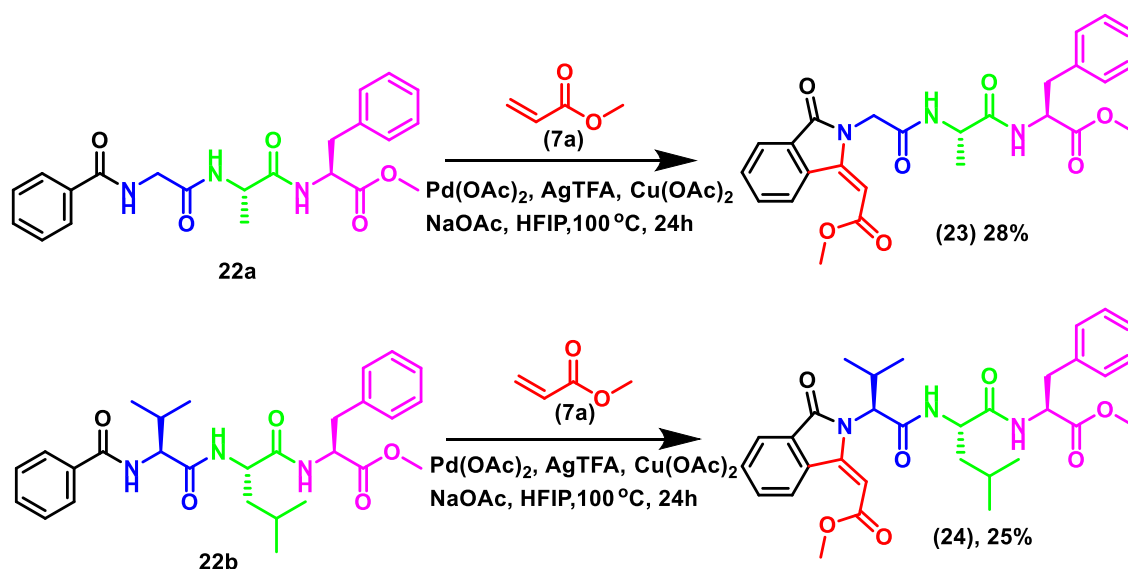
Scheme 4b.4 Synthesis of aryl substituted isoindolinonyl peptide derivatives



4b.2.5 Substrate scope using tripeptides

Further, we attempted to apply this methodology for synthesis of isoindolinone containing *tri*-peptides. Thus, we synthesized benzamide of *tri*-peptides such as BzNHGly-Ala-Phe (**22a**) and BzNHVal-Leu-Phe-OMe (**22b**). These peptides were subjected for Pd-catalysed olefination/activation reaction with olefin (**7a**) under above optimized reaction condition (Scheme 4b.5). Importantly, benzamide peptides **22a-22b** also produced respective isoindolinone derivative peptides **23/24** though their yields are quite low (~25-30%) as compared to dipeptides.

Scheme 4b.5 Synthesis of substituted isoindolinonyl *tri*-peptide



Herein we proposed reaction mechanism of isoindolinone-peptide synthesis through Pd(II)-catalyzed C(sp²)-H olefination/activation (Figure 4b.3). Additive Cu(OAc)₂ facilitates the formation of a stable palladacycle with amide carbonyl through N, O type chelation by preventing N,N covalent chelation. In the literature, the coordination of amide carbonyl with catalyst Pd(OAc)₂ is known as well.⁵⁷ Benzoyl amino acid residue of peptide (**reactant 6a**) acting as intrinsic directing group for the Pd-complexation (5-membered palladacycle) and proceeds for C(sp²)-H activation at ortho-position of its phenyl ring (**I-1**). Olefin has forms Pd-

complex **I-2** by displacement of ligand OAc, and then proceeds to **I-3** through 1,2-migration as intermediate **I-3**. This intermediate (**I-3**) leads to olefinated product (**6'**) via β -hydride elimination reaction. Again, palladacycle forming with benzoyl amino acid residue of olefinated peptide (**6'**) and proceeds for the $c(sp^2)$ -H activation at olefin as intermediate **I-4** that lead to stable isoindolinonyl peptides (**8a**) via reductive elimination. Regeneration of catalyst occur *in situ* through reoxidation.

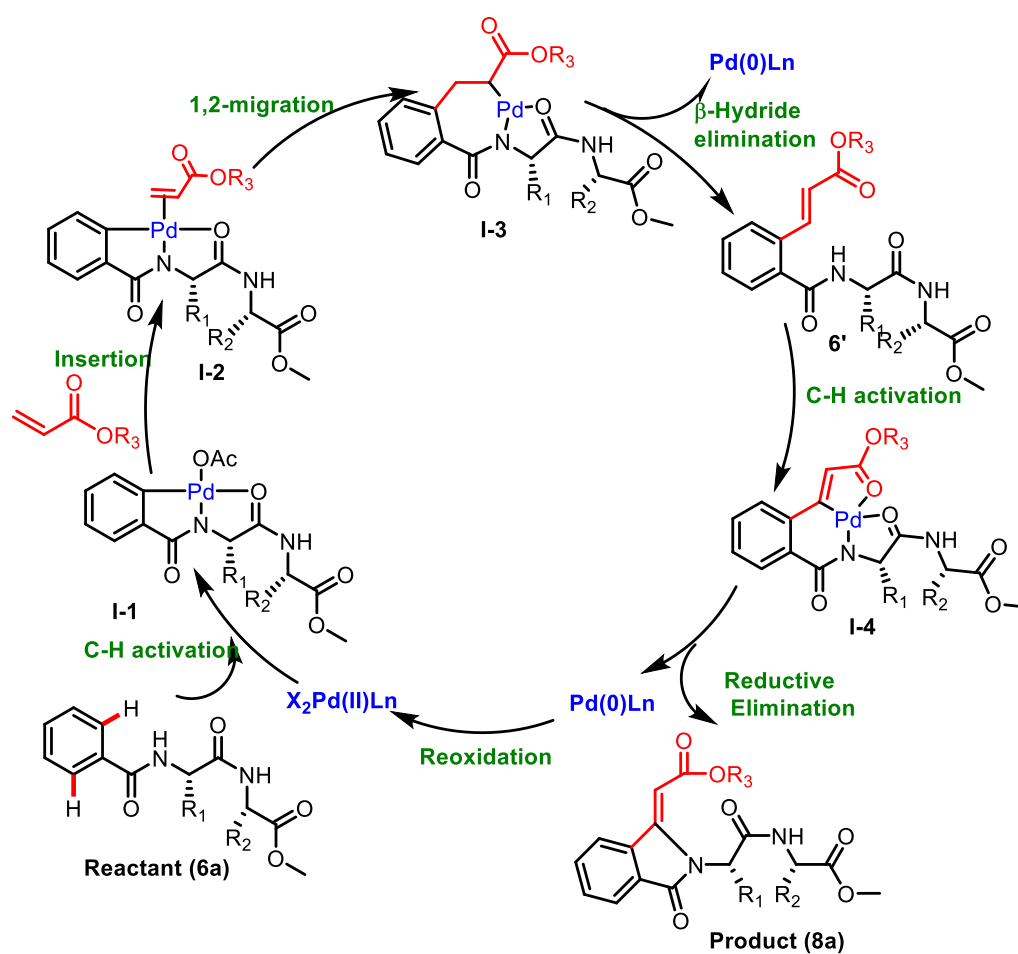


Figure 4b.3 The proposed mechanism for isoindolinone peptide synthesis.

4b.2.6 Conformational analyses

After successful synthesis of isoindolinonyl conjugated peptides through C-H activation, we attempted to find conformation of isoindolinyl tripeptides (**23**) in solution by NMR technique. We recorded its NMR spectra ($^1\text{H}/^1\text{H}$ - ^1H COSY/ ^1H - ^1H NOESY) only in DMSO- d_6 solvent because of poor solubility (or insolubility) in other solvents. The chemical shift of all protons was assigned from its COSY spectra, then its NOE cross peaks used to find interaction of non-vicinal protons. Our analyses helped to find the ^1H - ^1H interactions which are in proximity. In **Figure 4b.4**, phenyl ring proton (d) of isoindolinone residue interacts with methyl protons of acrylate residue. Olefin protons of acrylate residue exhibit two cross peaks with glycinate protons (a) and alaninyl methyl protons. Thus, orientation of isoindolinyl residue is in proximity with alanine methyl (i+2) to form a stable conformation in solution.

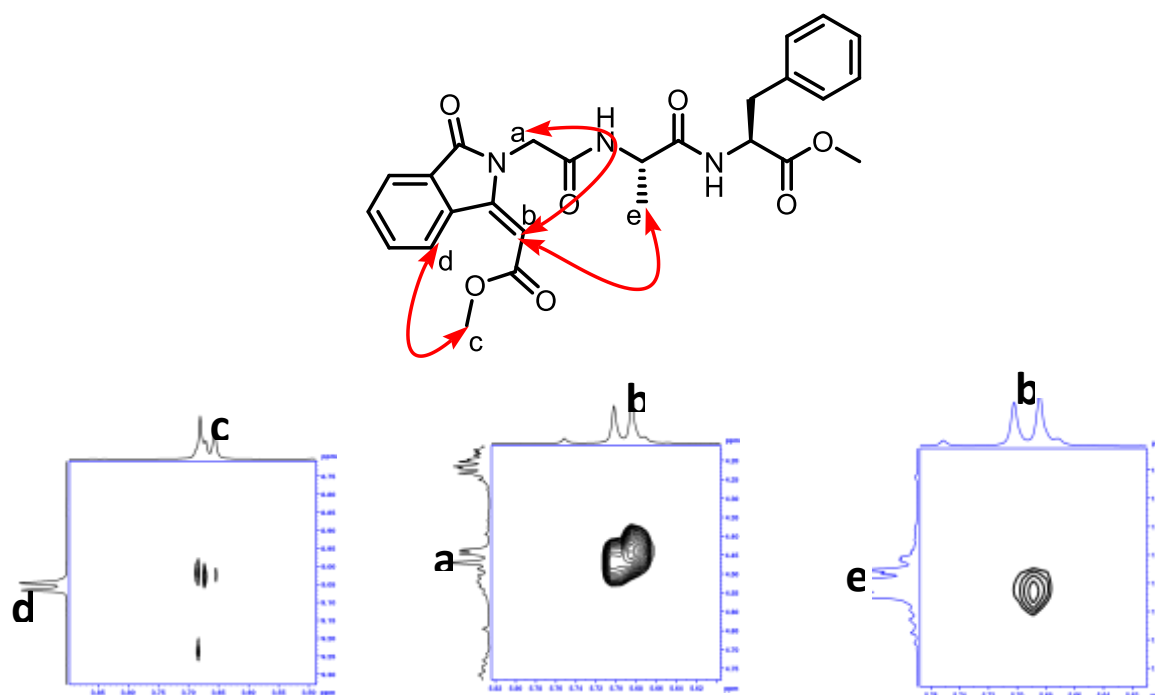


Figure 4b.4 NOESY spectra of isoindolinone derivative **23**.

4b.2.7 DMSO D6 Titration study

DMSO- d_6 titration NMR (^1H -NMR) experiment is well established technique to find the intramolecular hydrogen bonding N-H's in CDCl_3 .⁵⁸ Herein, we performed DMSO- d_6 titration ^1H -NMR experiment with representative isoindolinonyl peptides derived from methyl acrylates (**8a-11a/14a/14c/17a/17c**) and control peptide BzNHGly-ValOMe (**6b**). However, peptides **23/24** are insoluble in CDCl_3 (soluble only in DMSO). In **Figure 4b.5**, we have extracted a bar diagram Peptides vs $\Delta\delta(\text{ppm})$, where $\Delta\delta(\text{ppm}) = (\delta_{\text{final}} - \delta_{\text{initial}})$. Control peptide (**6b**) has two amide N-H's which titration profile shows that one N-H is unaffected while another has little downfield shift with DMSO- d_6 titration owing to the strong and moderate type intramolecular hydrogen bonding respectively. The isoindolinonyl peptides (**8a-11a/14a/14c/17a/17c**) have one amide N-H that exhibit little downfield shift (~ 0.4 - 1.3 ppm) with DMSO- d_6 titration possible due to intramolecular hydrogen bonding with amide N-H (**Figure 4b.5A & B**). The amide N-H of peptide **11a** and **9a** have little shifts as compared to other isoindolinonyl peptides (**Figure 4b.5B**). Thus, sequence specific isoindolinone carbonyl ($\text{C}=\text{O}$) has significant roles in the intramolecular hydrogen bonding with amide N-H which could be useful for tuning the peptide folding.

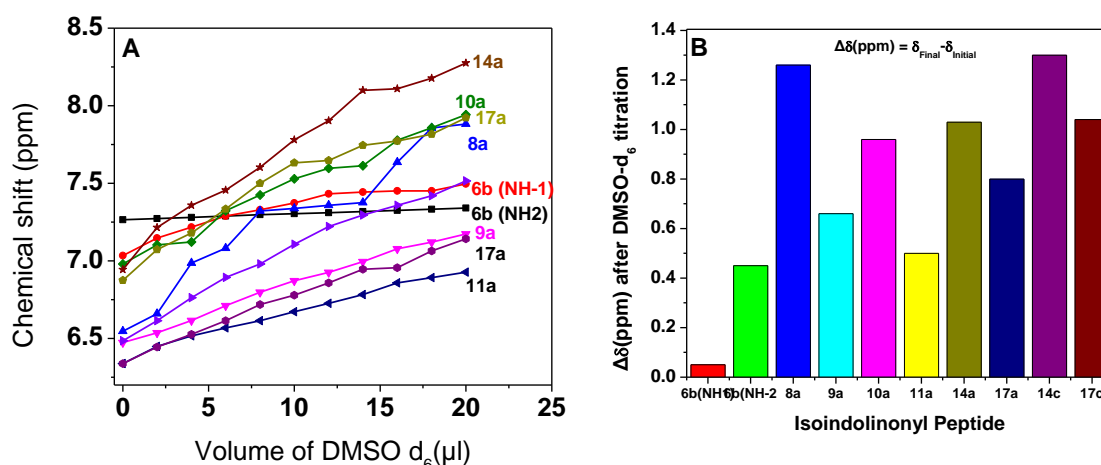


Figure 4b.5 DMSO d_6 titration NMR of isoindonyl derivatives.

4b.2.8 Theoretical study

Next, we performed computational studies with representative isoindolinonyl peptides derived from methyl acrylates (**8a-11a/14a/14c/17a/17c/23/24**) and control peptide BzNHGly-ValOMe (**6b**) using MMFF94 force field and GMMX. We visualized their conformations on PyMol (**Figure 4b.6**). Control peptide, without containing isoindolinone scaffold, (**6b**) exhibit hydrogen bonding between benzoyl carbonyl with second amino acid residue valine N-H (i+3) with bond distance 1.9Å (N-H---O=C) and bond angle \angle N-H-O \sim 148° that nearly matched with γ -turn. Isoindolinone containing dipeptides (**8a-11a/14a/14c/17a/17c**) exhibit an intramolecular hydrogen bonding between isoindolinone carbonyl (C=O) and N-H of second amino acid residue with bond distance (N-H---O) \sim 2.0 and bond angle \angle N-H-O \sim 150° with irrespective substituents of amino acid and nature of aryl group of isoindolinone residue. In the case of isoindolinonyl *tri*-peptides (**23/24**) it exhibits two intramolecular hydrogen bonding between isoindolinonyl carbonyl and amide i+3 amide (N-H-----O=C). The bond length/angle of hydrogen bonds are almost same \sim 2.0Å/ \sim 150° of peptide **23** and possibly lead to the formation of helix. In contrast for **24**, the bond length/angle of hydrogen bonds are different with bond length \sim 2.0Å/ \sim 150° (strong) & \sim 2.8Å/136° (weak) presumably due to leu residue at 2nd position and may leads to only γ -turn structure. These data strongly support that isoindolinone containing peptides are potential building blocks for the designing unique foldamers.

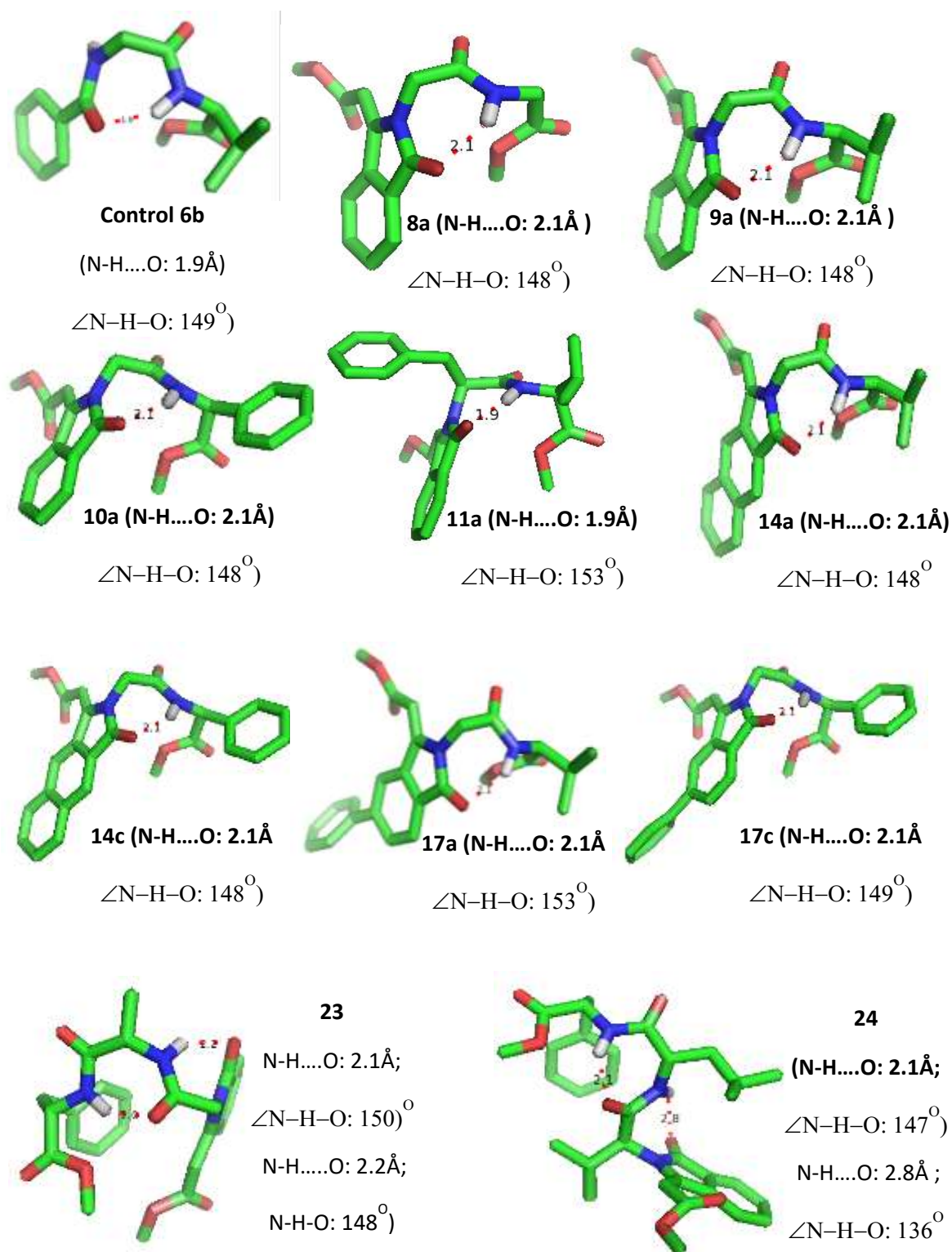
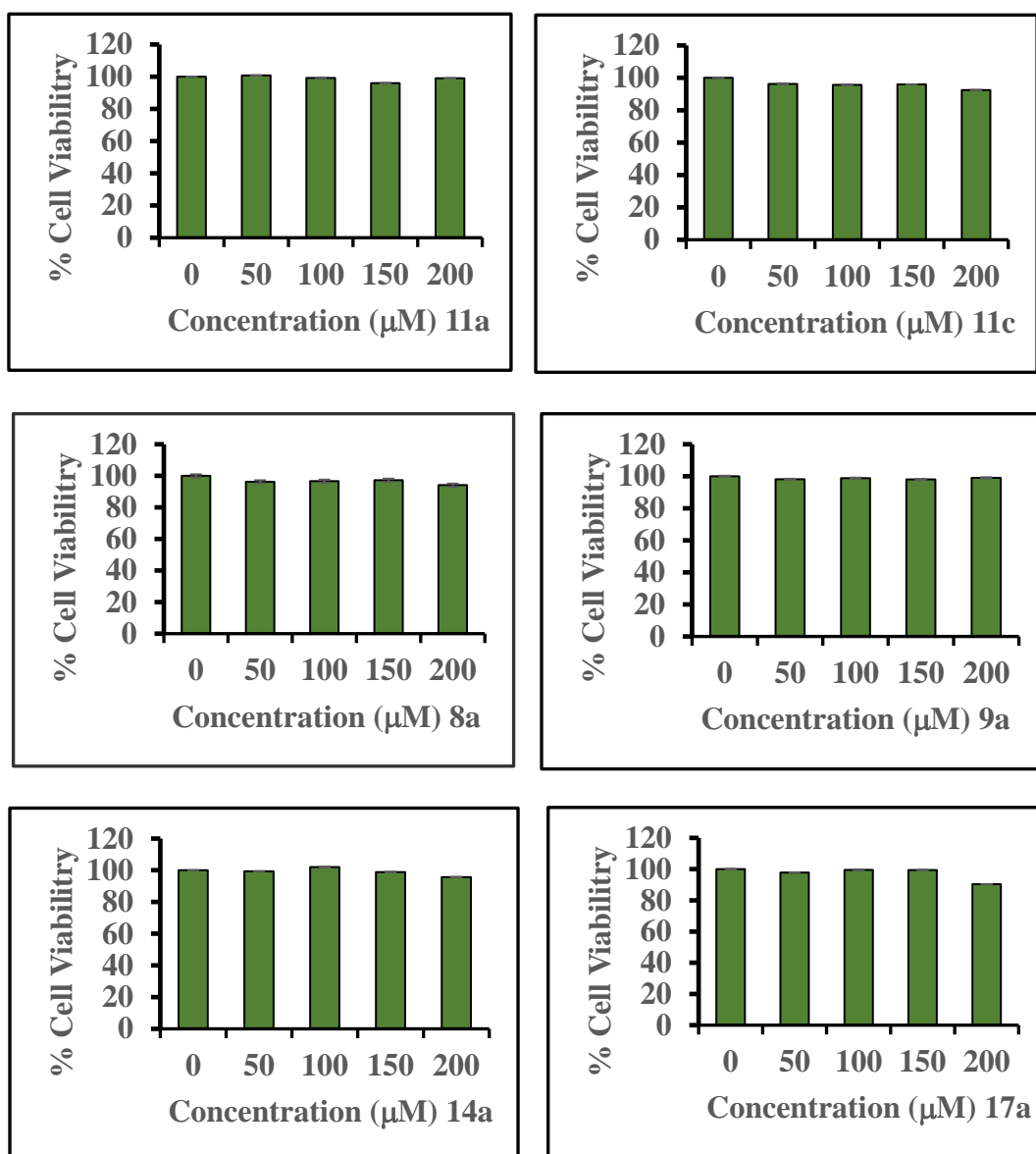


Figure 4b.6 Conformation of isoindolinone peptides (Computationally optimized structure of isoindolinone peptides MMFF94 and GMMX).

4b.2.9 Cell culture study

Finally, we examined the cell cytotoxicity of isoindolinonyl peptides derived from methyl acrylates (**8a-11a/11c/14a/17a/20a/21a/23**) with Hek293T cells using MTT assay. Their cytotoxicity data are provided below (**Figure 4b.7**) that indicate isoindolinonyl peptides have negligible cytotoxicity as compared to control (DMSO).



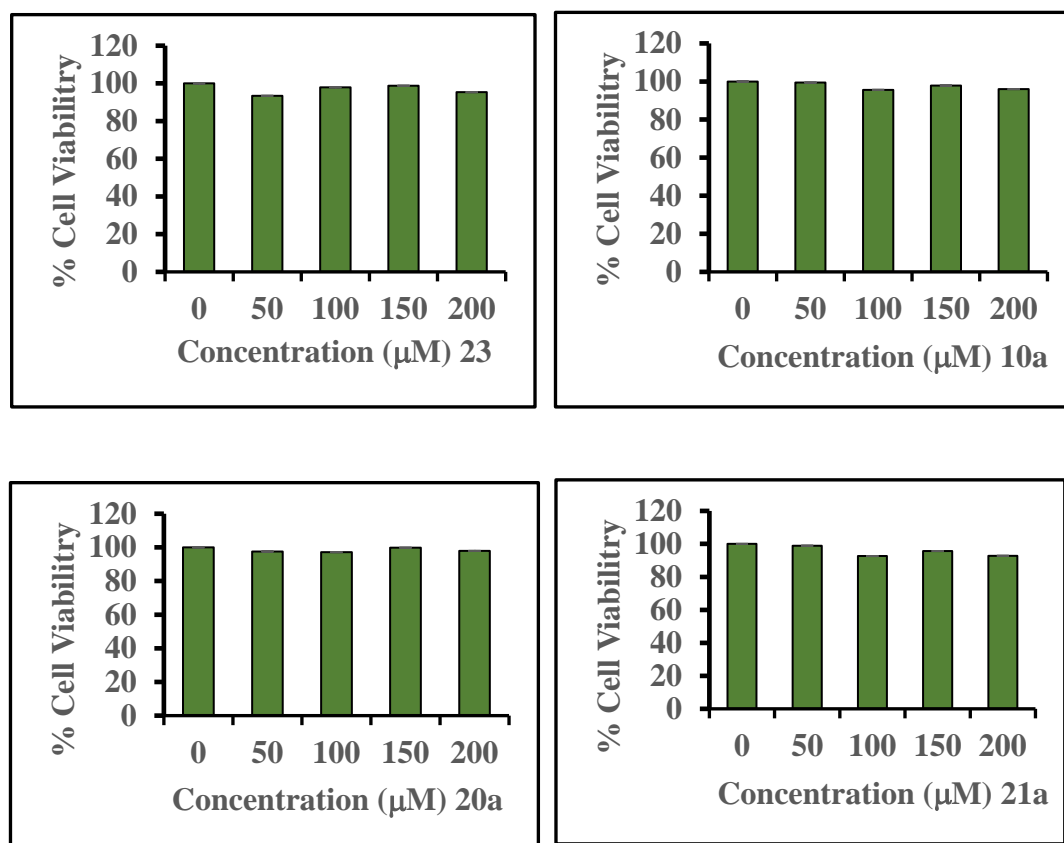


Figure 4b.7 Cell proliferation data of peptides.

4b.3 Conclusions

Isoindolinonyl incorporated cyclopeptides are emerging therapeutic target drug molecules and their synthesis involves multiple challenging steps. Herein, we have developed novel methodology for the synthesis of isoindolinone scaffold comprising *di/tri*-peptides through Pd(II)-catalyzed C(sp²)-H olefination/activation from various arylamide peptides and acrylate olefins. We have also studied the conformational changes of those peptides owing to the isoindolinone residue. Our conformational analyses strongly support the formation of γ -turn in *di*-peptide and helical formation in less steric tripeptides. Finally, these peptides are biocompatible owing to their negligible cytotoxicity effect on Hek293T cells. Hence

isolindolinone containing peptides are potential building blocks for novel foldamers with therapeutic values.

4b.4 Experimental Details

4b.4.1 Material and Instrumentation

All required materials were obtained from commercial suppliers and used without purification. The Dry DMF and ACN were freshly prepared by distilling over calcium hydride. Reactions were monitored by thin-layer chromatography, visualized by UV and Ninhydrin. Column chromatography was performed in 100-200 mesh silica. Mass spectra were obtained from Bruker Micro TOF-Q II Spectrometer. NMR spectra were recorded on Bruker AV-400 ^1H (400 MHz), ^{13}C (100.6 MHz). ^1H and ^{13}C NMR chemical shifts were recorded in ppm downfield from tetramethylsilane, splitting patterns are abbreviated as s, singlet; d, doublet; dd, doublet of doublet; t, triplet; q, quartet; dq, doublet of the quartet; m, multiplet.

4b.4.2 General Procedure for benzamide derivative peptide synthesis

Benzoic acid or its derivative was dissolved in DMF before the triethylamine TEA, (3.0 eq.), EDC.HCl (1.3 eq.) and HOAt (1.3 eq.) were added, followed by free *N*-terminal peptide methyl ester (1.2 eq.). Further, this mixture was heated to 60°C for 8-12 h. The reaction was monitored by TLC. The crude reaction mixture was concentrated under reduced pressure before water was added. The aqueous layer was extracted with EtOAc. The organic layer was combined, dried over anhydrous Na_2SO_4 , and concentrated under reduced pressure. The residue was purified with column chromatography by EtOAc/Hexane solvent system to yield corresponding substrates.

4b.4.3 General procedure for Pd-catalysed reactions

Typically, the amide substrates were placed in a 15 ml sealed reaction tube under indicated reaction conditions. The mixture was stirred at 100 °C for 12–24 h, cooled to room temperature, and then diluted with EtOAc. The resulting solution was filtered through a Celite pad, concentrated under reduced pressure and the product was further purified by column chromatography by EtOAc/Hexane solvent system and was typically obtained as a white solid.

4b.4.4 Chemical shift values of NMR

Methyl benzoylglcylglycinate (6a). ¹H NMR (400 MHz, CDCl₃) δ 7.85 (t, *J* = 8.0 Hz, 2H), 7.62 (d, *J* = 4.0 Hz, 1H), 7.50 (t, *J* = 8.0 Hz, 1H), 7.45 (s, 1H), 7.41 (d, *J* = 8.0 Hz, 2H), 4.21 (d, *J* = 4.0 Hz, 2H), 4.05 (d, *J* = 4.0 Hz, 2H), 3.72 (s, 3H). ¹³C NMR (101 MHz, CDCl₃) δ 170.28 (s), 169.88 (s), 168.04 (s), 133.35 (s), 131.91 (s), 128.59 (s), 127.23 (s), 52.41 (s), 43.57 (s), 41.20 (s). White solid (68% yield).ESI-HRMS *m/z* [M+H]⁺ calcd. for C₁₂H₁₄N₂O₄ 251.1032 found 251.1040.

Methyl(Z)-2-(2-(2-((2-methoxy-2-oxoethyl)amino)-2-oxoethyl)-3-oxoisindolin-1-ylidene)acetate (8a). ¹H NMR (400 MHz, CDCl₃) δ 9.07(d, *J* = 8.0 Hz, 1H), 7.88 (d, *J* = 8.0 Hz, 1H), 7.70 (d, *J* = 8.0 Hz, 1H), 7.61 (d, *J* = 8.0 Hz, 1H), 6.54 (s, 1H), 5.79 (s, 1H), 4.52 (s, 2H), 4.04 (d, *J* = 4.0 Hz, 2H), 3.81 (s, 3H), 3.72 (s, 3H). ¹³C NMR (101 MHz, CDCl₃) δ 169.77 (s), 167.26 (s), 166.82 (s), 166.08 (s), 147.65 (s), 133.88 (s), 133.79 (s), 131.55 (s), 129.32 (s), 128.27 (s), 123.56 (s), 99.68 (s), 52.49 (s), 51.82 (s), 43.39 (s), 41.23 (s). White solid (81% yield).ESI-HRMS *m/z* [M+Na]⁺ calcd. for C₁₂H₁₄N₂O₄ 355.0906 found 355.1041.

ethyl(Z)-2-(2-(2-((2-Methoxy-2-oxoethyl)amino)-2-oxoethyl)-3-oxoisindolin-1-

ylidene)acetate (8b). ¹H NMR (400 MHz, CDCl₃) δ 9.09 (d, *J* = 7.9 Hz, 1H), 7.90 (d, *J* = 7.4 Hz, 1H), 7.71 (t, *J* = 8.3 Hz, 1H), 7.62 (t, *J* = 7.9 Hz, 1H), 6.49 (d, *J* = 4.0 Hz, 1H), 5.80 (s, 1H), 4.54 (s, 2H), 4.28 (q, *J* = 8.0 Hz, 2H), 4.06 (d, *J* = 5.4 Hz, 2H), 3.74 (s, 3H), 1.36 (t, *J* = 8.0 Hz, 3H). ¹³C NMR (176 MHz, CDCl₃) δ 169.70 (s), 167.27 (s), 166.85 (s), 165.65 (s), 147.37 (s), 133.87 (s), 133.76 (s), 131.31 (s), 129.32 (s), 128.32 (s), 123.81 (s), 100.29 (s), 60.77 (s), 52.42 (s), 43.47 (s), 41.24 (s), 14.24 (s). White solid (71% yield).ESI-HRMS *m/z* [M+H]⁺ calcd. for C₁₇H₁₈N₂O₆ 347.1243 found 347.1243.

butyl(Z)-2-(2-(2-((2-Methoxy-2-oxoethyl)amino)-2-oxoethyl)-3-oxoisindolin-1-

ylidene)acetate (8c). ¹H NMR (400 MHz, CDCl₃) δ 9.10 (d, *J* = 8.0 Hz, 1H), 7.90 (d, *J* = 8.0 Hz, 1H), 7.71 (t, *J* = 8.0 Hz, 1H), 7.62 (t, *J* = 8.0 Hz, 1H), 6.47 (s, 1H), 5.81 (s, 1H), 4.54 (s, 2H), 4.23 (t, *J* = 8.0 Hz, 2H), 4.06 (d, *J* = 8.0 Hz, 2H), 3.74 (s, 3H), 1.72 – 1.67 (m, 2H), 1.49 – 1.41 (m, 2H), 0.98 (t, *J* = 8.0 Hz, 3H). ¹³C NMR (176 MHz, CDCl₃) δ 169.68 (s), 167.26 (s), 166.87 (s), 165.77 (s), 147.35 (s), 133.89 (s), 133.75 (s), 131.30 (s), 129.31 (s), 128.33 (s), 123.80 (s), 100.30 (s), 64.70 (s), 52.40 (s), 43.48 (s), 41.24 (s), 30.68 (s), 19.17 (s), 13.73 (s). White solid (61% yield).ESI-HRMS *m/z* [M+H]⁺ calcd. for C₁₉H₂₂N₂O₆ 375.1558 found 375.1553.

tert-Butyl(Z)-2-(2-(2-((2-methoxy-2-oxoethyl)amino)-2-oxoethyl)-3-oxoisindolin-1-

ylidene)acetate (8d). ¹H NMR (400 MHz, CDCl₃) δ 9.02(d, *J* = 8.0 Hz, 1H), 7.86 (d, *J* = 8.0 Hz, 1H), 7.68 (t, *J* = 8.0 Hz, 1H), 7.58(t, *J* = 8.0 Hz, 1H), 6.57 (s, 1H), 5.74 (s, 1H), 4.50 (s, 2H), 4.04 (d, *J* = 4.0 Hz, 2H), 3.71 (s, 3H), 1.55 (s, *J* = 8.0 Hz, 9H). ¹³C NMR (101 MHz, CDCl₃) δ 169.71 (s), 167.28 (s), 167.09 (s), 165.03 (s), 146.31 (s), 133.97 (s), 133.61 (s), 131.21 (s), 129.33 (s), 128.21 (s), 123.41 (s), 102.55 (s), 81.19 (s), 52.41 (s), 43.44 (s), 41.22 (s), 28.23

(s). White solid (64% yield).ESI-HRMS m/z $[M+H]^+$ calcd. for $C_{19}H_{22}N_2O_6$ 375.1556 found 375.1553.

Methyl benzoylglycyl-L-valinate (6b). 1H NMR (400 MHz, $CDCl_3$) δ 7.85 (d, $J = 8.0$ Hz, 2H), 7.56 – 7.38 (m, 4H), 7.27 (s, 1H), 4.55 (d, $J = 4.0$ Hz, 1H), 4.26 (d, $J = 4.0$ Hz, 2H), 3.73 (s, 3H), 2.25 – 2.13 (m, 1H), 0.94 (d,d, $J = 8.0$ Hz, 6H). ^{13}C NMR (101 MHz, $CDCl_3$) δ 172.21 (s), 169.34 (s), 167.93 (s), 133.53 (s), 131.86 (s), 128.59 (s), 127.21 (s), 57.52 (s), 52.25 (s), 43.78 (s), 31.07 (s), 19.05 (s), 17.79 (s). White solid (62% yield).ESI-HRMS m/z $[M+H]^+$ calcd. for $C_{15}H_{20}N_2O_4$ 293.1501 found 293.1498.

Methyl(Z)-(2-(1-(2-methoxy-2-oxoethylidene)-3-oxoisindolin-2-yl)acetyl)-L-valinate (9a). 1H NMR (400 MHz, $CDCl_3$) δ 9.14 – 9.05 (m, 1H), 7.90 (d, 1H), 7.71 (t, $J = 8.0$ Hz, 1H), 7.62 (t, $J = 8.0$ Hz, 1H), 6.47 (d, $J = 8.0$ Hz, 1H), 5.78 (s, 1H), 4.61 – 4.49 (m, 3H), 3.81 (s, 3H), 3.70 (s, 3H), 2.16 (d, $J = 8.0$ Hz, 1H), 0.88 (dd, $J = 8.0$ Hz, 6H). ^{13}C NMR (101 MHz, $CDCl_3$) δ 171.91 (s), 167.26 (s), 166.45 (s), 166.08 (s), 147.77 (s), 133.82 (s), 133.77 (s), 131.55 (s), 129.33 (s), 128.29 (s), 123.60 (s), 99.53 (s), 57.27 (s), 52.32 (s), 51.80 (s), 43.57 (s), 31.22 (s), 18.93 (s), 17.73 (s). White solid (71% yield).ESI-HRMS m/z $[M+H]^+$ calcd. for $C_{19}H_{22}N_2O_6$ 375.1556 found 375.1553.

Methyl (Z)-(2-(1-(2-ethoxy-2-oxoethylidene)-3-oxoisindolin-2-yl)acetyl)-L-valinate (9b).

1H NMR (400 MHz, $CDCl_3$) δ 9.09 (d, $J = 4.0$ Hz, 1H), 7.89 (d, $J = 4.0$ Hz, 1H), 7.69 (t, $J = 8.0$ Hz, 1H), 7.62 (t, 1H), 6.47 (d, $J = 8.0$ Hz, 1H), 5.77 (d, $J = 4.0$ Hz, 1H), 4.60 – 4.49 (m, 3H), 4.32 – 4.18 (m, 2H), 3.70 (s, 3H), 2.21 – 2.09 (m, 1H), 1.37 – 1.27 (m, 3H), 0.88 (dd, $J = 8.0$ Hz, 6H). ^{13}C NMR (101 MHz, $CDCl_3$) δ 171.90 (s), 167.26 (s), 166.50 (s), 165.63 (s), 133.82 (s), 133.73 (s), 131.48 (s), 129.33 (s), 128.32 (s), 123.58 (s), 100.13 (s), 60.67 (s), 57.26

(s), 52.31 (s), 43.59 (s), 31.23 (s), 18.95 (s), 17.72 (s), 14.28 (s). White solid (75% yield).ESI-HRMS m/z $[M+H]^+$ calcd. for $C_{20}H_{24}N_2O_6$ 389.1713 found 389.1714.

Methyl (Z)-(2-(1-(2-butoxy-2-oxoethylidene)-3-oxoisindolin-2-yl)acetyl)-L-valinate (9c).

1H NMR (400 MHz, $CDCl_3$) δ 9.10 (d, $J = 8.0$ Hz, 1H), 7.91 (d, $J = 8.0$ Hz, 1H), 7.71 (d, $J = 8.0$ Hz, 1H), 7.62 (t, $J = 8.0$ Hz, 1H), 6.36 (d, $J = 8.0$ Hz, 1H), 5.77 (s, 1H), 4.59 – 4.49 (m, 3H), 4.21 (d, $J = 8.0$ Hz, 2H), 3.70 (s, 3H), 2.20 – 2.11 (m, 1H), 1.67 (d, $J = 7.9$ Hz, 2H), 1.45 – 1.39 (m, 2H), 0.96 (d, $J = 4.0$ Hz, 3H), 0.93 – 0.83 (m, 6H). ^{13}C NMR (101 MHz, $CDCl_3$) δ 171.81 (s), 167.23 (s), 166.46 (s), 165.72 (s), 147.47 (s), 133.87 (s), 133.73 (s), 131.47 (s), 129.34 (s), 128.36 (s), 123.59 (s), 100.13 (s), 64.60 (s), 57.25 (s), 52.26 (s), 43.68 (s), 31.24 (s), 30.70 (s), 19.16 (s), 18.93 (s), 17.69 (s), 13.71 (s). White solid (62% yield).ESI-HRMS m/z $[M+H]^+$ calcd. for $C_{22}H_{28}N_2O_6$ 417.2026 found 417.2060.

Methyl(Z)-(2-(1-(2-(tert-butoxy)-2-oxoethylidene)-3-oxoisindolin-2-yl)acetyl)-L-valinate

(9d). 1H NMR (400 MHz, $CDCl_3$) δ 9.04 (d, $J = 8.0$ Hz, 1H), 7.89 (d, $J = 8.0$ Hz, 1H), 7.70 (d, $J = 8.0$ Hz, 1H), 7.60 (d, $J = 8.0$ Hz, 1H), 6.41 (d, $J = 8.7$ Hz, 1H), 5.71 (s, 1H), 4.60 – 4.46 (m, 3H), 3.69 (s, 3H), 2.20 – 2.11 (m, 1H), 1.53 (s, 9H), 1.02 – 0.75 (m, 6H). ^{13}C NMR (176 MHz, $CDCl_3$) δ 171.83 (s), 167.23 (s), 166.62 (s), 164.93 (s), 146.44 (s), 133.94 (s), 133.62 (s), 131.26 (s), 129.37 (s), 128.28 (s), 123.50 (s), 102.42 (s), 57.24 (s), 52.26 (s), 43.66 (s), 31.25 (s), 28.21 (s), 18.98 (s), 17.68 (s). White solid (67% yield).ESI-HRMS m/z $[M+H]^+$ calcd. for $C_{22}H_{28}N_2O_6$ 417.2026 found 417.2019.

Methyl (S)-2-(2-benzamidoacetamido)-2-phenylacetate (6c). 1H NMR (400 MHz, $CDCl_3$) δ 7.76 (d, $J = 8.0$ Hz, 2H), 7.59 (d, $J = 6.7$ Hz, 1H), 7.52 – 7.45 (m, 1H), 7.43 – 7.30 (m, 7H), 7.19 (s, 1H), 5.57 (d, $J = 8.0$ Hz, 1H), 4.32 – 4.13 (m, 2H), 3.70 (s, 3H). ^{13}C NMR (101 MHz, $CDCl_3$) δ 171.00 (s), 168.57 (s), 167.76 (s), 135.93 (s), 133.51 (s),

131.83 (s), 129.05 (s), 128.71 (s), 128.64 (d, $J = 12.4$ Hz), 128.58 (s), 127.36 (s), 127.18 (s), 56.77 (s), 52.89 (s), 43.57 (s). White solid (65% yield).ESI-HRMS m/z $[M+H]^+$ calcd. for $C_{18}H_{18}N_2O_4$ 327.1345 found 327.1369.

Methyl(S,Z)-2-(2-(1-(2-methoxy-2-oxoethylidene)-3-oxoisindolin-2-yl)acetamido)-2-phenylacetate (10a). 1H NMR (400 MHz, $CDCl_3$) δ 9.10 (d, $J = 8.0$ Hz, 1H), 7.91 (d, $J = 8.0$ Hz, 1H), 7.72 (d, $J = 8.0$ Hz, 1H), 7.63 (d, $J = 8.0$ Hz, 1H), 7.35 – 7.32 (m, 5H), 6.99 (d, $J = 8.0$ Hz, 1H), 5.75 (s, 1H), 5.57 (d, $J = 8.0$ Hz, 1H), 4.53 (s, 2H), 3.81 (s, 3H), 3.71 (s, 3H). ^{13}C NMR (101 MHz, $CDCl_3$) δ 170.77 (s), 167.21 (s), 166.03 (s), 165.90 (s), 147.74 (s), 135.85 (s), 133.82 (s), 133.75 (s), 131.51 (s), 129.36 (s), 129.02 (s), 128.67 (s), 128.28 (s), 127.23 (s), 123.62 (s), 99.57 (s), 56.58 (s), 52.94 (s), 51.74 (s), 43.43 (s). White solid (75% yield).ESI-HRMS m/z $[M+H]^+$ calcd. for $C_{22}H_{20}N_2O_6$ 409.1400 found 409.1739.

Methyl(S,Z)-2-(2-(1-(2-ethoxy-2-oxoethylidene)-3-oxoisindolin-2-yl)acetamido)-2-phenylacetate (10b). 1H NMR (400 MHz, $CDCl_3$) δ 9.08 (d, $J = 8.0$ Hz, 1H), 7.89 (d, $J = 8.0$ Hz, 1H), 7.69 (d, $J = 8.0$ Hz, 1H), 7.61 (t, $J = 8.0$ Hz, 1H), 7.37 – 7.28 (m, 5H), 6.95 (d, $J = 8.0$ Hz, 1H), 5.73 (s, 1H), 5.55 (d, $J = 7.0$ Hz, 1H), 4.51 (d, $J = 4.0$ Hz, 2H), 4.26 (d, $J = 8.0$ Hz, 2H), 3.69 (s, 3H), 1.34 (d, $J = 8.0$ Hz, 3H). ^{13}C NMR (101 MHz, $CDCl_3$) δ 170.80 (s), 167.24 (s), 166.03 (s), 165.64 (s), 147.55 (s), 133.85 (s), 133.69 (s), 131.44 (s), 129.37 (s), 129.00 (s), 128.85 – 128.75 (m), 128.66 (s), 128.30 (s), 127.24 (s), 123.57 (s), 100.13 (s), 60.67 (s), 56.57 (s), 52.95 (s), 43.36 (s), 14.31 (s).White solid (78% yield).ESI-HRMS m/z $[M+H]^+$ calcd. for $C_{25}H_{26}N_2O_6$ 423.1556 found 423.1570.

Methyl(S,Z)-2-(2-(1-(2-butoxy-2-oxoethylidene)-3-oxoisindolin-2-yl)acetamido)-2-phenylacetate (10c). ^1NMR (400 MHz,) δ 9.09 (d, J = 8.0 Hz, 1H), 7.89 (d, J = 8.0 Hz, 1H), 7.70 (t, J = 8.0 Hz, 1H), 7.61 (t, J = 8.0 Hz, 1H), 7.40 – 7.29 (m, 5H), 7.09 – 6.98 (m, 1H), 5.74 (s, 1H), 5.57 (d, J = 8.0 Hz, 1H), 4.53 (d, J = 4.0 Hz, 2H), 4.21 (t, J = 8.0 Hz, 2H), 3.69 (s, 3H), 1.74 – 1.64 (m, 2H), 1.48 – 1.39 (m, 2H), 0.98 (t, J = 8.0 Hz, 3H). ^1NMR (101 MHz,) δ 170.83 (s), 167.31 (s), 166.08 (s), 165.81 (s), 147.56 (s), 135.93 (s), 135.93 (s), 133.96 (s), 133.76 (s), 131.49 (s), 129.43 (s), 129.07 (s), 128.91 (s), 128.72 (s), 128.39 (s), 127.29 (s), 100.21 (s), 64.68 (s), 56.64 (s), 52.98 (s), 43.51 (s), 30.79 (s), 19.25 (s), 13.81 (s). White solid (67% yield). ESI-HRMS m/z $[\text{M}+\text{H}]^+$ calcd. for $\text{C}_{25}\text{H}_{26}\text{N}_2\text{O}_6$ 451.1869 found 451.1873.

Methyl(S,Z)-2-(2-(1-(2-(tert-butoxy)-2-oxoethylidene)-3-oxoisindolin-2-yl)acetamido)-2-phenylacetate (10d). ^1NMR (400 MHz,) δ 9.03 (d, J = 8.0 Hz, 1H), 7.89 (d, J = 8.0 Hz, 1H), 7.69 (t, J = 8.0 Hz, 1H), 7.59 (t, J = 8.0 Hz, 1H), 7.36 – 7.28 (m, 5H), 6.95 (d, J = 8.0 Hz, 1H), 5.69 (s, 1H), 5.55 (d, J = 8.0 Hz, 1H), 4.50 (m, 2H), 3.69 (s, 3H), 1.54 (s, 9H). ^1NMR (101 MHz,) δ 170.76 (s), 167.31 (s), 166.16 (s), 165.00 (s), 146.47 (s), 135.92 (s), 134.03 (s), 133.66 (s), 131.27 (s), 129.39 (s), 129.06 (s), 128.90 (s), 128.70 (s), 128.30 (s), 127.22 (s), 123.56 (s), 102.48 (s), 81.14 (s), 56.58 (s), 52.96 (s), 43.60 (s), 28.28 (s). White solid (64% yield). ESI-HRMS m/z $[\text{M}+\text{H}]^+$ calcd. for $\text{C}_{25}\text{H}_{26}\text{N}_2\text{O}_6$ 451.1869 found 451.1873.

Methyl benzoyl-L-phenylalanyl-L-valinate (6d). $^1\text{H NMR}$ (400 MHz, CDCl_3) δ 7.72 (d, J = 8.0 Hz, 2H), 7.50 (d, J = 8.0 Hz, 1H), 7.40 (d, J = 4.0 Hz, 2H), 7.32 – 7.21 (m, 5H), 6.95 (d, J = 8.0 Hz, 1H), 6.50 (d, J = 8.0 Hz, 1H), 4.94 (q, J = 8.0 Hz, 1H), 4.44 (dd, J = 4.0 Hz, 1H), 3.71 (s, 3H), 3.29 – 3.06 (m, 2H), 2.19 – 1.93 (m, 1H), 0.83 (d, J = 8.0 Hz, 6H). $^{13}\text{C NMR}$ (101 MHz, CDCl_3) δ 171.66 (s), 170.93 (s), 167.30 (s), 136.52 (s), 133.80 (s), 131.82 (s), 129.41 (s), 128.71 (s), 128.61 (s), 127.06 (s), 57.52 (s), 54.83 (s), 52.14 (s), 38.25 (s), 31.08 (s), 18.85

(s), 17.74 (s). White solid (60% yield).ESI-HRMS m/z $[M+H]^+$ calcd. for $C_{22}H_{26}N_2O_4$ 383.1971 found 383.1970.

Methyl((S)-2-((Z)-1-(2-methoxy-2-oxoethylidene)-3-oxoisindolin-2-yl)-3-phenylpropanoyl)-L-valinate (11a). 1H NMR (400 MHz, $CDCl_3$) δ 9.05 (d, $J = 8.0$ Hz, 1H), 7.79 (d, $J = 8.0$ Hz, 1H), 7.69 (t, $J = 8.0$ Hz, 1H), 7.59 (t, $J = 8.0$ Hz, 1H), 7.22 – 7.09 (m, 5H), 6.38 (s, 1H), 5.98 (s, 1H), 5.43 (s, 1H), 4.59 (dd, $J = 4.0$ Hz, 1H), 3.84 (s, 3H), 3.71 (s, 3H), 3.67 – 3.60 (m, 1H), 3.44 – 3.34 (m, 1H), 2.21 – 2.07 (m, 1H), 0.83 (dd, $J = 8.0$ Hz, 6H). ^{13}C NMR (101 MHz, $CDCl_3$) δ 171.78 (s), 168.59 (s), 167.36 (s), 166.04 (s), 136.70 (s), 133.69 (s), 133.55 (s), 131.43 (s), 128.97 (s), 128.72 (s), 128.55 (s), 128.03 (s), 126.91 (s), 101.06 (s), 57.53 (s), 52.24 (s), 51.80 (s), 34.05 (s), 31.14 (s), 29.21 (s), 18.88 (s), 17.76 (s). White solid (67% yield).ESI-HRMS m/z $[M+H]^+$ calcd. for $C_{26}H_{28}N_2O_6$ 465.1945 found 465.1995.

Methyl ((S)-2-((Z)-1-(2-ethoxy-2-oxoethylidene)-3-oxoisindolin-2-yl)-3-phenylpropanoyl)-L-valinate (11b). 1H NMR (400 MHz, $CDCl_3$) δ 9.05 (d, $J = 8.0$ Hz, 1H), 7.79 (d, $J = 8.0$ Hz, 1H), 7.68 (t, $J = 8.0$ Hz, 1H), 7.58 (t, $J = 8.0$ Hz, 1H), 7.23 – 7.08 (m, 4H), 6.40 (s, 1H), 5.94 (s, 1H), 5.45 (s, 1H), 4.60 (d, $J = 4.0$ Hz, 1H), 4.38 – 4.20 (m, 2H), 3.71 (s, 2H), 3.68 – 3.58 (m, 1H), 3.45 – 3.32 (m, 1H), 2.20 – 2.10 (m, 1H), 1.36 (t, $J = 8.0$ Hz, 3H), 0.87 (dd, $J = 8.0$ Hz, 6H). ^{13}C NMR (101 MHz, $CDCl_3$) δ 171.78 (s), 168.59 (s), 167.36 (s), 166.04 (s), 136.70 (s), 133.69 (s), 133.55 (s), 131.43 (s), 128.97 (s), 128.72 (s), 128.55 (s), 128.03 (s), 126.91 (s), 101.06 (s), 57.53 (s), 52.24 (s), 51.80 (s), 34.05 (s), 31.14 (s), 21.96 (s), 18.88 (s), 17.76 (s). White solid (51% yield).ESI-HRMS m/z $[M+H]^+$ calcd. for $C_{27}H_{30}N_2O_6$ 479.2182 found 479.2165.

Methyl ((S)-2-((Z)-1-(2-butoxy-2-oxoethylidene)-3-oxoisindolin-2-yl)-3-phenylpropanoyl)-L-valinate (11c). ^1H NMR (400 MHz,) δ 9.01 (d, J = 8.0 Hz, 1H), 7.74 (d, J = 8.0 Hz, 1H), 7.67 – 7.61 (t, J = 8.0 Hz, 1H), 7.55 – 7.51 (t, J = 8.0 Hz, 1H), 7.16 – 7.06 (m, 5H), 6.49 – 6.30 (s, 1H), 5.89 (s, 1H), 5.42 (s, 1H), 4.57 (d, J = 8.0 Hz, 1H), 4.30 – 4.10 (m, 2H), 3.64 (s, 3H), 3.62 – 3.59 (m, 1H), 3.35 (m, 1H), 2.16 – 2.06 (m, 1H), 1.71 – 1.63 (m, 2H), 1.46 – 1.37 (m, 2H), 0.96 (t, J = 8.0 Hz, 3H), 0.80 (d, J = 8.0 Hz, 6H). NMR (101 MHz,) δ 171.86 (s), 169.10 – 168.50 (m), 167.40 (s), 165.77 (s), 136.84 (s), 133.68 (s), 131.41 (s), 129.06 (s), 128.83 (s), 128.56 (s), 128.13 (s), 126.93 (s), 123.55 (s), 101.64 (s), 64.72 (s), 57.57 (s), 52.27 (s), 34.09 (s), 31.29 (s), 30.78 (s), 29.76 (s), 19.24 (s), 19.04 (s), 17.82 (s), 13.79 (s). White solid (58% yield). ESI-HRMS m/z $[\text{M}+\text{H}]^+$ calcd. for $\text{C}_{29}\text{H}_{34}\text{N}_2\text{O}_6$ 507.2498 found 507.2518.

Methyl((S)-2-((Z)-1-(2-(tert-butoxy)-2-oxoethylidene)-3-oxoisindolin-2-yl)-3-phenylpropanoyl)-L-valinate (11d). ^1H NMR (400 MHz,) δ 8.97 (d, J = 8.0 Hz, 1H), 7.76 (d, J = 8.0 Hz, 1H), 7.66 (t, J = 8.0 Hz, 1H), 7.55 (t, J = 8.0 Hz, 1H), 7.17 – 7.09 (m, 5H), 6.37 (s, 1H), 5.81 (s, 1H), 5.41 (s, 1H), 4.60 (dd, J = 8.0 Hz, 1H), 3.69 (s, 3H), 3.68 – 3.60 (m, 1H), 3.40 – 3.30 (m, 1H), 2.21 – 2.05 (m, 1H), 1.55 (s, 9H), 0.98 – 0.67 (dd J = 8.0 Hz, 6H). NMR (101 MHz, CDCl_3) δ 170.76 (s), 167.25 (s), 165.95 (s), 165.62 (s), 147.49 (s), 135.85 (s), 133.87 (s), 133.74 (s), 131.47 (s), 129.34 (s), 129.03 (s), 128.87 (s), 128.69 (s), 128.34 (s), 127.22 (s), 123.62 (s), 100.19 (s), 60.68 (s), 56.57 (s), 52.97 (s), 45.71 (s), 43.50 (s), 29.71 (s), 14.30 (s), 14.17 (s). White solid (55% yield). ESI-HRMS m/z $[\text{M}+\text{H}]^+$ calcd. for $\text{C}_{29}\text{H}_{34}\text{N}_2\text{O}_6$ 507.2498 found 507.2518.

Methyl (2-naphthoyl)glycyl-L-valinate (13a). ^1H NMR (400 MHz, CDCl_3) δ 8.37 (s, 1H), 8.07 (s, 1H), 7.89 (d, J = 4.0 Hz, 1H), 7.79 (t, J = 8.0 Hz, 1H), 7.71 (d, J = 8.0 Hz, 1H), 7.55 – 7.41 (m, 1H), 4.60 – 4.54 (m, 1H), 4.43 – 4.28 (m, 2H), 3.70 (s, 3H), 2.32 – 2.08 (m, 1H), 0.95 (dd,

$J = 8.0$ Hz, 6H). ^{13}C NMR (101 MHz, CDCl_3) δ 172.39 (s), 170.15 (s), 168.16 (s), 134.76 (s), 132.48 (s), 130.62 (s), 129.02 (s), 128.21 (s), 128.08 (s), 127.66 (s), 127.60 (s), 126.56 (s), 123.72 (s), 57.73 (s), 52.14 (s), 43.86 (s), 30.98 (s), 19.08 (s), 17.92 (s). Yellow solid (66% yield).ESI-HRMS m/z $[\text{M}+\text{H}]^+$ calcd. for $\text{C}_{19}\text{H}_{22}\text{N}_2\text{O}_4$ 343.1658 found 343.1658.

Methyl(Z)-(2-(1-(2-methoxy-2-oxoethylidene)-3-oxo-1,3-dihydro-2H-benzo[f]isoindol-2-yl)acetyl)-L-valinate (14a). ^1H NMR (400 MHz, CDCl_3) δ 9.70 (s, 1H), 8.40 (s, 1H), 8.12 – 8.06 (m, 1H), 8.06 – 7.98 (m, 1H), 7.78 – 7.49 (m, 2H), 6.46 (d, $J = 8.0$ Hz, 1H), 5.78 (s, 1H), 4.68 – 4.45 (m, 3H), 3.84 (s, 3H), 3.69 (s, 4H), 2.23 – 2.09 (m, 1H), 0.88 (dd, $J = 8.0$ Hz, 6H). ^{13}C NMR (101 MHz, CDCl_3) δ 171.83 (s), 167.17 (s), 166.50 (s), 166.34 (s), 148.26 (s), 136.02 (s), 133.87 (s), 130.52 (s), 129.96 (s), 129.65 (s), 128.64 (s), 128.54 (s), 126.11 (s), 125.20 (s), 124.73 (s), 97.97 (s), 57.32 (s), 52.26 (s), 51.69 (s), 43.93 (s), 31.20 (s), 18.91 (s), 17.72 (s). Yellow solid (60% yield).ESI-HRMS m/z $[\text{M}+\text{H}]^+$ calcd. for $\text{C}_{23}\text{H}_{24}\text{N}_2\text{O}_6$ 425.1713 found 425.1697.

Methyl(Z)-(2-(1-(2-ethoxy-2-oxoethylidene)-3-oxo-1,3-dihydro-2H-benzo[f]isoindol-2-yl)acetyl)-L-valinate (14b). ^1H NMR (400 MHz, CDCl_3) δ 9.71 (s, 1H), 8.41 (s, 1H), 8.12 – 8.06 (m, 1H), 8.05 – 7.99 (m, 1H), 7.71 – 7.57 (m, 2H), 6.47 (d, $J = 8.7$ Hz, 1H), 5.77 (s, 1H), 4.61 – 4.52 (m, 2H), 4.30 (q, $J = 8.0$ Hz, 2H), 3.70 (s, 2H), 2.23 – 2.12 (m, 1H), 1.37 (t, $J = 8.0$ Hz, 3H), 0.88 (dd, $J = 8.0$ Hz, 6H). ^{13}C NMR (101 MHz, CDCl_3) δ 171.82 (s), 167.19 (s), 166.38 (s), 166.05 (s), 147.98 (s), 136.03 (s), 133.86 (s), 130.52 (s), 129.98 (s), 129.65 (s), 128.69 (s), 128.62 (s), 128.51 (s), 126.15 (s), 124.72 (s), 98.61 (s), 60.53 (s), 57.31 (s), 52.27 (s), 43.98 (s), 31.22 (s), 18.94 (s), 17.71 (s), 14.35 (s). Yellow solid (57% yield).ESI-HRMS m/z $[\text{M}+\text{H}]^+$ calcd. for $\text{C}_{23}\text{H}_{24}\text{N}_2\text{O}_6$ 439.1869 found 439.1867.

Methyl ([1,1'-biphenyl]-4-carbonyl)glycyl-L-valinate (16a). ^1H NMR (400 MHz, CDCl_3) δ 8.07 – 8.01 (m, 1H), 7.93 (d, J = 8.0 Hz, 2H), 7.73 (d, J = 8.0 Hz, 1H), 7.55 (dd, J = 8.0 Hz, 4H), 7.44 – 7.31 (m, 3H), 4.57 (dd, J = 8.0 Hz, 1H), 4.31 (d, J = 4.0 Hz, 2H), 3.70 (s, 3H), 2.31 – 2.09 (m, 1H), 0.95 (dd, J = 6.0 Hz, 6H). ^{13}C NMR (101 MHz, CDCl_3) δ 172.33 (s), 170.04 (s), 167.85 (s), 144.40 (s), 139.92 (s), 132.18 (s), 128.89 (s), 127.99 (s), 127.89 (s), 127.15 (s), 127.08 (s), 57.69 (s), 52.15 (s), 43.83 (s), 31.03 (s), 19.08 (s), 17.91 (s). Yellow solid (62% yield). ESI-HRMS m/z $[\text{M}+\text{H}]^+$ calcd. for $\text{C}_{23}\text{H}_{24}\text{N}_2\text{O}_6$ 369.1814 found 369.1799.

Methyl(Z)-(2-(3-(2-methoxy-2-oxoethylidene)-1-oxo-5-phenylisoindolin-2-yl)acetyl)-L-valinate (17a). ^1H NMR (400 MHz, CDCl_3) δ 9.41 (s, 1H), 7.97 (d, J = 8.0 Hz, 1H), 7.85 (d, J = 4.0 Hz, 1H), 7.71 (d, J = 4.0 Hz, 1H), 7.51 (d, J = 8.0 Hz, 1H), 7.43 (d, J = 8.0 Hz, 1H), 6.36 (d, J = 1.0 Hz, 1H), 5.81 (s, 1H), 4.60 – 4.44 (m, 3H), 3.81 (s, 3H), 3.71 (s, 3H), 2.24 – 2.08 (m, 1H), 0.89 (dd, J = 6.0 Hz, 6H). NMR (101 MHz,) δ 171.93 (s), 167.20 (s), 166.49 (s), 166.12 (s), 147.82 (s), 147.14 (s), 140.09 (s), 134.59 (s), 130.46 (s), 129.17 (s), 128.47 (s), 127.97 (s), 127.65 (s), 127.25 (s), 124.04 (s), 99.77 (s), 57.34 (s), 52.41 (s), 51.96 (s), 43.81 (s), 31.31 (s), 19.01 (s), 17.81 (s). Yellow solid (64% yield). ESI-HRMS m/z $[\text{M}+\text{H}]^+$ calcd. for $\text{C}_{25}\text{H}_{26}\text{N}_2\text{O}_6$ 451.1869 found 451.1879.

Methyl(Z)-(2-(3-(2-ethoxy-2-oxoethylidene)-1-oxo-5-phenylisoindolin-2-yl)acetyl)-L-valinate (17b). ^1H NMR (400 MHz, CDCl_3) δ 9.43 (d, J = 4.0 Hz, 1H), 7.99 (d, J = 4.0 Hz, 1H), 7.87 (d, J = 4.0 Hz, 1H), 7.73 (d, J = 4.0 Hz, 2H), 7.53 (t, J = 8.0 Hz, 2H), 7.45 (t, J = 8.0 Hz, 1H), 6.37 (d, J = 8.0 Hz, 1H), 5.83 (s, 1H), 4.63 – 4.52 (m, 3H), 4.29 (d, J = 8.0 Hz, 2H), 3.73 (s, 3H), 2.25 – 2.12 (m, 1H), 1.35 (t, J = 8.0 Hz, 3H), 0.91 (dd, J = 8.0 Hz, 6H). NMR (101 MHz,) δ 171.91 (s), 167.20 (s), 166.54 (s), 165.66 (s), 147.52 (s), 147.12 (s), 140.12 (s), 134.63 (s), 130.41 (s), 129.16 (s), 128.45 (s), 127.99 (s), 127.66 (s), 127.14 (s), 124.02 (s), 100.40 (s),

60.79 (s), 57.33 (s), 52.40 (s), 43.84 (s), 31.33 (s), 19.03 (s), 17.80 (s), 14.38 (s). Yellow solid (60% yield).ESI-HRMS m/z $[M+H]^+$ calcd. for $C_{26}H_{28}N_2O_6$ 465.2026 found 465.2043.

Methyl (S)-2-(2-(2-naphthamido)acetamido)-2-phenylacetate (13b). 1H NMR (400 MHz, $CDCl_3$) δ 8.33 (s, 1H), 7.87 – 7.78 (m, 5H), 7.58 – 7.47 (m, 3H), 7.42 – 7.37 (m, 2H), 7.35 – 7.28 (m, 3H), 5.61 (d, J = 8.0 Hz, 1H), 4.46 – 4.22 (m, 2H), 3.70 (s, 3H). NMR (101 MHz,) δ 171.14 (s), 168.90 (s), 167.93 (s), 136.01 (s), 134.94 (s), 132.62 (s), 130.72 (s), 129.13 (s), 128.78 (s), 128.50 (s), 128.00 (s), 127.87 (s), 127.79 (s), 127.47 (s), 126.81 (s), 123.74 (s), 56.91 (s), 52.99 (s), 43.78 (s). Yellow solid (60% yield).ESI-HRMS m/z $[M+H]^+$ calcd. for $C_{22}H_{20}N_2O_4$ 465.1501 found 465.1418.

Methyl(S,Z)-2-(2-(1-(2-methoxy-2-oxoethylidene)-3-oxo-1,3-dihydro-2H-benzo[f]isoindol-2-yl)acetamido)-2-phenylacetate (14c). 1H NMR (400 MHz, $CDCl_3$) δ 9.70 (s, 1H), 8.39 (s, 1H), 8.12 – 8.07 (m, 1H), 8.04 – 7.98 (m, 1H), 7.67 – 7.61 (m, 2H), 7.37 – 7.29 (m, 5H), 7.00 (d, J = 8.0 Hz, 1H), 5.73 (s, 1H), 5.63 – 5.50 (m, 1H), 4.57 (s, 2H), 3.83 (s, 3H), 3.68 (s, 3H). ^{13}C NMR (101 MHz, $CDCl_3$) δ 170.76 (s), 167.15 (s), 166.47 (s), 165.80 (s), 148.27 (s), 136.02 (s), 135.86 (s), 133.87 (s), 130.53 (s), 129.96 (s), 129.66 (s), 129.02 (s), 128.88 (s), 128.67 (s), 128.64 (s), 128.54 (s), 127.24 (s), 126.12 (s), 124.77 (s), 98.02 (s), 56.60 (s), 52.95 (s), 51.67 (s), 43.75 (s). Yellow solid (62% yield).ESI-HRMS m/z $[M+H]^+$ calcd. for $C_{26}H_{22}N_2O_6$ 459.1556 found 459.1564.

Methyl(S,Z)-2-(2-(1-(2-ethoxy-2-oxoethylidene)-3-oxo-1,3-dihydro-2H-benzo[f]isoindol-2-yl)acetamido)-2-phenylacetate (14d). 1H NMR (400 MHz, $CDCl_3$) δ 9.75 (s, 1H), 8.44 (s, 1H), 8.17 – 8.11 (m, 1H), 8.07 – 8.02 (m, 1H), 7.71 – 7.64 (m, 2H), 7.42 – 7.30 (m, 7H), 6.97 (d, J = 6.8 Hz, 1H), 5.76 (s, 1H), 5.60 (d, J = 8.0 Hz, 1H), 4.60 (d, J = 2.7 Hz, 2H), 4.32 (d, J = 8.0

Hz, 2H), 3.71 (s, 2H), 1.38 (t, $J = 8.0$ Hz, 3H). ^{13}C NMR (101 MHz, CDCl_3) δ 170.75 (s), 167.21 (s), 166.07 (s), 165.83 (s), 148.01 (s), 136.05 (s), 135.86 (s), 133.87 (s), 130.54 (s), 130.02 (s), 129.67 (s), 129.21 (s), 129.04 (s), 128.89 – 128.87 (m), 128.69 (s), 128.65 (s), 127.22 (s), 126.14 (s), 124.79 (s), 98.66 (s), 60.57 (s), 56.58 (s), 52.98 (s), 43.83 (s), 14.38 (s). Yellow solid (58% yield). ESI-HRMS m/z $[\text{M}+\text{H}]^+$ calcd. for $\text{C}_{27}\text{H}_{24}\text{N}_2\text{O}_6$ 473.1713 found 473.1757.

Methyl (S)-2-(2-([1,1'-biphenyl]-4-carboxamido)acetamido)-2-phenylacetate (16b). ^1H NMR (400 MHz, CDCl_3) δ 7.88 (d, $J = 8.0$ Hz, 2H), 7.70 – 7.58 (m, 5H), 7.52 – 7.45 (m, 2H), 7.45 – 7.33 (m, 6H), 7.31 (s, 1H), 5.62 (d, $J = 8.0$ Hz, 1H), 4.39 – 4.14 (m, 2H), 3.74 (s, 3H). ^{13}C NMR (101 MHz,) δ 171.12 (s), 168.75 (s), 167.55 (s), 144.66 (s), 140.01 (s), 135.98 (s), 132.16 (s), 129.16 (s), 129.01 (s), 128.81 (s), 128.13 (s), 127.81 (s), 127.47 (s), 127.30 (s), 56.87 (s), 53.02 (s), 43.67 (s). Yellow solid (55% yield). ESI-HRMS m/z $[\text{M}+\text{H}]^+$ calcd. for $\text{C}_{24}\text{H}_{22}\text{N}_2\text{O}_4$ 403.1658 found 403.1653.

Methyl(S,Z)-2-(2-(3-(2-methoxy-2-oxoethylidene)-1-oxo-5-phenylisoindolin-2-yl)acetamido)-2-phenylacetate (17c). ^1H NMR (400 MHz, CDCl_3) δ 9.39 (d, $J = 0.8$ Hz, 1H), 7.94 (d, $J = 8.0$ Hz, 1H), 7.86 – 7.80 (m, $J = 7.9, 1.4$ Hz, 1H), 7.73 – 7.66 (m, 2H), 7.50 (t, $J = 8.0$ Hz, 2H), 7.43 (d, $J = 8.0$ Hz, 1H), 7.35 – 7.29 (m, 5H), 6.96 (d, $J = 6.9$ Hz, 1H), 5.76 (s, 1H), 5.56 (d, $J = 8.0$ Hz, 1H), 4.53 (d, $J = 4.0$ Hz, 2H), 3.80 (s, 3H), 3.69 (s, 3H). ^{13}C NMR (101 MHz, CDCl_3) δ 170.78 (s), 167.08 (s), 166.02 (s), 165.92 (s), 147.75 (s), 147.05 (s), 140.04 (s), 135.86 (s), 134.55 (s), 130.34 (s), 129.09 (s), 129.03 (s), 128.69 (s), 128.38 (s), 127.94 (s), 127.57 (s), 127.24 (s), 127.15 (s), 123.96 (s), 99.72 (s), 56.58 (s), 52.96 (s), 51.82 (s), 43.55 (s). Yellow solid (58% yield). ESI-HRMS m/z $[\text{M}+\text{H}]^+$ calcd. for $\text{C}_{28}\text{H}_{24}\text{N}_2\text{O}_6$ 485.1713 found 485.1740.

Methyl(S,Z)-2-(2-(3-(2-ethoxy-2-oxoethylidene)-1-oxo-5-phenylisoindolin-2-yl)acetamido)-2-phenylacetate (17d). ¹H NMR (400 MHz, CDCl₃) δ 9.39 (d, *J* = 0.9 Hz, 1H), 7.95 (d, *J* = 8.0 Hz, 1H), 7.86 – 7.80 (m, 1H), 7.72 – 7.66 (m, 2H), 7.53 – 7.46 (m, 2H), 7.46 – 7.39 (m, 1H), 7.38 – 7.27 (m, 5H), 6.96 (d, *J* = 6.9 Hz, 1H), 5.76 (s, 1H), 5.56 (d, *J* = 8.0 Hz, 1H), 4.59 – 4.44 (m, 2H), 4.26 (d, *J* = 8.0 Hz, 2H), 3.70 (s, 3H), 1.33 (d, *J* = 8.0 Hz, 3H). ¹³C NMR (101 MHz, CDCl₃) δ 170.77 (s), 167.11 (s), 165.99 (s), 165.59 (s), 147.47 (s), 147.03 (s), 140.08 (s), 135.88 (s), 134.60 (s), 130.30 (s), 129.08 (s), 129.03 (s), 128.69 (s), 128.36 (s), 127.95 (s), 127.58 (s), 127.23 (s), 127.18 (s), 123.94 (s), 100.33 (s), 60.70 (s), 56.58 (s), 52.96 (s), 43.58 (s), 14.32 (s). Yellow solid (56% yield).ESI-HRMS *m/z* [M+H]⁺ calcd. for C₂₉H₂₆N₂O₆ 498.1869 found 498.1845.

Methyl (4-methylbenzoyl)-L-phenylalanylvalinate (19a). ¹H NMR (400 MHz, CDCl₃) δ 7.62 (d, *J* = 8.1 Hz, 2H), 7.32 – 7.18 (m, 7H), 6.87 (d, *J* = 7.1 Hz, 1H), 6.53 (d, *J* = 7.9 Hz, 1H), 5.00 – 4.85 (m, 1H), 4.43 (d, *J* = 8.0 Hz, 1H), 3.71 (s, 3H), 3.28 – 3.11 (m, *J* = 8.0 Hz, 2H), 2.38 (s, 3H), 2.12 – 2.04 (m, 1H), 0.98 – 0.71 (m, *J* = 8.0 Hz, 6H). ¹³C NMR (101 MHz, CDCl₃) δ 171.68 (s), 170.99 (s), 167.26 (s), 142.31 (s), 136.59 (s), 130.95 (s), 129.41 (s), 129.27 (s), 128.69 (s), 127.06 (s), 127.03 (s), 57.51 (s), 54.74 (s), 52.12 (s), 38.19 (s), 31.07 (s), 21.46 (s), 18.85 (s), 17.74 (s). White solid (40% yield).ESI-HRMS *m/z* [M+H]⁺ calcd. for C₂₃H₂₈N₂O₄ 397.2127 found 397.2145.

Methyl((S)-2-((Z)-3-(2-methoxy-2-oxoethylidene)-5-methyl-1-oxoisindolin-2-yl)-3-phenylpropanoyl)-L-valinate (20a). ¹H NMR (400 MHz,) δ 8.85 (s,1H), 7.64 (d, *J* = 8.0 Hz,1H), 7.36 (d, *J* = 8.0 Hz,1H), 7.19 – 7.02 (m,5H), 6.40 (s,1H), 5.92 (s,1H), 5.41 (s,1H), 4.56 (dd, *J* = 8.0 Hz,1H), 3.81 (s,3H), 3.67 (s,3H), 3.64 – 3.56 (m,1H), 3.42 – 3.30 (m,1H), 2.50 (s,3H), 2.16 – 1.98 (m, 1H), 0.82 (dd, *J* = 8.0 Hz, 6H). NMR (101 MHz,) δ 171.87 (s), 168.81

(s), 167.41 (s), 166.20 (s), 144.34 (s), 136.86 (s), 133.93 (s), 132.34 (s), 129.04 (s), 128.56 (d, $J = 3.0$ Hz), 126.91 (s), 126.31 (s), 123.42 (s), 100.40 (s), 57.59 (s), 52.27 (s), 51.83 (s), 34.03 (s), 31.19 (s), 29.72 (s), 22.42 (s), 18.96 (s), 17.84 (s). White solid (40% yield).ESI-HRMS m/z $[M+H]^+$ calcd. for $C_{27}H_{30}N_2O_6$ 479.2182 found 479.2209.

Methyl((S)-2-((Z)-3-(2-ethoxy-2-oxoethylidene)-5-methyl-1-oxoisindolin-2-yl)-3-phenylpropanoyl)-Lvalinate (20b). 1H NMR (400 MHz,) δ 8.83 (s, 1H), 7.62 (d, $J = 8.0$ Hz, 1H), 7.34 (d, $J = 8.0$ Hz, 1H), 7.18 – 7.05 (m, 5H), 6.40 (s, 1H), 5.86 (s, 1H), 5.39 (s, 1H), 4.56 (dd, $J = 8.0$ Hz, 1H), 4.29 – 4.21 (m, 2H), 3.65 (s, 3H), 3.64 – 3.57 (m, 1H), 3.41 – 3.26 (m, 1H), 2.49 (s, 3H), 2.17 – 2.03 (m, 1H), 1.33 (t, $J = 8.0$ Hz, 3H), 0.80 (dd, $J = 8.0$ Hz, 6H).NMR (101 MHz,) δ 171.86 (s), 168.88 (s), 167.40 (s), 165.74 (s), 144.73 (s), 136.96 (s), 133.99 (s), 132.29 (s), 129.06 (s), 128.55 (s), 126.90 (s), 126.38 (s), 123.41 (s), 101.26 (s), 60.72 (s), 57.58 (s), 52.21(s), 34.03 (s), 31.24 (s), 29.81 (s), 22.39 (s), 19.04 (s), 17.83 (s), 14.38 (s).White solid (40% yield).ESI-HRMS m/z $[M+H]^+$ calcd. for $C_{28}H_{32}N_2O_6$ 492.2339 found 492.2367.

Methyl (4-(tert-butyl)benzoyl)-L-phenylalanyl-L-valinate (19b). 1H NMR (400 MHz, $CDCl_3$) δ 7.67 (d, $J = 8.0$ Hz, 2H), 7.43 – 7.39 (m, 2H), 7.30 – 7.19 (m, 6H), 6.98 (d, $J = 8.0$ Hz, 1H), 6.66 (d, $J = 8.1$ Hz, 1H), 4.96 (q, $J = 8.0$ Hz, 1H), 4.45 (dd, $J = 8.0$ Hz, 1H), 3.71 (s, 3H), 3.28 – 3.13 (m, 2H), 2.14 – 2.00 (m, 1H), 1.32 (s, 9H), 0.83 (dd, $J = 8.0$ Hz, 6H). ^{13}C NMR (101 MHz, $CDCl_3$) δ 171.70 (s), 171.12 (s), 167.28 (s), 155.35 (s), 136.62 (s), 130.88 (s), 129.41 (s), 128.67 (s), 126.97 (d, $J = 4.6$ Hz), 125.53 (s), 125.22 (s), 57.50 (s), 54.73 (s), 52.11 (s), 38.13 (s), 34.94 (s), 31.14 (s), 31.08 (s), 18.86 (s), 17.75 (s). White solid (55% yield).ESI-HRMS m/z $[M+H]^+$ calcd. for $C_{26}H_{34}N_2O_4$ 439.2597 found 439.2552.

Methyl((S)-2-((Z)-5-(tert-butyl)-3-(2-methoxy-2-oxoethylidene)-1-oxoisindolin-2-yl)-3-phenylpropanoyl)-L-valinate (21a). ¹H NMR (400 MHz, CDCl₃) δ 9.18 (d, *J* = 4.0 Hz, 1H), 7.70 (d, *J* = 8.0 Hz, 1H), 7.61 (d, *J* = 8.0 Hz, 1H), 7.20 – 7.05 (m, 5H), 6.34 (s, 1H), 5.91 (s, 1H), 5.38 (s, 1H), 4.60 – 4.52 (m, 1H), 3.82 (s, 3H), 3.69 (s, 3H), 3.66 – 3.59 (m, 1H), 3.45 – 3.28 (m, 1H), 2.16 – 2.00 (m, 1H), 1.41 (s, 9H), 0.82 (d, *J* = 8.0 Hz, 7H). ¹³C NMR (101 MHz, CDCl₃) δ 171.79 (s), 168.72 (s), 166.08 (s), 157.92 (s), 146.94 (s), 136.89 (s), 133.75 (s), 129.34 (s), 128.99 (s), 128.75 (s), 128.54 (s), 126.84 (s), 126.12 (s), 125.31 (s), 123.13 (s), 100.68 (s), 57.55 (s), 52.22 (s), 51.80 (s), 35.87 (s), 34.09 (s), 31.34 (s), 31.19 (s), 29.70 (s), 18.89 (s), 17.84 (s). White solid (35% yield). ESI-HRMS *m/z* [M+H]⁺ calcd. for C₃₀H₃₆N₂O₆ 521.2651 found 521.2672

Methyl((S)-2-((Z)-5-(tert-butyl)-3-(2-ethoxy-2-oxoethylidene)-1-oxoisindolin-2-yl)-3-phenylpropanoyl)-L-valinate (21b). ¹H NMR (400 MHz, CDCl₃) δ 9.17 (d, *J* = 1.1 Hz, 1H), 7.69 (d, *J* = 8.0 Hz, 1H), 7.60 (dd, *J* = 8.0, 1.6 Hz, 1H), 7.21 – 7.08 (m, 1H), 6.37 (s, 1H), 5.88 (s, 1H), 5.40 (s, 1H), 4.58 (dd, *J* = 8.6, 5.0 Hz, 1H), 4.35 – 4.20 (m, 1H), 3.68 (s, 1H), 3.67 – 3.61 (m, 1H), 3.42 – 3.30 (m, 1H), 2.20 – 2.07 (m, 1H), 1.40 (s, 9H), 1.34 (t, *J* = 8.0 Hz, 3H), 0.84 (d, *J* = 8.0 Hz, 6H). ¹³C NMR (101 MHz, CDCl₃) δ 171.80 (s), 168.80 (s), 165.62 (s), 157.86 (s), 136.94 (s), 133.79 (s), 129.00 (s), 128.96 (s), 128.69 (s), 128.51 (s), 126.82 (s), 126.14 (s), 125.31 (s), 123.10 (s), 101.15 (s), 60.62 (s), 57.56 (s), 52.22 (s), 35.86 (s), 34.09 (s), 31.34 (s), 31.24 (s), 29.70 (s), 18.97 (s), 17.86 (s), 14.34 (s). White solid (32% yield). ESI-HRMS *m/z* [M+H]⁺ calcd. for C₃₁H₃₈N₂O₆ 535.2730 found 535.2773.

Methyl((S)-2-((Z)-3-(2-butoxy-2-oxoethylidene)-5-(tert-butyl)-1-oxoisindolin-2-yl)-3-phenylpropanoyl)-L-valinate (21c). ¹H NMR (400 MHz, CDCl₃) δ 9.19 (s, 1H), 7.71 (d, *J* = 8.0 Hz, 1H), 7.62 (d, *J* = 9.4 Hz, 1H), 7.21 – 7.10 (m, 3H), 6.41 (s, 1H), 5.89 (s, 1H), 5.43 (s,

1H), 4.60 (dd, $J = 8.6, 4.9$ Hz, 1H), 4.31 – 4.16 (m, 2H), 3.69 (s, 2H), 3.67 – 3.62 (m, 1H), 3.44 – 3.30 (m, 1H), 2.19 – 2.10 (m, 1H), 1.74 – 1.65 (m, 2H), 1.49 – 1.44 (m, 2H), 1.42 (s, 9H), 0.99 (t, $J = 8.0$ Hz, 3H), 0.86 (dd, $J = 8.0$ Hz, 6H). ^{13}C NMR (101 MHz, CDCl_3) δ 171.79 (s), 168.81 (s), 165.74 (s), 157.85 (s), 150.88 (s), 136.95 (s), 133.81 (s), 129.00 (s), 128.68 (s), 128.50 (s), 128.25 (s), 126.81 (s), 126.14 (s), 125.31 (s), 123.09 (s), 101.17 (s), 64.58 (s), 57.55 (s), 52.21 (s), 35.86 (s), 34.07 (s), 31.34 (s), 31.27 (s), 30.75 (s), 29.70 (s), 19.18 (s), 18.97 (s), 17.85 (s), 13.75 (s). White solid (30% yield). ESI-HRMS m/z $[\text{M}+\text{H}]^+$ calcd. for $\text{C}_{33}\text{H}_{42}\text{N}_2\text{O}_6$ 563.3121 found 563.3135.

Methyl ((S)-2-((Z)-3-(2-(tert-butoxy)-2-oxoethylidene)-5-(tert-butyl)-1-oxoisindolin-2-yl)-3-phenylpropanoyl)-L-valinate (21d). ^1H NMR (400 MHz, CDCl_3) δ 9.03 (s, 1H), 7.67 (d, $J = 8.0$ Hz, 1H), 7.62 – 7.55 (m, 1H), 7.21 – 7.08 (m, 5H), 6.40 (s, 1H), 5.78 (s, 1H), 5.39 (s, 1H), 4.63 – 4.55 (m, 1H), 3.68 (s, 3H), 3.66 – 3.62 (m, 1H), 3.42 – 3.26 (m, 1H), 2.13 (m, 1H), 1.55 (s, 9H), 1.39 (s, 9H), 0.86 (dd, $J = 8.0$ Hz, 6H). ^{13}C NMR (101 MHz, CDCl_3) δ 171.78 (s), 168.95 (s), 165.01 (s), 157.60 (s), 137.08 (s), 133.91 (s), 129.03 (s), 128.95 (s), 128.47 (s), 128.28 (s), 126.77 (s), 126.17 (s), 124.83 (s), 123.01 (s), 103.33 (s), 81.00 (s), 57.57 (s), 52.21 (s), 35.81 (s), 34.08 (s), 31.30 (s), 31.24 (s), 29.70 (s), 28.21 (s), 19.10 (s), 17.87 (s). White solid (32% yield). ESI-HRMS m/z $[\text{M}+\text{H}]^+$ calcd. for $\text{C}_{33}\text{H}_{42}\text{N}_2\text{O}_6$ 563.3043 found 563.3095.

Methyl (3-nitrobenzoyl)-L-phenylalanyl-L-valinate (19c). ^1H NMR (400 MHz, CDCl_3) δ 8.59 (s, 1H), 8.35 (d, $J = 8.0$ Hz, 1H), 8.08 (d, $J = 8.0$ Hz, 1H), 7.61 (t, $J = 8.0$ Hz, 1H), 7.41 (d, $J = 8.0$ Hz, 1H), 7.36 – 7.25 (m, 5H), 6.46 (d, $J = 8.0$ Hz, 1H), 4.97 (q, $J = 8.0$ Hz, 1H), 4.48 (dd, $J = 8.0$ Hz, 1H), 3.75 (s, 3H), 3.23 (m, 1H), 2.21 – 2.09 (m, 1H), 0.88 (dd, $J = 8.0$ Hz, 6H). ^{13}C NMR (101 MHz, CDCl_3) δ 171.61 (s), 170.89 (s), 164.79 (s), 148.27 (s), 136.21 (s), 135.38 (s), 132.92 (s), 129.73 (s), 129.37 (s), 128.78 (s), 127.25 (s), 126.27 (s), 122.36 (s), 57.64 (s),

55.23 (s), 52.22 (s), 38.47 (s), 31.08 (s), 18.87 (s), 17.77 (s). White solid (53% yield).ESI-HRMS m/z $[M+H]^+$ calcd. for $C_{22}H_{25}N_2O_4$ 428.1822 found 428.1808.

Methyl benzoylglycyl-L-alanyl-L-phenylalaninate (22a). 1H NMR (400 MHz, $CDCl_3$) δ 7.83 (d, $J = 7.3$ Hz, 1H), 7.51 (t, $J = 7.3$ Hz, 1H), 7.45 – 7.38 (m, 1H), 7.32 (d, $J = 7.5$ Hz, 1H), 7.24 – 7.15 (m, 1H), 7.10 – 7.02 (m, 1H), 4.88 – 4.79 (m, 1H), 4.58 (t, $J = 8.0$ Hz, 1H), 4.12 – 4.07 (m, 2H), 3.68 (s, 3H), 3.13 (m, 1H), 3.04 (m, 1H), 1.34 (d, $J = 8.0$ Hz, 2H). ^{13}C NMR (101 MHz, $CDCl_3$) δ 171.82 (s), 168.98 (s), 167.88 (s), 166.79 (s), 135.82 (s), 133.50 (s), 131.89 (s), 129.23 (s), 128.58 (s), 128.51 (s), 127.28 (s), 127.09 (s), 53.31 (s), 52.39 (s), 48.98 (s), 43.47 (s), 37.80 (s), 18.18 (s). White solid (50% yield).ESI-HRMS m/z $[M+H]^+$ calcd. for $C_{22}H_{26}N_3O_5$ 412.1873 found 412.1873.

Methyl(2-((Z)-1-(2-methoxy-2-oxoethylidene)-3-oxoisindolin-2-yl)acetyl)-L-alanyl-L-phenylalaninate (23). 1H NMR (400 MHz, $CDCl_3$) δ 9.05 (d, $J = 7.9$ Hz, 1H), 7.85 (d, $J = 7.4$ Hz, 1H), 7.71 – 7.63 (m, $J = 9.6, 5.7$ Hz, 1H), 7.61 – 7.54 (m, $J = 13.2, 5.9$ Hz, 1H), 7.29 – 7.17 (m, 1H), 7.07 (d, $J = 6.8$ Hz, 1H), 6.98 (t, $J = 8.8$ Hz, 1H), 6.74 (t, $J = 7.9$ Hz, 1H), 5.68 (s, 1H), 4.78 (m, 1H), 4.59 – 4.49 (m, 1H), 4.44 (s, 2H), 3.75 (s, 3H), 3.68 (s, 3H), 3.16 – 2.97 (m, 2H), 1.32 (d, $J = 7.0$ Hz, 3H). ^{13}C NMR (101 MHz, $CDCl_3$) δ 171.62 (s), 171.53 (s), 167.20 (s), 166.33 (s), 166.04 (s), 147.96 (s), 135.60 (s), 133.78 (s), 133.66 (s), 131.48 (s), 129.42 (s), 129.22 (s), 128.60 (s), 128.25 (s), 127.19 (s), 123.51 (s), 99.13 (s), 53.43 (s), 52.43 (s), 51.73 (s), 48.91 (s), 43.06 (s), 37.74 (s), 18.37 (s). White solid (28% yield).ESI-HRMS m/z $[M+H]^+$ calcd. for $C_{26}H_{27}N_3O_7$ 493.1849 found 493.4983.

Methyl benzoyl-L-valyl-L-leucyl-L-phenylalaninate (22b). 1H NMR (400 MHz, DMSO) δ 8.17 (d, $J = 8.1$ Hz, 1H), 7.94 (d, $J = 8.2$ Hz, 1H), 7.90 – 7.82 (m, 1H), 7.55 – 7.48 (m, 1H), 7.44

(dd, $J = 9.2, 4.1$ Hz, 1H), 7.23 (t, $J = 7.1$ Hz, 1H), 7.17 (d, $J = 5.8$ Hz, 1H), 4.53 (d, $J = 8.0$ Hz, 1H), 4.41 (q, $J = 8.0$ Hz, 1H), 4.32 (t, $J = 8.0$ Hz, 1H), 3.58 (s, 3H), 2.99 (m, 2H), 2.13 (m, 1H), 1.59 (m, 1H), 1.43 (t, $J = 8.0$ Hz, 2H), 0.94 – 0.79 (m, 12H). ^{13}C NMR (101 MHz, DMSO) δ 172.32 (s), 171.91 (s), 171.14 (s), 167.07 (s), 137.21 (s), 134.86 (s), 131.48 (s), 129.30 (s), 128.50 (s), 128.44 (s), 127.82 (s), 126.82 (s), 59.56 (s), 53.62 (s), 52.05 (s), 51.67 – 51.39 (m), 41.45 (s), 37.16 (s), 30.59 (s), 24.49 (s), 23.28 (s), 22.11 (s), 19.76 (s), 19.06 (s). White solid (42% yield). ESI-HRMS m/z $[\text{M}+\text{H}]^+$ calcd. for $\text{C}_{28}\text{H}_{38}\text{N}_3\text{O}_5$ 496.2812 found 496.3018.

Methyl ((S)-2-((Z)-1-(2-methoxy-2-oxoethylidene)-3-oxoisindolin-2-yl)-3-methylbutanoyl) - L-leucyl-L-phenylalaninate (24). ^1H NMR (400 MHz, CDCl_3) δ 9.06 (d, $J = 7.9$ Hz, 1H), 7.95 (d, $J = 15.8$ Hz, 1H), 7.86 (d, $J = 7.4$ Hz, 1H), 7.69 (td, $J = 7.8, 1.1$ Hz, 1H), 7.61 (t, $J = 7.2$ Hz, 1H), 7.29 (dd, $J = 16.1, 6.9$ Hz, 1H), 7.15 (d, $J = 7.4$ Hz, 1H), 6.75 (d, $J = 7.7$ Hz, 1H), 6.41 (d, $J = 15.7$ Hz, 1H), 6.26 (s, 1H), 4.78 (d, $J = 8.0$ Hz, 1H), 4.46 – 4.38 (m, 1H), 3.80 (s, 3H), 3.78 (s, 3H), 3.65 (m, 2H), 3.34 – 3.16 (m, 2H), 1.62 – 1.53 (m, 1H), 1.48 – 1.38 (m, 2H), 1.13 – 0.67 (m, 12H). ^{13}C NMR (101 MHz, CDCl_3) δ 171.29 (s), 171.25 (s), 168.93 (s), 167.58 (s), 166.27 (s), 141.77 (s), 135.84 (s), 133.73 (s), 133.52 (s), 131.34 (s), 131.14 (s), 130.22 (s), 128.83 (s), 128.02 (s), 127.72 (s), 126.74 (s), 123.46 (s), 119.69 (s), 101.51 (s), 53.14 (s), 52.45 (s), 51.83 (s), 51.73 (s), 39.94 (s), 34.87 (s), 31.92 (s), 29.70 (s), 24.69 (s), 22.80 (s), 21.40 (s), 20.84 (s), 14.13 (s). White solid (25% yield). ESI-HRMS m/z $[\text{M}+\text{Na}]^+$ calcd. for $\text{C}_{32}\text{H}_{39}\text{N}_3\text{O}_7$ 601.2686 found 601.4069.

4b.5 References

1. Şener, B.; Gözler, B.; Minard, R. D.; Shamma, M., Alkaloids of *Fumaria vaillantii*. *Phytochemistry* **1983**, 22 (9), 2073-2075.
2. Blaskó, G.; Gula, D. J.; Shamma, M., The phthalideisoquinoline alkaloids. *J. Nat. Prod.* **1982**, 45 (2), 105-122.
3. Upadhyay, S. P.; Thapa, P.; Sharma, R.; Sharma, M., 1-Isoindolinone scaffold-based natural products with a promising diverse bioactivity. *Fitoterapia* **2020**, 104722.
4. Räder, A. F. B.; Weinmüller, M.; Reichart, F.; Schumacher-Klinger, A.; Merzbach, S.; Gilon, C.; Hoffman, A.; Kessler, H., Orally Active Peptides: Is There a Magic Bullet? *Angew Chem Int Ed Engl* **2018**, 57 (44), 14414-14438.
5. Zhang, H.; Wu, J.; Wang, J.; Xiao, S.; Zhao, L.; Yan, R.; Wu, X.; Wang, Z.; Fan, L.; Jin, Y., Novel Isoindolinone-Based Analogs of the Natural Cyclic Peptide Fenestin A: Synthesis and Antitumor Activity. *ACS Medicinal Chemistry Letters* **2022**, 13 (7), 1118-1124.
6. Yoon, U. C.; Jin, Y. X.; Oh, S. W.; Park, C. H.; Park, J. H.; Campana, C. F.; Cai, X.; Duesler, E. N.; Mariano, P. S., A synthetic strategy for the preparation of cyclic peptide mimetics based on SET-promoted photocyclization processes. *Journal of the American Chemical Society* **2003**, 125 (35), 10664-10671.
7. Li, B.; Wang, L.; Chen, X.; Chu, X.; Tang, H.; Zhang, J.; He, G.; Li, L.; Chen, G., Extendable stapling of unprotected peptides by crosslinking two amines with o-phthalaldehyde. *Nature Communications* **2022**, 13 (1), 311.
8. Horne, W. S.; Stout, C. D.; Ghadiri, M. R., A heterocyclic peptide nanotube. *Journal of the American Chemical Society* **2003**, 125 (31), 9372-9376.
9. Boto, A.; González, C. C.; Hernández, D.; Romero-Estudillo, I.; Saavedra, C. J., Site-selective modification of peptide backbones. *Organic Chemistry Frontiers* **2021**, 8 (23), 6720-6759.
10. Yang, H.; Du, Y.; Wan, S.; Trahan, G. D.; Jin, Y.; Zhang, W., Mesoporous 2D covalent organic frameworks based on shape-persistent arylene-ethynylene macrocycles. *Chemical Science* **2015**, 6 (7), 4049-4053.
11. Thapa, P.; Corral, E.; Sardar, S.; Pierce, B. S.; Foss Jr, F. W., Isoindolinone Synthesis: Selective Dioxane-Mediated Aerobic Oxidation of Isoindolines. *J. Org. Chem.* **2018**, 84 (2), 1025-1034.
12. Anamimoghadam, O.; Mumtaz, S.; Nietsch, A.; Saya, G.; Motti, C. A.; Wang, J.; Junk, P. C.; Qureshi, A. M.; Oelgemöller, M., The photodecarboxylative addition of carboxylates to phthalimides as a key-step in the synthesis of biologically active 3-arylmethylene-2, 3-dihydro-1H-isoindolin-1-ones. *Beilstein J. Org. Chem.* **2017**, 13 (1), 2833-2841.

13. Abell, A.; Oldham, M.; Taylor, J., Synthesis of Cyclic Acylated Enamino Esters from Enol Lactones, 4-Keto Amides, and 5-Hydroxy Lactams. *J. Org. Chem.* **1995**, *60* (5), 1214-1220.
14. Gupta, M. K.; Jena, C. K.; Sharma, N. K., Pd-Catalyzed C (sp²)-H olefination: synthesis of N-alkylated isoindolinone scaffolds from aryl amides of amino acid esters. *Organic & Biomolecular Chemistry* **2021**, *19* (46), 10097-10104.
15. Chalker, J. M.; Bernardes, G. J.; Davis, B. G., A “tag-and-modify” approach to site-selective protein modification. *Accounts of chemical research* **2011**, *44* (9), 730-741.
16. Ali, W.; Prakash, G.; Maiti, D., Recent development in transition metal-catalysed C-H olefination. *Chem. Sci.* **2021**, *12* (8), 2735-2759.
17. Reddy, M. C.; Jeganmohan, M., Total synthesis of aristolactam alkaloids via synergistic C-H bond activation and dehydro-Diels-Alder reactions. *Chem. Sci.* **2017**, *8* (5), 4130-4135.
18. Deb, A.; Hazra, A.; Peng, Q.; Paton, R. S.; Maiti, D., Detailed mechanistic studies on palladium-catalyzed selective C-H olefination with aliphatic alkenes: a significant influence of proton shuttling. *J. Am. Chem. Soc.* **2017**, *139* (2), 763-775.
19. Bag, S.; Patra, T.; Modak, A.; Deb, A.; Maity, S.; Dutta, U.; Dey, A.; Kancherla, R.; Maji, A.; Hazra, A., Remote para-C-H functionalization of arenes by a D-shaped biphenyl template-based assembly. *Journal of the American Chemical Society* **2015**, *137* (37), 11888-11891.
20. Deb, A.; Bag, S.; Kancherla, R.; Maiti, D., Palladium-catalyzed aryl C-H olefination with unactivated, aliphatic alkenes. *J. Am. Chem. Soc.* **2014**, *136* (39), 13602-13605.
21. Seth, K.; Bera, M.; Brochetta, M.; Agasti, S.; Das, A.; Gandini, A.; Porta, A.; Zanoni, G.; Maiti, D., Incorporating unbiased, unactivated aliphatic alkenes in Pd (II)-catalyzed olefination of benzyl phosphoramidate. *ACS Catal.* **2017**, *7* (11), 7732-7736.
22. Thrimurtulu, N.; Dey, A.; Singh, A.; Pal, K.; Maiti, D.; Volla, C. M., Palladium Catalyzed Regioselective C4-Arylation and Olefination of Indoles and Azaindoles. *Adv. Synth. Catal.* **2019**, *361* (6), 1441-1446.
23. Maity, S.; Hoque, E.; Dhawa, U.; Maiti, D., Palladium catalyzed selective distal C-H olefination of biaryl systems. *Chem. Commun.* **2016**, *52* (97), 14003-14006.
24. Manoharan, R.; Sivakumar, G.; Jeganmohan, M., Cobalt-catalyzed C-H olefination of aromatics with unactivated alkenes. *Chem. Commun.* **2016**, *52* (69), 10533-10536.
25. Patra, T.; Watile, R.; Agasti, S.; Naveen, T.; Maiti, D., Sequential meta-C-H olefination of synthetically versatile benzyl silanes: effective synthesis of meta-olefinated toluene, benzaldehyde and benzyl alcohols. *Chem. Commun.* **2016**, *52* (10), 2027-2030.
26. Achar, T. K.; Ramakrishna, K.; Pal, T.; Porey, S.; Dolui, P.; Biswas, J. P.; Maiti, D., Regiocontrolled remote C-H olefination of small heterocycles. *Chem. Euro. J.* **2018**, *24* (68), 17906-17910.

27. Achar, T. K.; Maiti, S.; Jana, S.; Maiti, D., Transition metal catalyzed enantioselective C (sp²)–H bond functionalization. *ACS Catalysis* **2020**, *10* (23), 13748-13793.
28. Dutta, U.; Maiti, S.; Bhattacharya, T.; Maiti, D., Arene diversification through distal C (sp²)–H functionalization. *Science* **2021**, *372* (6543), eabd5992.
29. Saha, A.; Guin, S.; Ali, W.; Bhattacharya, T.; Sasmal, S.; Goswami, N.; Prakash, G.; Sinha, S. K.; Chandrashekar, H. B.; Panda, S., Photoinduced regioselective olefination of arenes at proximal and distal sites. *Journal of the American Chemical Society* **2022**, *144* (4), 1929-1940.
30. Dutta, U.; Maiti, S.; Pimparkar, S.; Maiti, S.; Gahan, L. R.; Krenseke, E. H.; Lupton, D. W.; Maiti, D., Rhodium catalyzed template-assisted distal para-C–H olefination. *Chem. Sci.* **2019**, *10* (31), 7426-7432.
31. Maity, S.; Dolui, P.; Kancherla, R.; Maiti, D., Introducing unactivated acyclic internal aliphatic olefins into a cobalt catalyzed allylic selective dehydrogenative Heck reaction. *Chem. Sci.* **2017**, *8* (7), 5181-5185.
32. Baccalini, A.; Vergura, S.; Dolui, P.; Maiti, S.; Dutta, S.; Maity, S.; Khan, F. F.; Lahiri, G. K.; Zanoni, G.; Maiti, D., Cobalt-Catalyzed C (sp²)–H Allylation of Biphenyl Amines with Unbiased Terminal Olefins. *Org. Lett.* **2019**, *21* (21), 8842-8846.
33. Xia, C.; White, A. J.; Hii, K. K. M., Synthesis of isoindolinones by Pd-catalyzed coupling between N-methoxybenzamide and styrene derivatives. *J. Org. Chem.* **2016**, *81* (17), 7931-7938.
34. Zhu, C.; Falck, J., N-acylsulfonamide assisted tandem C–H olefination/annulation: synthesis of isoindolinones. *Org. Lett.* **2011**, *13* (5), 1214-1217.
35. Youn, S. W.; Ko, T. Y.; Kim, Y. H.; Kim, Y. A., Pd (II)/Cu (II)-Catalyzed regio- and stereoselective synthesis of (E)-3-arylmethyleneisoindolin-1-ones using air as the terminal oxidant. *Org. Lett.* **2018**, *20* (24), 7869-7874.
36. Noisier, A. F.; Brimble, M. A., C–H functionalization in the synthesis of amino acids and peptides. *Chemical Reviews* **2014**, *114* (18), 8775-8806.
37. Gong, W.; Zhang, G.; Liu, T.; Giri, R.; Yu, J.-Q., Site-selective C (sp³)–H functionalization of di-, tri-, and tetrapeptides at the N-terminus. *J. Am. Chem. Soc.* **2014**, *136* (48), 16940-16946.
38. Chen, G.; Zhuang, Z.; Li, G. C.; Saint-Denis, T. G.; Hsiao, Y.; Joe, C. L.; Yu, J. Q., Ligand-Enabled β-C–H Arylation of α-Amino Acids Without Installing Exogenous Directing Groups. *Angew. Chem. Int. Ed. Engl.* **2017**, *56* (6), 1506-1509.
39. Liu, T.; Qiao, J. X.; Poss, M. A.; Yu, J. Q., Palladium (II)-Catalyzed Site-Selective C (sp³)–H Alkynylation of Oligopeptides: A Linchpin Approach for Oligopeptide–Drug Conjugation. *Angewandte Chemie International Edition* **2017**, *56* (36), 10924-10927.

40. Mendive-Tapia, L.; Preciado, S.; García, J.; Ramón, R.; Kielland, N.; Albericio, F.; Lavilla, R., New peptide architectures through C–H activation stapling between tryptophan–phenylalanine/tyrosine residues. *Nature communications* **2015**, *6* (1), 1-9.
41. Noisier, A. F.; García, J.; Ionuț, I. A.; Albericio, F., Stapled Peptides by Late-Stage C (sp³)–H Activation. *Angewandte Chemie* **2017**, *129* (1), 320-324.
42. Tran, L. D.; Daugulis, O., Nonnatural amino acid synthesis by using carbon-hydrogen bond functionalization methodology. *Angew. Chem. Int. Ed. Engl.* **2012**, *51* (21), 5188-91.
43. Lu, Y.; Wang, D.-H.; Engle, K. M.; Yu, J.-Q., Pd (II)-catalyzed hydroxyl-directed C–H olefination enabled by monoprotected amino acid ligands. *J. Am. Chem. Soc.* **2010**, *132* (16), 5916-5921.
44. He, J.; Li, S.; Deng, Y.; Fu, H.; Laforteza, B. N.; Spangler, J. E.; Homs, A.; Yu, J.-Q., Ligand-controlled C (sp³)–H arylation and olefination in synthesis of unnatural chiral α -amino acids. *Science* **2014**, *343* (6176), 1216-1220.
45. Sevov, C. S.; Hartwig, J. F., Iridium-catalyzed oxidative olefination of furans with unactivated alkenes. *J. Am. Chem. Soc.* **2014**, *136* (30), 10625-10631.
46. Lu, M.-Z.; Chen, X.-R.; Xu, H.; Dai, H.-X.; Yu, J.-Q., Ligand-enabled ortho-C–H olefination of phenylacetic amides with unactivated alkenes. *Chem. Sci.* **2018**, *9* (5), 1311-1316.
47. Bera, M.; Modak, A.; Patra, T.; Maji, A.; Maiti, D., Meta-selective arene C–H bond olefination of arylacetic acid using a nitrile-based directing group. *Org. Lett.* **2014**, *16* (21), 5760-5763.
48. Agasti, S.; Mondal, B.; Achar, T. K.; Sinha, S. K.; Sarala Suseelan, A.; Szabo, K. J.; Schoenebeck, F.; Maiti, D., Orthogonal selectivity in C–H olefination: synthesis of branched vinylarene with unactivated aliphatic substitution. *ACS Catal.* **2019**, *9* (10), 9606-9613.
49. Bera, M.; Sahoo, S. K.; Maiti, D., Room-temperature meta-functionalization: Pd (II)-catalyzed synthesis of 1, 3, 5-trialkenyl arene and meta-hydroxylated olefin. *ACS Catal.* **2016**, *6* (6), 3575-3579.
50. Achar, T. K.; Zhang, X.; Mondal, R.; Shanavas, M.; Maiti, S.; Maity, S.; Pal, N.; Paton, R. S.; Maiti, D., Palladium-catalyzed directed meta-selective C–H allylation of arenes: Unactivated internal olefins as allyl surrogates. *Angew. Chem. Int. Ed. Engl.* **2019**, *131* (30), 10461-10468.
51. Achar, T. K.; Biswas, J. P.; Porey, S.; Pal, T.; Ramakrishna, K.; Maiti, S.; Maiti, D., Palladium-catalyzed template directed C-5 selective olefination of thiazoles. *J. Org. Chem.* **2019**, *84* (12), 8315-8321.
52. Bag, S.; Jana, S.; Pradhan, S.; Bhowmick, S.; Goswami, N.; Sinha, S. K.; Maiti, D., Imine as a linchpin approach for meta-C–H functionalization. *Nat. Commun.* **2021**, *12* (1), 1-8.

53. Bag, S.; Maiti, D., Palladium-catalyzed olefination of aryl C–H bonds by using directing scaffolds. *Synthesis* **2016**, 48 (06), 804-815.
54. Tang, J.; Chen, H.; He, Y.; Sheng, W.; Bai, Q.; Wang, H., Peptide-guided functionalization and macrocyclization of bioactive peptidosulfonamides by Pd (II)-catalyzed late-stage C–H activation. *Nature communications* **2018**, 9 (1), 1-8.
55. Savela, R.; Méndez-Gálvez, C., Isoindolinone Synthesis via One-Pot Type Transition Metal Catalyzed C– C Bond Forming Reactions. *Chemistry (Weinheim an der Bergstrasse, Germany)* **2021**, 27 (17), 5344.
56. Gupta, M. K.; Sharma, N. K., A new amino acid, hybrid peptides and BODIPY analogs: synthesis and evaluation of 2-aminotroponyl-L-alanine (ATA) derivatives. *Organic & Biomolecular Chemistry* **2022**, 20 (47), 9397-9407.
57. Tang, J.; Chen, H.; He, Y.; Sheng, W.; Bai, Q.; Wang, H., Peptide-guided functionalization and macrocyclization of bioactive peptidosulfonamides by Pd (II)-catalyzed late-stage C–H activation. *Nature Communications* **2018**, 9 (1), 3383.
58. Palai, B. B.; Sharma, N. K., N-Arylated peptide: troponyl residue influences the structure and conformation of N-troponylated-(di/tri)-peptides. *CrystEngComm* **2021**, 23 (1), 131-139.

CHAPTER-5

Synthesis of isoquinolone by Ru(II)-catalyzed annulation of *N*-naphthoyl amino ester at room temperature

TABLE OF CONTENTS

Chapter 5	159
5.1 Introduction.....	159
5.1.1 Hypothesis and objective	161
5.2 Result and discussion	161
5.2.1 Annulation of <i>N</i>-naphthoyl amino ester	163
5.2.2 Substrate scopes naphthoyl amino esters and naphthoyl aminoacid.....	164
5.2.3 Substrate scopes various peptides with diphenyl acetylene	165
5.2.4 The proposed reaction mechanism	166
5.3 Conclusion	167
5.4 Experimental Section.....	168
5.4.1 Materials and instrumentation	168
5.4.2 General procedure for amide synthesis.....	168
5.4.2 General procedure for Ru-catalysed reactions	169
5.4.3 Chemical shift values of NMR	169
5.5 Appendix	182
Contents	182
5.6 References	209

Chapter 5

5.1 Introduction

One of the significant nitrogen-heterocyclic compounds with a wide range of pharmacological and physiological activities are isoquinolones (isoquinolin-1(2H)-ones), and their synthesis techniques have advanced significantly in recent years. It has been extensively studied in synthetic chemistry that annulation protocols using unsaturated hydrocarbons are essential and effective ways to synthesise cyclic molecules with high atom-utilization and step-economy.¹⁻⁴ Isoquinolones are useful synthetic building blocks in addition to being intriguing and significant nitrogen-heterocyclic molecules with a variety of pharmacological and physiological functions.⁵⁻⁸ Jin Zhu has demonstrated the first direct synthesis of cobaltacycles via C–H activation and document N-chloroamide-enabled room temperature construction of heterocycles.⁹ The first Ru(II)-catalysed C–H activation of *N*-chlorobenzamides with 1,3-diynes for the synthesis of isoquinolone derivatives via [4+2] annulation was reported by Pawar.¹⁰ However, these methods suffer from at least one of the following limitations: use of a precious transition metal such as rhodium, high reaction temperature, requirement of an external oxidant, and bidentate directing group.

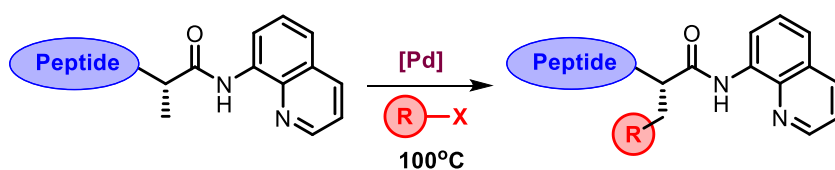
The modern pharmaceutical industry has been greatly influenced by peptides contributing significantly to the improvement of biological and chemical science.¹¹⁻¹⁴ Unlike small molecules, peptides are a special class of compounds as they disrupt protein-protein interactions, target or inhibit intracellular molecules, and have unique biological and therapeutic properties. The chemo- and regio-selective derivatization of peptides is a vital synthetic transformation in modern chemistry owing to the ability to fine-tune structural characteristics that assist in modulating physicochemical and biological properties. To treat cancer and deliver medications to specific locations, peptide conjugation to bioactive

substances including lipids, carbohydrates, and pharmaceuticals is a widespread practise.¹⁵⁻¹⁶

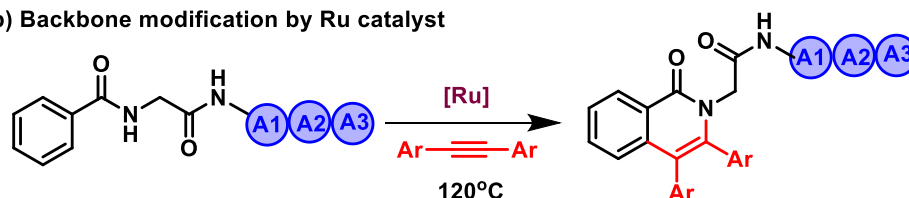
Real-time tracking in physiological condition requires peptide ligation to fluorescent labels, which is in great demand.¹⁷⁻¹⁸ Selective peptide modification is a desirable strategy in drug discovery to enhance bioavailability, metabolic stability, and membrane permeability.¹⁹⁻²²

But many of these covalent transforms are limited to the side chains of peptides rather than the peptide backbone. Although traditional reactions and cross-couplings have been used for the chemoselective diversification and bioorthogonal ligation of peptides, they primarily rely on prefunctionalizations, which can be time-consuming, result in undesirable by products, and racemize the peptide scaffold. For instance, C(sp³)H arylation of the Ala residue in peptides has been employed by the use of 8-aminoquinoline as a bidentate directing group (**Figure 5.1a**).²³⁻²⁸ Peptide backbone diversification employing the amide bonds of peptide backbone acting as the bidentate directing group through Ru(II)-catalysed C–H activation/annulation has been reported. (**Figure 5.1b**).²⁹ Lys-based peptides are modified chemo- and siteselectively using Rh(III)-catalysed C-H activation/annulation (**Figure 5.1c**).³⁰ These peptide modification requires harsh reaction condition or installation of directing group.

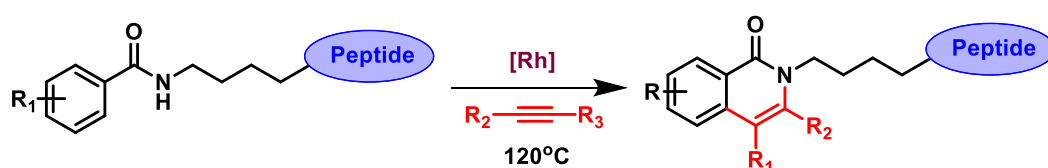
(a) C-H activation of ala residue via bidentate directing group



(b) Backbone modification by Ru catalyst



(c) Lys-based peptides are modification by Rh(III) catalyst



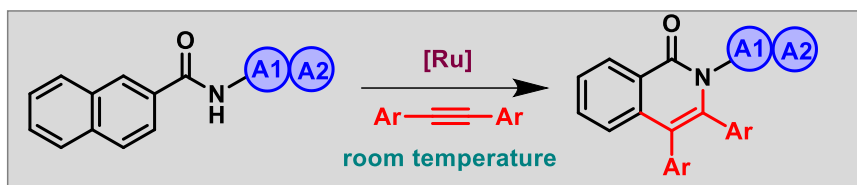
(d) C-H activation/annulation in *N*-naphthoyl amino ester in rt

Figure 5.1 (a) C-H activation of ala residue via bidentate directing group (b) Backbone modification by Ru catalyst (c) Lys-based peptides are modification by Rh(III) catalyst (d) C-H activation/annulation in *N*-naphthoyl amino ester in rt.

Here in we report eco-friendly and versatile Ru-catalysed C-H activation/annulation of *N*-naphthoyl amino ester/peptides at room temperature in a minimal duration of 2h. The modification of a peptide backbone by a Ru-catalyst at room temperature is being reported for the first time in this work (**Figure 5.1d**).

5.1.1 Hypothesis and objective

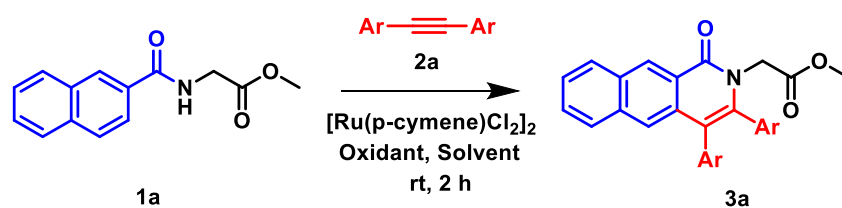
This paper describes the synthesis of isoquinolone derivatives from *N*-naphthoyl amino ester/peptide and *N*-biphenyl amino ester/peptide via Ru-catalysed C(sp²)-H annulation at room temperature. Herein, the amino acid ester/amide residue acts as a directing group for annulation at the aryl ring, and then cyclization occurs at the amide NH. Hence, this methodology could be helpful to transform standard amino acids/peptides into respective chiral isoquinolone derivatives at room temperature.

5.2 Result and discussion

We began our study with optimizing the Ru(II)-catalysed C-H activation/annulation of amino acid **1a** and diphenylacetylene **2a** (**Table 5.1**). Based on previous work on the diversification of oligopeptides Ru(II)-catalysed C-H activation/annulation by Erik V. Van der Eycken³¹⁻³² we employed [Ru(cymene)Cl₂]₂ as catalyst and Cu(OAc)₂ as oxidant in HFIP at rt for 2 h; the functionalized isoquinolone **3a** was isolated in 70% yield (**Table 5.1, entry 11**). When 1 mol%

of Ru(II) catalyst was used, **3a** was isolated in 43% yield and when [RhCp*Cl₂]₂ (5 mol%) was used instead of [Ru(*p*-cymene)Cl₂]₂, isolated yield was 54%. Other solvents, such as TFE, DCE, ^tAmOH gave lower yields whereas solvents like DMF, DMSO, ^tBuOH and Toluene gave trace amount of yields (**Table 5.1**). Various oxidants and additives were screened, leading to lower yields.

Table 5.1 Optimized reaction condition



Entry	Solvent	Oxidant 2 eq.	T (°C)	Yield (%)
1	TFE	AgOAc	rt	60
2	^t AmOH	AgOAc	rt	50
3	TFE	Ag ₂ CO ₃	rt	53
4	TFE	Cs ₂ OAc	rt	45
5	TFE	NaOAc	rt	Trace
6	HFIP	KOAc	rt	Trace
7	TFE	AgTFA	rt	Trace
8	TFE	Cu(OAc) ₂	rt	-
9	TFE	Cs ₂ CO ₃	rt	Trace
10	TFE	K ₂ CO ₃	rt	Trace
11	HFIP	Cu(OAc)₂	rt	70
12	DCE	AgOAc	rt	40
13	Butanol	AgOAc	rt	-
14	Toluene	AgOAc	rt	-
15	DMF	AgOAc	rt	-
16 ^a	HFIP	Cu(OAc) ₂	rt	43
17 ^b	HFIP	Cu(OAc) ₂	rt	54
18	DMSO	AgOAc	rt	-

1a (50 mg, 0.2 mmol, 1 eq.), **2a** (54.9 mg, 0.3 mmol, 1.5 eq.), $[\text{Ru}(p\text{-cymene})\text{Cl}_2]_2$ (6.3 mg, 0.05 mmol, 5 mol%), oxidant (74.45mg, 0.41 mmol, 2 eq.), solvent (1 mL, 0.1 M), rt, 2h.

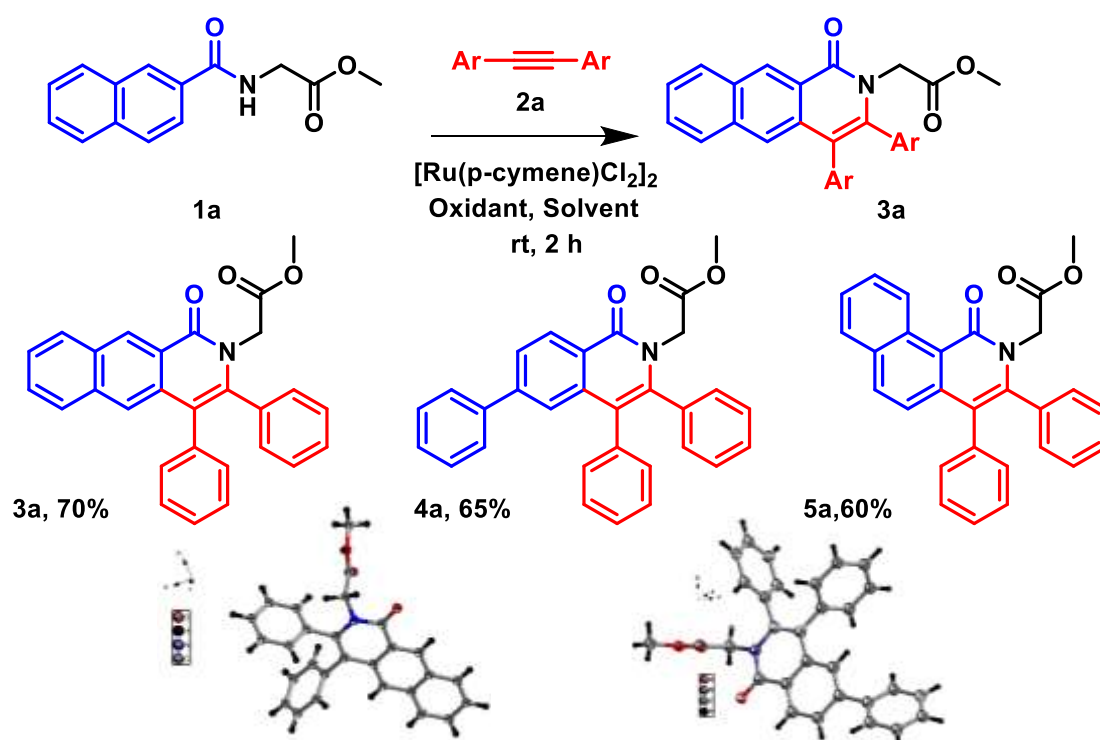
^a $[\text{Ru}(p\text{-cymene})\text{Cl}_2]_2$ (1 mol%) was used instead of (5 mol%).

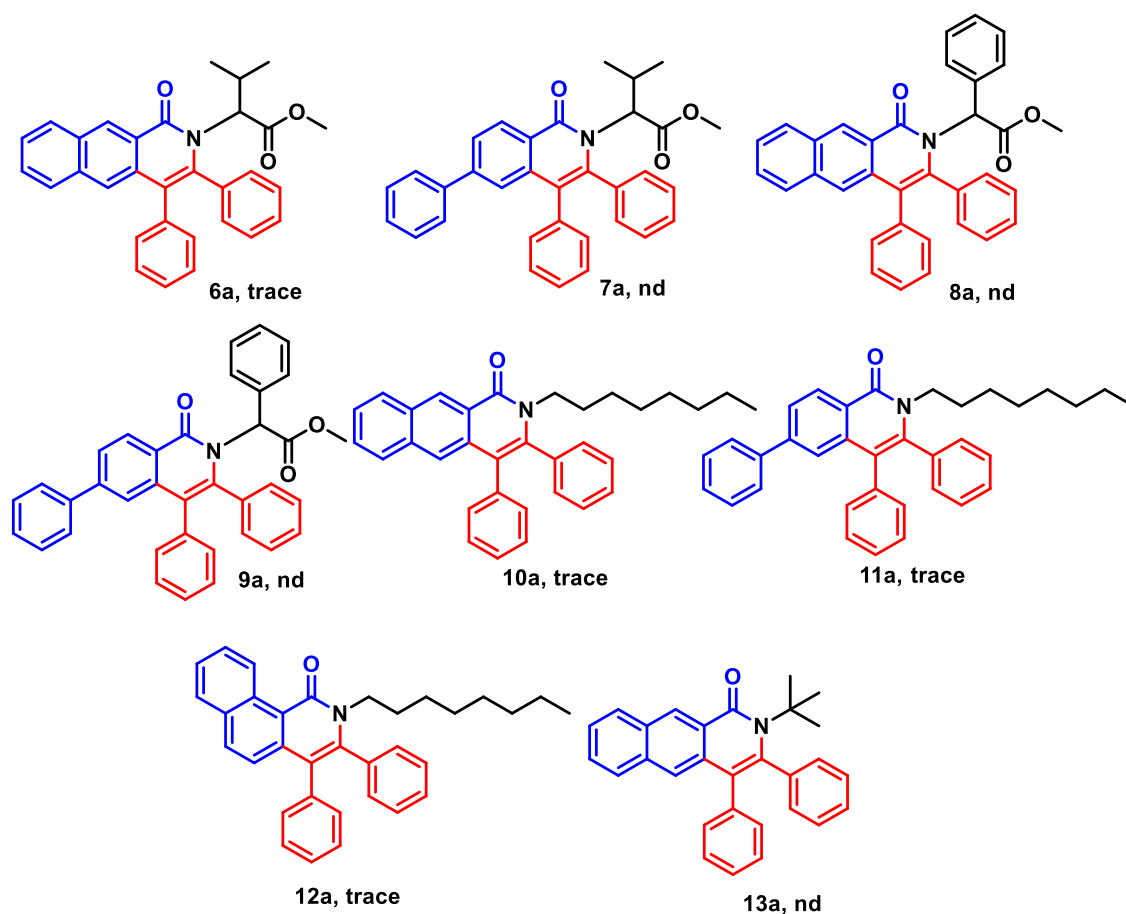
^b $[\text{RhCp}^*\text{Cl}_2]_2$ (5 mol%) was used instead of $[\text{Ru}(p\text{-cymene})\text{Cl}_2]_2$.

5.2.1 Annulation of *N*-naphthoyl amino ester

With the optimized reaction conditions in hand (**Scheme 5.1**), we evaluated the scope of the methodology. Initially, the influence of the 2-Napthoic α -amino ester, 1-Napthoic α -amino ester and 1,4-Biphenayl α -amino ester moiety on the reaction was studied with 1,2-diphenayl acetylene. We were pleased to observe that diphenyl acetylene was well tolerated to afford isoquinolone **3a** in 70% yield, **4a** in 65% yield, **5a** in 60% yield (**Scheme 5.1**). On the other hand, when a tertiary α -carbon amino ester was introduced on the substrate, trace amount of product formed as a result of the steric hindrance (**6a-13a**).

Scheme 5.1 Annulation of *N*-naphthoyl amino ester

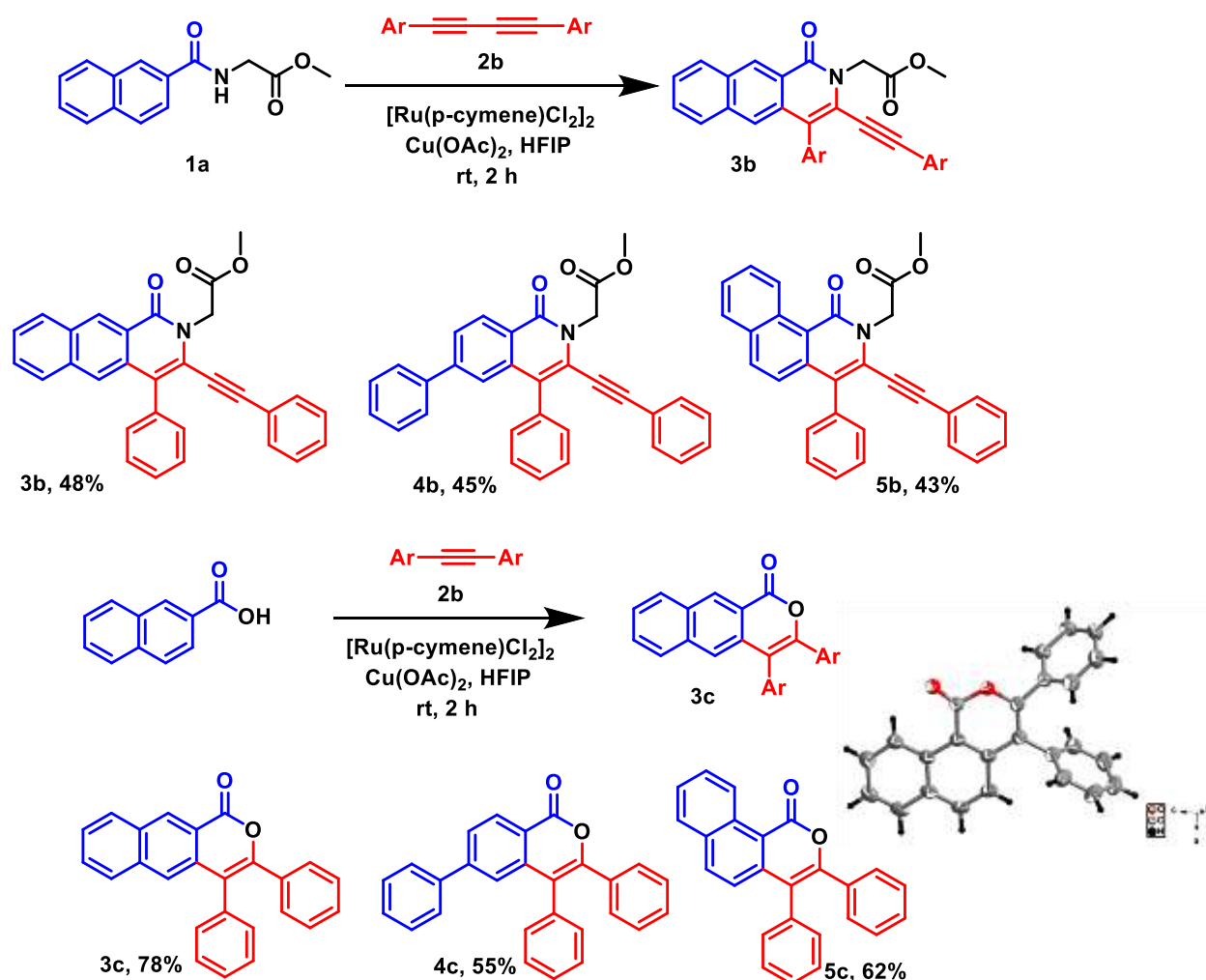




5.2.2 Substrate scopes naphthoyl amino esters and naphthoyl aminoacid.

Next, the reaction scope was evaluated with respect to 1,4-diphenylbutadiyne with 2-Napthoic α -amino ester, 1-Napthoic α -amino ester, 1,4-Biphenayl α -amino ester and 2-Napthoic acid, 1-Napthoic acid, 1,4-Biphenayl carboxylic acid (**Scheme 5.2**). All substrates form corresponding isoquinolone products in moderate to good yields (**3b-5b** and **3c-5c**).

Scheme 5.2 isoquinolone derivative using peptides and 1,3-diyne

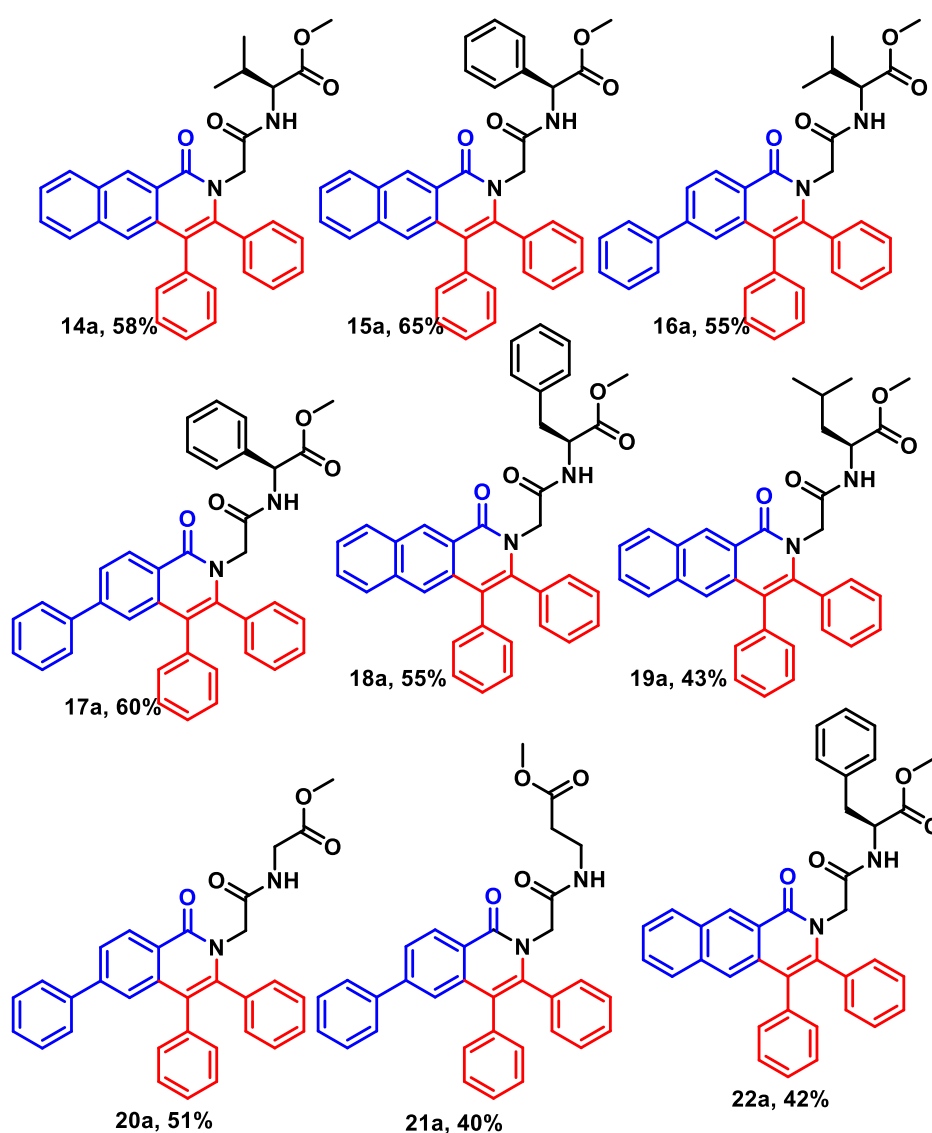


5.2.3 Substrate scopes various peptides with diphenyl acetylene

After demonstrating the success of this Ru(II)-catalysed C–H activation/annulation process in the site selective modification of α -amino ester and acid, we were encouraged to further explore the derivatization of oligopeptides (**Scheme 5.3**). A variety of oligopeptides bearing functionalized amino acids were examined. *Di*-peptides gly-val, gly-phe, gly-gly, gly- β -ala

were well tolerated with both 2-napthoic acid and 4-biphenyl carboxylic acid affording the peptide-isoquinolone conjugates **14a-22a** in 40–65% yields.

Scheme 5.3 isoquinolone derivative using peptides and diphenyl acetylene



5.2.4 The proposed reaction mechanism

Thus, based on the above results, preliminary mechanistic studies and previous reports a plausible mechanism is presented (**Figure 5.2**).³¹ First, $[\text{RuCl}_2(\text{p-cymene})]_2$ undergoes ligand

exchange with $\text{Cu}(\text{OAc})_2$ to give the active catalytic species, which coordinates to the nitrogen atom of the *N*-benzoyl glycine ester **1** moiety via NH deprotonation. This is followed by C-H activation through elimination of AcOH , forming a five membered ruthenacycle. Further coordination of alkyne **2**, followed by insertion and reductive elimination afforded the final product **3**. The active catalyst species is then regenerated by $\text{Cu}(\text{OAc})_2$ and air for the next catalytic cycle.

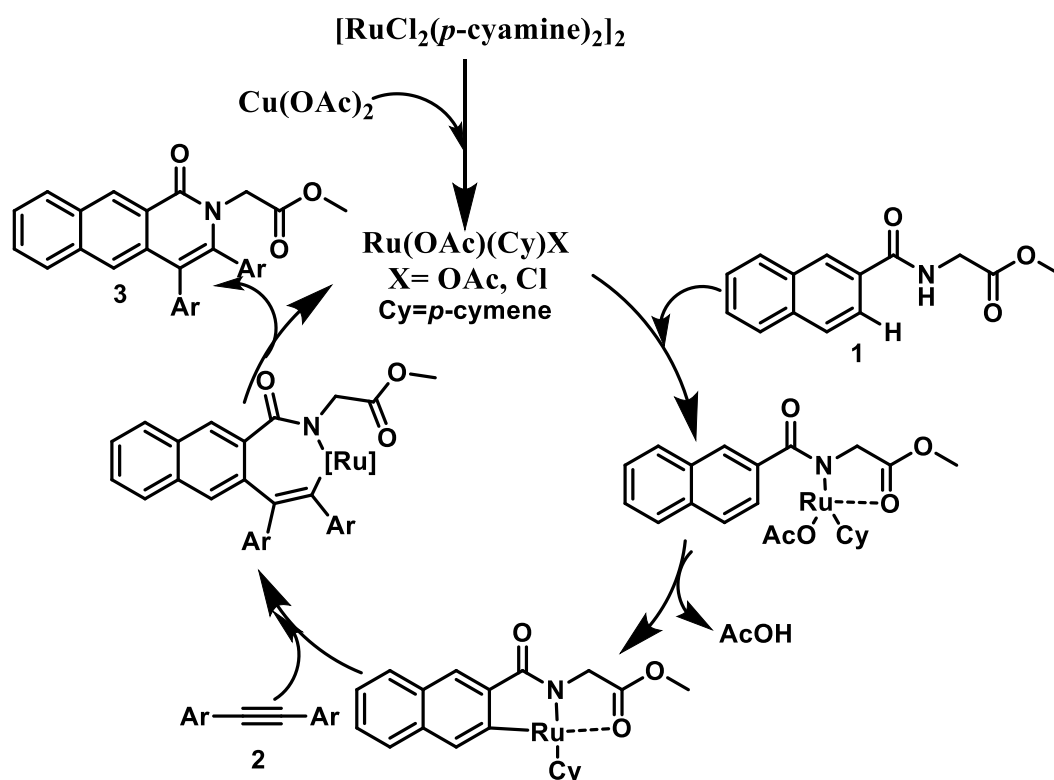


Figure 5.2. Proposed mechanistic pathway.

5.3 Conclusion

We developed a flexible and effective method for chemo selective annulation of *N*-Naphoyl amino acid/peptides with 1,2-diphenylethyne that offers fair to outstanding regioselectivity in a time-efficient manner in ambient temperature. We propose that the NH-amido and carbonyl ester/peptide groups both play a significant role in the catalytic reaction based on the experimental findings and spectroscopic investigations. This technique was additionally

expanded to include the synthesis of isoquinoline with 1,4-diphenylbuta-1,3-diyne. For further research, this class of isoquinolone compounds with an amino acid ester side chain represents potential bioactive molecule. The developed methodology is easy to use, inexpensive, avoids tedious workup procedures, and functions effectively at ambient temperature.

5.4 Experimental Section

5.4.1 Materials and instrumentation

All the required materials were obtained from commercial suppliers and used without purification. The dry DMF and ACN were freshly prepared by distilling them over calcium hydride. The reactions were monitored using thin-layer chromatography, and visualized using UV light and ninhydrin. Column chromatography was performed through 100–200 mesh silica. Mass spectra were obtained using a Bruker micrO TOF-Q II spectrometer. The ^{13}C - and ^1H -NMR spectra were recorded on a Bruker AV-400 NMR spectrometer ^1H (400 MHz), ^{13}C (100.6 MHz). ^1H and ^{13}C -NMR chemical shifts were recorded in ppm downfield from the tetramethyl silane, and the splitting patterns are abbreviated as s, singlet; d, doublet; dd, doublet of doublets; t, triplet; q, quartet; dq, doublet of a quartet; m, multiplet.

5.4.2 General procedure for amide synthesis

Benzoic acid was dissolved in DMF and then the triethylamine (TEA, 3.0 eq.), EDC·HCl (1.3 eq.) and HOAt (1.3 eq.) were added, followed by the resulting amino acid methyl ester (1.2 eq.). Next, this mixture was heated to 60 °C for 8–12 h, and the reaction was monitored by TLC. The crude reaction mixture was concentrated under reduced pressure before water was added. The aqueous layer was extracted with EtOAc. The organic layer was combined, dried over anhydrous Na_2SO_4 , and concentrated under reduced pressure. The residue was purified by column chromatography with an EtOAc/hexane solvent system to yield the corresponding substrates.

5.4.2 General procedure for Ru-catalysed reactions

Typically, the amide substrates were placed in a 25 ml round bottom flask under the indicated reaction conditions. The mixture was stirred at rt for 2–4 h and then diluted with EtOAc. The resulting solution was filtered through a Celite pad, concentrated under reduced pressure and the product was further purified by column chromatography with an EtOAc/hexane solvent system and was typically obtained as a white solid.

5.4.3 Chemical shift values of NMR

methyl (2-naphthoyl) glycinate (3). ¹H NMR (400 MHz, CDCl₃) δ 8.25 (s, 1H), 7.79 (m, 4H), 7.51 – 7.39 (m, 2H), 6.89 (s, 1H), 4.22 (d, *J* = 4.0 Hz, 2H), 3.72 (s, 3H). ¹³C NMR (101 MHz, CDCl₃) δ 170.66 (s), 167.58 (s), 134.89 (s), 132.57 (s), 130.86 (s), 129.01 (s), 128.52 (s), 127.81 (s), 127.75 (s), 126.80 (s), 123.55 (s), 52.51 (s), 41.85 (s). White solid (85% yield). ESI-HRMS *m/z* [M+H]⁺ calcd. for C₁₄H₁₃NO₃ 347.1243 found 347.1243.

*methyl 2-(1-oxo-3,4-diphenylbenzo[*g*]isoquinolin-2(1*H*)-yl) acetate (3a).* ¹H NMR (400 MHz, CDCl₃) δ 9.14 (s, 1H), 8.09 – 8.04 (m, 1H), 7.76 – 7.71 (m, 1H), 7.52 – 7.47 (m, 1H), 7.27 – 7.13 (m, 11H), 4.58 (s, 2H), 3.70 (s, 3H). ¹³C NMR (101 MHz, CDCl₃) δ 169.31 (s), 163.15 (s), 139.27 (s), 136.63 (s), 135.43 (s), 134.48 (s), 133.78 (s), 131.68 (s), 131.59 (s), 130.24 (s), 129.43 (s), 129.36 (s), 128.57 (s), 128.30 (s), 128.07 (t, *J* = 3.5 Hz), 126.97 (s), 126.18 (s), 124.46 (s), 123.31 (s), 119.29 (s), 52.36 (s), 47.69 (s). Pale yellow solid (70% yield). ESI-HRMS *m/z* [M+H]⁺ calcd. for C₁₈H₂₁NO₃ 420.1600 found 420.1571.

*methyl 2-(1-oxo-4-phenyl-3-(phenylethynyl)benzo[*g*]isoquinolin-2(1*H*)-yl)acetate (3b).* ¹H NMR (400 MHz, CDCl₃) δ 9.11 (s, 1H), 8.10 – 8.04 (m, 1H), 7.82 – 7.77 (m, 1H), 7.75 (s, 1H), 7.62 – 7.46 (m, 7H), 7.33 – 7.22 (m, 3H), 7.10 (d, *J* = 8.0 Hz, 2H), 5.26 (s, 2H), 3.80 (s, 3H).

^{13}C NMR (101 MHz, CDCl_3) δ 169.17 (s), 162.31 (s), 136.59 – 136.30 (m), 135.31 (s), 132.78 (s), 132.08 (s), 131.29 (s), 131.23 (s), 129.84 (s), 129.40 (s), 129.16 (s), 128.45 (s), 128.42 (s), 128.24 (s), 128.09 (s), 126.69 (s), 124.91 (s), 123.60 (s), 122.84 (s), 121.63 (s), 99.67 (s), 52.57 (s), 47.45 (s). Pale yellow solid (48% yield).ESI-HRMS m/z $[\text{M}+\text{H}]^+$ calcd. for $\text{C}_{30}\text{H}_{21}\text{NO}_3$ 444.1521 found 444.1530.

3,4-diphenyl-1H-benzo[g]isochromen-1-one (3c). ^1H NMR (400 MHz, CDCl_3) δ 9.03 (s), 8.05 (d, $J = 7.9$ Hz), 7.76 (d, $J = 8.1$ Hz), 7.61 – 7.57 (m, $J = 4.4, 2.3$ Hz), 7.56 (d, $J = 1.9$ Hz), 7.49 – 7.44 (m), 7.38 – 7.33 (m), 7.24 – 7.18 (m). ^{13}C NMR (101 MHz, CDCl_3) δ 162.67 (s), 149.44 (s), 136.42 (s), 134.79 (s), 134.01 (s), 133.18 (s), 132.18 (s), 131.93 (s), 131.42 (s), 129.53 (s), 129.33 (s), 129.20 (s), 128.88 (s), 128.30 (s), 128.23 (s), 127.91 (s), 127.00 (s), 124.53 (s), 118.94 (s), 116.97 (s). Pale yellow solid (78% yield).ESI-HRMS m/z $[\text{M}+\text{H}]^+$ calcd. for $\text{C}_{25}\text{H}_{16}\text{NO}_2$ 349.1229 found 349.1244.

methyl ([1,1'-biphenyl]-4-carbonyl) glycinate (**4**). ^1H NMR (400 MHz, CDCl_3) δ 7.89 (d, $J = 8.0$ Hz, 2H), 7.66 (d, $J = 8.0$ Hz, 2H), 7.61 (d, $J = 8.0$ Hz, 2H), 7.46 (t, $J = 8.0$ Hz, 2H), 7.40 (t, $J = 8.0$ Hz, 1H), 6.80 (s, 1H), 4.27 (d, $J = 4.0$ Hz, 2H), 3.81 (s, 3H). ^{13}C NMR (101 MHz, CDCl_3) δ 170.61 (s), 167.19 (s), 144.65(s), 139.95 (s), 132.31 (s), 128.94 (s), 128.06 (s), 127.64 (s), 127.29 (s), 127.23 (s), 52.52 (s), 41.78 (s). White solid (78% yield).ESI-HRMS m/z $[\text{M}+\text{H}]^+$ calcd. for $\text{C}_{16}\text{H}_{15}\text{NO}_3$ 270.1130 found 270.1161.

methyl 2-(1-oxo-3,4,6-triphenylisoquinolin-2(1H)-yl) acetate (**4a**). ^1H NMR (400 MHz, CDCl_3) δ 8.60 (d, $J = 8.0$ Hz, 1H), 7.74 (d, $J = 8.0$ Hz, 1H), 7.49 (d, $J = 8.0$ Hz, 2H), 7.37 (m, 4H), 7.26 – 7.11 (m, 10H), 4.58 (s, 2H), 3.71 (s, 3H). ^{13}C NMR (101 MHz, CDCl_3) δ 169.19 (s), 162.37 (s), 145.33 (s), 140.99 (s), 140.34 (s), 137.94 (s), 136.16 (s), 134.33 (s), 131.49 (s),

130.08 (s), 128.89 (s), 128.68 (s), 128.36 (s), 128.07 (s), 127.51 (s), 127.03 (s), 126.16 (s), 123.84 (s), 123.67 (s), 119.48 (s), 52.43 (s), 47.87 (s). Pale yellow solid (65% yield).ESI-HRMS m/z $[M+H]^+$ calcd. for $C_{30}H_{23}NO_3$ 446.1756 found 446.1770.

methyl 2-(1-oxo-4,6-diphenyl-3-(phenylethynyl)isoquinolin-2(1H)-yl)acetate (**4b**). 1H NMR (400 MHz, $CDCl_3$) δ 8.58 (d, $J = 8$ Hz, 1H), 7.77 – 7.73 (m, 1H), 7.56 – 7.47 (m, 10H), 7.44 – 7.37 (m, 2H), 7.32 – 7.23 (m, 2H), 7.11 (d, $J = 4$ Hz, 1H), 7.09 (d, $J = 4$ Hz, 1H), 5.27 (s, 2H), 3.80 (s, 3H). ^{13}C NMR (101 MHz, $CDCl_3$) δ 169.00 (s), 161.63 (s), 145.49 (s), 140.08 (s), 137.00 (s), 136.01 (s), 131.31 (s), 131.21 (s), 131.03 (s), 129.53 (s), 129.32 (s), 129.01 (s), 128.94 (s), 128.45 (s), 128.23 (s), 128.14 (s), 127.50 (s), 126.97 (s), 125.67 (s), 124.42 (s), 123.91 (s), 121.44 (s), 52.63 (s), 47.63 (s). Pale yellow solid (45% yield).ESI-HRMS m/z $[M+H]^+$ calcd. for $C_{32}H_{23}NO_3$ 470.1756 found 470.1800.

3,4,6-triphenyl-1H-isochromen-1-one (**4c**). 1H NMR (400 MHz, $CDCl_3$) δ 8.47 (d, $J = 8$ Hz, 1H), 7.75 (dd, $J = 8$ Hz 1H), 7.52 – 7.48 (m, 2H), 7.46 – 7.38 (m, 7H), 7.36 – 7.33 (m, 2H), 7.32 – 7.29 (m, 2H), 7.25 – 7.18 (m, 3H). ^{13}C NMR (101 MHz, $CDCl_3$) δ 162.32 (s), 151.42 (s), 147.57 (s), 139.78 (s), 139.38 (s), 134.31 (s), 133.02 (s), 131.33 (s), 130.27 (s), 129.34 (s), 129.21 (s), 129.09 (s), 128.65 (s), 128.29 (s), 127.95 (s), 127.52 (s), 127.27 (s), 123.69 (s), 119.24 (s), 117.10 (s). Pale yellow solid (55% yield).ESI-HRMS m/z $[M+H]^+$ calcd. for $C_{27}H_{18}O_2$ 375.1385 found 375.1361.

methyl (1-naphthoyl)glycinate (**5**). 1H NMR (400 MHz, $CDCl_3$) δ 8.36 (d, $J = 8$ Hz, 1H), 7.93 (d, $J = 8$ Hz, 1H), 7.87 (d, $J = 8$ Hz, 1H), 7.67 (d, $J = 8$ Hz, 1H), 7.59 – 7.50 (m, 2H), 7.48 – 7.42 (m, 1H), 6.57 (s, 1H), 4.32 (d, $J = 8$ Hz, 2H), 3.81 (s, 3H). ^{13}C NMR (101 MHz, $CDCl_3$) δ 170.42 (s), 169.67 (s), 133.68 (s), 133.54 (s), 131.01 (s), 130.13 (s), 128.33 (s), 127.28 (s), 126.51 (s), 125.38 (s), 125.35 (s), 124.70 (s), 52.53 (s), 41.68 (s). White solid (76% yield).ESI-HRMS m/z $[M+H]^+$ calcd. for $C_{14}H_{13}NO_3$ 244.0974 found 244.0938.

methyl 2-(1-oxo-3,4-diphenylbenzo[h]isoquinolin-2(1H)-yl)acetate (5a). ^1H NMR (400 MHz, CDCl_3) δ 10.29 (d, $J = 8.7$ Hz, 1H), 7.92 (dd, $J = 12.3, 8.5$ Hz, 1H), 7.81 – 7.74 (m, 1H), 7.67 – 7.61 (m, 1H), 7.30 – 7.19 (m, 3H), 7.17 – 7.13 (m, 1H), 4.70 (s, 2H), 3.77 (s, 3H). ^{13}C NMR (101 MHz, CDCl_3) δ 169.30 (s), 162.59 (s), 142.43 (s), 138.95 (s), 136.88 (s), 134.51 (s), 133.85 (s), 132.20 (s), 131.87 (s), 131.74 (s), 129.87 (s), 128.70 (s), 128.56 (s), 128.36 (s), 128.19 (s), 128.09 (s), 127.74 (s), 127.01 (s), 126.53 (s), 123.52 (s), 119.64 (s), 118.36 (s), 52.47 (s), 48.69 (s). Pale yellow solid (60% yield). ESI-HRMS m/z $[\text{M}+\text{H}]^+$ calcd. for $\text{C}_{30}\text{H}_{21}\text{NO}_3$ 420.1600 found 420.1607.

methyl 2-(1-oxo-4-phenyl-3-(phenylethynyl)benzo[h]isoquinolin-2(1H)-yl)acetate (5b). ^1H NMR (400 MHz, CDCl_3) δ 10.27 (d, $J = 8.8$ Hz, 1H), 7.93 – 7.84 (m, 2H), 7.79 – 7.72 (m, 1H), 7.65 – 7.58 (m, 1H), 7.56 – 7.48 (m, 1H), 7.27 – 7.18 (m, 10H), 7.15 – 7.11 (m, 2H), 4.67 (s, 2H), 3.75 (s, 3H). ^{13}C NMR (101 MHz, CDCl_3) δ 169.29 (s), 162.58 (s), 142.44 (s), 138.94 (s), 136.88 (s), 134.52 (s), 133.84 (s), 132.21 (s), 131.88 (s), 131.74 (s), 131.42 (s), 129.87 (s), 128.69 (s), 128.55 (s), 128.36 (s), 128.19 (s), 128.09 (s), 127.75 (s), 127.01 (s), 126.52 (s), 123.52 (s), 119.63 (s), 118.36 (s), 52.45 (s), 48.68 (s). Pale yellow solid (43% yield). ESI-HRMS m/z $[\text{M}+\text{H}]^+$ calcd. for $\text{C}_{30}\text{H}_{21}\text{NO}_3$ 444.1600 found 444.1599.

3,4-diphenyl-1H-benzo[h]isochromen-1-one (5c). ^1H NMR (400 MHz, CDCl_3) δ 9.85 (d, $J = 8$ Hz, 1H), 7.96 (d, $J = 8$ Hz, 1H), 7.84 (d, $J = 8.0$ Hz, 1H), 7.79 – 7.73 (m, 1H), 7.64 – 7.56 (m, 1H), 7.47 – 7.41 (m, 3H), 7.41 – 7.35 (m, 2H), 7.31 – 7.25 (m, 2H), 7.25 – 7.17 (m, 5H). ^{13}C NMR (101 MHz, CDCl_3) δ 161.51 (s), 152.59 (s), 141.13 (s), 135.99 (s), 134.86 (s), 132.87 (s), 132.72 (s), 131.60 (s), 129.57 (s), 129.33 (s), 129.30 (s), 129.21 (s), 128.60 (s), 128.33 (s), 128.02 (s), 127.15 (s), 127.12 (s), 122.77 (d, $J = 2.2$ Hz), 117.52 (s), 114.02 (s).

Pale yellow solid (62% yield).ESI-HRMS m/z $[M+H]^+$ calcd. for $C_{25}H_{16}O_2$ 349.1229 found 349.1206.

methyl (2-naphthoyl)valinate (6). 1H NMR (400 MHz, $CDCl_3$) δ 8.32 (s, 1H), 7.95 – 7.79 (m, 4H), 7.59 – 7.45 (m, 2H), 6.89 (d, $J = 8$ Hz, 1H), 4.85 (dd, $J = 8$ Hz, 1H), 3.78 (s, 3H), 2.40 – 2.21 (m, 1H), 1.03 (t, $J = 8$ Hz, 6H). ^{13}C NMR (101 MHz, $CDCl_3$) δ 172.79 (s), 167.40 (s), 134.86 (s), 132.59 (s), 131.34 (s), 128.97 (s), 128.50 (s), 127.75 (s), 127.60 (s), 126.79 (s), 123.64 (s), 57.61 (s), 52.27 (s), 31.68 (s), 19.06 (s), 18.10 (s). White solid (90% yield).ESI-HRMS m/z $[M+H]^+$ calcd. for $C_{18}H_{21}NO_3$ 420.1600 found 420.1571.

methyl ([1,1'-biphenyl]-4-carbonyl)valinate (7). 1H NMR (400 MHz, $CDCl_3$) δ 7.89 (d, $J = 8.4$ Hz, 2H), 7.67 (d, $J = 8.4$ Hz, 2H), 7.63 – 7.58 (m, 2H), 7.47 (dd, $J = 10.2, 4.7$ Hz, 2H), 7.42 – 7.35 (m, 1H), 6.70 (d, $J = 8$ Hz, 1H), 4.82 (dd, $J = 8$ Hz, 1H), 3.79 (s, 3H), 2.37 – 2.21 (m, 1H), 1.02 (dd, $J = 8$ Hz, 6H). ^{13}C NMR (101 MHz, $CDCl_3$) δ 172.73 (s), 166.99 (s), 144.60 (s), 140.01 (s), 132.80 (s), 128.94 (s), 128.05 (s), 127.61 (s), 127.30 (s), 127.24 (s), 57.46 (s), 52.28 (s), 31.70 (s), 19.03 (s), 18.02 (s). White solid (87% yield).ESI-HRMS m/z $[M+H]^+$ calcd. for $C_{19}H_{21}NO_3$ 312.1600 found 312.1603.

methyl (2-naphthoyl)phenylalaninate (8). 1H NMR (400 MHz, $CDCl_3$) δ 8.23 (s, 1H), 7.90 – 7.81 (m, 3H), 7.77 (d, $J = 8$ Hz, 1H), 7.53 (m, 2H), 7.33 – 7.22 (m, 3H), 7.20 – 7.12 (m, 2H), 6.82 (d, $J = 8$ Hz, 1H), 5.23 – 5.05 (m, 1H), 3.77 (s, 3H), 3.39 – 3.18 (m, 2H). ^{13}C NMR (101 MHz, $CDCl_3$) δ 172.21 (s), 166.96 (s), 135.95 (s), 134.90 (s), 132.58 (s), 131.08 (s), 129.41 (s), 129.02 (s), 128.67 (s), 128.54 (s), 127.81 (s), 127.76 (s), 127.70 (s), 127.25 (s), 126.81 (s), 123.53 (s), 53.70 (s), 52.49 (s), 37.96 (s). White solid (83% yield).ESI-HRMS m/z $[M+H]^+$ calcd. for $C_{21}H_{19}NO_3$ 334.1443 found 334.1447.

methyl ([1,1'-biphenyl]-4-carbonyl)phenylalaninate (9). ^1H NMR (400 MHz, CDCl_3) δ 7.80 (d, $J = 8.3$ Hz, 1H), 7.66 – 7.56 (m, 2H), 7.49 – 7.41 (m, 1H), 7.39 (d, $J = 7.3$ Hz, 1H), 7.33 – 7.22 (m, 2H), 7.15 (d, $J = 6.8$ Hz, 1H), 6.63 (s, 1H), 6.63 (s, 1H), 5.12 (m, 1H), 3.77 (s, 3H), 3.28 (m, 2H). ^{13}C NMR (101 MHz, CDCl_3) δ 172.11 (s), 166.54 (s), 144.64 (s), 139.97 (s), 135.88 (s), 132.52 (s), 129.38 (s), 128.94 (s), 128.67 (s), 128.06 (s), 127.57 (s), 127.31 (s), 127.23 (s), 53.56 (s), 52.47 (s), 37.95 (s). White solid (80% yield). ESI-HRMS m/z $[\text{M}+\text{H}]^+$ calcd. for $\text{C}_{23}\text{H}_{21}\text{NO}_3$ 360.1600 found 360.1613.

N-ethyl-2-naphthamide (10). ^1H NMR (400 MHz, CDCl_3) δ 8.28 (s, 1H), 7.89 – 7.71 (m, 4H), 7.47 (m, 2H), 6.90 (s, 1H), 3.44 (dd, $J = 12, 8$ Hz, 2H), 1.64 – 1.50 (m, 2H), 1.37 – 1.12 (m, 10H), 0.86 (t, $J = 8$ Hz, 4H). ^{13}C NMR (101 MHz, CDCl_3) δ 167.78 (s), 134.62 (s), 132.62 (s), 132.08 (s), 128.89 (s), 128.28 (s), 127.69 (s), 127.47 (s), 127.39 (s), 126.60 (s), 123.78 (s), 40.35 (s), 31.85 (s), 29.75 (s), 29.38 (s), 29.29 (s), 27.11 (s), 22.70 (s), 14.16 (s). White solid (90% yield). ESI-HRMS m/z $[\text{M}+\text{H}]^+$ calcd. for $\text{C}_{19}\text{H}_{25}\text{NO}$ 284.2014 found 284.2045.

N-ethyl-[1,1'-biphenyl]-4-carboxamide (11). ^1H NMR (400 MHz, CDCl_3) δ 7.84 (d, $J = 8.1$ Hz, 1H), 7.67 – 7.57 (m, 1H), 7.45 (t, $J = 7.5$ Hz, 1H), 7.39 (d, $J = 7.4$ Hz, 1H), 6.29 (s, 1H), 3.46 (dd, $J = 12, 8$ Hz, 2H), 1.68 – 1.57 (m, 2H), 1.42 – 1.20 (m, 10H), 0.88 (t, $J = 8$ Hz, 3H). ^{13}C NMR (101 MHz, CDCl_3) δ 167.25 (s), 144.10 (s), 140.06 (s), 133.52 (s), 128.93 (s), 127.97 (s), 127.41 (s), 127.21 (s), 40.19 (s), 31.83 (s), 29.73 (s), 29.34 (s), 29.26 (s), 27.06 (s), 22.68 (s), 14.13 (s). White solid (88% yield). ESI-HRMS m/z $[\text{M}+\text{H}]^+$ calcd. for $\text{C}_{21}\text{H}_{27}\text{NO}$ 310.2171 found 310.2250.

N-ethyl-1-naphthamide (12). ^1H NMR (400 MHz, CDCl_3) δ 8.26 (d, $J = 8.6$ Hz, 1H), 7.90 – 7.79 (m, 1H), 7.56 – 7.46 (m, 1H), 7.40 (dd, $J = 8.2, 7.1$ Hz, 1H), 6.12 (s, 1H), 3.52 – 3.42 (m,

2H), 1.66 – 1.55 (m, 2H), 1.42 – 1.21 (m, 10H), 0.89 (t, $J = 8$ Hz, 3H). ^{13}C NMR (101 MHz, CDCl_3) δ 169.68 (s), 134.95 (s), 133.72 (s), 130.44 (s), 130.19 (s), 128.34 (s), 127.09 (s), 126.44 (s), 125.50 (s), 124.83 (s), 124.79 (s), 40.14 (s), 31.89 (s), 29.75 (s), 29.36 (s), 29.32 (s), 27.08 (s), 22.74 (s), 14.20 (s). White solid (85% yield). ESI-HRMS m/z $[\text{M}+\text{H}]^+$ calcd. for $\text{C}_{19}\text{H}_{25}\text{NO}$ 284.2014 found 284.2045.

N-(*tert*-butyl)-2-naphthamide (**13**). ^1H NMR (400 MHz, CDCl_3) δ 8.22 (s, 1H), 7.93 – 7.83 (m, 1H), 7.79 (dd, $J = 8.6, 1.7$ Hz, 1H), 7.58 – 7.50 (m, 1H), 6.12 (s, 1H), 1.52 (s, 1H). ^{13}C NMR (101 MHz, CDCl_3) δ 167.01 (s), 134.55 (s), 133.11 (s), 132.63 (s), 128.85 (s), 128.38 (s), 127.74 (s), 127.47 (s), 126.97 (s), 126.70 (s), 123.60 (s), 51.78 (s), 28.94 (s). White solid (88% yield). ESI-HRMS m/z $[\text{M}+\text{H}]^+$ calcd. for $\text{C}_{15}\text{H}_{17}\text{NO}$ 228.1388 found 228.1419.

methyl (2-naphthoyl)glycyl-L-valinate (**14**). ^1H NMR (400 MHz, CDCl_3) δ 8.37 (s, 1H), 8.07 (s, 1H), 7.89 (d, $J = 4.0$ Hz, 1H), 7.79 (t, $J = 8.0$ Hz, 1H), 7.71 (d, $J = 8.0$ Hz, 1H), 7.55 – 7.41 (m, 1H), 4.60 – 4.54 (m, 1H), 4.43 – 4.28 (m, 2H), 3.70 (s, 3H), 2.32 – 2.08 (m, 1H), 0.95 (dd, $J = 8.0$ Hz, 6H). ^{13}C NMR (101 MHz, CDCl_3) δ 172.39 (s), 170.15 (s), 168.16 (s), 134.76 (s), 132.48 (s), 130.62 (s), 129.02 (s), 128.21 (s), 128.08 (s), 127.66 (s), 127.60 (s), 126.56 (s), 123.72 (s), 57.73 (s), 52.14 (s), 43.86 (s), 30.98 (s), 19.08 (s), 17.92 (s). Yellow solid (66% yield). ESI-HRMS m/z $[\text{M}+\text{H}]^+$ calcd. for $\text{C}_{19}\text{H}_{22}\text{N}_2\text{O}_4$ 343.1658 found 343.1658.

N-(2-methyl-4-oxopentan-3-yl)-2-(1-oxo-3,4-diphenylbenzo[*g*]isoquinolin-2(1H)-yl)acetamide (**14a**). ^1H NMR (400 MHz, CDCl_3) δ 9.16 (s, 1H), 8.12 – 8.05 (m, 1H), 7.78 – 7.71 (m, 1H), 7.51 (dt, $J = 5.4, 3.1$ Hz, 1H), 7.28 – 7.14 (m, 2H), 6.49 (d, $J = 8.6$ Hz, 1H), 4.57 (td, $J = 8.7, 4.9$ Hz, 1H), 4.16 (qd, $J = 16.9, 4.9$ Hz, 1H), 3.72 (s, 1H), 2.23 – 2.11 (m, 1H), 0.99 – 0.90 (m, 1H). ^{13}C NMR (101 MHz, CDCl_3) δ 172.34 (s), 167.77 (s), 163.44 (s), 139.66 (s),

136.67 (s), 135.44 (s), 134.39 (s), 133.75 (s), 131.69(s), 131.60 (s), 130.55 (s), 130.50 (s), 129.43 (s), 129.34 (s), 128.48 (s), 128.17 (s), 128.12 (s), 128.05 (s), 128.01 (s), 126.93 (s), 126.17 (s), 124.48(s), 123.26 (s), 119.54 (s), 57.20 (s), 52.20 (s), 49.62 (s), 31.52 (s), 18.98 (s), 17.73 (s). Pale yellow solid (58% yield).ESI-HRMS m/z $[M+H]^+$ calcd. for $C_{33}H_{30}N_2O_4$ 519.2284 found 519.2203.

methyl (S)-2-(2-(2-naphthamido)acetamido)-2-phenylacetate (15). 1H NMR (400 MHz, $CDCl_3$) δ 8.33 (s, 1H), 7.87 – 7.78 (m, 5H), 7.58 – 7.47 (m, 3H), 7.42 – 7.37 (m, 2H), 7.35 – 7.28 (m, 3H), 5.61 (d, J = 8.0 Hz, 1H), 4.46 – 4.22 (m, 2H), 3.70 (s, 3H). NMR (101 MHz,) δ 171.14 (s), 168.90 (s), 167.93 (s), 136.01 (s), 134.94 (s), 132.62 (s), 130.72 (s), 129.13 (s), 128.78 (s), 128.50 (s), 128.00 (s), 127.87 (s), 127.79 (s), 127.47 (s), 126.81 (s), 123.74 (s), 56.91 (s), 52.99 (s), 43.78 (s). Yellow solid (60% yield).ESI-HRMS m/z $[M+H]^+$ calcd. for $C_{22}H_{20}N_2O_4$ 465.1501 found 465.1418.

N-(2-oxo-1-phenylpropyl)-2-(1-oxo-3,4-diphenylbenzo[g]isoquinolin-2(1H)-yl)acetamide (15a). 1H NMR (400 MHz, $CDCl_3$) δ 9.14 (s, 1H), 8.10 – 8.04 (m, 1H), 7.76 – 7.70 (m, 1H), 7.59 (s, 1H), 7.51 (dd, J = 6.6, 2.7 Hz, 1H), 7.36 – 7.28 (m, 1H), 7.24 – 7.18 (m, 1H), 7.17 – 7.11 (m, 2H), 7.11 – 7.05 (m, 1H), 6.99(d, J = 8.0 Hz, 1H), 5.56 (d, J = 8.0 Hz, 1H), 4.58 (m, 2H), 3.70 (s, 3H). ^{13}C NMR (101 MHz, $CDCl_3$) δ 171.08 (s), 167.29 (s), 163.49 (s), 139.58 (s), 136.66 (s), 136.26 (s), 135.44 (s), 134.39 – 134.22 (m), 133.75 (s), 131.59 (s), 130.46 (s), 129.52 (s), 129.35 (s), 128.89 (s), 128.47 (s), 128.42 (s), 128.16 (s), 128.11 (s), 128.09 (s), 128.04 (s), 127.99 (s), 127.31 (s), 126.91 (s), 126.15 (s), 124.44 (s), 123.26 (s), 119.51 (s), 56.53 (s), 52.85 (s), 49.45 (s). Pale yellow solid (65% yield).ESI-HRMS m/z $[M+H]^+$ calcd. for $C_{36}H_{28}N_2O_4$ 553.2127 found 553.2231.

methyl ([1,1'-biphenyl]-4-carbonyl)glycyl-L-valinate (16). 1H NMR (400 MHz, $CDCl_3$) δ 8.07 – 8.01 (m, 1H), 7.93 (d, J = 8.0 Hz, 2H), 7.73(d, J = 8.0 Hz, 1H), 7.55 (dd, J = 8.0 Hz, 4H),

7.44 – 7.31 (m, 3H), 4.57 (dd, $J = 8.0$ Hz, 1H), 4.31 (d, $J = 4.0$ Hz, 2H), 3.70 (s, 3H), 2.31 – 2.09 (m, 1H), 0.95 (dd, $J = 6.0$ Hz, 6H). ^{13}C NMR (101 MHz, CDCl_3) δ 172.33 (s), 170.04 (s), 167.85 (s), 144.40 (s), 139.92 (s), 132.18 (s), 128.89 (s), 127.99 (s), 127.89 (s), 127.15 (s), 127.08 (s), 57.69 (s), 52.15 (s), 43.83 (s), 31.03 (s), 19.08 (s), 17.91 (s). Yellow solid (62% yield). ESI-HRMS m/z $[\text{M}+\text{H}]^+$ calcd. for $\text{C}_{23}\text{H}_{24}\text{N}_2\text{O}_6$ 369.1814 found 369.1799.

methyl (2-(1-oxo-3,4,6-triphenylisoquinolin-2(1H)-yl)acetyl)-L-valinate (16a). ^1H NMR (400 MHz, CDCl_3) δ 8.61 (d, $J = 8$ Hz, 1H), 7.74 (dd, $J = 8.0$ 1H), 7.49 (d, $J = 8$ Hz, 2 H), 7.42 – 7.31 (m, 4 H), 7.23 – 7.09 (m, 10 H), 6.45 (d, $J = 8$ Hz, 1H), 4.68 - 4.43 (m, 3H), 3.73 (s, 3H), 2.25 – 2.00 (m, 1H), 0.91 (dd, $J = 24, 8$ Hz, 6H). ^{13}C NMR (101 MHz, CDCl_3) δ 172.24 (s), 167.60 (s), 162.65 (s), 145.34 (s), 141.41 (s), 140.33 (s), 137.92 (s), 136.21 (s), 134.21 (s), 131.50 (s), 130.43(s), 130.37 (s), 128.87 (s), 128.69 (s), 128.58 (s), 128.20 (s), 128.05 (s), 127.49 (s), 126.98 (s), 126.13 (s), 123.82 (s), 123.64 (s), 119.72 (s), 57.25 (s), 52.19 (s), 49.84 (s), 31.51 (s), 20.26 – 19.05 (m), 17.55 – 16.62 (m). Pale yellow solid (55% yield). ESI-HRMS m/z $[\text{M}+\text{H}]^+$ calcd. for $\text{C}_{35}\text{H}_{32}\text{N}_2\text{O}_4$ 545.2440 found 545.2468.

methyl(S)-2-(2-([1,1'-biphenyl]-4-carboxamido)acetamido)-2-phenylacetate (17). ^1H NMR (400 MHz, CDCl_3) δ 7.88 (d, $J = 8.0$ Hz, 2H), 7.70 – 7.58 (m, 5H), 7.52 – 7.45 (m, 2H), 7.45 – 7.33 (m, 6H), 7.31 (s, 1H), 5.62 (d, $J = 8.0$ Hz, 1H), 4.39 – 4.14 (m, 2H), 3.74 (s, 3H). ^{13}C NMR (101 MHz,) δ 171.12 (s), 168.75 (s), 167.55 (s), 144.66 (s), 140.01 (s), 135.98 (s), 132.16 (s), 129.16 (s), 129.01 (s), 128.81 (s), 128.13 (s), 127.81 (s), 127.47 (s), 127.30 (s), 56.87 (s), 53.02 (s), 43.67 (s). Yellow solid (55% yield). ESI-HRMS m/z $[\text{M}+\text{H}]^+$ calcd. for $\text{C}_{24}\text{H}_{22}\text{N}_2\text{O}_4$ 403.1658 found 403.1653.

methyl(S)-2-(2-(1-oxo-3,4,6-triphenylisoquinolin-2(1H)-yl)acetamido)-2-phenylacetate (17a)
 ^1H NMR (400 MHz, CDCl_3) δ 8.60 (d, $J = 8.3$ Hz, 1H), 7.74 (dd, $J = 8.4, 1.6$ Hz, 1H), 7.51 – 7.46 (m, 1H), 7.42 – 7.31 (m, 2 H), 7.21 – 7.06 (m, 10 H), 6.98 (d, $J = 8$ Hz, 1H), 5.56 (d, $J =$

8 Hz, 1H), 4.69 (d, $J = 12$ Hz, 1H), 4.47 (d, $J = 12$ Hz, 1H), 3.72 (s, 3H). ^{13}C NMR (101MHz, CDCl_3) δ 171.05 (s), 167.11 (s), 162.69 (s), 145.34 (s), 141.30 (s), 140.34 (s), 137.91 (s), 136.23 (s), 134.12 (s), 131.48 (s), 130.32 (s), 128.91 (s), 128.86 (s), 128.75 (s), 128.50 (s), 128.19 (s), 128.06 (s), 127.49 (s), 127.31 (s), 126.96 (s), 126.12 (s), 123.80 (s), 123.60 – 123.47 (m), 119.70 (s), 56.56 (s), 52.88 (s), 49.64 (s). Pale yellow solid (60% yield). ESI-HRMS m/z $[\text{M}+\text{H}]^+$ calcd. for $\text{C}_{38}\text{H}_{30}\text{N}_2\text{O}_4$ 579.2284 found 579.2360.

methyl (2-naphthoyl)glycyl-L-phenylalaninate (18). ^1H NMR (400 MHz, CDCl_3) δ 8.32 (s, 1H), 8.10 (t, $J = 5.1$ Hz, 1H), 7.85 (d, $J = 8.5$ Hz, 1H), 7.73 (t, $J = 7.9$ Hz, 2H), 7.49 – 7.36 (m, $J = 15.0, 7.2$ Hz, 1H), 7.18 – 7.04 (m, 2H), 4.87 (dd, $J = 13.5, 7.4$ Hz, 1H), 4.26 – 4.07 (m, $J = 16.6, 5.3$ Hz, 1H), 3.60 (s, 1H), 3.17 – 2.94 (m, $J = 21.2, 13.8, 6.5$ Hz, 1H). ^{13}C NMR (101 MHz, CDCl_3) δ 172.06 (s), 169.85 (s), 168.07 (s), 136.07 (s), 134.83 (s), 132.54 (s), 130.64 (s), 129.24 (s), 129.08 (s), 128.56 (s), 128.30 (s), 128.12 (s), 127.75 (s), 127.67 (s), 127.04 (s), 126.66 (s), 123.77 (s), 53.74 (s), 52.34 (s), 43.75 (s), 37.84 (s). Yellow solid (65% yield). ESI-HRMS m/z $[\text{M}+\text{H}]^+$ calcd. for $\text{C}_{23}\text{H}_{22}\text{N}_2\text{O}_4$ 391.658 found 391.1679.

methyl(2-(1-oxo-3,4-diphenylbenzo[g]isoquinolin-2(1H)-yl)acetyl)-L-phenylalaninate (18a). ^1H NMR (400 MHz, CDCl_3) δ 9.17 (s), 8.09 (dd, $J = 5.5, 4.2$ Hz), 7.77 – 7.72 (m), 7.61 (s), 7.54 – 7.48 (m), 7.24 – 7.16 (m), 7.15 – 7.11 (m, $J = 7.1, 3.4, 1.8$ Hz), 7.10 – 7.05 (m), 7.03 – 6.99 (m), 6.52 (d, $J = 5.2$ Hz), 4.87 – 4.81 (m, 1H), 4.49 (t, $J = 12$ Hz, 2H), 3.69 (s, 1H), 3.14 – 3.02 (m, $J = 12$ Hz, 2H). ^{13}C NMR (101 MHz, CDCl_3) δ 171.74 (s), 167.60 (s), 163.46 (s), 139.66 (s), 136.70 (s), 135.77 (s), 135.53 (s), 134.33 (s), 133.82 (s), 131.78 (s), 131.68 (s), 131.60 (s), 130.60 (s), 130.56 (s), 129.56 (s), 129.40 (s), 128.57 (s), 128.28 (s), 128.23 (s), 128.15 (s), 128.11 (s), 127.07 (s), 127.03 (s), 126.31 (s), 124.56 (s), 123.33 (d, $J = 2.4$ Hz), 119.63 (s), 53.23 (s), 52.42 (s), 49.63 (s), 37.86 (s). Pale yellow solid (55% yield). ESI-HRMS m/z $[\text{M}+\text{H}]^+$ calcd. for $\text{C}_{37}\text{H}_{30}\text{N}_2\text{O}_4$ 567.2284 found 567.2334.

methyl (2-naphthoyl)glycyl-L-leucinate (19). ^1H NMR (400 MHz, CDCl_3) δ 8.37 (s, 1H), 7.95 (t, $J = 5.0$ Hz, 1H), 7.89 (d, $J = 8.5$ Hz, 1H), 7.81 (t, $J = 7.5$ Hz, 1H), 7.65 (d, $J = 8.4$ Hz, 1H), 7.56 – 7.42 (m, 1H), 4.68 – 4.50 (m, 1H), 4.34 (d, $J = 4$ Hz, 2H), 3.69 (s, 3H), 1.97 – 1.82 (m, 1H), 1.57 – 1.30 (m, 1H), 1.31 – 1.12 (m, 1H), 0.99 – 0.80 (m, 6H). ^{13}C NMR (101 MHz, CDCl_3) δ 172.27 (s), 169.63 (s), 168.08 (s), 134.83 (s), 132.54 (s), 130.72 (s), 129.02 (s), 128.33 (s), 127.98 (s), 127.72 (s), 127.66 (s), 126.66 (s), 123.68 (s), 56.91 (s), 52.11 (s), 43.86 (s), 37.61 (s), 25.12 (s), 15.54 (s), 11.50 (s). Yellow solid (65% yield). ESI-HRMS m/z $[\text{M}+\text{H}]^+$ calcd. for $\text{C}_{20}\text{H}_{24}\text{N}_2\text{O}_4$ 357.1814 found 357.1825.

methyl (2-(1-oxo-3,4-diphenylbenzo[g]isoquinolin-2(1H)-yl)acetyl)-L-leucinate (19a). ^1H NMR (400 MHz, CDCl_3) δ 9.15 (s), 8.09 – 8.02 (m), 7.74 – 7.68 (m, $J = 5.0, 4.6$ Hz), 7.59 (s), 7.52 – 7.44 (m, 2H), 7.24 – 7.13 (m, 10 H), 6.51 (d, $J = 8$ Hz, 1H), 4.66 (d, $J = 16$ Hz, 1H), 4.59 (dd, $J = 8, 4$ Hz, 1H), 4.46 (d, $J = 16$ Hz, 1H), 3.69 (s, 3H), 1.90 – 1.81 (m, 1H), 1.39 – 1.32 (m, 1H), 1.18 – 1.09 (m, 1H), 0.86 (t, $J = 8$ Hz, 6H). ^{13}C NMR (101 MHz, CDCl_3) δ 172.30 (s), 167.70 (s), 163.49 (s), 139.77 (s), 136.77 (s), 135.49 (s), 134.48 (s), 133.84 (s), 131.74 (s), 131.67 (s), 130.64 (s), 130.57 (s), 129.52 (s), 129.41 (s), 128.53 (s), 128.23 (s), 128.16 (s), 128.11 (s), 126.99 (s), 126.21 (s), 124.51 (s), 123.36 (s), 119.54 (s), 56.60 (s), 52.18 (s), 49.64 (s), 38.14 (s), 25.18 (s), 15.52 (s), 11.65 (s). Pale yellow solid (43% yield). ESI-HRMS m/z $[\text{M}+\text{H}]^+$ calcd. for $\text{C}_{34}\text{H}_{32}\text{N}_2\text{O}_4$ 532.2362 found 532.2390.

methyl (2-naphthoyl)glycylglycinate (20). ^1H NMR (400 MHz, CDCl_3) δ 8.31 (d, $J = 8.7$ Hz, 1H), 7.90 (d, $J = 8.2$ Hz, 1H), 7.85 (dd, $J = 6.2, 2.9$ Hz, 1H), 7.64 (d, $J = 7.0$ Hz, 1H), 7.55 – 7.47 (m, 1H), 7.41 (t, $J = 7.7$ Hz, 1H), 7.26 (d, $J = 4.9$ Hz, 1H), 7.17 (s, 1H), 4.26 (d, $J = 4.0$ Hz, 2H), 4.01 (d, $J = 4.0$ Hz, 2H), 3.70 (s, 3H). ^{13}C NMR (101 MHz, CDCl_3) δ 170.16 (s), 170.11 (s), 169.34 (s), 133.66 (s), 133.22 (s), 131.07 (s), 130.11 (s), 128.34 (s), 127.25 (s),

126.47 (s), 125.54 (s), 125.32 (s), 124.68 (s), 52.37 (s), 43.49 (s), 41.19 (s). Yellow solid (55% yield). ESI-HRMS m/z $[M+H]^+$ calcd. for $C_{16}H_{16}N_2O_4$ 301.1188 found 301.1184.

methyl (2-(1-oxo-3,4-diphenylbenzo[g]isoquinolin-2(1H)-yl)acetyl)glycinate (20a). 1H NMR (400 MHz, $CDCl_3$) δ 10.25 (d, $J = 8$ Hz, 1H), 7.90 (dd, $J = 12, 8$ Hz, 2H), 7.76 (d, $J = 8$ Hz, 1H), 7.62 (t, $J = 8$ Hz, 1H), 7.22 (m, 9H), 7.15 – 7.10 (m, 2H), 6.64 (s, 1H), 4.66 (s, 2H), 4.09 (d, $J = 8, 2$ Hz), 3.74 (s, 3H). ^{13}C NMR (101 MHz, $CDCl_3$) δ 142.92 (s), 139.02 (s), 136.79 (s), 133.98 (s), 131.72 (s), 130.18 (s), 128.70 (s), 128.55 – 128.49 (m), 128.26 (s), 128.08 (s), 127.65 (s), 127.02 (s), 126.58 (s), 123.55 (s), 52.39 (s), 50.66 (s), 41.30 (s). Pale yellow solid (51% yield). ESI-HRMS m/z $[M+H]^+$ calcd. for $C_{30}H_{24}N_2O_4$ 477.1814 found 477.1826.

methyl 3-(2-(2-naphthamido)acetamido)propanoate (21). 1H NMR (400 MHz, $CDCl_3$) δ 8.32 (d, $J = 8.5$ Hz, 1H), 7.92 (d, $J = 8.2$ Hz, 1H), 7.87 (d, $J = 7.4$ Hz, 1H), 7.66 (d, $J = 7.0$ Hz, 1H), 7.58 – 7.49 (m, 1H), 7.44 (t, $J = 7.6$ Hz, 1H), 7.11 (s, 1H), 7.06 (s, 1H), 4.18 (d, $J = 4.0$ Hz, 2H), 3.66 (s, 3H), 3.54 (q, $J = 4.0$ Hz, 2H), 2.55 (t, $J = 4.0$ Hz, 2H). ^{13}C NMR (101 MHz, $CDCl_3$) δ 172.71 (s), 169.99 (s), 168.85 (s), 133.68 (s), 133.34 (s), 131.03 (s), 130.12 (s), 128.34 (s), 127.22 (s), 126.46 (s), 125.49 (s), 125.32 (s), 124.68 (s), 51.84 (s), 43.58 (s), 35.06 (s), 33.72 (s). Yellow solid (53% yield). ESI-HRMS m/z $[M+H]^+$ calcd. for $C_{17}H_{18}N_2O_4$ 315.1345 found 315.1343.

N-(2-acetamidoethyl)-2-(1-oxo-3,4-diphenylbenzo[g]isoquinolin-2(1H)-yl)acetamide (21a). 1H NMR (400 MHz, $CDCl_3$) δ 10.25 (d, $J = 8$ Hz, 1H), 7.94 – 7.84 (m, 2H), 7.80 – 7.69 (m, 1H), 7.62 (t, $J = 8$ Hz, 1H), 7.25 – 7.18 (m, 9H), 7.15 – 7.10 (m, 2H), 6.50 (s, 1H), 4.59 (s, 2H), 3.62 (s, 3H), 3.54 (d, $J = 8$ Hz, 2H), 2.55 (t, $J = 8$ Hz, 2H). ^{13}C NMR (101 MHz, $CDCl_3$) δ 172.96 (s), 167.97 (s), 162.78 (s), 142.78 (s), 138.95 (s), 136.89 (s), 133.89 (s), 131.73 (s), 130.13 (s), 128.61 (s), 128.51 (s), 128.20 (s), 128.07 (s), 127.70 (s), 127.00 (s), 126.53 (s),

123.56 (s), 119.90 (s), 51.79 (s), 50.61 (s), 35.00 (s), 33.69 (s). Pale yellow solid (40% yield).ESI-HRMS m/z $[M+H]^+$ calcd. for $C_{31}H_{26}N_2O_4$ 491.1971 found 491.1794.

methyl (1-naphthoyl)glycyl-L-phenylalaninate (**22**). 1H NMR (400 MHz, $CDCl_3$) δ 8.33 – 8.28 (m, J = 6.2, 3.5 Hz, 1H), 7.88 (d, J = 8.2 Hz, 1H), 7.86 – 7.82 (m, J = 6.7, 3.4 Hz, 1H), 7.57 (d, J = 7.0 Hz, 1H), 7.52 – 7.47 (m, 1H), 7.42 (d, J = 7.8 Hz, 1H), 7.36 (t, J = 7.6 Hz, 1H), 7.21 (t, J = 7.7 Hz, 1H), 7.12 (d, J = 6.3 Hz, 1H), 4.86 (dd, J = 8 Hz, 1H), 4.27 – 4.09 (m, 2H), 3.65 (s, 3H), 3.20 – 2.90 (m, 2H). ^{13}C NMR (101 MHz, $CDCl_3$) δ 171.90 (s), 170.05 (s), 169.05 (s), 135.94 (s), 133.64 (s), 133.24 (s), 130.99 (s), 130.16 (s), 129.25 (s), 128.59 (s), 128.32 (s), 127.20 (s), 127.09 (s), 126.42 (s), 125.60 (s), 125.46 (s), 124.65 (s), 53.60 (s), 52.36 (s), 43.50 (s), 37.79 (s). Yellow solid (58% yield).ESI-HRMS m/z $[M+H]^+$ calcd. for $C_{23}H_{22}N_2O_4$ 391.1658 found 391.1678.

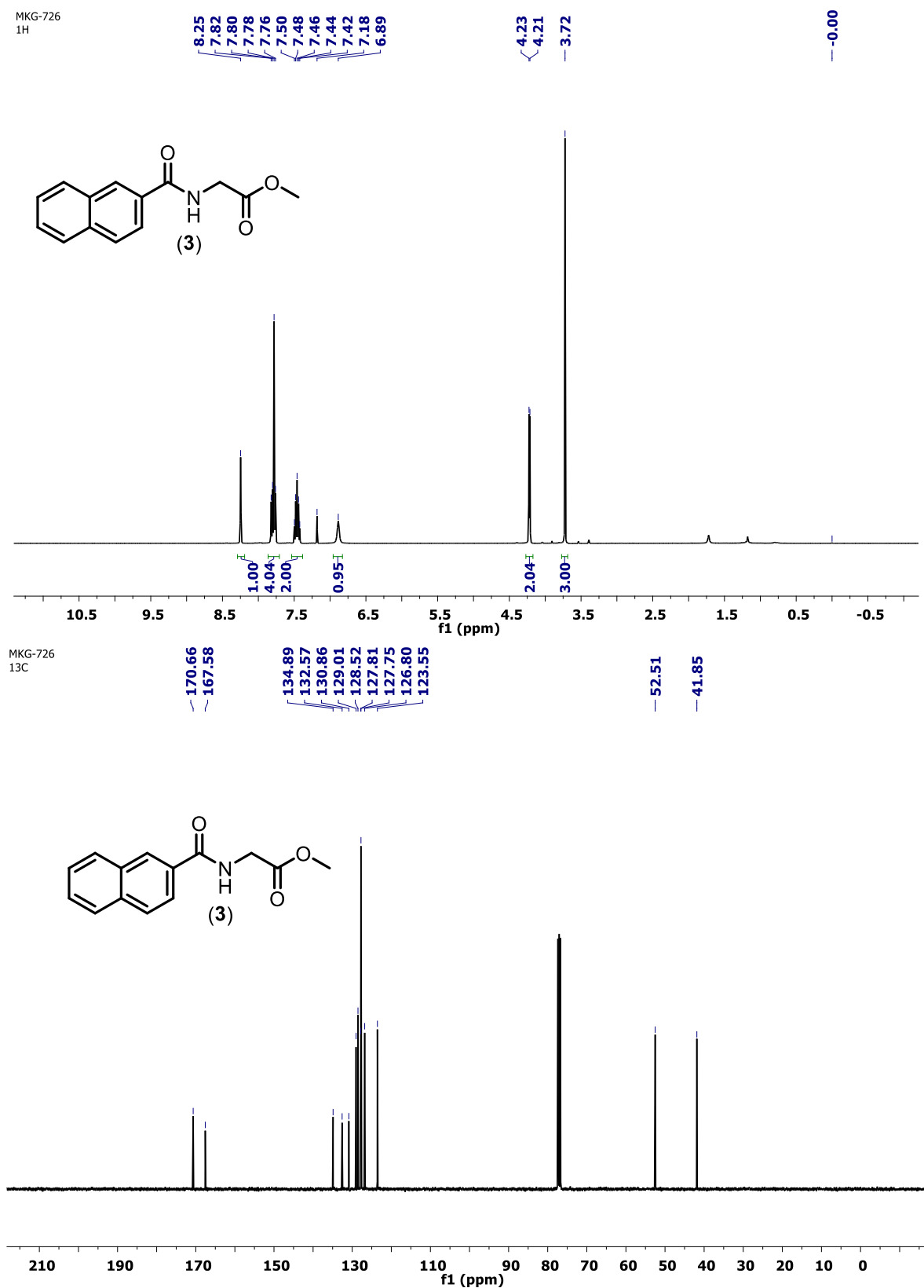
methyl (2-(1-oxo-3,4-diphenylbenzo[h]isoquinolin-2(1H)-yl)acetyl)phenylalaninate (22a).

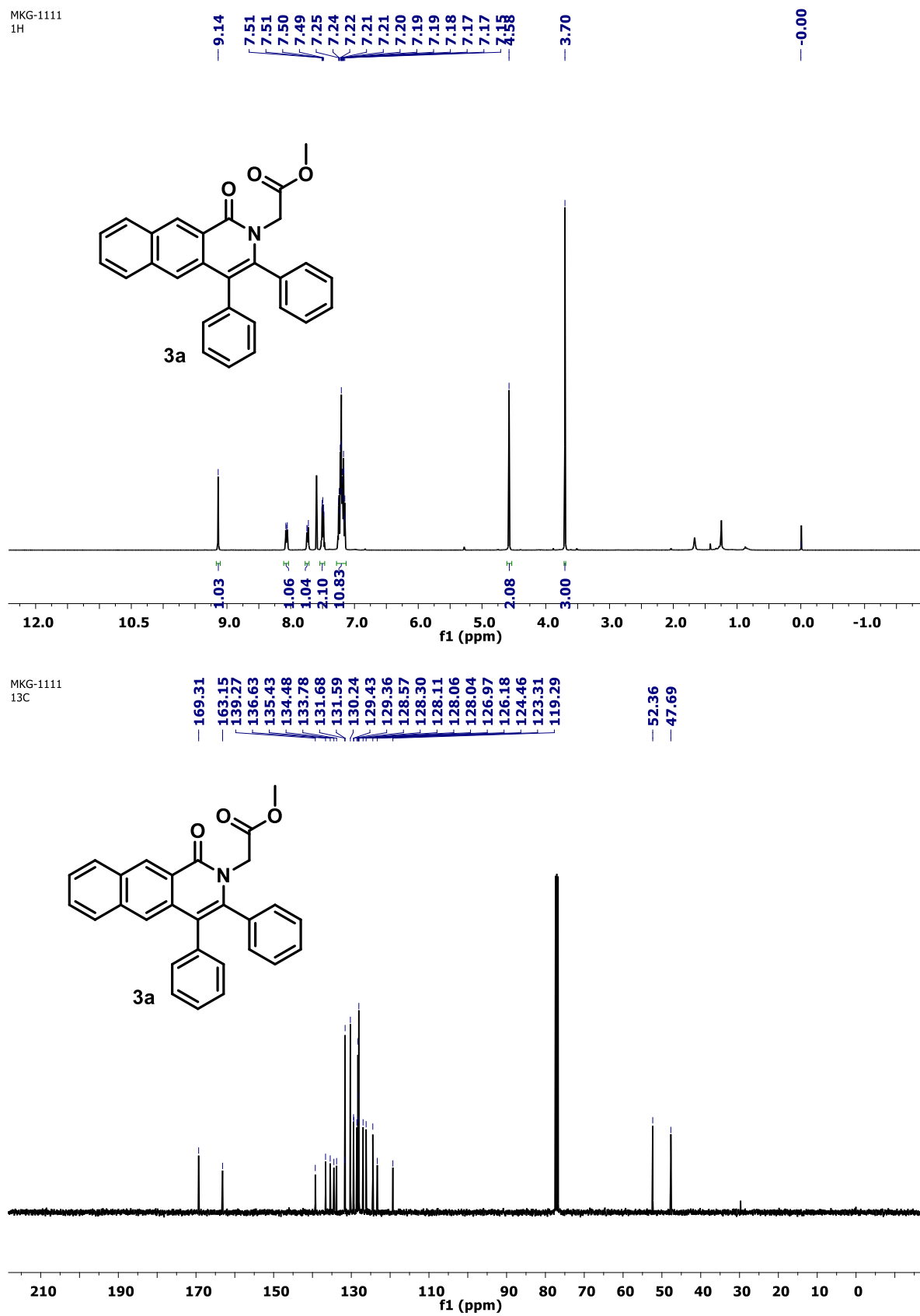
1H NMR (400 MHz, $CDCl_3$) δ 10.32 (d, J = 8 Hz, 1H), 7.90 (t, J = 8 Hz, 2H), 7.81 – 7.75 (m, 1H), 7.66 – 7.60 (m, 1H), 7.23 – 7.16 (m, 7H), 7.11 – 7.04 (m, 5H), 7.02 – 6.99 (m, 4H), 6.61 (d, J = 8 Hz, 1H), 4.92 – 4.84 (m, 1H), 4.72 – 4.49 (m, 2H), 3.70 (s, 3H), 3.21 – 2.98 (m, 2H). ^{13}C NMR (101 MHz, $CDCl_3$) δ 171.73 (s), 167.60 (s), 162.83 (s), 142.87 (s), 139.05 (s), 136.92 (s), 135.72 (s), 134.31 (s), 134.03 (s), 132.33 (s), 131.99 (s), 131.82 (s), 131.74 (s), 130.26 (s), 130.19 (s), 129.41 (s), 128.70 (s), 128.53 (s), 128.35 (s), 128.26 (s), 128.13 (s), 127.85 (s), 127.08 (s), 127.04 (s), 126.66 (s), 123.63 (s), 119.99 (s), 118.41 (s), 53.26 (s), 52.42 (s), 50.60 (s), 37.78 (s). Pale yellow solid (42% yield).ESI-HRMS m/z $[M+H]^+$ calcd. for $C_{37}H_{30}N_2O_4$ 567.2284 found 567.2264.

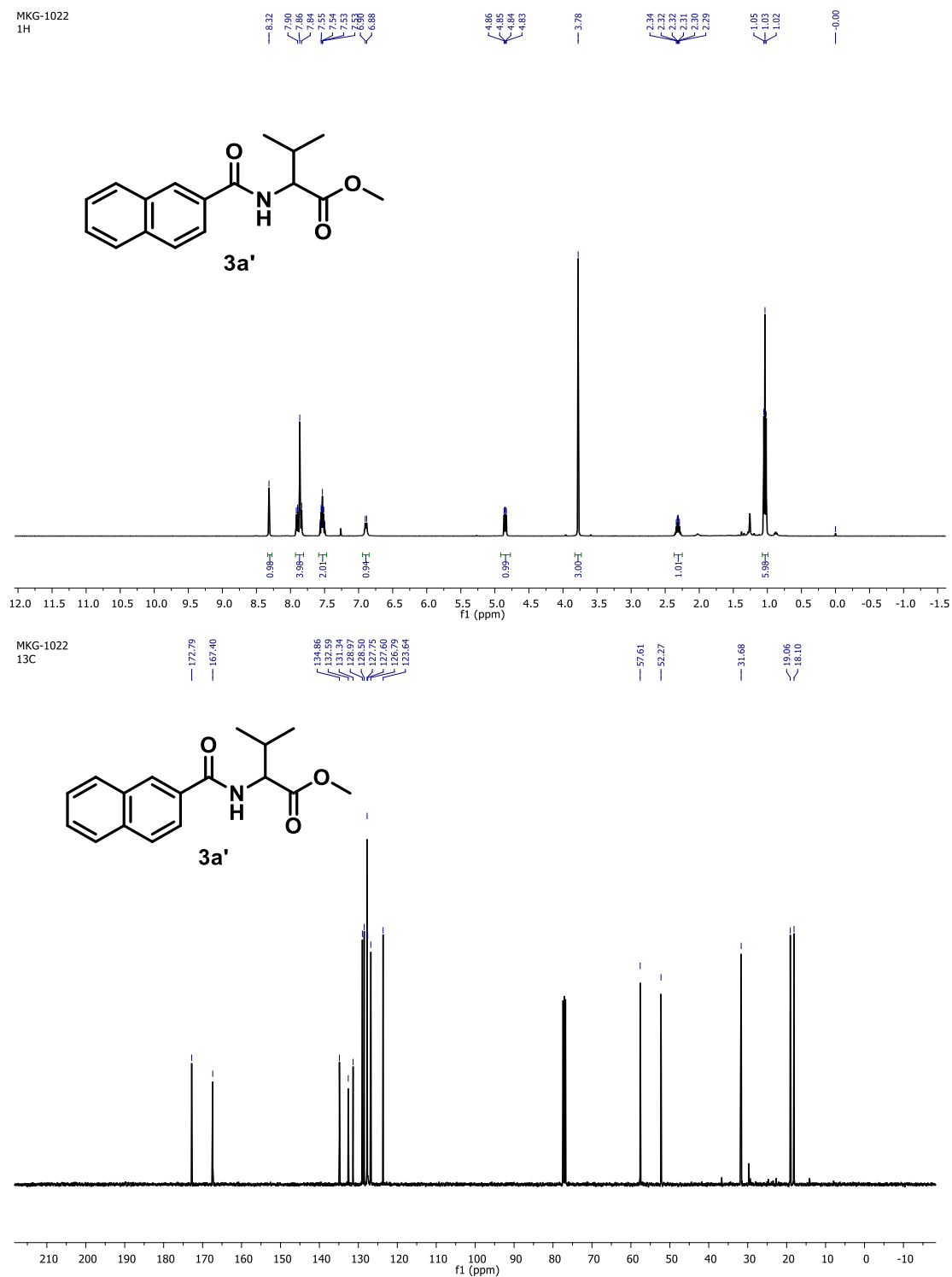
5.5 Appendix

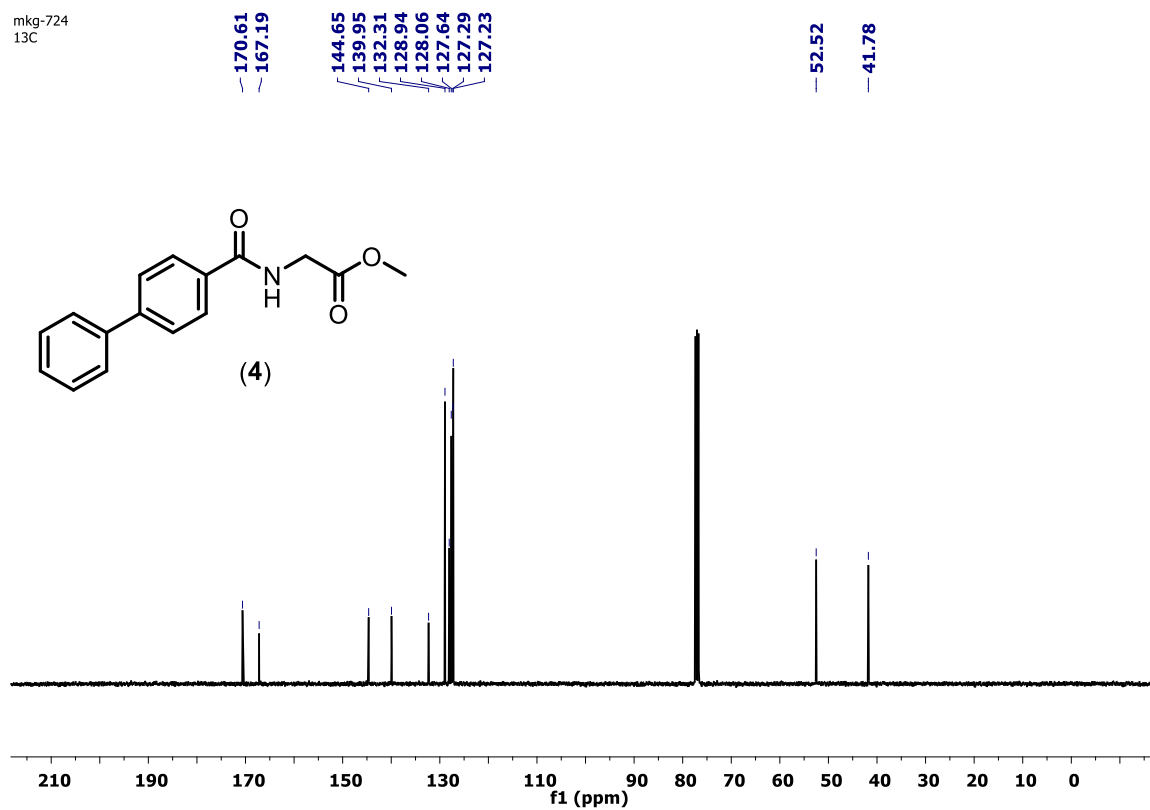
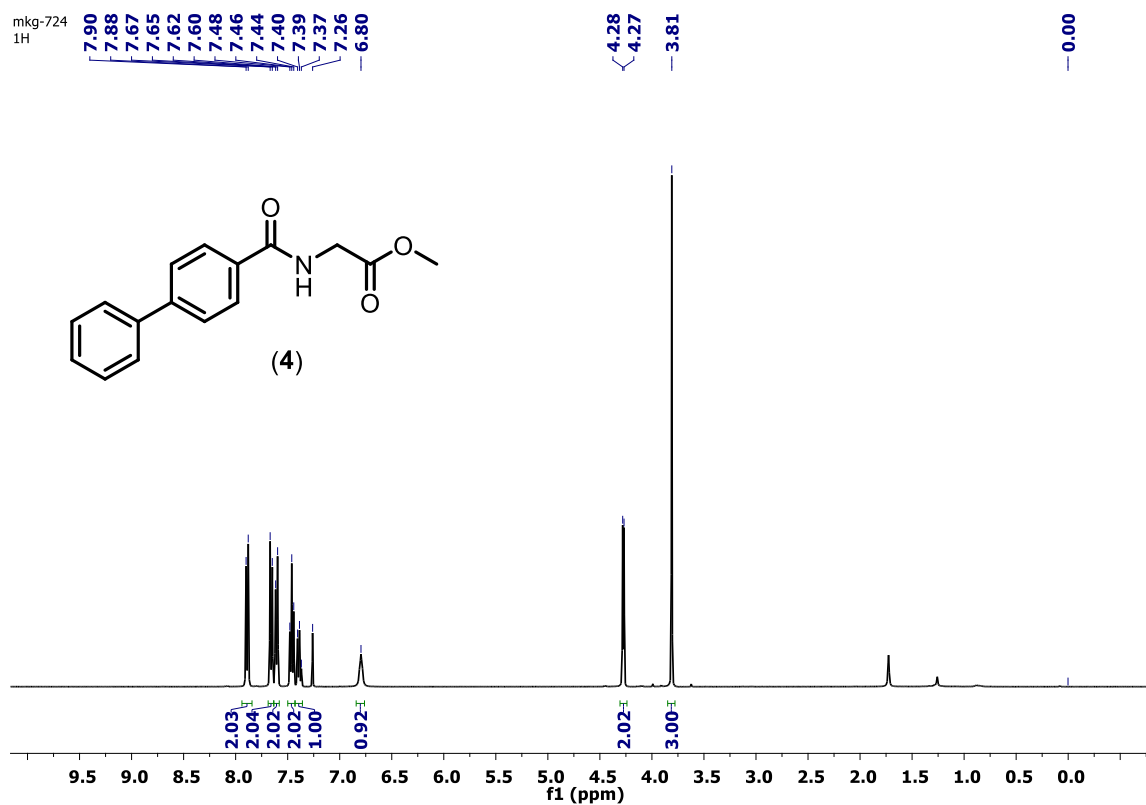
Contents

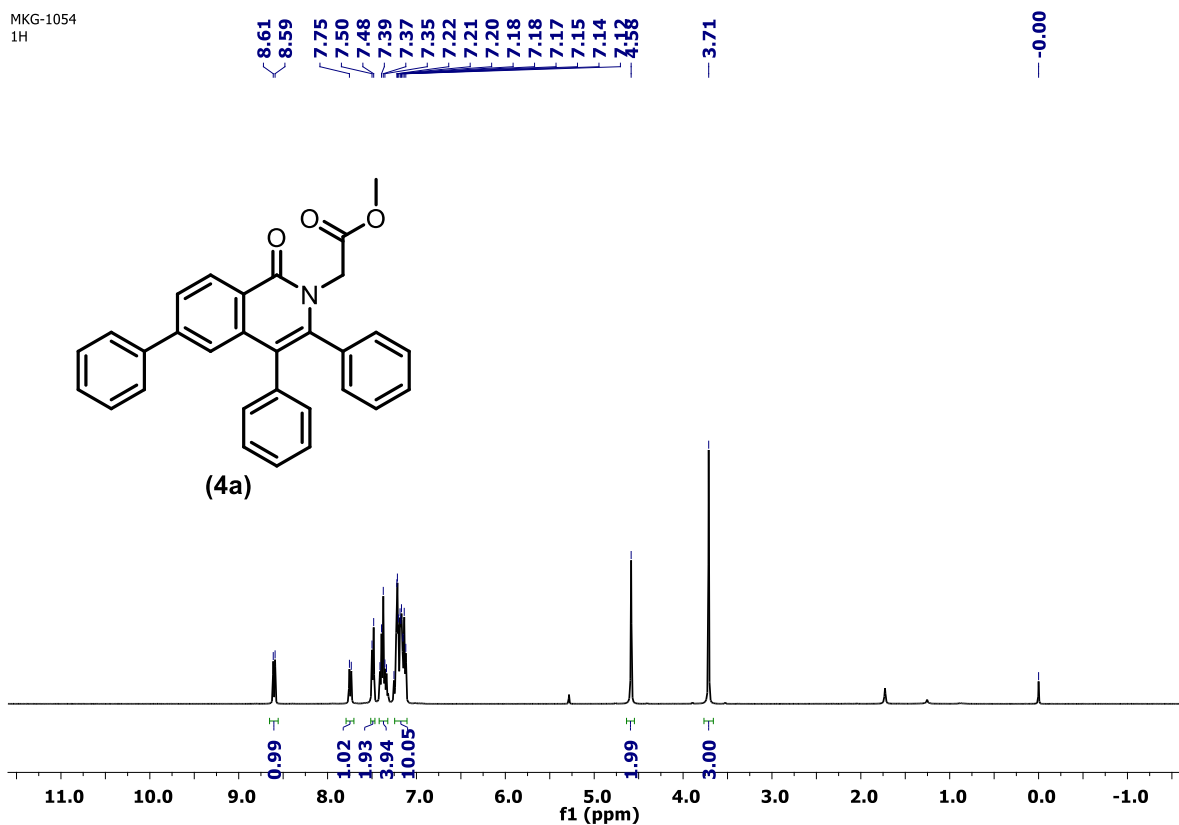
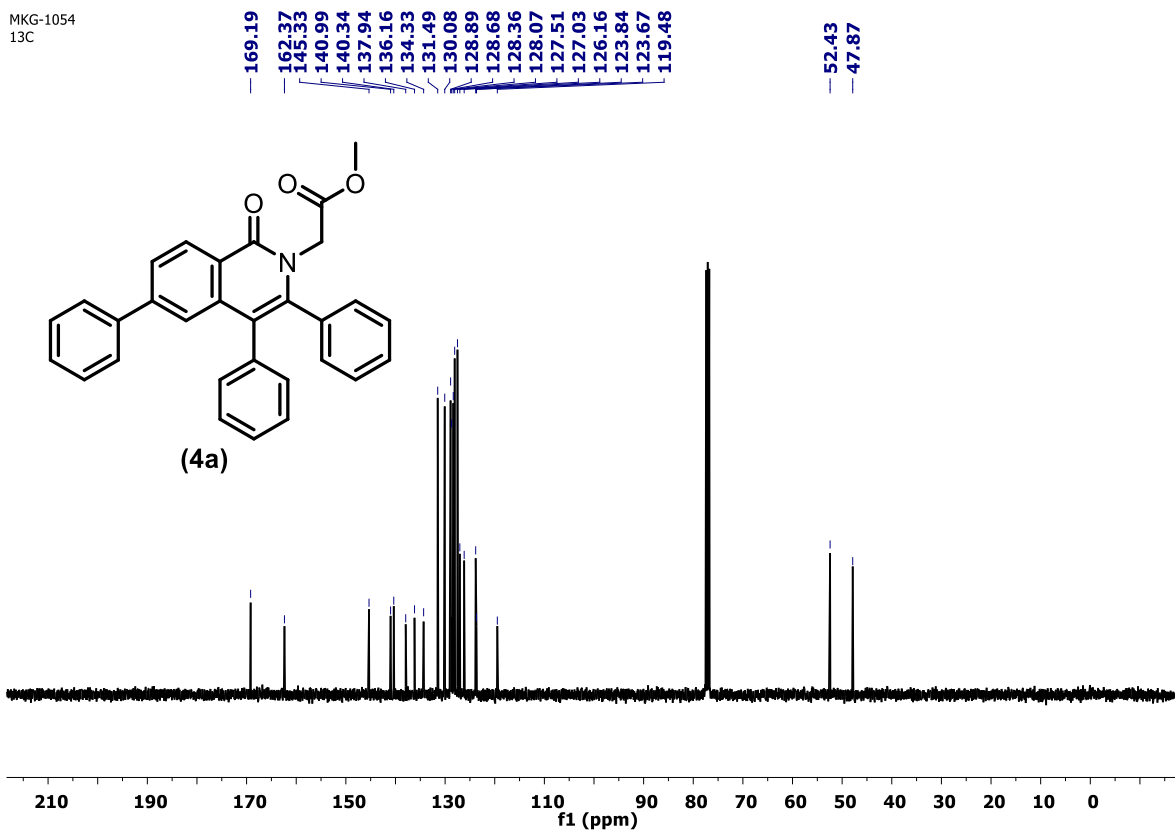
Figure S 1 ^1H , ^{13}C NMR spectra of Compound 3	183
Figure S 2 ^1H , ^{13}C NMR spectra of Compound 3a	184
Figure S 3 ^1H , ^{13}C NMR spectra of Compound 3a'	185
Figure S 4 ^1H , ^{13}C NMR spectra of Compound 4	186
Figure S 5 ^1H , ^{13}C NMR spectra of Compound 4a	187
Figure S 6 ^1H , ^{13}C NMR spectra of Compound 4a'	188
Figure S 7 ^1H , ^{13}C NMR spectra of Compound 5	189
Figure S 8 ^1H , ^{13}C NMR spectra of Compound 5a	190
Figure S 9 ^1H , ^{13}C NMR spectra of Compound 5a'	191
Figure S 10 ^1H , ^{13}C NMR spectra of Compound 6	192
Figure S 11 ^1H , ^{13}C NMR spectra of Compound 6a	193
Figure S 12 ESI HRMS spectra of Compound 6	194
Figure S 13 ^1H , ^{13}C NMR spectra of Compound 6a'	195
Figure S 14 ^1H , ^{13}C NMR spectra of Compound 7	196
Figure S 15 ^1H , ^{13}C NMR spectra of Compound 7a	197
Figure S 16 ESI HRMS spectra of Compound 7	198
Figure S 17 ^1H , ^{13}C NMR spectra of Compound 8	199
Figure S 18 ^1H , ^{13}C NMR spectra of Compound 8a	200
Figure S 19 ESI HRMS spectra of Compound 8	201
Figure S 20 ^1H , ^{13}C NMR spectra of Compound 9	202
Figure S 21 ^1H , ^{13}C NMR spectra of Compound 9a	203
Figure S 22 ESI HRMS spectra of Compound 9	204
Figure S 23 ^1H , ^{13}C NMR spectra of Compound 10	205
Figure S 24 ^1H , ^{13}C NMR spectra of Compound 10a	206
Figure S 25 ^1H , ^{13}C NMR spectra of Compound 11	207
Figure S 26 ^1H , ^{13}C NMR spectra of Compound 11a	208

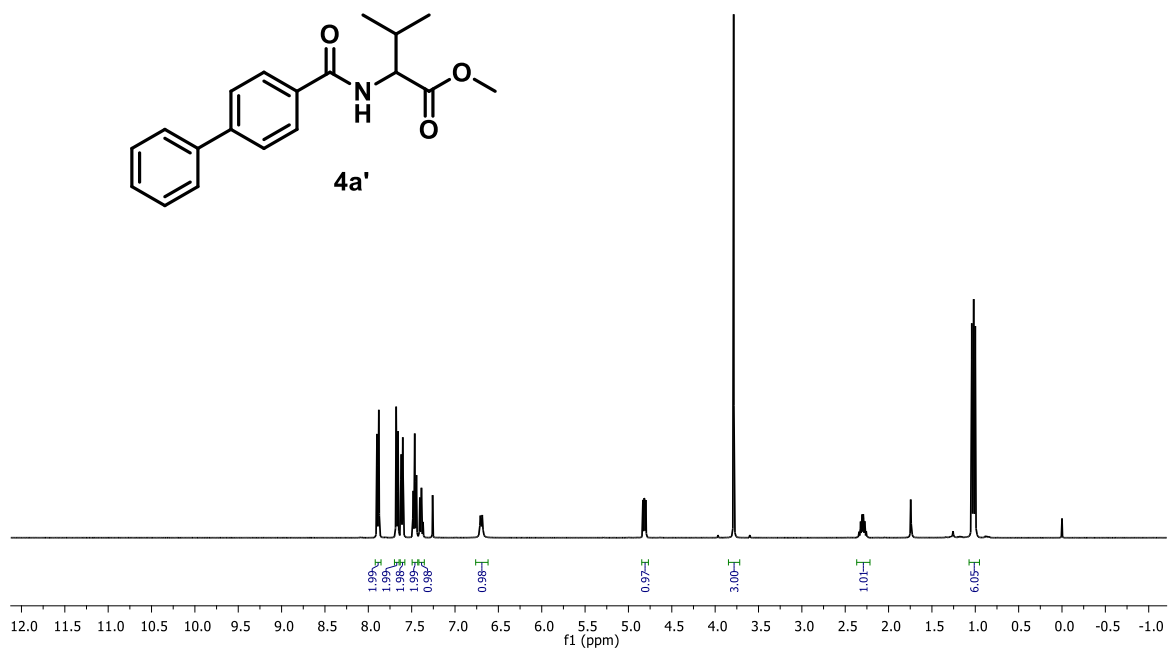
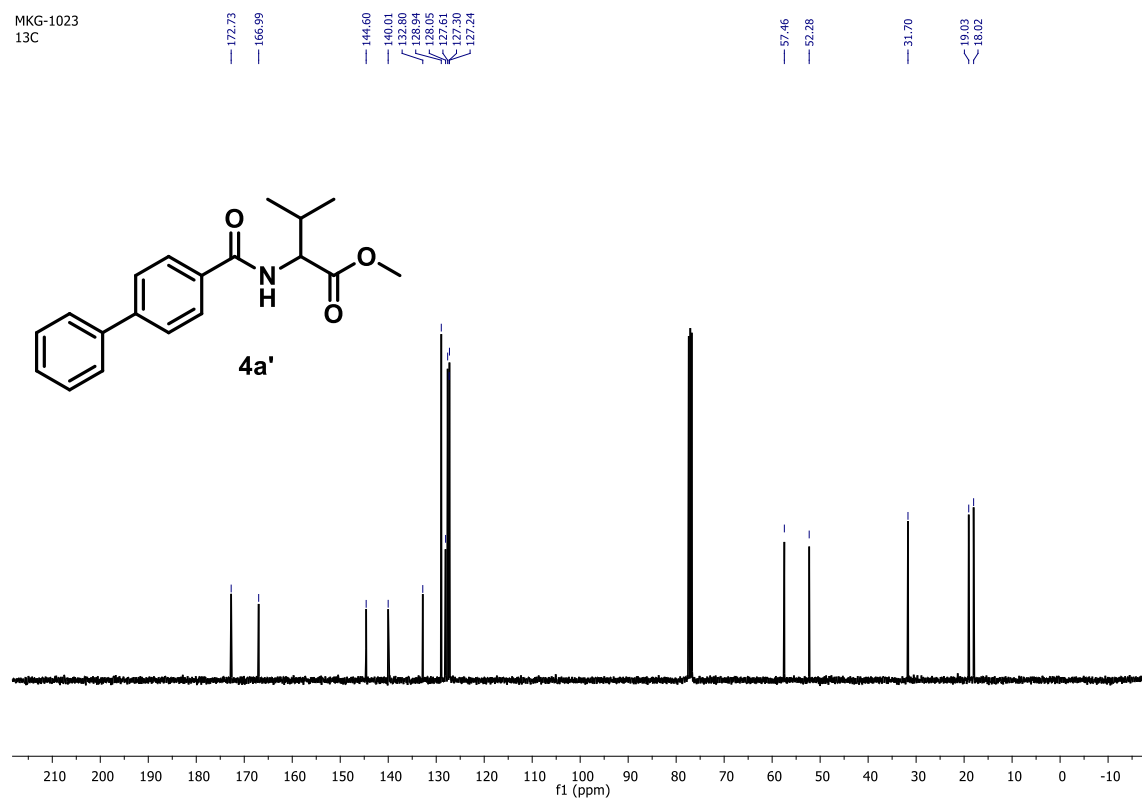
Figure S 1 ¹H, ¹³C NMR spectra of Compound 3

Figure S 2 ^1H , ^{13}C NMR spectra of Compound 3a

Figure S 3 ¹H, ¹³C NMR spectra of Compound **3a'**

Figure S 4 ^1H , ^{13}C NMR spectra of Compound 4

MKG-1054
1HMKG-1054
13CFigure S 5 ¹H, ¹³C NMR spectra of Compound 4a

MKG-1023
1HMKG-1023
13CFigure S 6 ¹H, ¹³C NMR spectra of Compound 4a'

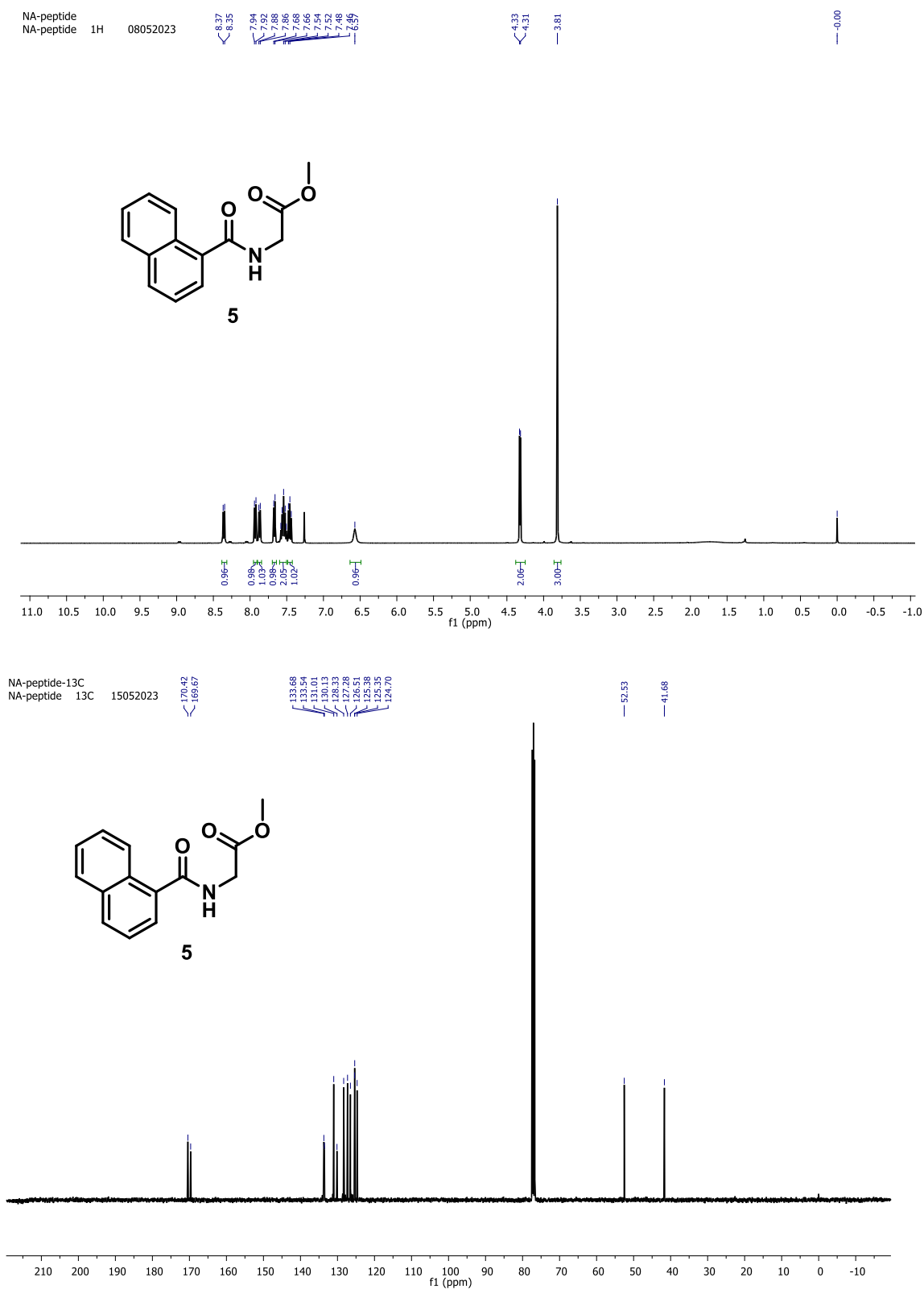
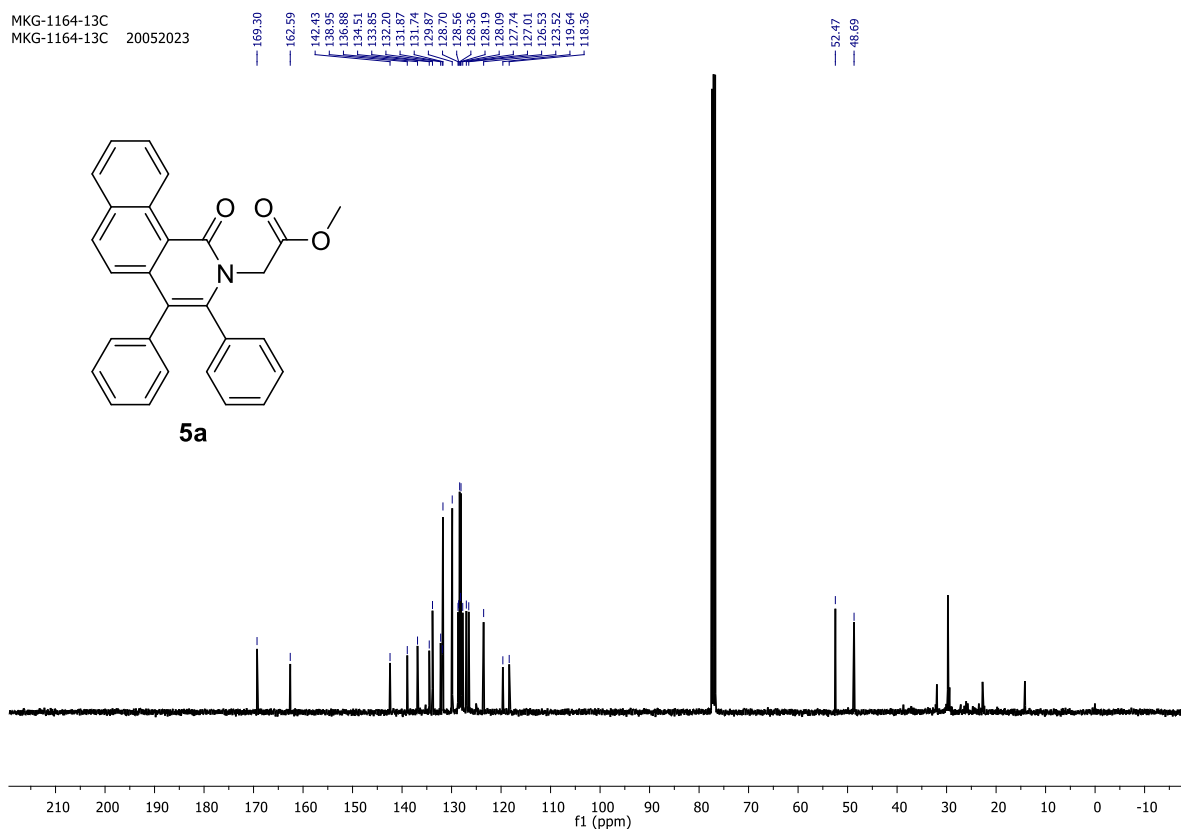
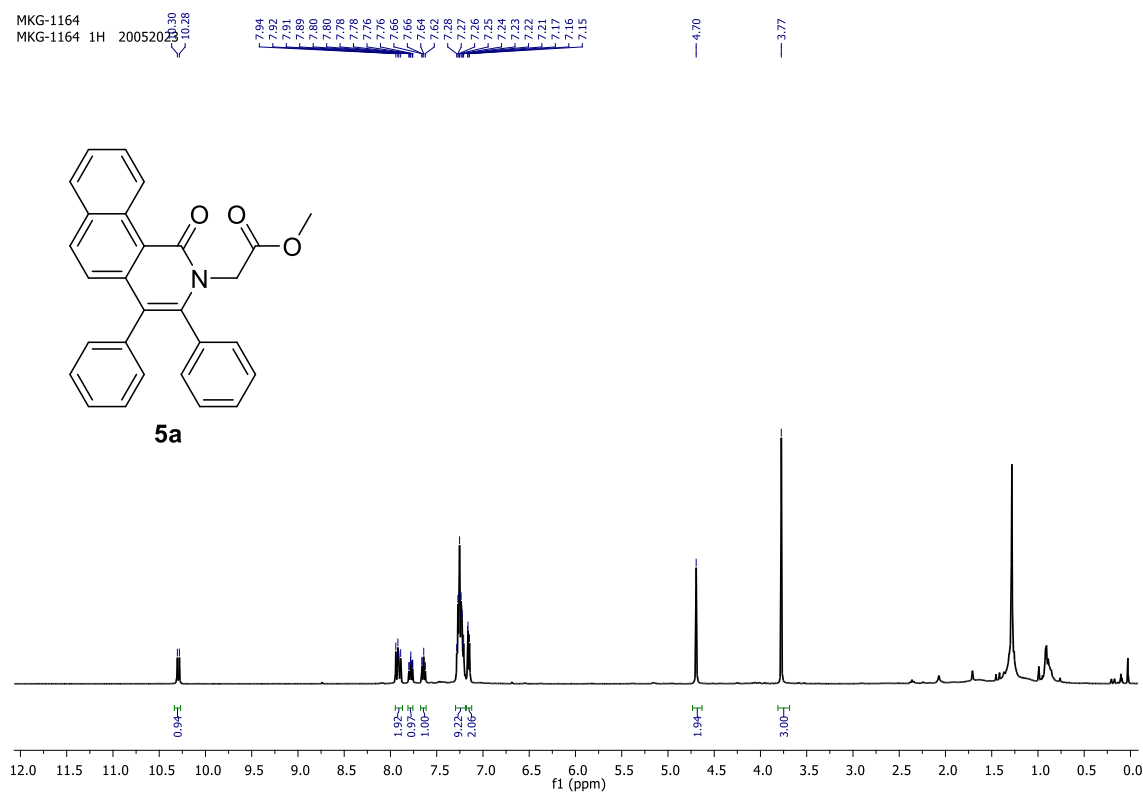


Figure S 7 ^1H , ^{13}C NMR spectra of Compound 5

Figure S 8 ^1H , ^{13}C NMR spectra of Compound **5a**

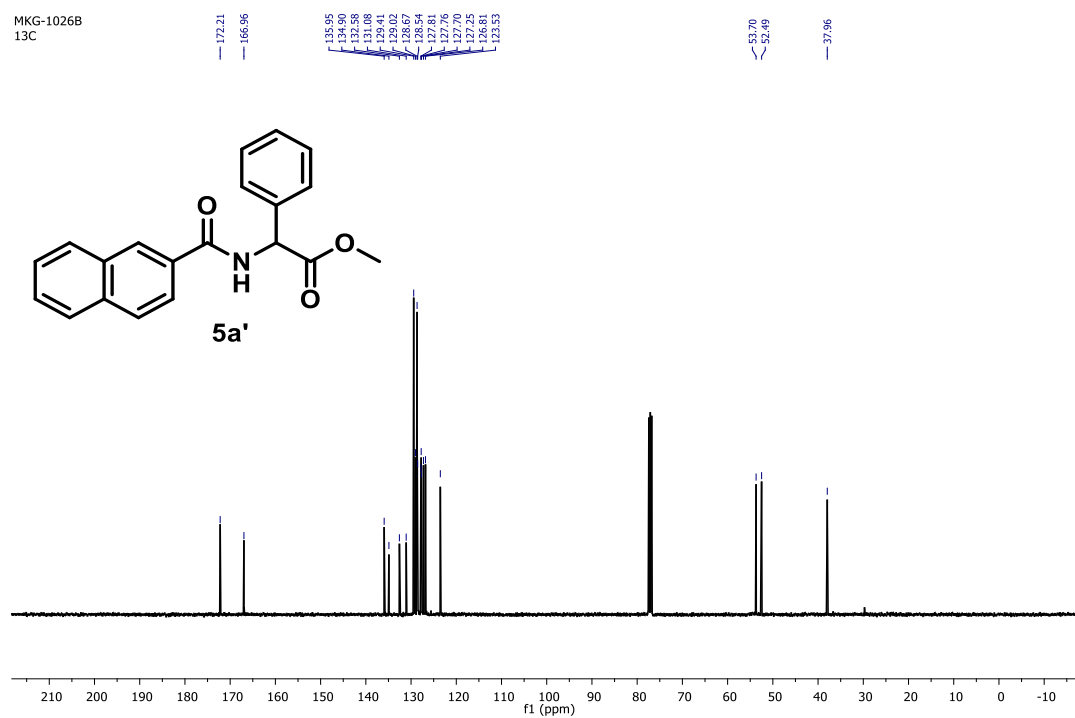
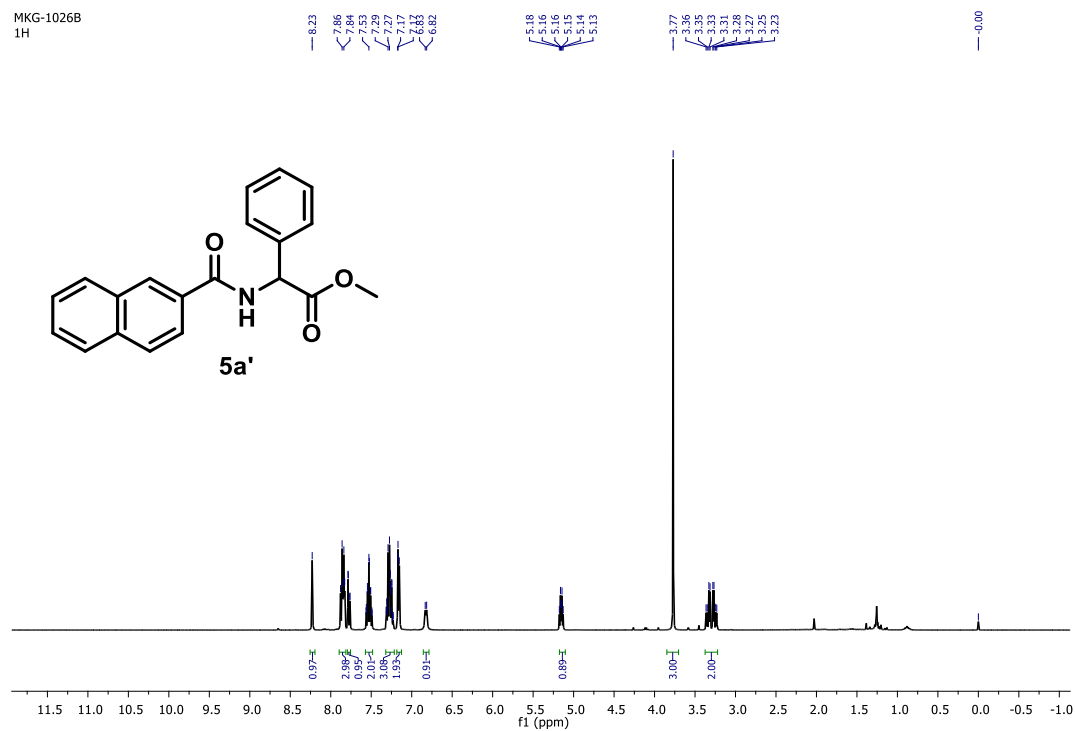
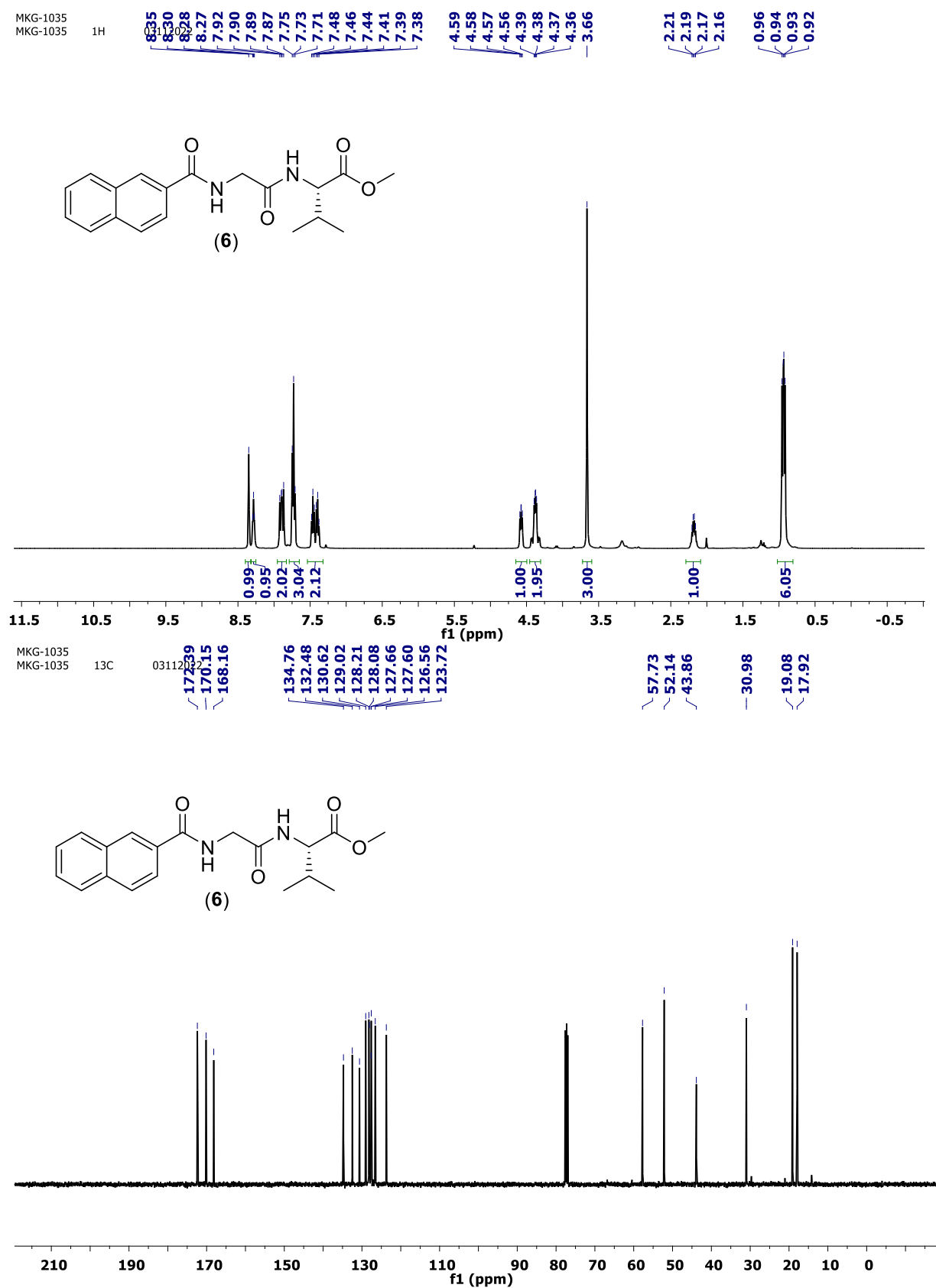
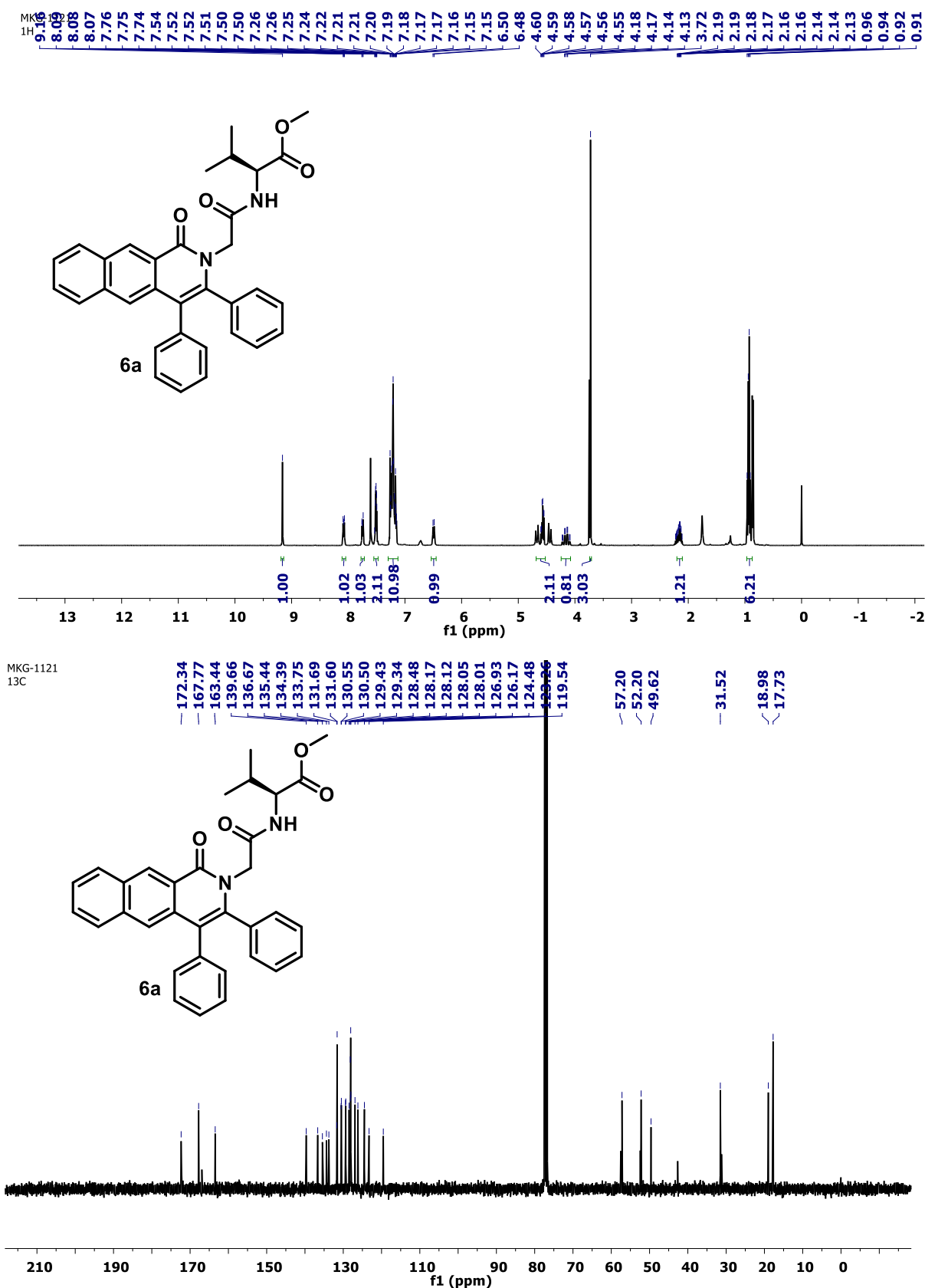


Figure S 9 ^1H , ^{13}C NMR spectra of Compound **5a'**

Figure S 10 ^1H , ^{13}C NMR spectra of Compound 6

Figure S 11 ^1H , ^{13}C NMR spectra of Compound 6a

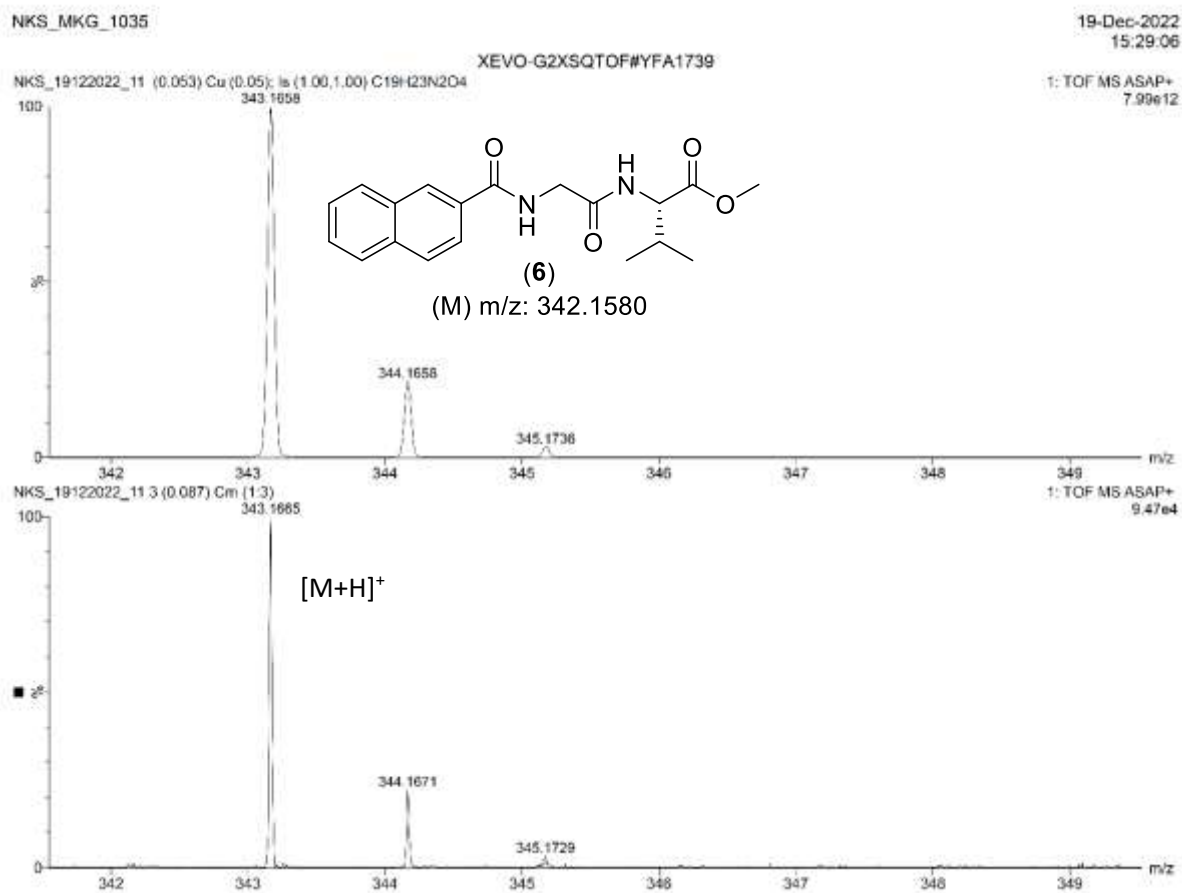


Figure S 12 ESI HRMS spectra of Compound 6

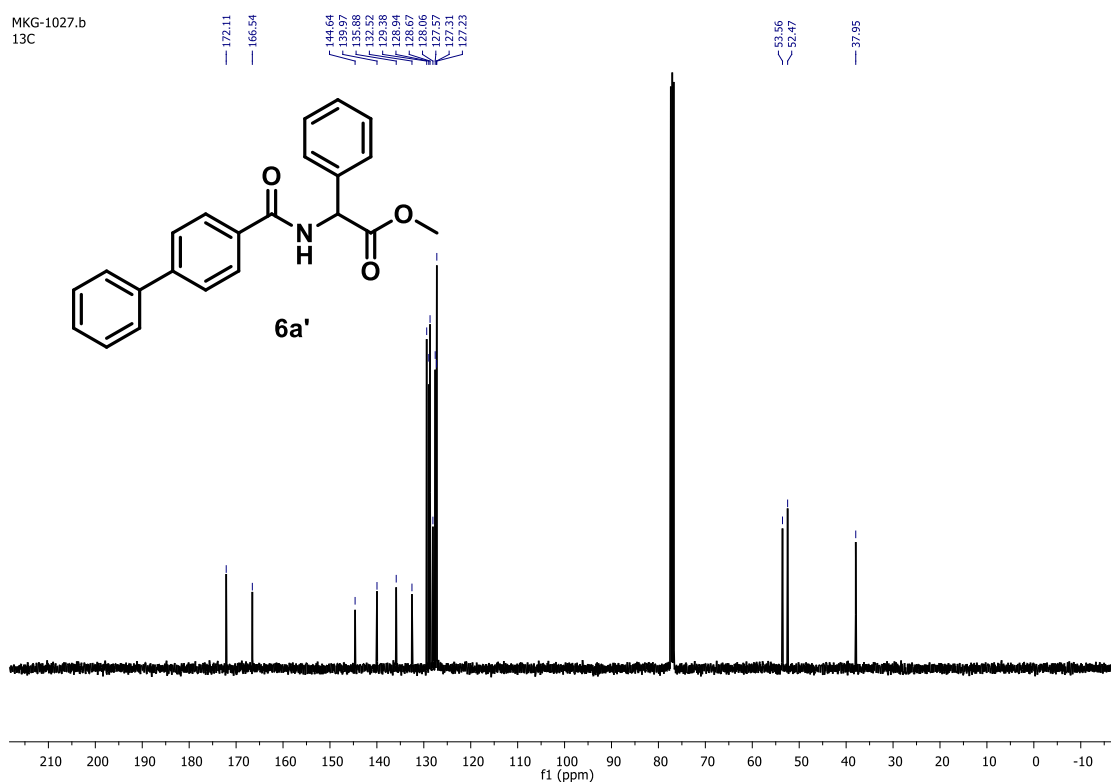
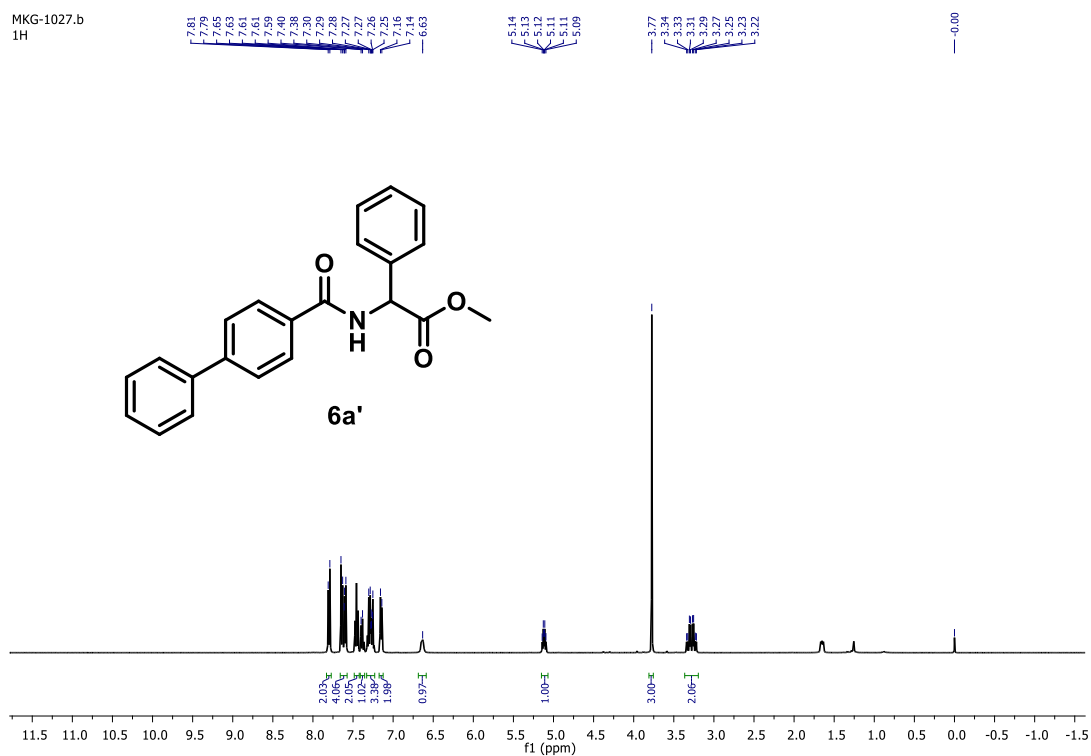
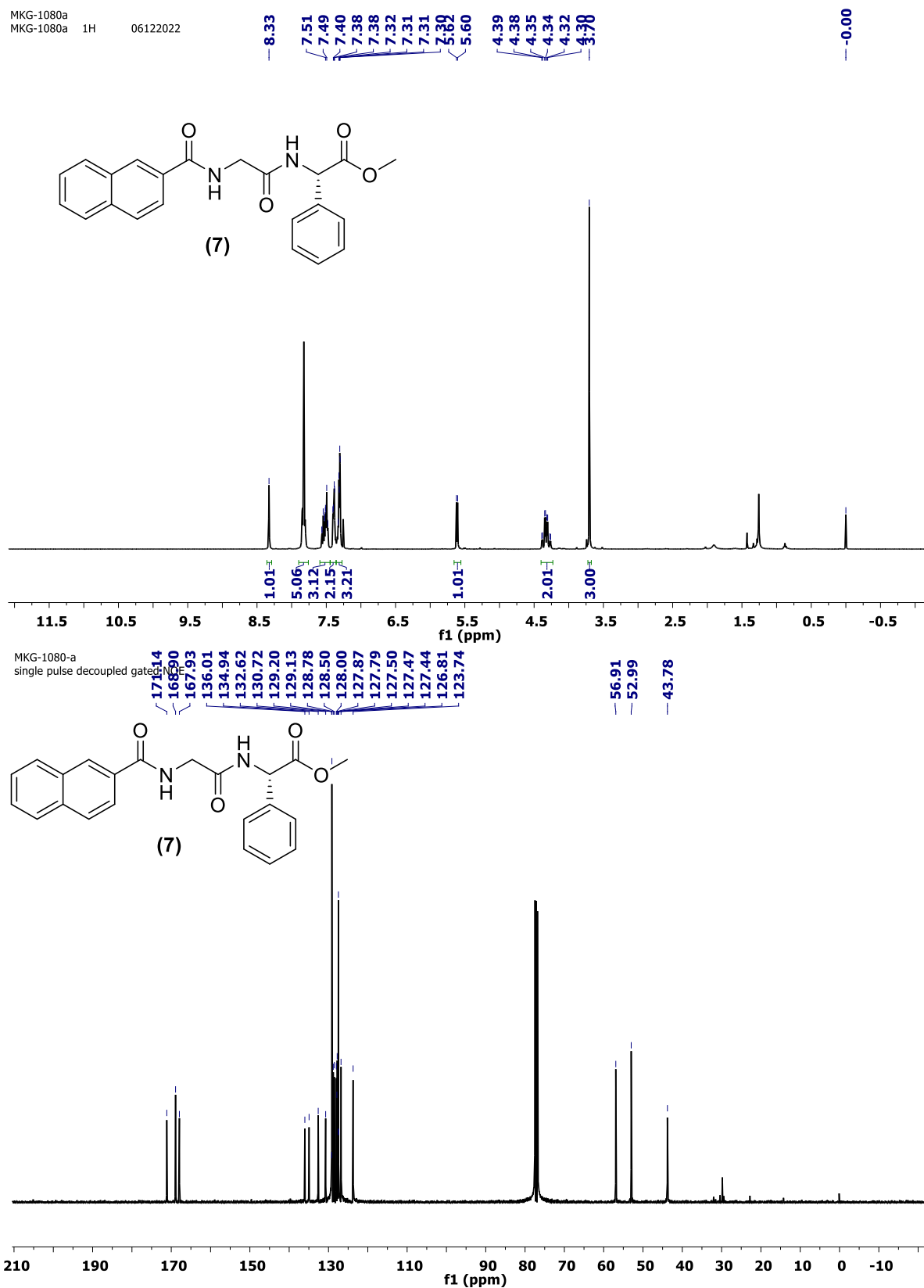
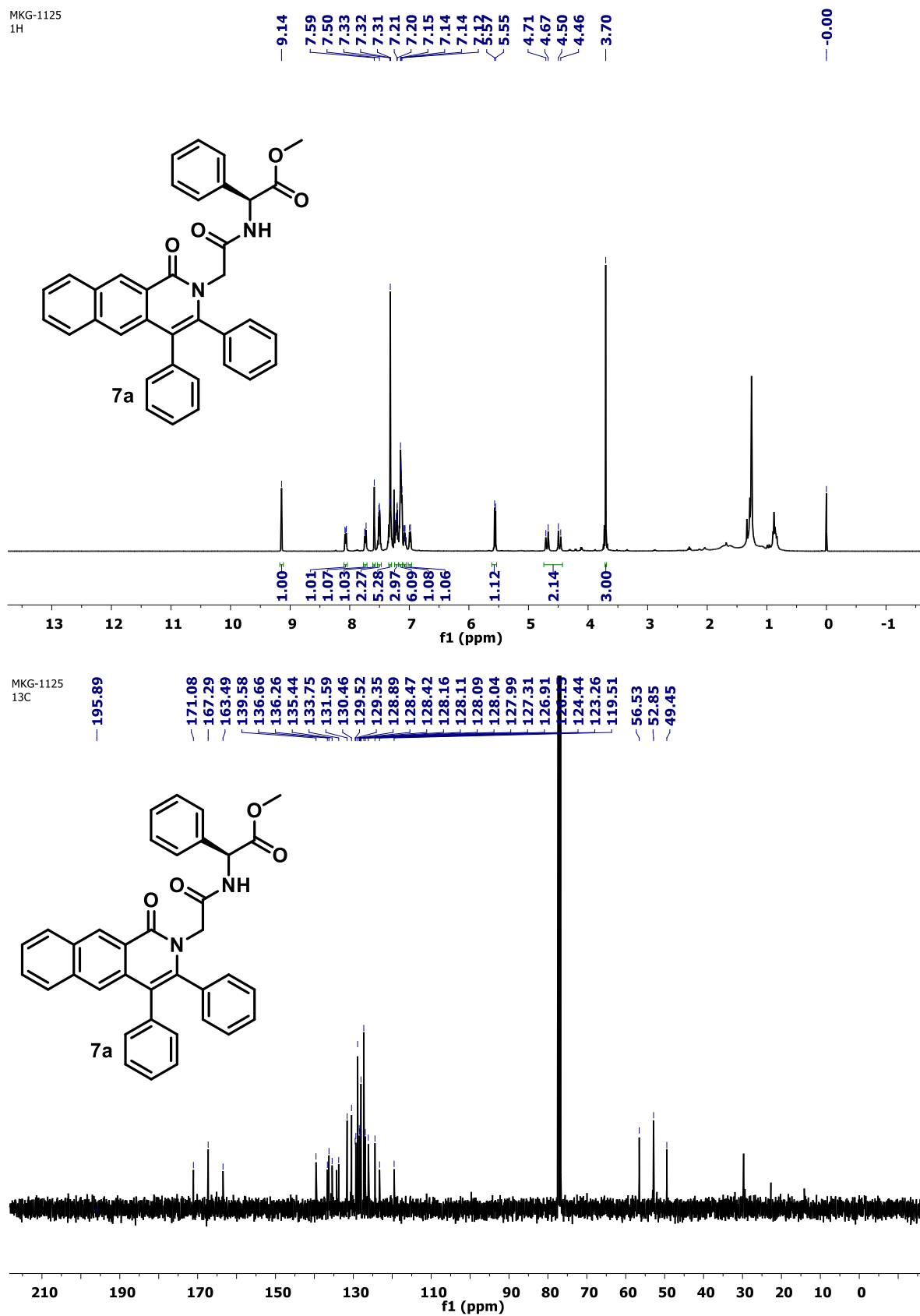


Figure S 13 ^1H , ^{13}C NMR spectra of Compound **6a'**

Figure S 14 ¹H, ¹³C NMR spectra of Compound 7

Figure S 15 ^1H , ^{13}C NMR spectra of Compound 7a

MKG_1080_A_re

12-Jan-2023

16:53:28

XEVO-G2XSQTOF#YFA1739

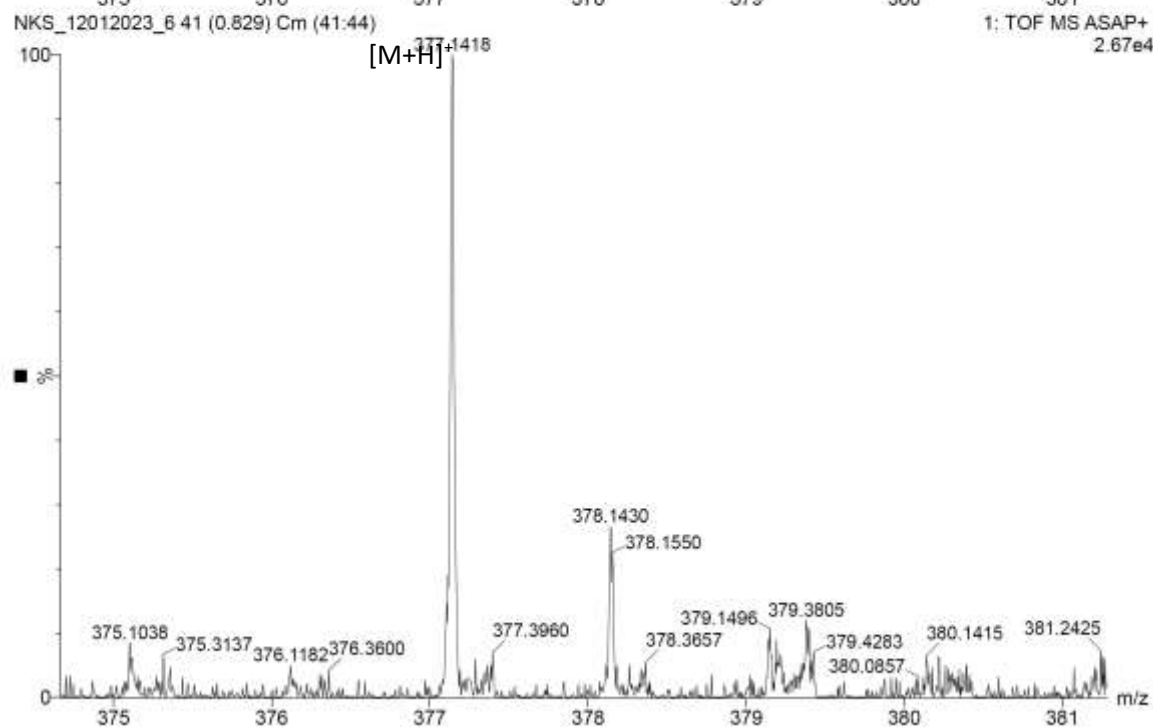
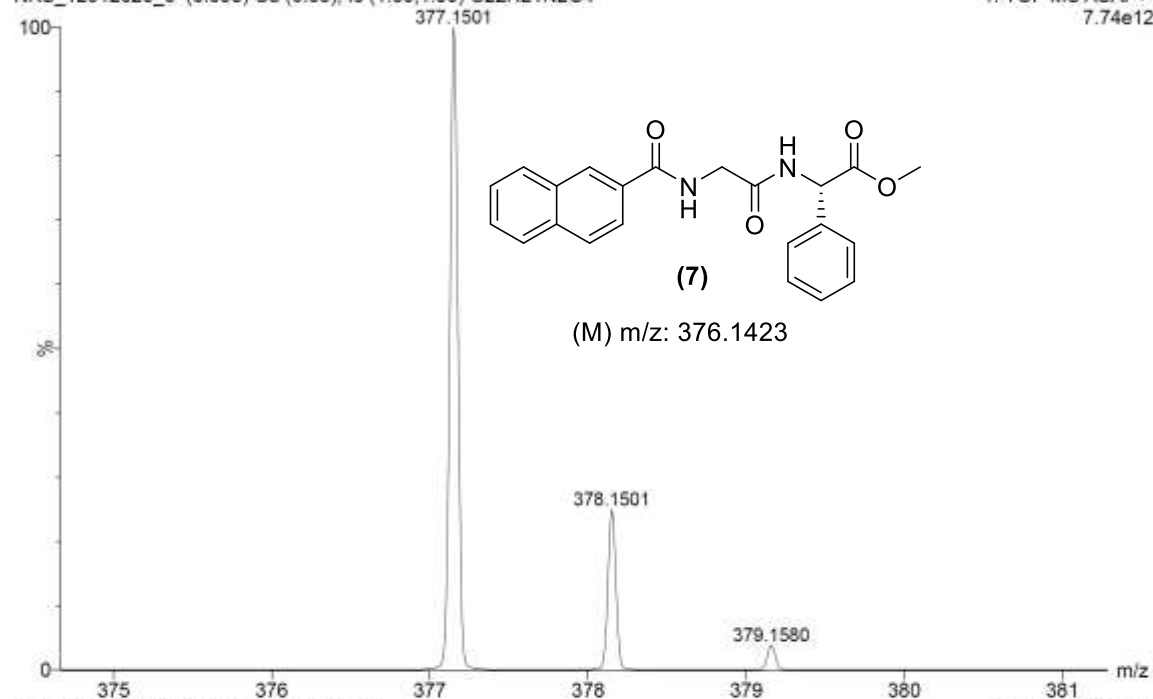
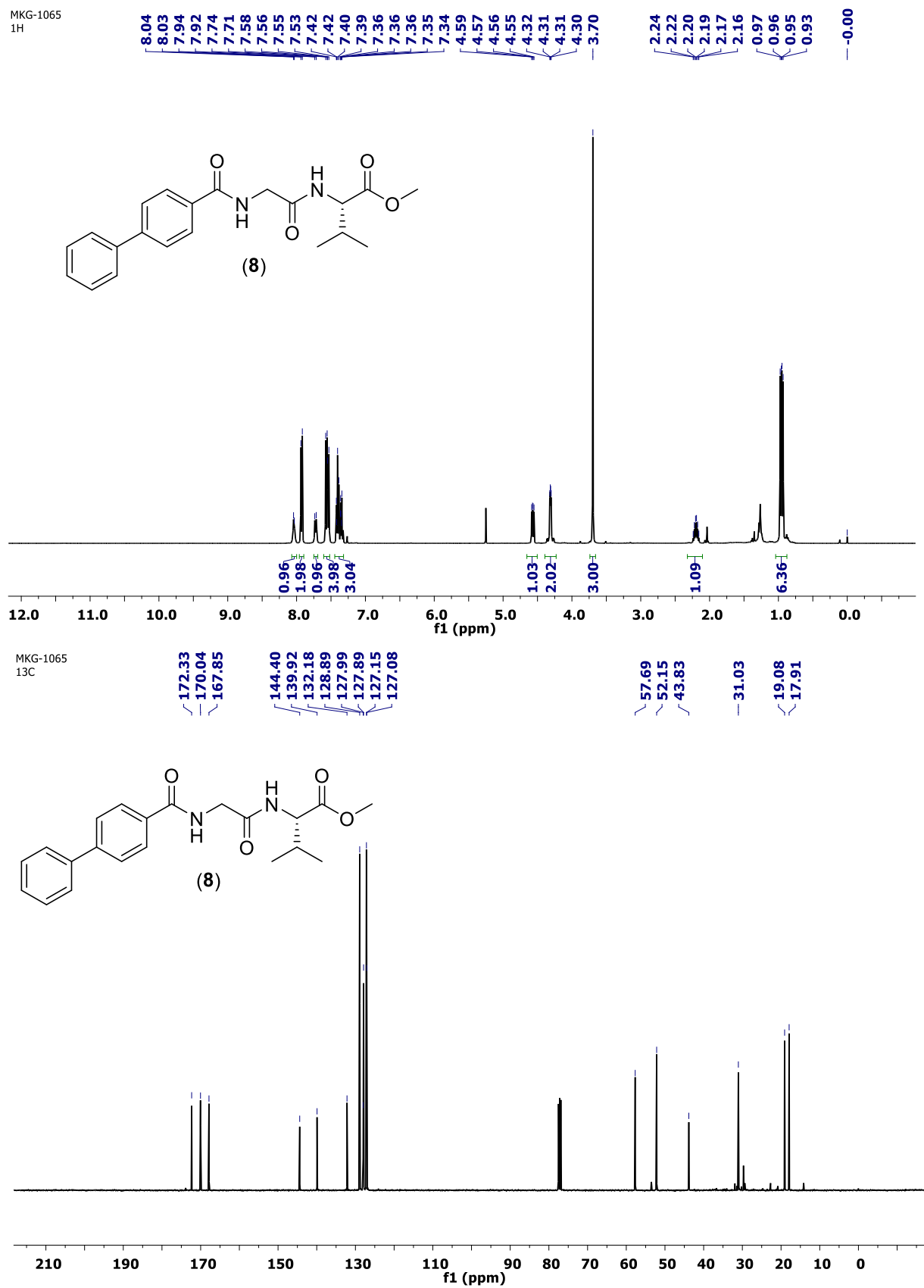
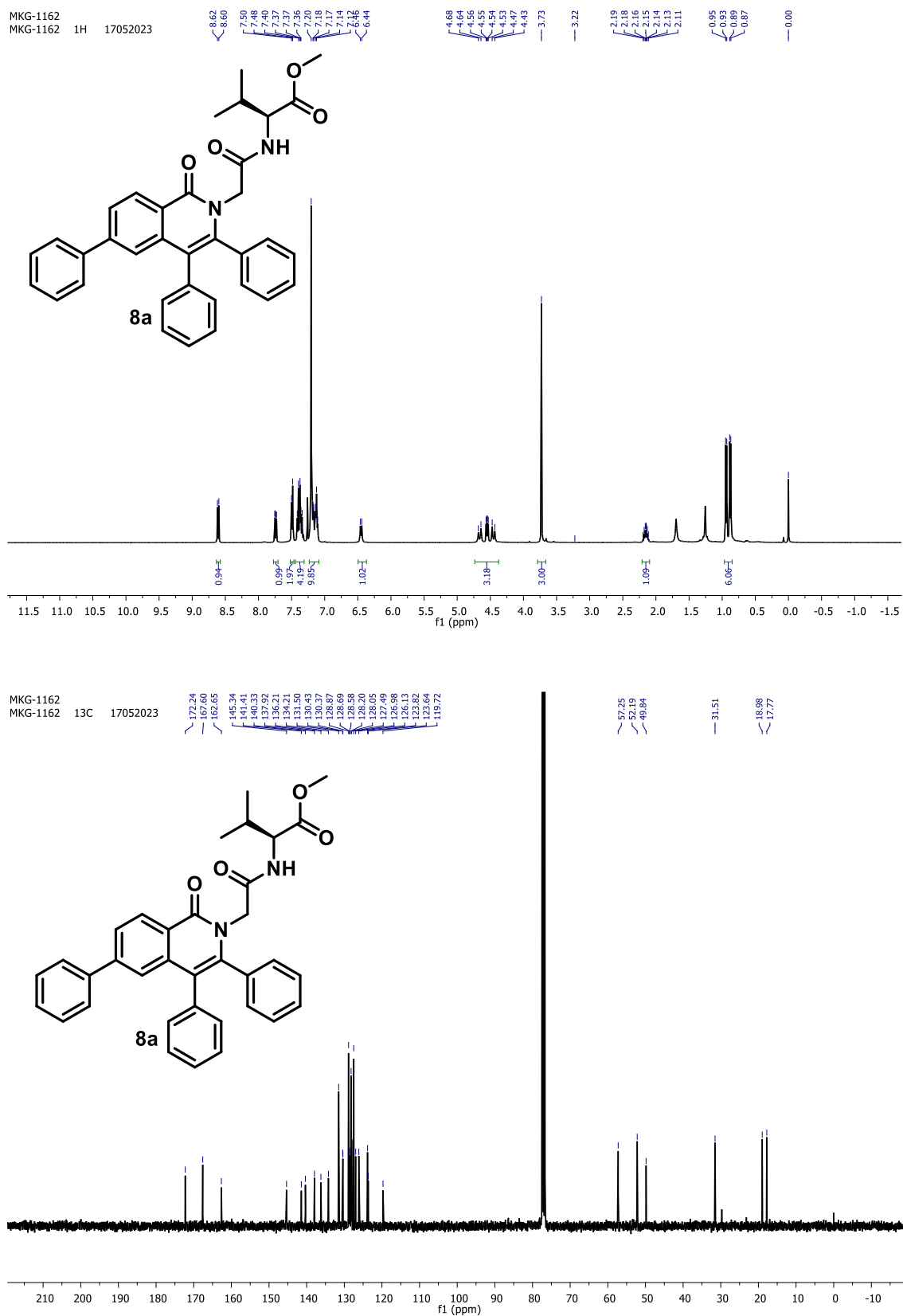
NKS_12012023_6 (0.053) Cu (0.05); Is (1.00,1.00) C₂₂H₂₁N₂O₄1: TOF MS ASAP+
7.74e12

Figure S 16 ESI HRMS spectra of Compound 7

Figure S 17 ^1H , ^{13}C NMR spectra of Compound 8

Figure S 18 ^1H , ^{13}C NMR spectra of Compound 8a

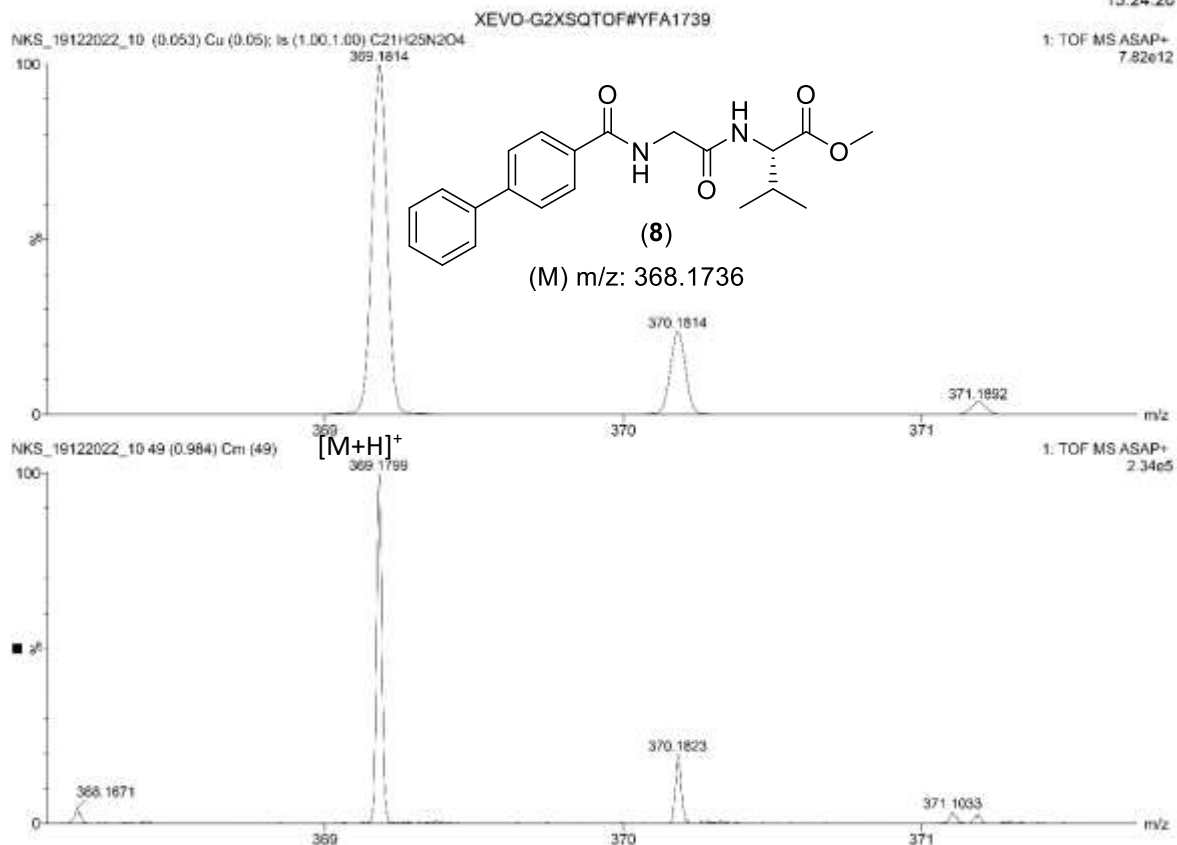
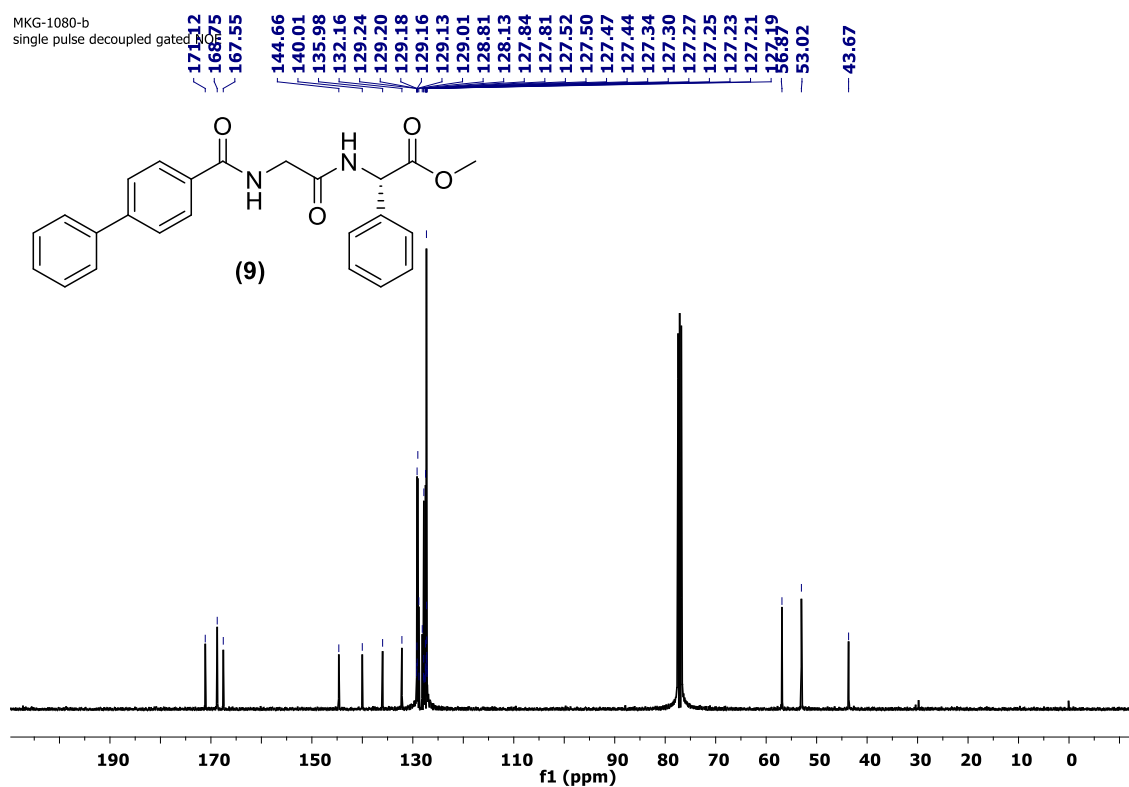
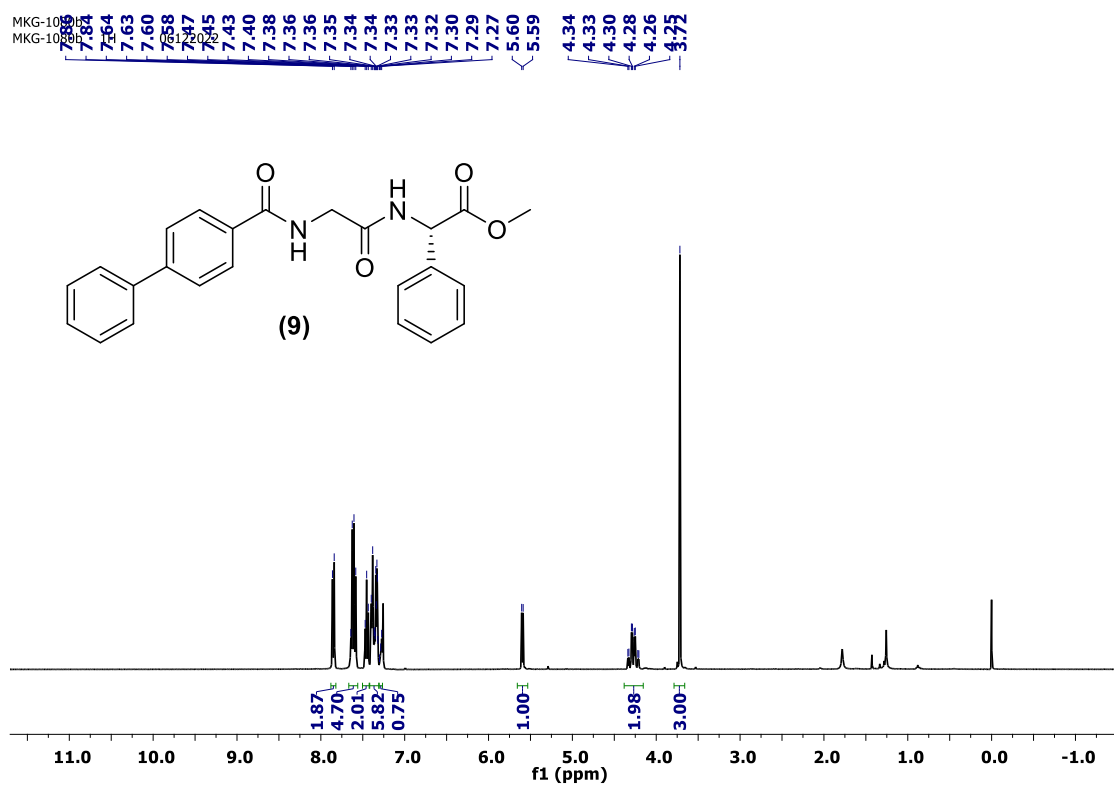
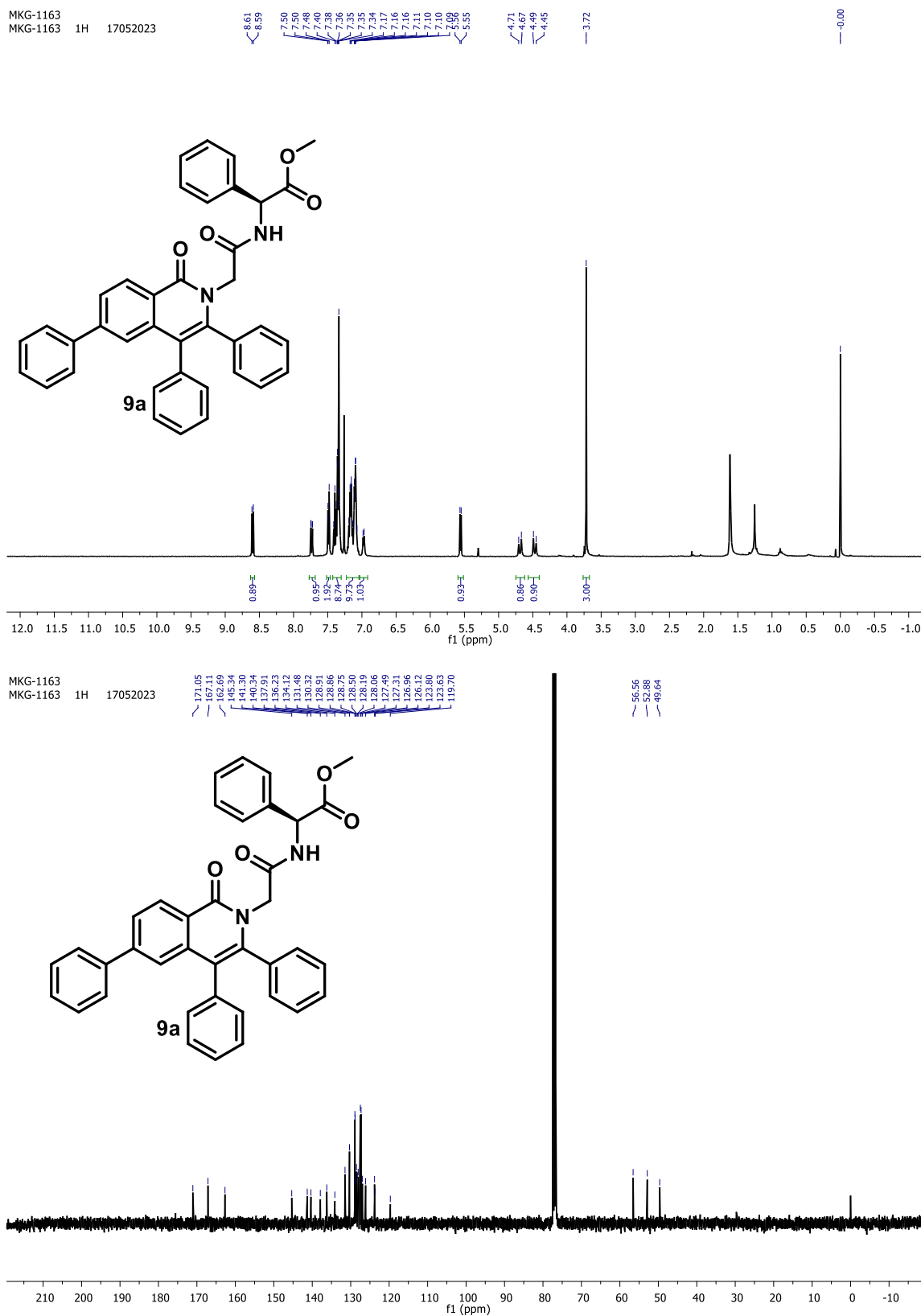


Figure S 19 ESI HRMS spectra of Compound **8**

Figure S 20 ^1H , ^{13}C NMR spectra of Compound 9

Figure S 21 ^1H , ^{13}C NMR spectra of Compound 9a

NKS_MKG_1080_B

19-Dec-2022

15:38:03

XEVO-G2XSQTOF#YFA1739

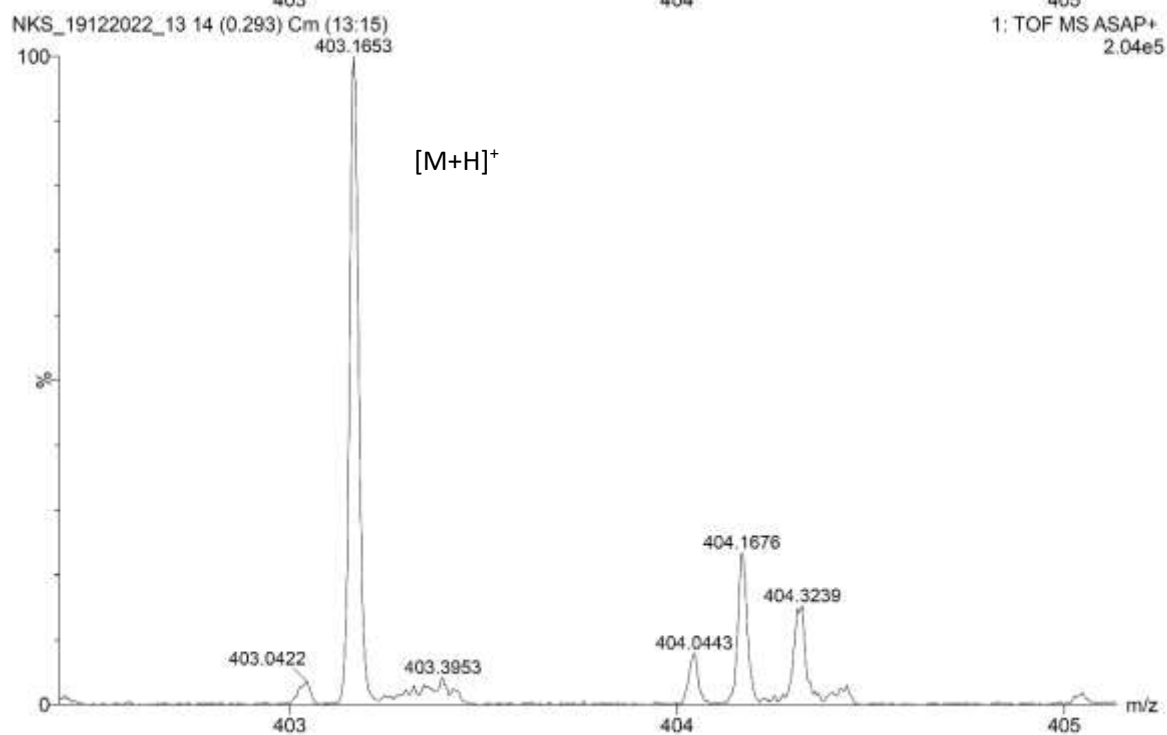
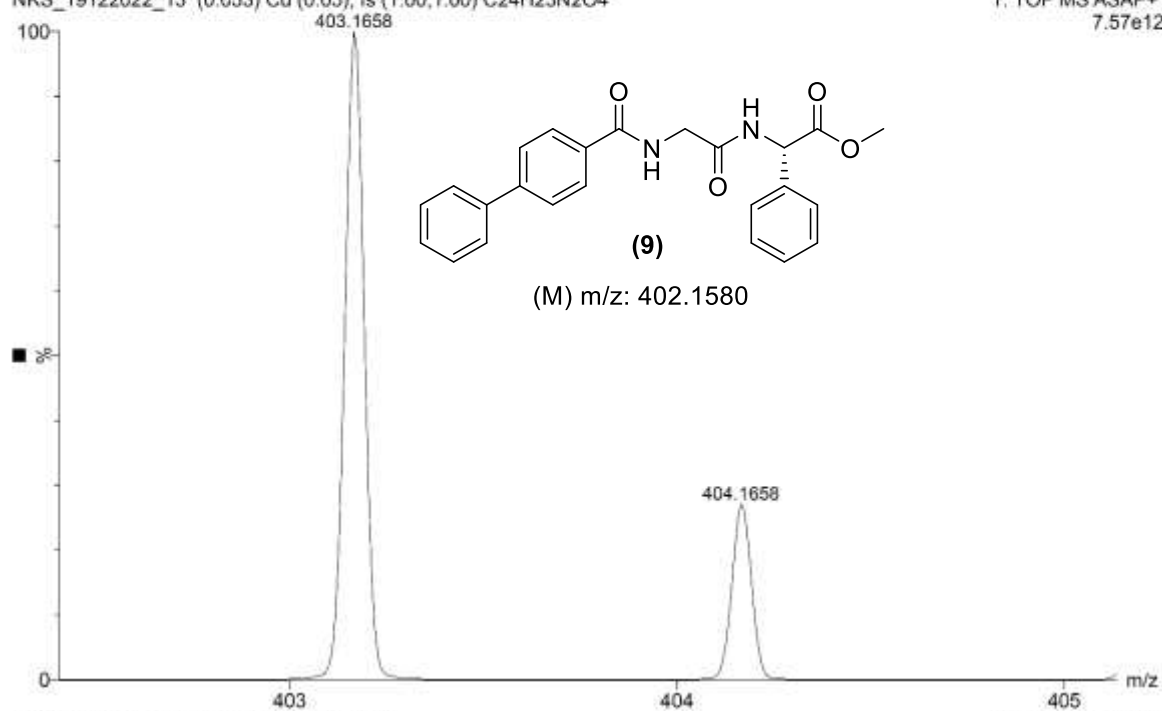
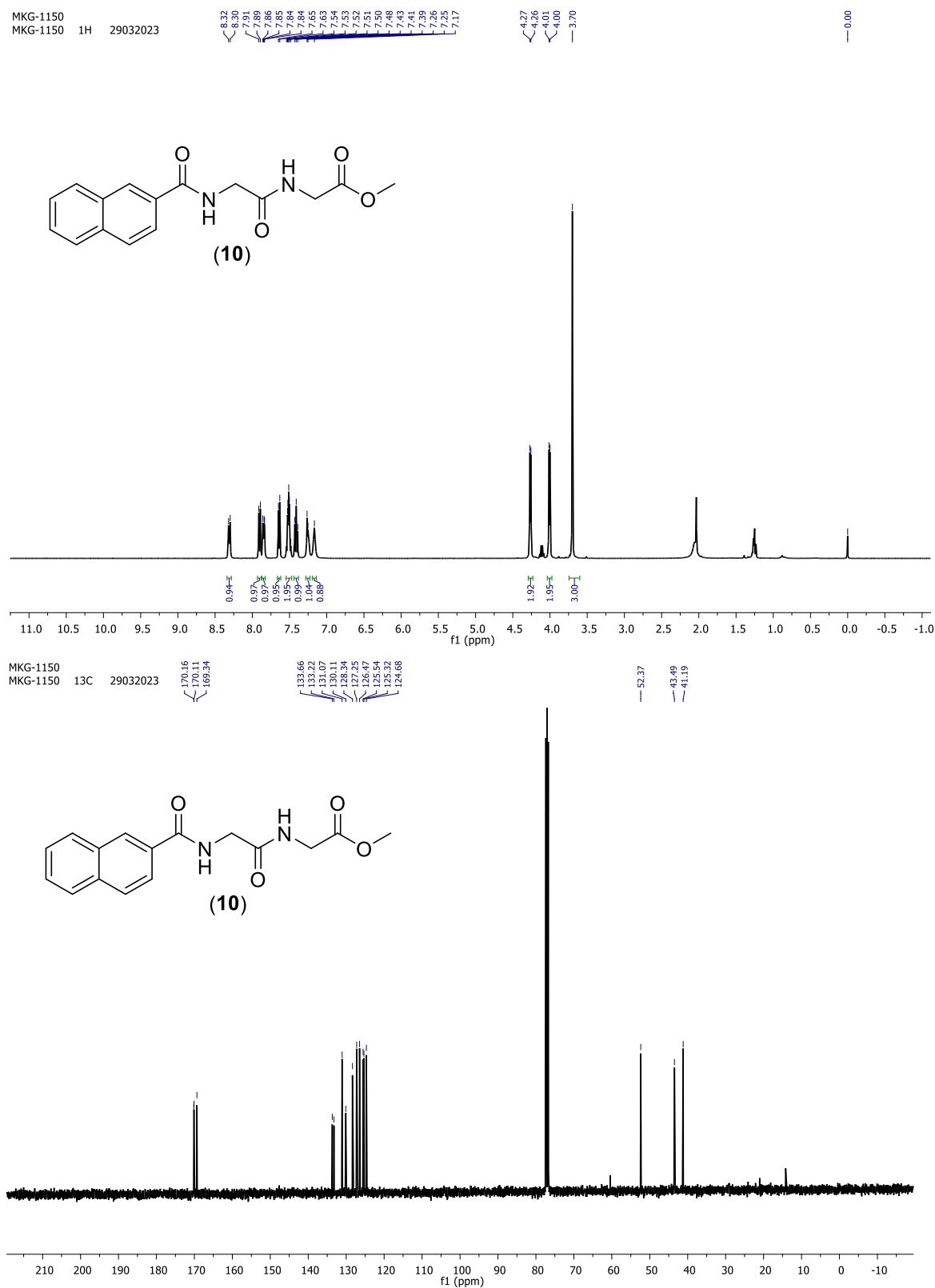
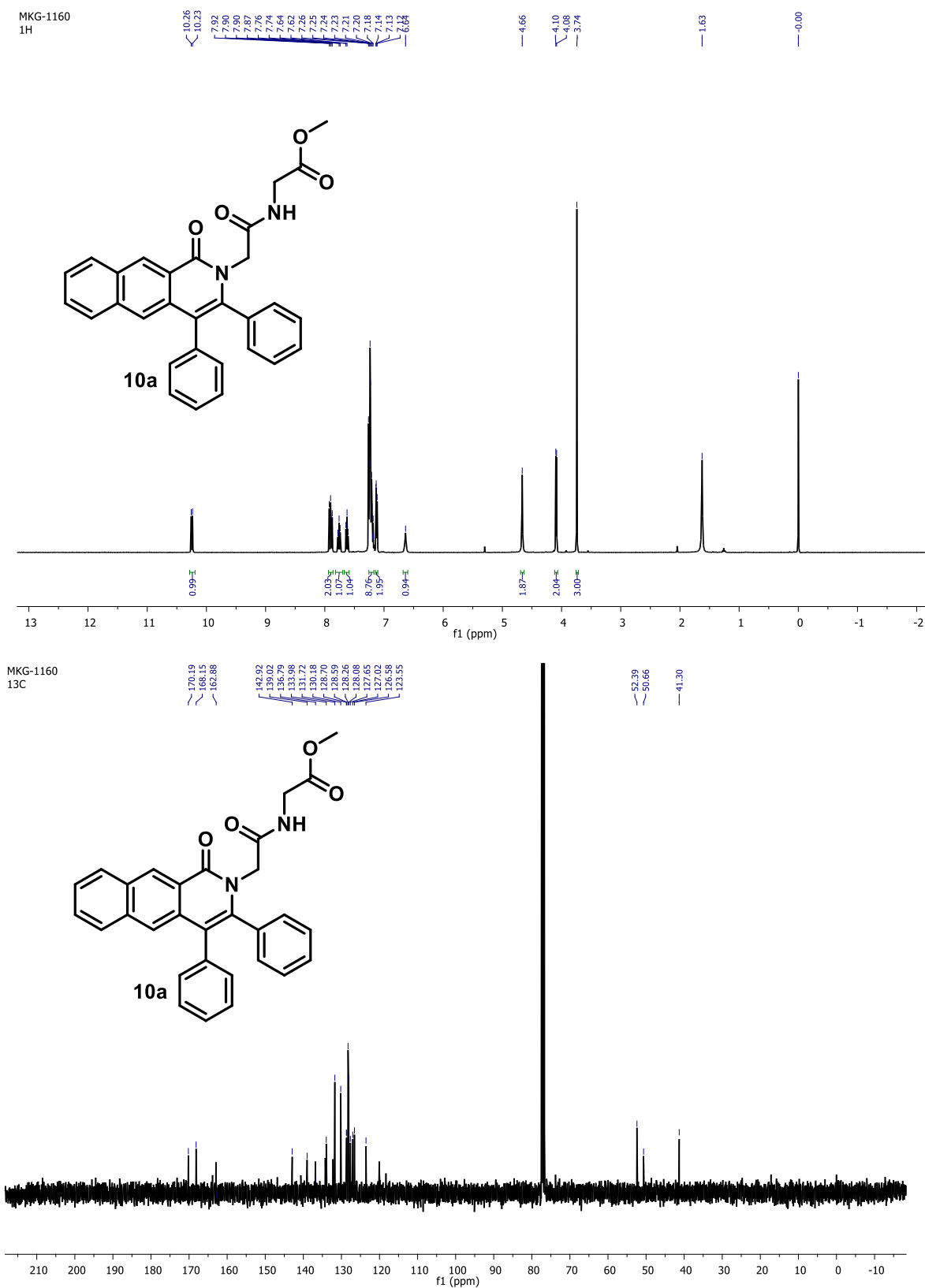
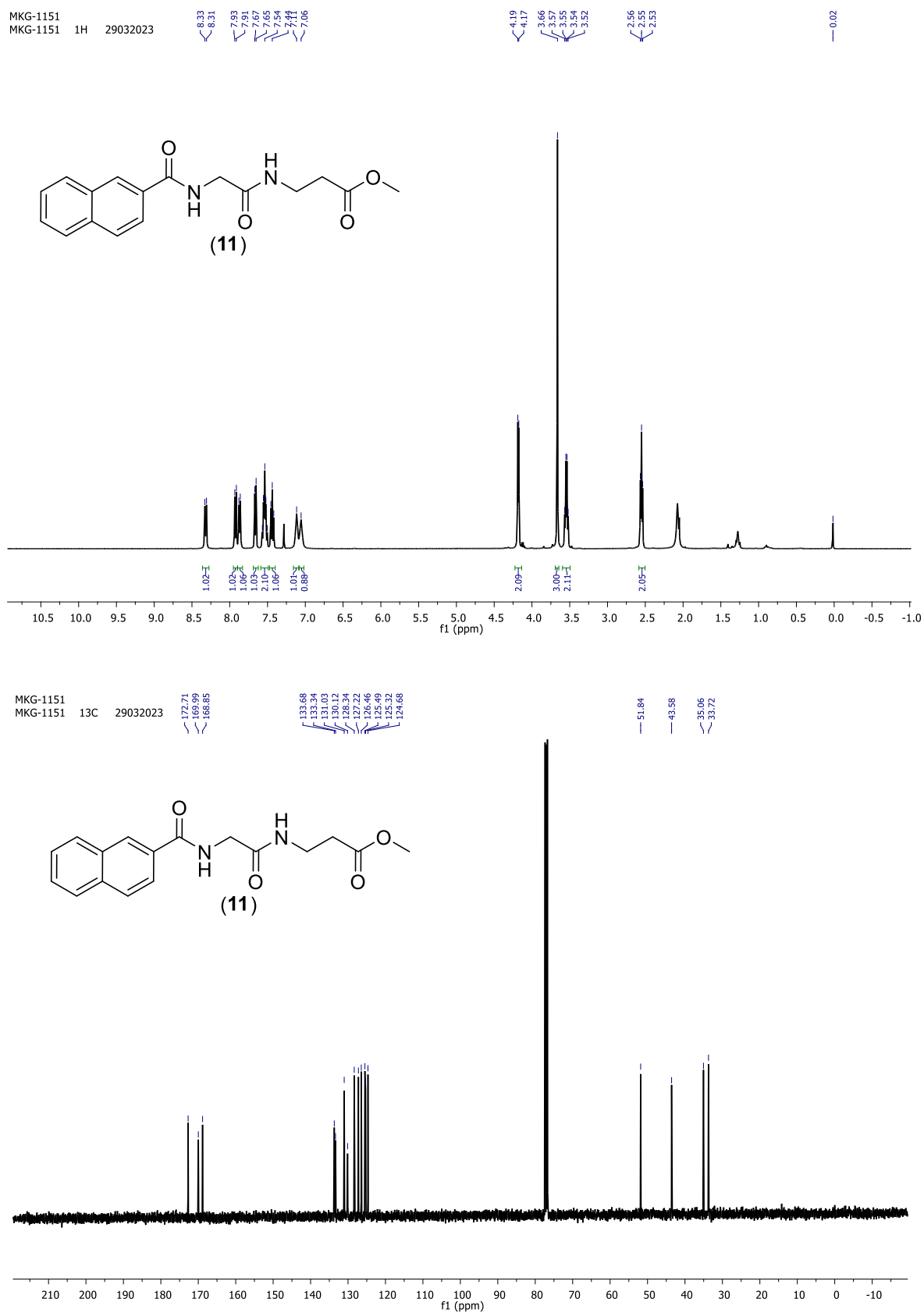
NKS_19122022_13 (0.053) Cu (0.05); Is (1.00,1.00) C₂₄H₂₃N₂O₄1: TOF MS ASAP+
7.57e12

Figure S 22 ESI HRMS spectra of Compound 9

Figure S 23 ^1H , ^{13}C NMR spectra of Compound 10

Figure S 24 ¹H, ¹³C NMR spectra of Compound 10a

Figure S 25 ^1H , ^{13}C NMR spectra of Compound 11

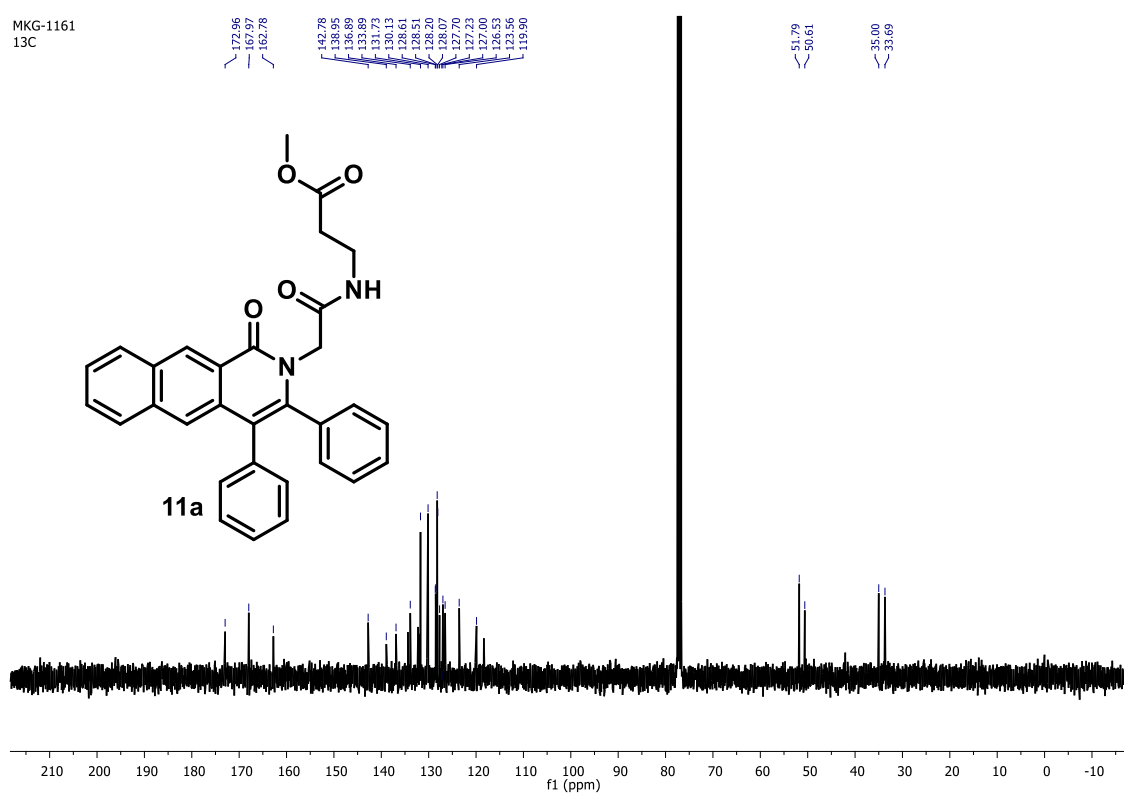
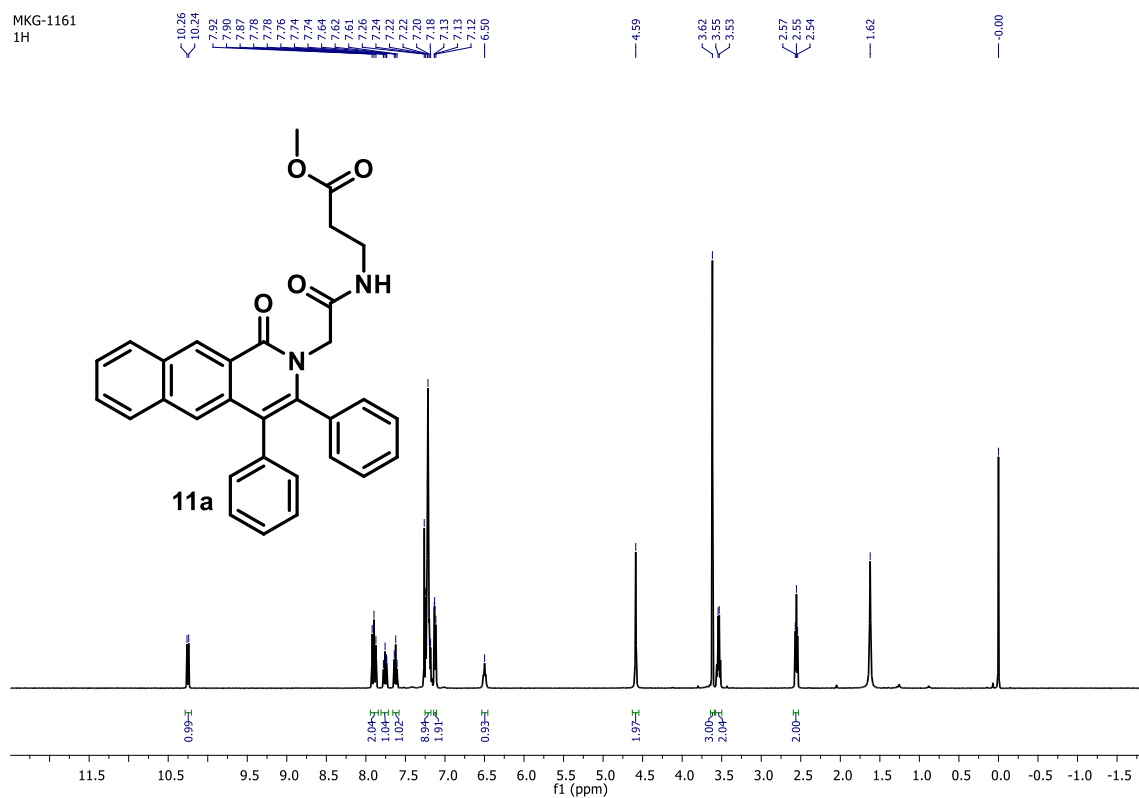


Figure S 26 ^1H , ^{13}C NMR spectra of Compound 11a

5.6 References

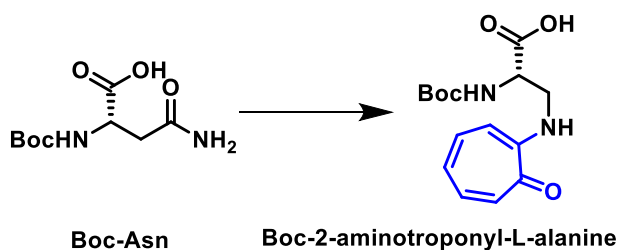
1. Huang, M.-H.; Hao, W.-J.; Li, G.; Tu, S.-J.; Jiang, B., Recent advances in radical transformations of internal alkynes. *Chemical Communications* **2018**, 54 (77), 10791-10811.
2. Zheng, L.; Hua, R., C–H activation and alkyne annulation via automatic or intrinsic directing groups: towards high step economy. *The Chemical Record* **2018**, 18 (6), 556-569.
3. Hua, R.; Nizami, T. A., Synthesis of heterocycles by using propargyl compounds as versatile synthons. *Mini-Reviews in Organic Chemistry* **2018**, 15 (3), 198-207.
4. Zheng, L.; Hua, R., Recent advances in construction of polycyclic natural product scaffolds via one-pot reactions involving alkyne annulation. *Frontiers in Chemistry* **2020**, 8, 580355.
5. Strumberg, D.; Pommier, Y.; Paull, K.; Jayaraman, M.; Nagafuji, P.; Cushman, M., Synthesis of cytotoxic indenoisoquinoline topoisomerase I poisons. *Journal of medicinal chemistry* **1999**, 42 (3), 446-457.
6. Glushkov, V.; Shklyayev, Y. V., Synthesis of 1 (2H)-Isoquinolones. *Chemistry of Heterocyclic Compounds* **2001**, 37, 663-687.
7. Cappelli, A.; Pericot Mohr, G. I.; Giuliani, G.; Galeazzi, S.; Anzini, M.; Mennuni, L.; Ferrari, F.; Makovec, F.; Kleinrath, E. M.; Langer, T., Further studies on imidazo [4, 5-b] pyridine AT1 angiotensin II receptor antagonists. Effects of the transformation of the 4-phenylquinoline backbone into 4-phenylisoquinolinone or 1-phenylindene scaffolds. *Journal of medicinal chemistry* **2006**, 49 (22), 6451-6464.
8. Li, B.; Feng, H.; Wang, N.; Ma, J.; Song, H.; Xu, S.; Wang, B., Ruthenium-Catalyzed Oxidative Coupling/Cyclization of Isoquinolones with Alkynes through C-H/N-H Activation: Mechanism Study and Synthesis of Dibenzo [a, g] quinolizin-8-one Derivatives. *Chemistry–A European Journal* **2012**, 18 (40), 12873-12879.
9. Yu, X.; Chen, K.; Guo, S.; Shi, P.; Song, C.; Zhu, J., Direct access to cobaltacycles via C–H activation: N-Chloroamide-enabled room-temperature synthesis of heterocycles. *Organic letters* **2017**, 19 (19), 5348-5351.
10. Ghosh, A.; Sapkal, G. T.; Pawar, A. B., Ru (II)-Catalyzed Regioselective Redox-Neutral [4+ 2] Annulation of N-Chlorobenzamides with 1, 3-Diynes at Room Temperature for the Synthesis of Isoquinolones. *The Journal of Organic Chemistry* **2023**, 88 (7), 4704-4719.
11. deGruyter, J. N.; Malins, L. R.; Baran, P. S., Residue-Specific Peptide Modification: A Chemist's Guide. *Biochemistry* **2017**, 56 (30), 3863-3873.
12. Ohata, J.; Martin, S. C.; Ball, Z. T., Metal-Mediated Functionalization of Natural Peptides and Proteins: Panning for Bioconjugation Gold. *Angewandte Chemie International Edition* **2019**, 58 (19), 6176-6199.
13. Rodríguez, J.; Martínez-Calvo, M., Transition-Metal-Mediated Modification of Biomolecules. *Chemistry–A European Journal* **2020**, 26 (44), 9792-9813.

14. Wang, S.; Zhou, Q.; Zhang, X.; Wang, P., Site-Selective Itaconation of Complex Peptides by Photoredox Catalysis. *Angewandte Chemie International Edition* **2022**, *61* (5), e202111388.
15. Haase, C.; Seitz, O., Chemical synthesis of glycopeptides. *Glycopeptides and Glycoproteins: Synthesis, Structure, and Application* **2007**, 1-36.
16. Hoppenz, P.; Els-Heindl, S.; Beck-Sickinger, A. G., Peptide-drug conjugates and their targets in advanced cancer therapies. *Frontiers in chemistry* **2020**, *8*, 571.
17. Marks, K. M.; Nolan, G. P., Chemical labeling strategies for cell biology. *Nature methods* **2006**, *3* (8), 591-596.
18. Sinkeldam, R. W.; Greco, N. J.; Tor, Y., Fluorescent analogs of biomolecular building blocks: design, properties, and applications. *Chemical reviews* **2010**, *110* (5), 2579-2619.
19. Craik, D. J.; Fairlie, D. P.; Liras, S.; Price, D., The future of peptide-based drugs. *Chemical biology & drug design* **2013**, *81* (1), 136-147.
20. Gracia, S. R.; Gaus, K.; Sewald, N., Synthesis of chemically modified bioactive peptides: recent advances, challenges and developments for medicinal chemistry. *Future medicinal chemistry* **2009**, *1* (7), 1289-1310.
21. Chatterjee, J.; Rechenmacher, F.; Kessler, H., N-methylation of peptides and proteins: an important element for modulating biological functions. *Angewandte Chemie International Edition* **2013**, *52* (1), 254-269.
22. Reguera, L.; Rivera, D. G., Multicomponent reaction toolbox for peptide macrocyclization and stapling. *Chemical reviews* **2019**, *119* (17), 9836-9860.
23. Zhang, X.; Lu, G.; Sun, M.; Mahankali, M.; Ma, Y.; Zhang, M.; Hua, W.; Hu, Y.; Wang, Q.; Chen, J.; He, G.; Qi, X.; Shen, W.; Liu, P.; Chen, G., A general strategy for synthesis of cyclophane-braced peptide macrocycles via palladium-catalysed intramolecular (sp^3) C-H arylation. *Nature chemistry* **2018**, *10* (5), 540-548.
24. Wang, Q.; An, S.; Deng, Z.; Zhu, W.; Huang, Z.; He, G.; Chen, G., Palladium-catalysed C–H glycosylation for synthesis of C-aryl glycosides. *Nature Catalysis* **2019**, *2* (9), 793-800.
25. Chen, K.; Shi, B. F., Sulfonamide-Promoted Palladium (II)-Catalyzed Alkylation of Unactivated Methylene C (sp^3)-H Bonds with Alkyl Iodides. *Angewandte Chemie* **2014**, *126* (44), 12144-12148.
26. Zhan, B. B.; Li, Y.; Xu, J. W.; Nie, X. L.; Fan, J.; Jin, L.; Shi, B. F., Site-Selective δ -C (sp^3)-H Alkylation of Amino Acids and Peptides with Maleimides via a Six-Membered Palladacycle. *Angewandte Chemie International Edition* **2018**, *57* (20), 5858-5862.
27. Wang, Q.; Fu, Y.; Zhu, W.; An, S.; Zhou, Q.; Zhu, S.-F.; He, G.; Liu, P.; Chen, G., Total synthesis of C- α -mannosyl tryptophan via palladium-catalyzed C–H glycosylation. *CCS Chemistry* **2021**, *3* (6), 1729-1736.

28. He, G.; Wang, B.; Nack, W. A.; Chen, G., Syntheses and transformations of α -amino acids via palladium-catalyzed auxiliary-directed sp³ C–H functionalization. *Accounts of Chemical Research* **2016**, 49 (4), 635-645.
29. Song, L.; Ojeda-Carralero, G. M.; Parmar, D.; González-Martínez, D. A.; Van Meervelt, L.; Van der Eycken, J.; Goeman, J.; Rivera, D. G.; Van der Eycken, E. V., Chemoselective Peptide Backbone Diversification and Bioorthogonal Ligation by Ruthenium-Catalyzed C–H Activation/Annulation. *Advanced Synthesis & Catalysis* **2021**, 363 (13), 3297-3304.
30. Song, L.; Lv, Z.; Li, Y.; Zhang, K.; Van der Eycken, E. V.; Cai, L., Construction of Peptide–Isoquinolone Conjugates via Rh (III)-Catalyzed C–H Activation/Annulation. *Organic Letters* **2023**.
31. Sharma, N.; Bahadur, V.; Sharma, U. K.; Saha, D.; Li, Z.; Kumar, Y.; Colaers, J.; Singh, B. K.; Van der Eycken, E. V., Microwave-Assisted Ruthenium-Catalysed ortho-C–H Functionalization of N-Benzoyl α -Amino Ester Derivatives. *Advanced Synthesis & Catalysis* **2018**, 360 (16), 3083-3089.
32. Naikawadi, P. K.; Mucherla, L.; Dandela, R.; Sambari, M.; Kumar, K. S., One-Pot Two-Step Double Annulation of N-Methoxybenzamides with Alkynes and Alkenes: Regioselective Construction of Isoindolo [2, 1-b] isoquinolin-5 (7H)-ones. *Advanced Synthesis & Catalysis* **2021**, 363 (15), 3796-3802.

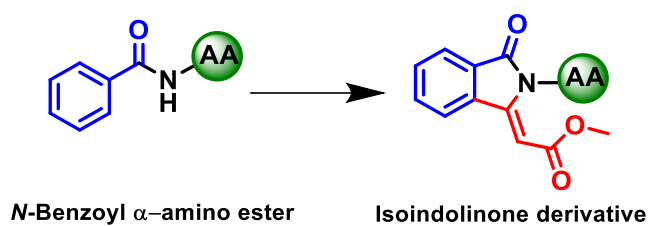
THESIS SUMMARY

Chapter-2



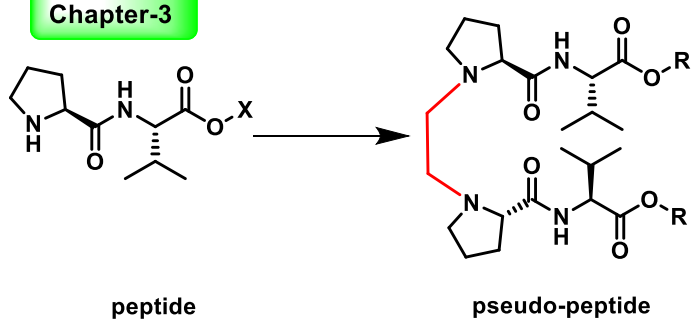
Org. Biomol. Chem. 2022, 20, 9397-9407

Chapter-4a



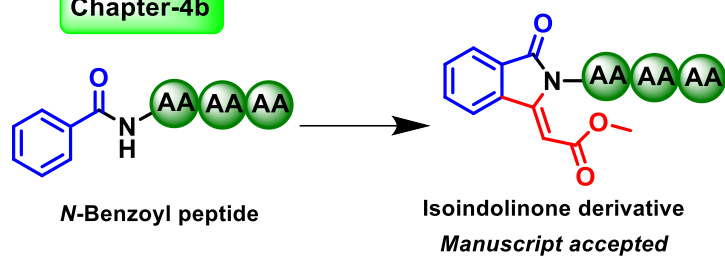
Org. Biomol. Chem. 2021, 19, 10097-10104

Chapter-3



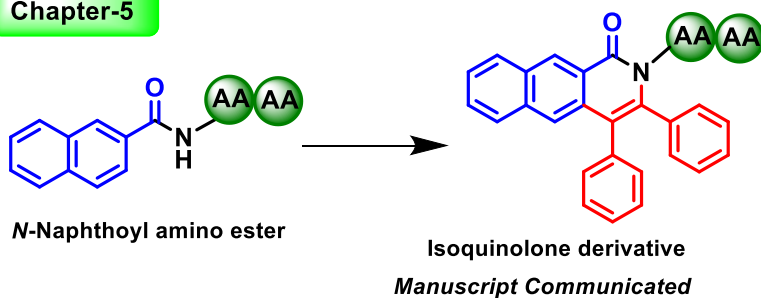
J. Org. Chem. 2021, 86, 16327-16336

Chapter-4b



Manuscript accepted

Chapter-5



Manuscript Communicated

ANNEXURE

Native peptides and proteins are derived from twenty proteogenic α -amino acids. However, many other amino acids and their derivatives are also occurred in various natural products. Recently, unnatural amino acids are synthesized and explored to tune the structure, function and bioactivity of native peptides. Pre-synopses of my thesis describe the synthesis and conformational analyses of unnatural amino acids/hybrid-peptides comprising non-benzenoid aromatic scaffold (2-aminotropone), Ethylenedipropyl pseudopeptides, isoindolinonyl peptides, isoquinolonyl peptides. Herein a couple of new synthetic methodologies have been developed including Pd/Ru-catalysed C(sp²)-H activation. The 2-aminotroponyl peptides form α -helix through non-covalent interactions and become scaffolds for synthesis of BODIPY analogues (Chapter-2). Its BODIPY analogues exhibit fluorescence. Interestingly, ethylenedipropyl pseudopeptides form β -/ γ -/ turn type structures and are considered potential entities to develop hairpin-forming peptides structure (Chapter-3). These pseudopeptides also form a metal complex with Cu(II) ions. Isoindolinonyl peptides are synthesized from *N*-Arylamide of amino acids/peptides through Pd(II) catalysed C(sp²)-H olefination/activation with different olefins and amino acid derivatives. Notably, isoindolinone's carbonyl plays a significant role in the folding of peptide structure through hydrogen bonding with the nearest amide N-H (Chapter-4). Isoquinolonyl peptides are synthesized from *N*-Arylamide of amino acids/peptides through Ru(II) catalysed C(sp²)-H activation/annulation from various alkynes at room temperature (Chapter-5). Interestingly these peptides are fluorescent which could be applicable for labeling the peptides. Hence newly synthesized unnatural amino acids and their hybrid peptides have shown characteristic conformations and functions including fluorescence.

PAPER

View Article Online

View Journal | View Issue



Cite this: *Org. Biomol. Chem.*, 2022, 20, 9397

A new amino acid, hybrid peptides and BODIPY analogs: synthesis and evaluation of 2-aminotroponyl-L-alanine (ATA) derivatives†

Manish K. Gupta^{a,b} and Nagendra K. Sharma^{a,b}

Natural aromatic α -amino acid residues play critical roles in the structural and functional organization of proteins owing to π -interactions. Their aromatic residues are derived from benzenoid scaffolds. Non-benzenoid aromatic scaffolds such as tropone and tropolone are also constituents of troponoid natural products. Tropolone has also the ability to exhibit π -interactions along with additional hydrogen bonding. Thus, amino acids comprising troponyl could be potential building blocks of novel peptidomimetics. This report describes the synthesis of the L-aminotroponylalanine amino acid (ATA) and its unusual activity with the peptide coupling agent EDC. Importantly, its di-peptides form β -sheet/-turn type secondary structures in organic solvents owing to the troponyl residue. This amino acid is an excellent scaffold for the synthesis of fluorescent amino acids such as BODIPY amino acid analogs. Nevertheless, this amino acid and its BODIPY derivatives can enter HeLa cells without exhibiting significant cytotoxicity at low concentrations (~ 50 μ M). Hence, ATA and its BODIPY derivatives are promising aromatic amino acids for the construction of potential peptidomimetics and fluorescent labelling of target peptides.

Received 18th October 2022,
Accepted 11th November 2022

DOI: 10.1039/d2ob01905a

rsc.li/obc

Introduction

Native aromatic α -amino acids such as phenylalanine (Phe), tyrosine (Tyr), tryptophan (Trp), and histidine (His) are derived from benzenoid scaffolds and play pivotal roles in the structural and functional organization of peptides/proteins.¹ The functional group-containing aromatic amino acids (Tyr, His, and Trp) are found in the active sites of various enzymes and play critical roles in their catalytic activity.² Moreover, Trp is a fluorescent amino acid. Generally, the structural modifications of native amino acids significantly alter their structure and functions. As reported in the literature, structurally modified aromatic amino acid analogs have emerged as potential building blocks of various peptidomimetics and foldamers.^{3–5} For example, Svendsen has demonstrated the role of bulky aromatic amino acid-containing bovine lactoferricin peptides in increasing antibacterial activity.⁶ Huc has rationally designed aromatic oligoamides from unnatural aromatic amino acids

and they form β -sheet type foldamers owing to the face-to-face π - π interaction between the aromatic residues.⁷ Aromatic amino acids are also involved in the formation of amyloid self-assembly structures owing to π - π interactions.⁸ Sanjayan has explored an anthranilic acid-associated α/β -hybrid peptide oligomer which forms unique (1-2) type helical turns.⁹ Sutherland has reported benzotriazole-derived unnatural aromatic acids which exhibit charge transfer-based fluorescent compounds with mega Stokes shifts.¹⁰ Cate has shown the initiation of protein synthesis with unnatural aromatic amino acids derived from phenylalanine using an engineered initiator tRNA *in vivo*.¹¹ Recently, a phenylalanine analog has been reported to form a hydrogel even with single amino acid derivatives that exhibit potent antimicrobial activity.¹² Parang has synthesized a series of cyclic peptides comprising the diphenylalanine residue and evaluated their transportation efficiency.¹³ Tannenbaum has evaluated aromatic amino acids as potential biomarkers in breast cancer by Raman spectroscopy analysis.¹⁴ Most unnatural aromatic amino acids are derived from the benzenoid aromatic ring. However, non-benzenoid aromatic scaffolds such as tropolone are constituents of troponoid natural products.^{15,16} It exhibits intramolecular proton transfer and metal complexing properties with coordinating metal ions. It also exhibits unique photophysical properties owing to π - π^* , n - π^* interactions, and charge transfer. Tropolone-related compounds exhibit numerous types of bioactivities including antimicrobial, antiviral, antifungal,

^aSchool of Chemical Sciences, National Institute of Science Education and Research (NISER)-Bhubaneswar, Jatni Campus, Bhubaneswar-752050, Odisha, India.

E-mail: nagendra@niser.ac.in; Fax: +91 (674)2494004; Tel: +674-249-4141

^bHBN-Mumbai, Mumbai, India

† Electronic supplementary information (ESI) available: Spectroscopic (MS and NMR) and crystallographic data. CCDC 2174977 and 2212187. For ESI and crystallographic data in CIF or other electronic format see DOI: <https://doi.org/10.1039/d2ob01905a>

Unusual Pseudopeptides: Syntheses and Structural Analyses of Ethylenediproyl Peptides and Their Metal Complexes with Cu(II) Ion

Manish K. Gupta,[§] Chinmay K. Jena,[§] Chenikkayala Balachandra, and Nagendra K. Sharma*

Cite This: *J. Org. Chem.* 2021, 86, 16327–16336

Read Online

ACCESS |

Metrics & More

Article Recommendations

Supporting Information

ABSTRACT: The synthetic unnatural amino acids and their peptides as peptidomimetics have shown remarkable structural and functional properties. In the repertoire of synthetic peptides, pseudopeptides have emerged as attractive small peptidomimetics that are capable of forming the characteristic secondary structures in the solid/solution phase, as in natural peptides. This report describes the synthesis and structural analyses of novel pseudopeptides as ethylenediproyl (*etpro*) tetra/hexapeptides, comprising a chiral diaminedicarboxylate scaffold. Their NMR and CD spectral analyses strongly support the formation of the β -turn-type structures in organic solvents (ACN/MeOH). Further, the single-crystal X-ray studies of tetrapseudopeptide confirm the formation of a unique self-assembly structure as β -strand type in the solid state through hydrogen bonding. Importantly, their diamine moiety influences the formation of Cu-complexes with Cu(II) ions. A tetrapseudopeptide monocarboxylate-Cu(II) complex forms the single crystal that is studied by the single-crystal X-ray diffractometer. The crystal structure of the tetrapseudopeptide-Cu(II) complex confirms the formation of the distorted square planar geometry structure, almost like the amyloid β (A β)-peptide-Cu(II) complex structural geometry. Hence, these *etpro*-pseudopeptides are emerging peptidomimetics that form β -turn types of structures and metal complexes mainly with Cu(II) ions. These molecules could be considered for the development of peptide-based catalysts and peptide-based therapeutic drug candidates.



INTRODUCTION

Protein–protein interactions (PPIs) and protein–nucleic acid interactions (PNIs) are involved in numerous biological processes.^{1,2} The development of molecules to target such interactions provides a significant therapeutic potential. However, small molecules barely target such interactions because of the large and shallow binding surface. In the repertoire of macromolecular ligands, the structured peptides have shown encouraging results as binding with protein and nucleic acids and are considered as potential therapeutic drug candidates.^{3,4} Protein and peptides form characteristic secondary structures such as α -helix, β -sheet, and β -turn to regulate the various biochemical processes.^{5–7} However, peptides likely lose the secondary structure in solutions and are prone to proteolysis, lowering the target selectivity. Peptides have other drawbacks, such as poor cell permeability and poor selectivity.⁸ To overcome these challenges, various structurally modified unnatural amino acids and their peptides are synthesized as peptidomimetics by restricting the conformational flexibility to improve metabolic stability and target specificity.^{9,10} The various peptidomimetics of α -helix, β -sheet, and β -turn are prepared and explored for various applications including therapeutic behaviors and catalytic properties in chemical synthesis.^{7,11–17} Another important peptidomimetics is β -hairpin, formed by connection of two β -strands through a loop in an antiparallel fashion.^{18–22} The antiparallel- β -hairpin peptides provide enormous opportunity

for selective binding with antibodies and the development of new peptide based nanomaterials.²³ The incorporation of the D-Pro/L-Pro, D-Pro/L-Gly turn into peptides is used for synthesis of stable β -hairpins. However, the β -hairpin with parallel strands is rare in nature. Gellman and co-workers have synthesized novel parallel β -hairpin peptides by using a dimethyl diamine linker and extensively studied their conformational analyses by NMR and X-ray studies.²⁴ Moreover the amide bonds/functional side-chain of peptides are natural ligands of coordinating metals. For example, peptide–metal complexes of metal ions (Fe/Cu/Zn ions) have significant roles in regulating the essential biological processes.²⁵ Metallopeptides are primarily engaged in a redox reaction, including regulating reactive oxygen species (ROS) production in living systems, the emerging area of biochemical research for developing therapeutic drugs and diagnosis probes.^{26,27} For example, the most common copper-peptide as GHK-Cu(II) is considered as natural antioxidant and collagen stimulating agents, which are found in human plasma

Received: July 14, 2021

Published: November 16, 2021



Cite this: *Org. Biomol. Chem.*, 2021, **19**, 10097

Pd-Catalyzed C(sp²)-H olefination: synthesis of *N*-alkylated isoindolinone scaffolds from aryl amides of amino acid esters†

Manish K. Gupta,^{a,b} Chinmay K. Jena^{a,b} and Nagendra K. Sharma^{a,b}

Isoindolinone is a constituent of various natural products and synthetic biologically active compounds. The classical multi-step synthetic methods used to prepare various indolinone derivatives are tedious and challenging. One-pot synthetic methods are attractive and economical. Transition-metal-catalyzed C-H activation is an emerging tool for synthesizing natural products and small organic molecules via reducing the number of synthetic steps necessary. This paper describes the synthesis of *N*-alkyl-3-methenyl chiral isoindolinone derivatives from aryl amides of L-amino acids and non-activated alkene via Pd-catalyzed C(sp²)-H olefination. Herein, the amino acid residue acts as a directing group for olefination at the aryl ring, and then cyclization occurs at the amide NH. Hence, this methodology could be helpful to transform standard amino acids into respective chiral isoindolinone derivatives.

Received 12th October 2021,
Accepted 4th November 2021
DOI: 10.1039/d1ob01997j
rsc.li/obc

Introduction

The isoindolinone (benzo-fused γ -lactam) scaffold is chemical constituent of various natural products and synthetic biologically active molecules. For example, *N*-C3-substituted isoindolinone derivatives are found in pagoclone, indoprofen, erinacins, lennoxamine, lenalidomide, isohericenone, pazinaclole (Fig. 1a).^{1–3} These molecules show antimicrobial, antioxidant, antifungal, antiviral, anxiolytic, anti-Parkinson's, anti-inflammatory, antihypertension, and anticancer activities. The classical synthesis of isoindolinone derivatives involves challenging multi-step synthetic strategies.^{4–6} In recent times, transition metal-catalyzed C-H activation and C-H olefination are emerging as synthetic methodologies for synthesizing various natural products and their precursors.^{7–10} For example, Maiti and co-workers have developed several remarkable C(sp²)-H olefination methodologies with a Pd-catalyst.^{10–18} Maiti has also explored Co-/Rh-catalyzed substrate-specific C(sp²)-H olefination.^{19–21}

The synthesis of isoindolinone derivatives has also been achieved using activated arylamides and non-reactive olefins in the presence of transition metal catalysts (Au, Co, Cu, In, Ir,

Ni, Pd, Rh, Ru, Sc, Yb, and Zn) (Fig. 1b).²² The tolyl sulfonate (Ts)/methyl sulfonate (Ms)/alkoxides containing arylamides are active for metal complexation in the presence of external ligands.

The directing group containing acrylamides has also been used to synthesize isoindolinone derivatives from non-activated olefins through C(sp²)-H olefination.²³ For example, the quinoline directing group containing arylamides gives *N*-quinolinyl substituted isoindolinones from acrylate in the presence of a Pd(II)-catalyst. However, *N*-tosylated benzamide requires the ligand to prepare isoindolinone derivatives from olefins using Pd-catalyzed olefination.^{24,25} Amino acids and peptides are natural ligands of various transition metals and have been used as directing groups/ligands in the different transition metal-catalyzed C-H activation/C-H olefination.²⁶ Yu and co-workers have explored using amino acids/peptides as the ligand or directing group in the metal-catalyzed C(sp²)-H functionalization of di-/tri/tetra-peptides at the N-terminus/site-specific C-H alkynylation/ β -C-H arylation.^{27–29} Albericio has shown the synthesis of stapled-peptides by the late-stage C(sp²)-H activation of peptides.^{30,31} Tran and Daugulis have used 2-thiomethylaniline as a directing group for C(sp²)-H functionalization of *N*-protected amino acids at the β -position with different aryl halides.³² The metal-catalyzed C-H olefination of amino acid/peptide-related compounds have generated opportunities to prepare various synthetic and natural peptide analogues.^{33,34} Metal catalyzed olefination of ligand enabled aryl amide with olefins is an emerging synthetic methodology that has attracted attention for the synthesis of substituted aryl amide derivatives.^{16,35–41} Recently, Maiti and co-workers

^aSchool of Chemical Sciences, National Institute of Science Education and Research (NISER)-Bhubaneswar, Jatni campus, Bhubaneswar-752050, Odisha, India.
E-mail: nagendra@niser.ac.in; Fax: +91 (674)2494004; Tel: +91 674-249-4141

^bHBTI-Mumbai, Mumbai, India

† Electronic supplementary information (ESI) available: Spectroscopic (MS and NMR) and crystallographic data. CCDC 2098113. For ESI and crystallographic data in CIF or other electronic format see DOI: 10.1039/d1ob01997j



Cite this: DOI: 10.1039/d3ob00742a

Synthesis of *N*-isoindolinonyl peptides via Pd-catalyzed C(sp²)-H olefination-activation and their conformational studies†

Manish K. Gupta,^{†a,b} Ankita Panda,^{†a,b} Subhasish Panda^{‡a,b} and Nagendra K. Sharma^{‡a,b}

Isoindolinone is a constituent of several natural products that show a wide range of bioactivity, such as anticancer, antimicrobial, antiviral and anti-inflammatory properties. It would be interesting to explore the carbonyl group (H-bond acceptor) of isoindolinone and its structural and conformational changes. However, the synthesis of isoindolinone-comprising peptides in short steps is challenging. Herein, we have developed a synthetic methodology for introducing the isoindolinone residue to peptides via Pd-catalyzed C(sp²)-H activation/olefination, and demonstrated the conformational changes owing to the isoindolinone scaffold. Hence, isoindolinonyl peptides provide an avenue for the synthesis of novel foldamers and therapeutic agents.

Received 12th May 2023
Accepted 22nd May 2023
DOI: 10.1039/d3ob00742a
rsc.li/obc

Introduction

Isoindolinone is heterocyclic compound with a benzo fused γ -lactam scaffold that is a constituent of various natural products and synthetic bioactive molecules such as pagoclone, indoprofen, erinaccerins, lennoxamine, lenalidomide, isohericenone, and pazinaclone (Fig. 1a).^{1–3} These molecules show antimicrobial, antioxidant, antifungal, antiviral, anxiolytic, anti-Parkinson's, anti-inflammatory, antihypertension, and anticancer activities.⁴ In the repertoire of isoindoline scaffolding into peptides, the incorporation of isoindolinone moiety into naturally occurring bioactive cyclic peptides enhances their bioactivity. Fenestin A and zygosporamide are marine-derived natural cyclic peptides possessing a wide range of bioactivity, including anticancer. Jin has synthesized Fenestin analogues containing isoindolinone derivatives that improved their apoptosis of tumor cells and led to cycle arrest in the G2/M phase.⁵ Zygosporamide cyclic depsipeptides isolated from marine-derived fungus and their analogues are also synthesized by incorporating the isoindolinone moiety, which sig-

nificantly improved their bioactivity (Fig. 1b).⁶ Nevertheless, Chen has synthesized various stapled peptides by incorporating isoindolinone derivatives (Fig. 1c).⁷ Thus, the demand for isoindolinone-containing peptides has suddenly increased and become a lucrative research area for both chemists and biol-

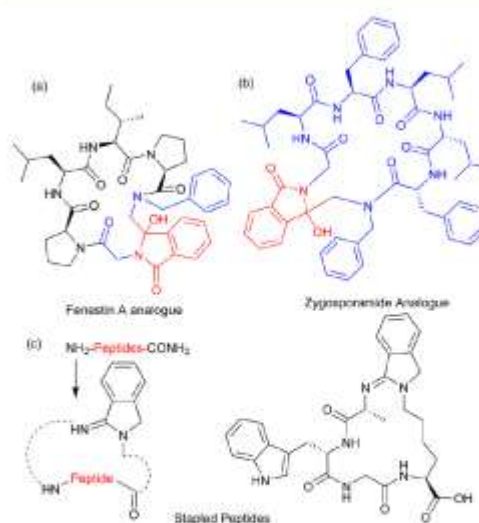


Fig. 1 Isoindolinone derivative: (a,b) isoindolinone related natural peptides; (c) stapled peptides.

^aSchool of Chemical Sciences, National Institute of Science Education and Research (NISER), Bhubaneswar, Jatani-752050, Odisha, India. E-mail: nagendra@niser.ac.in; Tel: +91-674-249-1141

^bHomi Bhabha National Institute (HBNI), Training School Complex, Anushaktinagar, Mumbai, 400094, India

[†]Electronic supplementary information (ESI) available: NMR and mass data of all new compounds are provided. 2D NMR of compound 19a and DMSO-titration spectra are also provided. Computational study outcomes (energy vs. conformation profiles) are also provided. See DOI: <https://doi.org/10.1039/d3ob00742a>

[‡]These authors are equally contributed.